LBL-12119
EEB-W-81-02
W-79

HIGH-PERFORMANCE SOLAR-CONTROL WINDOWS

FINAL REPORT

W. J. King*

Lawrence Berkeley Laboratory
University of California
Berkeley, California 94720

April 1980

The work described in this report was funded by the Assistant Secretary for Conservation and Solar Energy, Office of Buildings and Community Systems, Buildings Division of the U.S. Department of Energy under Contract No. W-7405-ENG-48.

*Kinetic Coatings, Inc.
Burlington, Massachusetts 01803
Subcontract No. 4335902

ABSTRACT

This report describes investigations carried out during a 23-month period on the use of ion-beam sputtered, metal-dielectric layers for fabricating high-performance solar-control windows for office buildings and residences. As such it represents a continuation and extension of a previous LBL contract (No. 1667000) and proprietary KCI developments.

Two basic types of windows were studied. The first was optimized for rejecting incident solar energy during the cooling season while maintaining high daylight transmittance. The second was optimized for transmission of solar energy and reduction of thermal losses in the heating season by maximizing reflectivity in the long-wave infrared (i.e., transparent heat mirror). Various compromise configurations for performing both functions were also considered. The program covered original equipment (glass) and retrofit (plastic) substrate materials. Various metal-dielectric combinations, including Cu-SiO_2, Bs-SiO_2 (Bs ≡ brass), Bs-Al_2O_3, AG-SiO_2, and Ag-Al_2O_3, were used to obtain the necessary optical characteristics. Extensive weathering tests were conducted to demonstrate that the final systems developed are capable of extended life in a practical environment.

Roll-to-roll (1' wide) coating was demonstrated for retrofit office and residential windows on various forms of polyester. Comparable window performance was achieved on polypropylene and teflon FEP substrates.

A brief economic analysis is presented which indicates that KCI's processing is completely consistent with the price structure in the solar-control film industry.

FOREWORD

This report was prepared by Kinetic Coatings, Inc., Burlington, Massachusetts 01803, and describes work performed from February 1978 to December 1979 on Lawrence Berkeley Laboratory Contract 4335902.

S. Selkowitz was Project Monitor for Lawrence Berkeley Laboratory.

W.J. King was Program Manager and was assisted in the research by E.R. Berman and William J. King, Jr.

This work was conducted as part of the Lawrence Berkeley Laboratory's Windows and Daylighting Program with support provided by the U.S. Department of Energy. For further information regarding related program activities, please contact:

Windows and Daylighting Program
Building 90, Room 3111
Lawrence Berkeley Laboratory
Berkeley, California 94720
(415) 486-5605

TABLE OF CONTENTS

1. Project Background

As the energy problem has become more acute, the structure, function and overall architectural characteristics of windows have been subjected to increasingly thorough analysis in terms of energy conservation. From an historical perspective, based on their extensive use, it is obvious that windows are a desirable building element and should continue to find extensive use in modern buildings. Recent design changes make it possible to retain the aesthetic value of windows, while ensuring minimum energy consumption or in some cases (passive solar heating) actually gaining energy.

Actual design characteristics depend critically on application (e.g. office vs. residential) and geographical location. A previous LBL funded program (Report LBL 7825) at KCI was concerned with demonstrating the use of ion beam sputtered metal-dielectric layers to achieve the necessary characteristics. The primary emphasis of the present program was originally to demonstrate a medium sized scale-up of basic production methods for glass (original equipment glazing) substrates with a secondary emphasis on the optical and weathering characteristics of selected deposited materials. Because it appeared that the shortest term energy pay-off could be achieved using retrofit (i. e. plastic substrates) techniques, the primary emphasis was shifted during the program to a demonstration of medium scale production methods on roll (1' wide) plastic substrates.

The basic philosophy was that any techniques demonstrated on plastic substrates could be directly applied to glass substrates. As a result of accelerated weathering studies, it now appears that the preferred coating materials for glass substrates may differ from those preferred for plastic substrates. Due to factors that may not exist under a real environment, the accelerated weathering tests may have eliminated some materials which would be acceptable under standard conditions. However, any materials which survived the accelerated testing used at KCI are believed acceptable under most real conditions.

In order to cover the varying requirements of original equipment office windows (OW), office window retrofits (OWR), original equipment residential windows (RW) and retrofit residential windows (RWR), the material studies were expanded to include five metal-dielectric combinations (see Section 2) and two plastic substrates (polyester and teflon FEP). A third substrate (polypropylene) was investigated by KCI after the end of the program and some results are included here for completeness.

The present program was not concerned with defining and/or analyzing all of the multiple design factors and energy considerations that may occur in real building designs. Considerable consideration was given to these factors in the first program and pre-program planning, and also by LBL in their overall window development project. Rather, it was primarily concerned with demonstrating optical performance and manufacturing methods capable of satisfying any, and all, window requirements, with variations easily included for performance optimization at any geographical location. Actual estimates of thermal transfer and associated energy losses, gains, or savings may be made for any specific application from the performance data presented herein. Examples of such calculations are given in the Final Report (LBL 7825) of the original program. Much more sophisticated analysis is required for each and every real situation and as such is beyond the scope of this report. The concept of being able to tailor the coating and substrate materials as well as optical characteristics can, however, be relied on to achieve optimum performance.

The primary factors affecting window heat transfer are radiation, convection/conduction and air leakage due to improper fitting or aging. Only properly designed and installed windows are considered for the present discussion, since air infiltration could otherwise eliminate any benefits derived from reduction of losses due to the other factors. Thermal radiation and convection losses are considered roughly equivalent so that savings due to low emittance coatings, which constitute the primary focus of the present program, may range up to 50% although they are likely to be significantly lower in practice. Proper control of thermal radiation and solar radiation, however, when combined with convection/conduction control could lead to window related energy savings greater than 50%.

An overall view of the general requirements may be obtained from Figure 1 which gives the Air Mass 2 (AM2) solar spectrum at the earth, a typical room temperature radiation spectrum and the basic desired performance characteristics of office windows and residential windows. For office windows, where reduction of air conditioning energy consumption is the prime factor, it is desirable to reflect all incident solar energy above 0.7 μ (visible limit) back to the atmosphere. In the visible region, reflectivity should be reduced to allow enough transmitted light (40-50%) for normal functioning on a sunny day without the need for extensive internal lighting, since the latter increases the energy load. Reasonable transmission is also necessary from an aesthetic point of view in order that the coating does not defeat the primary purpose of the window.

For moderate to northerly climates it is also preferable for the window to reflect most of the room temperature (thermal) radiant energy from walls machines, people etc. back into the room to reduce heat loss during cooler months. Of necessity, this heat mirror requirement conflicts with the primary function of reducing air conditioning loads and overall window design should be based on a yearly cycle energy balance. Obviously, for a southern climate, the heat retention function is less important so there is greater freedom in choosing the coating and its placement (inside or outside etc.) for optimum performance and weatherability.

Some of the possible variations for solar control office windows are shown in Figures 2(a) - 2(h). In discussing these configurations the results of this project are anticipated and it is assumed that the reflecting layers are protected by a dielectric overcoat from environmental factors or physical damage. It is also assumed that the reflectivity for room temperature (~300°K) radiation is approximately 95% (see Section 3.6).

Figures 2(a) and 2(b) show a single glazed configuration. If the functional layer is applied directly to glass (OW - Office Window) for original equipment installation, the reflecting layers may be on the outside (Fig. 2(a))

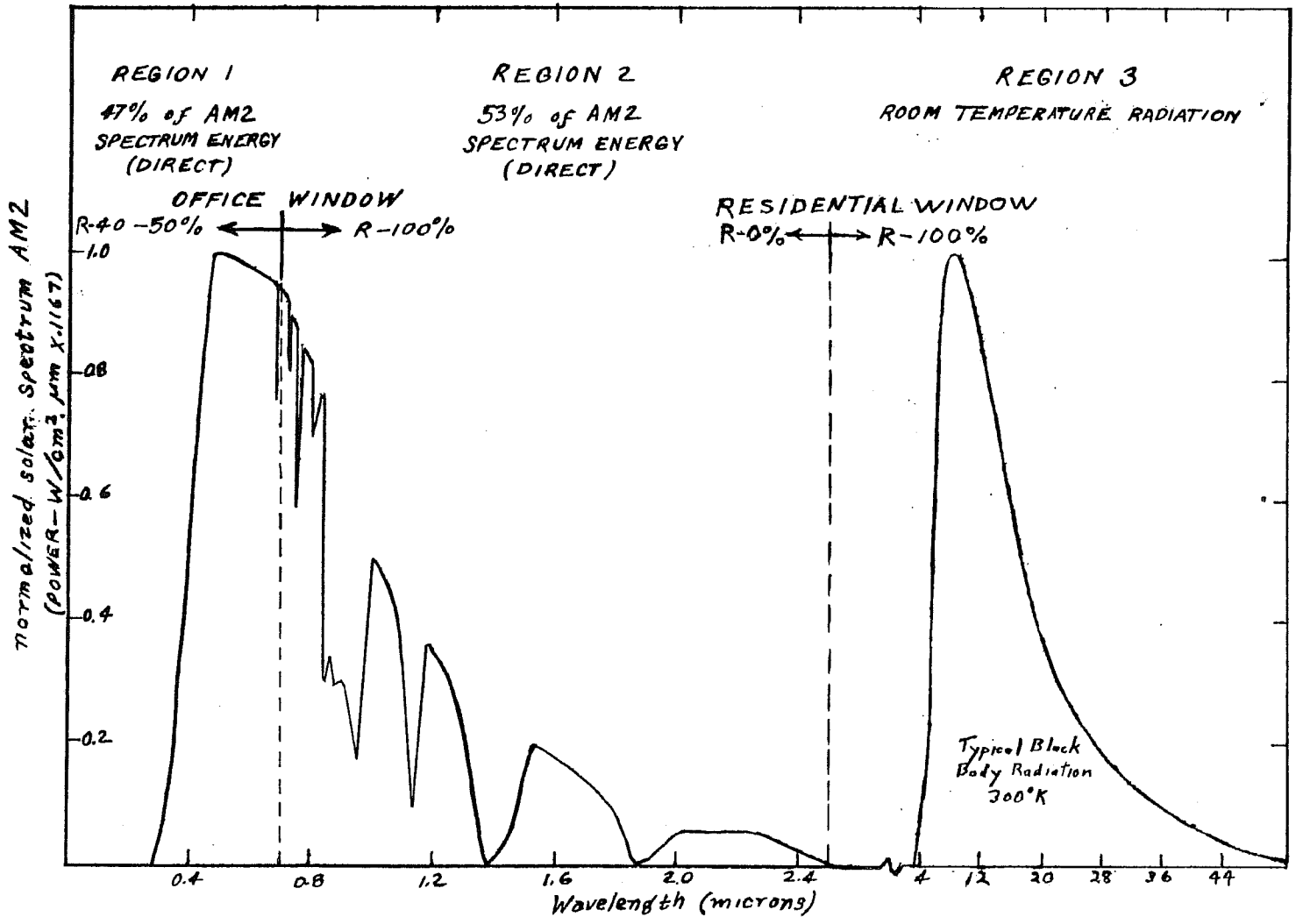

FIGURE 1 – RADIATION REGIONS FOR WINDOW DESIGN

OFFICE WINDOWS

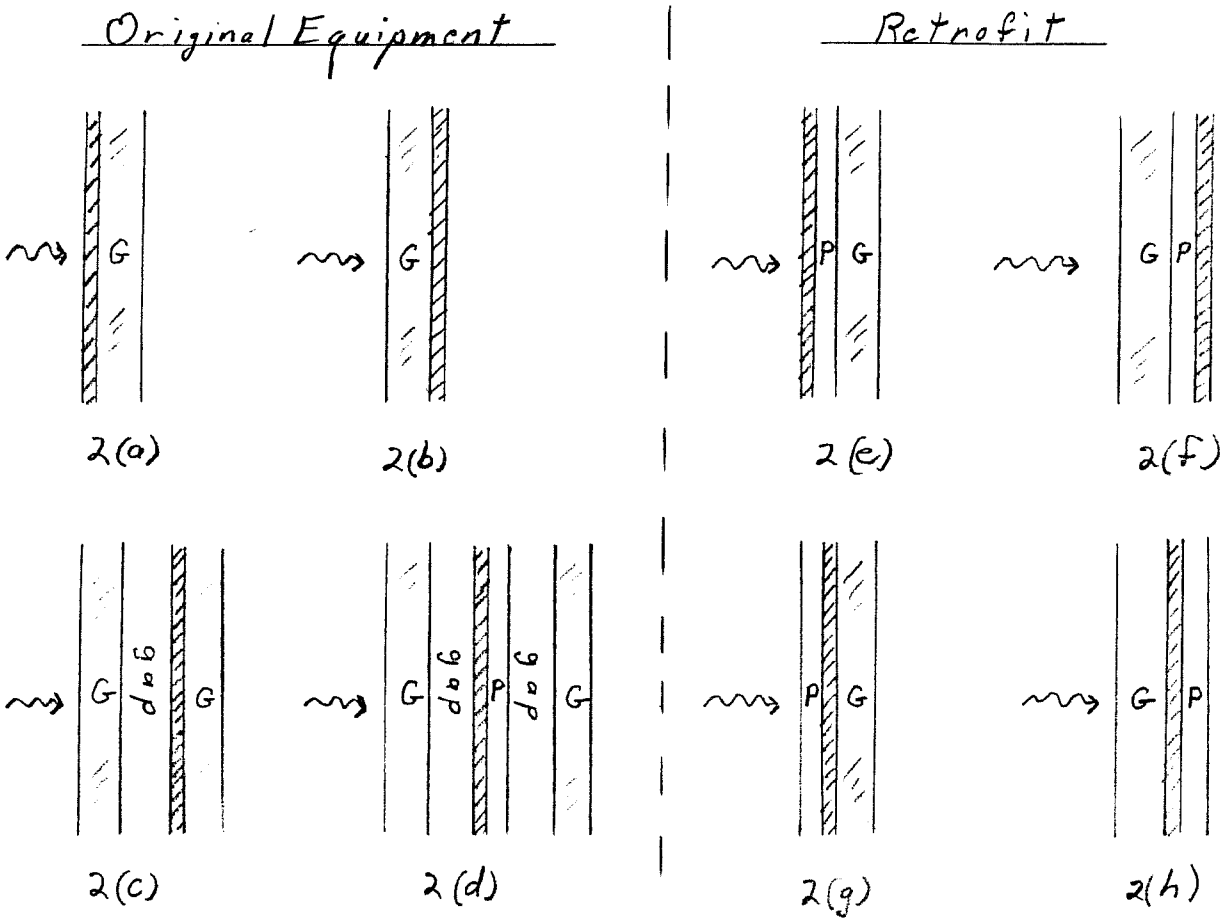

RESIDENTIAL WINDOWS

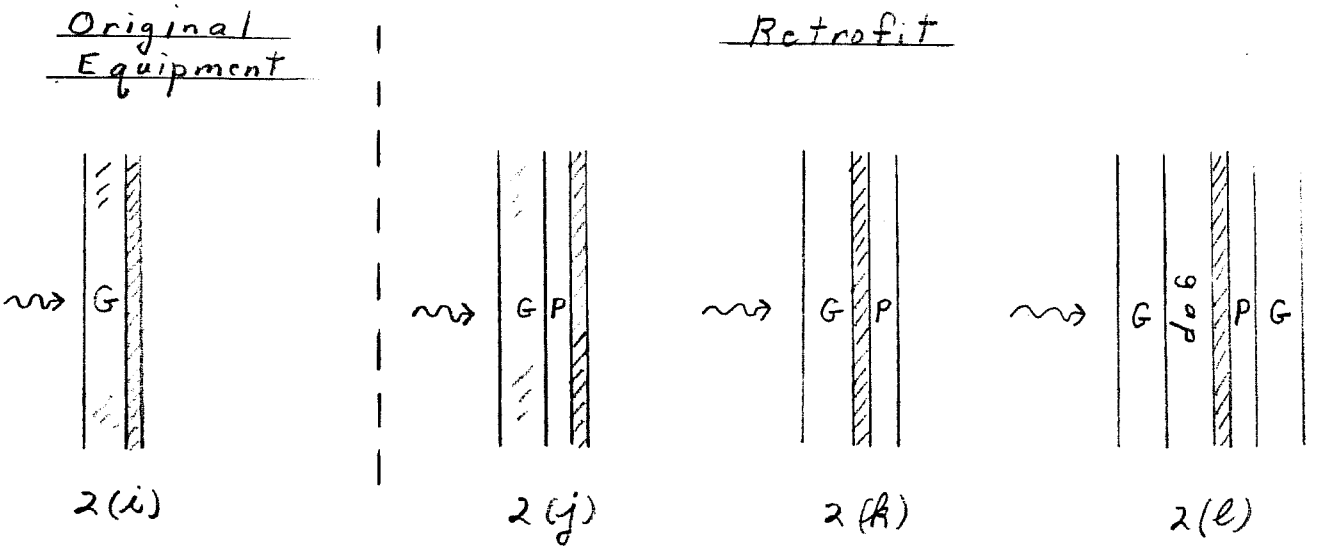

Legend: G ≡ glass ▨ ≡ deposited film (Note: Schematics not to scale)
P ≡ plastic ⇝ ≡ outdoor side

Fig. 2 Window Configurations

or on the inside (Fig. 2(b)). In the former case, it will have the maximum effect on reducing air conditioning loads but will be practically ineffective as a heat mirror on the indoor side due to the high emissivity of the glass for room temperature radiation, and will have only a minimal effect on the outdoor film coefficient since that term is normally dominated by convection. This is therefore the optimum configuration for southern climates.

With the coating inside, the glass is less effective as a solar reflector due to absorption of part (~7% for 3/32" thick window glass; higher if thicker) of the reflected solar radiation during two passes through the glass. Some of this absorbed energy will be conducted to the cooler inside where it can be transferred to the interior by convection; the remainder will be rejected to the outside. This configuration, however, will have maximum effect as a heat mirror due to the 95% reflectivity for thermal radiation and is therefore an excellent compromise for cooler climates. Since the inside of this reflecting glass will tend to be cooler in the winter, condensation problems may occur, depending on outdoor temperatures and interior humidity levels. Such condensation would tend to lower the effectiveness of a heat mirror due to the much higher emissivity of the condensed layer of water. That is, the water will absorb the radiant energy which can then be partly transferred to the cooler outside by conduction and convection.

Double glazing, as shown in Fig. 2(c) effectively avoids all of the potential loss mechanisms or problems mentioned above. The reflecting layer in this case should be on one of the interior glass surfaces facing the dead space. For the metal-dielectric combinations discussed in this report the gap side of the inner glass is the optimum position. During the cooling season, to a first approximation, solar energy absorbed in the outside glass can only reach the interior by radiation, due to the dead air space. The reflectivity of the deposited layer for this reradiated energy, however, is 95%, so that it is essentially all returned to the outside glass with very little absorbed in the inside glass. The effectiveness in cooling seasons is therefore comparable to a reflecting layer on the outside glass surface in terms of preventing undesirable solar radiation from reaching the interior. Overall performance will be superior to single glazing since energy absorbed in the outside glass from the hot air also cannot reach the

interior as it can by conduction in single glaze installations. Nor can it reach the interior by reradiation as it can in conventional double glazing.

During heating seasons, radiant internal energy is absorbed in the glass in a conventional manner. Again since conduction/convection effects are reduced by the dead air space, this absorbed energy (including that due to convection on the inside glass surface) is partially transferred to the outside glass through reradiation at longer wavelengths. The 95% reflecting layer will return essentially all of this energy to the inside glass. Since the inside glass will be warmer than in the non-reflecting case, condensation effects will actually be reduced.

The reflecting layer could be directly applied to the glass or could be applied to a plastic which is then glued to the glass with essentially the same performance. Alternately, superior performance could be achieved by putting the reflecting layer on a plastic and stretching the plastic film at the mid-point (Fig. 2(d)) of the air space with the reflecting layer facing the outside. This provides two separate conduction/convection blocks, and requires two absorptions and reradiations for radiant energy transfer. As before, the reflecting layer will return most of the reradiated energy to the inside glass. A transparent (in long wavelength IR) plastic substrate would be an improvement over conventional absorbing plastics. The additional manufacturing complexity and higher cost required to stretch the plastic film to maintain good optical clarity make it a questionable improvement over the simple one-gap case, particularly if the overall air space dimension is small. If the film suspension problem can be economically solved, this configuration becomes one of the best performers for cold climates.

Various coated plastic retrofit (OWR - Office Window Retrofit) structures (plastic glued on glass) are shown in Figs. 2(e)-2(h). Figs 2(e) and 2(f) show the same simple single glazed cases as 2(a) and 2(b). Performance should be essentially the same as in the original equipment cases. The inside configuration for the plastic substrate might be preferred in some severe climates because of its lower vulnerability to atmospheric attack. For these climates, the inside case is probably preferable in any event due to its heat mirror action during the heating season. Performance during the cooling season will be slightly

inferior to deposition directly on the glass ue to additional absorption in the plastic before reflection.

The general approach pursued by KCI is to protect the reflecting layer with a transparent dielectric overcoat. Additional protection can be provided by applying the retrofit plastic with the reflecting side glued to the glass as shown in Figs. 2(g) and 2(h). For outside configuration (primarily cooling climates) the primary requirements on the plastic substrates are that they be bondable and resistant to UV degradation. Two candidates are the relatively new ICI Melenex OW films (stabilized polyester) and the well documented FEP film. The former is more expensive (approx. $4¢/ft^2$ at .002" than conventional .001" polyester because of its higher manufacturing costs and larger minimum available thickness (.002" vs. .001"). It is, however, much cheaper than the Teflon FEP which is estimated to cost approximately $15¢/ft^2$ (.001") in large volumes (> 1M ft^2).

This stabilized polyester film is essentially untested under real conditions, whereas the FEP film has been demonstrated to withstand more than 15 years of continuous outdoor exposure in Florida without any significant degradation. From a maintenance point-of-view, the FEP is soft but cleans very easily and could be preferred for some applications where the higher costs would be overcome by its long life. Application could be difficult because of its very flexible nature and heavier gauges are not attractive due to the higher cost. Both types of material have been investigated at KCI.

Inside installation is more desirable in climates that have both heating and cooling seasons. For all-season performance it is necessary that the plastic be transparent to long wavelength IR as well as to solar radiation. FEP is much more transparent than polyester but is still not adequate when the absorption losses due to two passes are considered. Some polyethylene and polypropylene materials have the necessary transparancy. Samples of .001" very clear polypropylene have been obtained by KCI and successfully demonstrated for this application. On the basis of accelerated UV weathering tests, the potential negative factor of UV degradation appears to be surmountable for inside applications with the coated side of the film glued to the glass. In

addition, with this configuration it is also possible to add UV absorbing constituents to the glue, if necessary, for longer life.

For residential windows, it is assumed that the primary requirement is the reduction of heat loads during the heating season. In this case, the most efficient design is one which allows the maximum solar energy to reach the inside of the house while effectively retaining all energy radiated by room temperature components. To do this, the window should be as transparent as possible in regions 1 and 2 (Figure 1) and reflect as much radiant energy (region 3) as possible back into the interior. For single glazed applications, the reflecting layer must be on the inside of the glass as shown in the original equipment configuration in Fig. 2(i). Otherwise the internal radiant energy will be absorbed in the glass and partly transferred to the outside by conduction/convection effects.

Various configurations are possible in the retrofit case as shown in Figs. 2(j), 2(k), and 2(l). The simplest, in principle, is to glue the plastic film to the inside of the glass with the reflecting layer facing the interior (Fig. 2(j)). UV absorbers can be used in the glue to extend the plastic lifetime if the amount of UV radiation penetrating the glass is sufficient to cause long term damage to the plastic being used. The cheapest and most convenient substrate is simple .001" polyester (e.g. Melinex 442) with more sophisticated and more expensive variations being stabilized polyester (Melinex OW) or Teflon (FEP). For this configuration, the plastic need only be transparent to solar radiation in order to achieve high optical performance.

Alternately, in order to give the reflecting layer additional protection, the plastic film may be glued with the reflecting layer to the glass if the plastic substrate is sufficiently transparent to long wavelength IR. KCI has achieved the best performance with .001" polypropylene. FEP film has also been used but has significantly poorer performance due to its lower transmission.

Finally, for optimum performance, the plastic films can be inserted in double glazed original equipment either on an interior glass surface (Fig 2(l), or mid-gap as in the OWR case (Fig. 2(d)). Basically, a rule of thumb is that the

addition of a heat mirror is equivalent to adding an additional glazing plus air space. Nominal U-values of approximately .8 BTU/ft^2-hr-°F can be achieved on single glazing with heat mirrors having emissivities of .15 (reflectivity of 85%) at long IR wavelengths. Comparable values for double glazing with air gap and heat mirror are approximately .3 BTU/ft^2-hr-°F for emissivities of .15.

As in the office window case, any potential condensation problems are substantially reduced with the double glazing approach. An interesting additional point results from KCI's ability to continuously vary the characteristics of the coating from those of an optimum office window (cooling predominating) to those of an optimum residential window (heating predominating). For an intermediate climate requiring both substantial cooling and heating, an intermediate characteristic in a residential application could provide the best overall energy saving. This results because raising the visible reflectivity above that of a heat mirror will help in the cooling function (more solar radiation reflected) and also in the heating function (higher long wavelength IR reflectivity). These gains will be partly balanced by some loss in solar transmission and therefore decreased solar heating duringthe heating season, as well as reduced intensity of the outside as viewed from the inside. The question of overall energy balance and optimum window design is therefore strongly dependent on the climate in which the building is situated as well as the building function. KCI's goal has been to develop the capability of easily modifying window characteristics during manufacture (either original equipment or retrofit material) to achieve the optimum performance under any conditions. The results of the program presented here indicate that this flexibility has been achieved.

The basic deposition methods and many of the techniques used in fabricating these films are proprietary to KCI. It was the primary objective of the program to demonstrate the manufacturing capability of the basic process and to continue some material studies. Where desirable for completeness, KCI data have been included in the report.

2. General Program

Various aspects of five basic metal-dielectric material combinations were studied during this program. These combinations included Cu-SiO_2, Bs-SiO_2 (Bs ≡ brass), Bs-Al_2O_3, Ag-SiO_2 and Ag-Al_2O_3. Some Al-Al_2O_3 data was obtained as a check on earlier work on Al performance which was found to be greatly inferior to that of Ag or Cu based materials.

Originally the intent was to chose the optimum combination and then to demonstrate manufacturing on 12" wide glass by running the glass over an aperture defining a uniform beam of depositing material. Investigations were to be made on glass with plastic substrates for retrofit applications being demonstrated as convenient. As the program progressed, however, it became obvious that the quickest and most important contribution to overall energy conservation could be made in the retrofit area. For this reason the program was reoriented to plastic substrates with the manufacturing demonstration to be carried out on roll film. It was clear from program results that anything that could be accomplished on plastic could more easily be done on glass. Two plastic substrates, polyester and Teflon FEP, were included in the program. Subsequent to the program KCI extended the results to polypropylene (see discussion - Section 1) and some in-house results are included here for reference.

All of the materials investigations were conducted in a small experimental ion beam sputtering system (IBSS) including those for samples for weathering tests etc. Targets for larger systems are expensive so the concept was to choose the optimum materials combination or combinations and then modify a larger IBS system for roll coating demonstration. Changes could be rapidly effected in the small system so that more variables could be investigated.

At the beginning of the program some of these material variations were concerned with continuing the demonstration of proprietary KCI coloring techniques initiated under the previous program. After initial demonstrations on glass and plastic these studies were discontinued, per se, since the technology was well advanced and capable of implementation at any time. More importantly, the program was becoming too complex to demonstrate all coloring variations as well as the multiplicity of material combinations. Emphasis was

placed on optical performance, weathering characteristics and manufacturing demonstration.

Even with this restriction, in the second half of the program the materials studies continued to be extremenly complex as the result of weathering results which dictated changes. This report attempts to cover the critical aspects of all systems studied and to summarize the most important results. Sufficient data are presented in all cases to allow the reader to evaluate the relative characteristics of the various metal-dielectric systems for either glass or plastic substrates. The results are intended to be a general summation of what is possible with KCI's proprietary IBSS methods. Relative performance for other deposition methods in attempting to duplicate these results will depend on the methods and techniques used.

Money was not available in this program to build special vacuum chambers or deposition equipment. However KCI had a medium sized IBSS in which a small roller system could be inserted for demonstration of manufacturing capability. This system was modified to include the metal and dielectric elements and the roller system. Space was very tight as the result of the total number of elements that ended up inside the chamber. This forced some difficult compromises on overall performance (e. g. slightly lower transmission due to cross-contamination of sputtering targets) and uniformity of demonstration samples. Their performance, however, was only slightly inferior to that achieved in the smaller system and more than exceeded requirements in all cases. In a full scale production system none of these compromises would be necessary and performance would equal the best achieved.

Weathering studies initiated under the previous contract were continued throughout this program. These investigations basically involved the use of a 2. 5 sun level weatherometer with rain cycle for accelerated life testing. Additional factors introduced under the present contract included testing for resistance to solvents and cleaning agents as well as accelerated UV testing in selected cases (glued plastic on glass samples).

Material studies are presented in Section 3, weathering results in Section 4, and demonstration results in Section 5. A preliminary cost analysis is also presented in Section 6 as an aid in evaluating the economic factors

associated with the energy savings achievable with these windows.

3 Material Studies

3.1 General

As discussed previously, material studies were carried out to demonstrate the capability of optimizing any of the window forms shown in Fig. 2 and to compare weathering factors. Five metal-dielectric combinations (Cu-SiO_2, Bs-SiO_2, Bs-Al_2O_3, Ag-SiO_2 and Ag-Al_2O_3) were investigated on glass and plastic (polyester, teflon FEP and polypropylene) substrates.

For office windows the basic objectives were:

1. 40-50% transmission in visible
2. Reflectivity of .75-.85 at 1 μ, > .9 at 2.5 μ and >.95 at 10 μ and throughout most of long wavelength IR range (4-50 μ).
3. Color variability if desired
4. Use of glass or retrofit plastic substrates
5. Long term weatherability under conditions consistent with window form and use (see Fig. 2)
6. Operational cost savings over depreciation period equal to or greater than incremental cost of reflecting layer (including plastic substrate and installation for retrofit) added to basic glass; i.e. minimum cost.

In residential windows the basic objectives were:

1. 70-80% transmission in visible
2. Reflectivity of >.35 at 1 μ, > .75 at 2.5 μ and > .85 (i.e., emissivity <.15) at 10 μ and throughout most of long wavelength IR range (4-25 μ).
3. Minimum neutral coloring
4. Use of glass or retrofit plastic substrates
5. Long term weatherability consistent with use
6. Reasonable pay-back period

The choices on reflectivity (R) and transmission (T) above are not

hard numbers, but approximations, since real values are dependent on the window configuration used. It should be noted that the values in the transition or threshold region (1-2.5 μ) are based on practical considerations combining reflectivity characteristics achievable with the present techniques with those of the solar spectrum (Fig. 1).

In the case of residential windows, much higher transmission can be achieved in the visible and near IR by lowering R in the 1-2.5 μ region. Substantial T gains can be made in this region while only decreasing R at longer wavelengths from .85 to .80 and might be desirable for certain configurations and climates.

Optimum values are, in fact, difficult to predict without a more exact definition of the end use. KCI's intent in the present program was to demonstrate that almost any reasonable practical characteristic could be achieved and this has clearly been accomplished.

All thin film deposition for these investigations were made with proprietary KCI sputtering techniques. Actual values of film thicknesses were not monitored but were based on proprietary theoretical considerations combined with detailed knowledge of the IBSS deposition parameters. Thicknesses are known from previous measurements (see LBL-7825) to run approximately 30-120 Å for the metals used and from less than .05 μ to more than .5 μ for the dielectrics. Characteristics were simply controlled through precise variations in beam current and deposition time, based on historical data. For any other deposition method having the capability of depositing the films with the required characteristics, the same simple empirical method should yield equivalent results. Optical data on the window was obtained in three primary spectral regions; .35-.8 μ, .5-2.5 μ, and 2.5-50 μ. Some UV data was also generated relative to weathering considerations.

In general, reflectivity (R) and transmissivity (T) data were obtained for most samples in the .35-2.5 μ range using a Beckman DK-2A spectroreflectometer. This instrument, which was also used for UV measurements, was ideally suited for this project. The particular instrument used measures total reflectance using an integrating sphere to simultaneously collect both the

specular and diffuse reflected components. For total reflectance measurements the angle of incidence is 5°. The diffuse component alone can be obtained by changing the angle of incidence to 0° whereby the specular component is reflected back out of the sphere leaving only the diffuse component to be collected. R and T data at longer wavelengths were obtained primarily on a Perkin Elmer 337 spectrometer.

During early phases of the program, MgO reference standards were used for almost all measurements on the DK-2A. These standards have high absolute reflectance values in the visible and up to .9 μ. Above this they fall off compared, for example, to a fresh Ag standard. KCI developed some protected Cu standards which had >99% reflectivity compared to fresh Ag above 2.5 μ and these have continuously been used at these wavelengths. In the region from 1-2.5 μ, MgO was used for convenience, with conversion to real numbers, based on calculations, being made as required.

In the middle of the program, a switch was made to Eastman Kodak "White Reflectance Coating" (No. 6080) as the standard in the visible and up to 2.5 μ. This material is specified for the .2-2.5 μ region over which it has essentially 100% reflectance. Since it can be sprayed on it is much more easily applied and reproducible than the MgO. Four standard plates were made up at the same time, one of which (No. 1) was then semi-permanently attached to the integrating sphere of the Beckman DK-2A. The other three were then run against it, after 100% was set at 1.5 μ (.5-2.5 scale) or .55 μ (.35-.8 μ scale) using standard No. 2. One of the old MgO standards and a KCI Cu standard were then run on the same curve to evaluate the accuracy of the older results.

Figures 3 and 4 give the results (note double scale) for the .5-2.5 μ and .35-.8 μ ranges. Standards 2, 3, and 4 are essentially identical throughout the range and are completly interchangeable. As a secondary check, samples 1 (reference channel) and 2 were run against each other using 100% as full scale on the .5-2.5 μ range and using each one in the reference channel. As shown by Fig. 3, the results are essentially identical. This was not the case using MgO standards where the difference in characteristics between standards altered the curve shapes depending on which standard was in which channel.

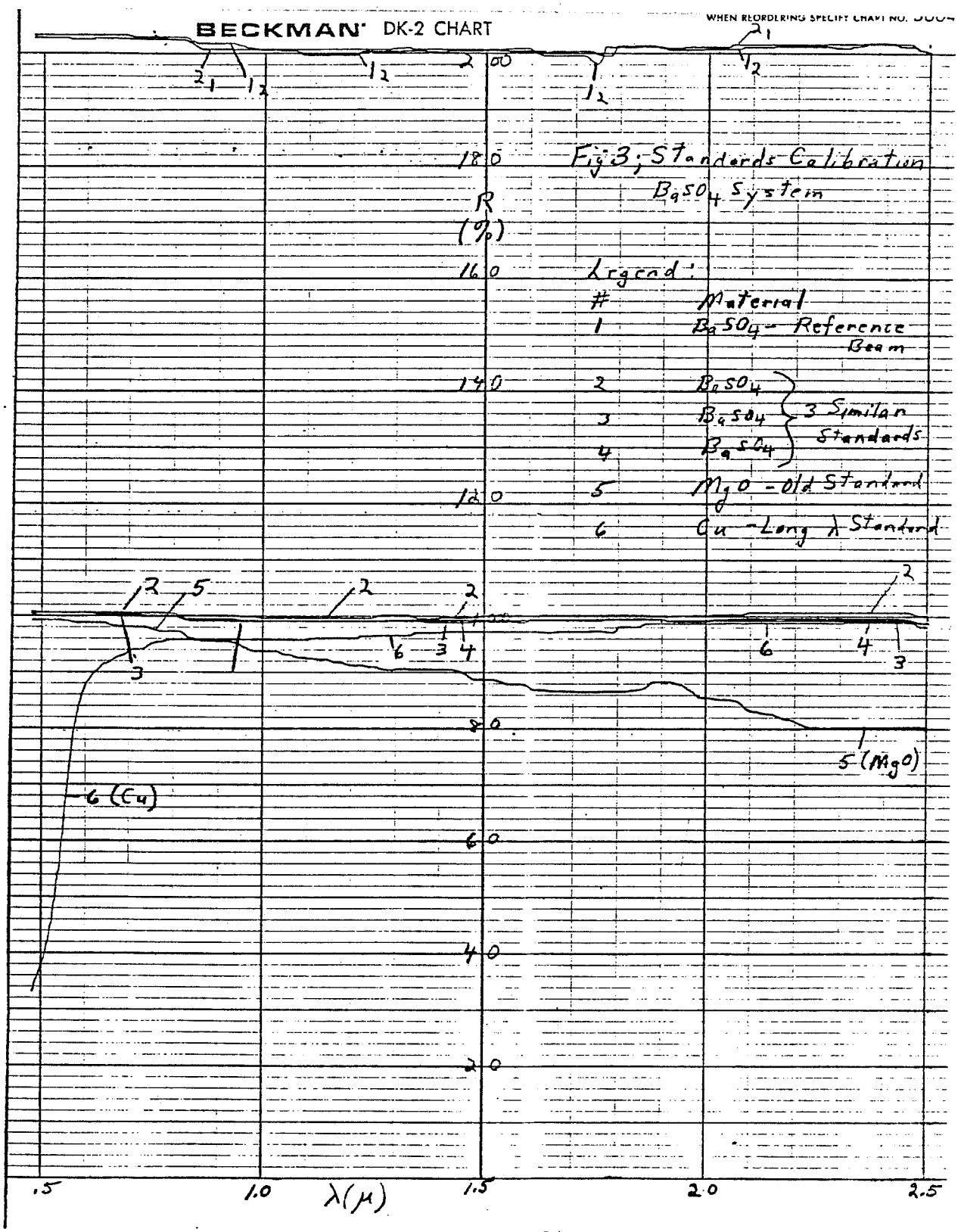
BECKMAN DK-2 CHART
WHEN REORDERING SPECIFY CHART NO.
Fig 3; Standards Calibration
$BaSO_4$ System
R (%)
Legend:
Material
1 $BaSO_4$ - Reference Beam
2 $BaSO_4$
3 $BaSO_4$
4 $BaSO_4$
3 Similar Standards
5 MgO - Old Standard
6 Cu - Long λ Standard
100
80
60
40
20
5 (MgO)
6 (Cu)
.5
1.0
λ(μ)
1.5
2.0
2.5

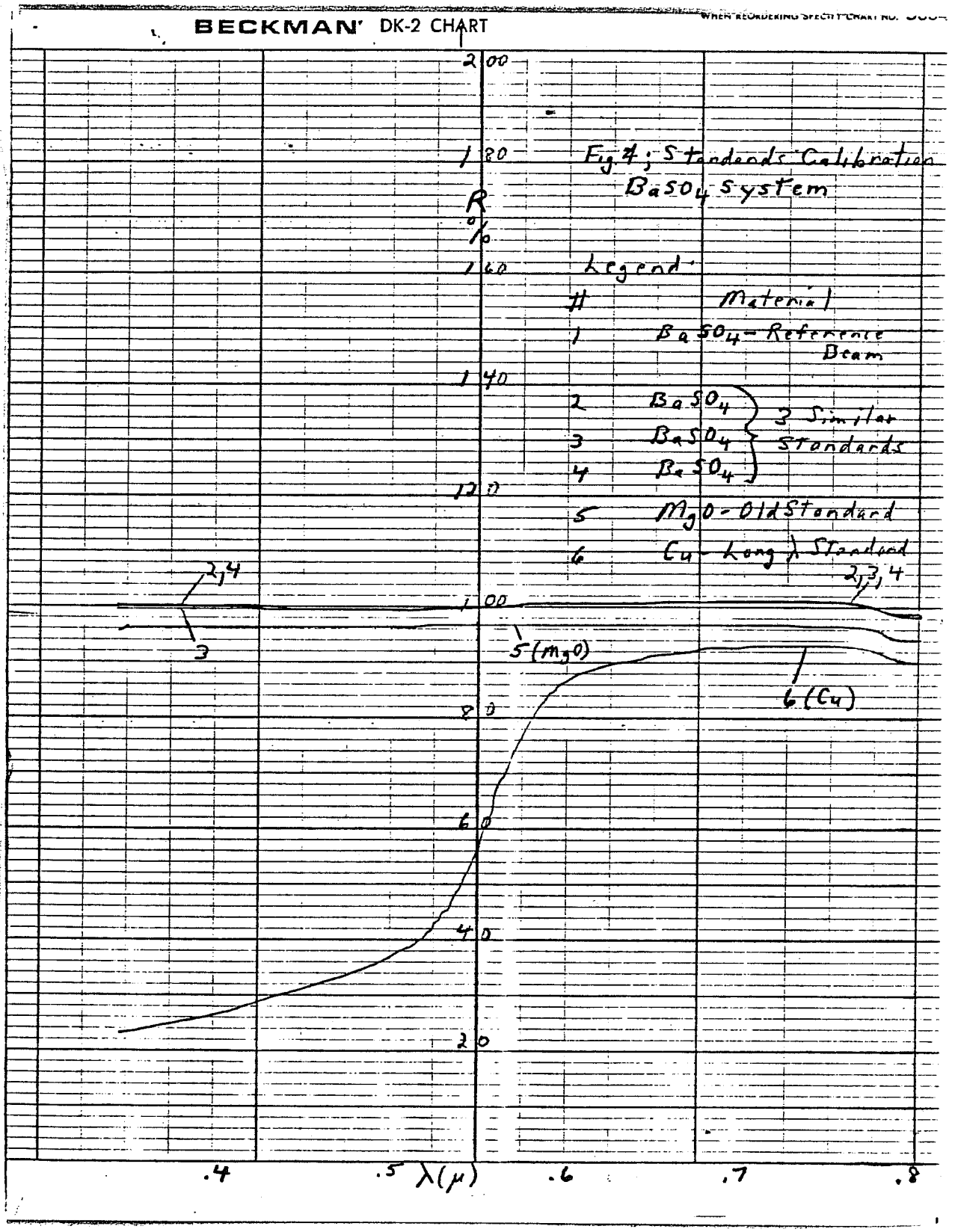
BECKMAN DK-2 CHART
Fig 4; Standards Calibration
BaSO4 System
R
%
Legend:
Material
1 BaSO4 - Reference Beam
2 BaSO4
3 BaSO4
4 BaSO4
3 Similar Standards
5 MgO - Old Standard
6 Cu - Long λ Standard
200
180
160
140
120
100
80
60
40
20
2,4
3
5 (MgO)
6 (Cu)
2,3,4
.4
.5
λ(μ)
.6
.7
.8

This point was not fully appreciated in earlier work and was responsible for some "small" (1-3%) variations observed for measurements made at different times. These variations had been attributed to spectrometer changes but the exact explanation was unknown since the MgO standards were considered interchangeable

As expected, the Cu standard gives almost 100% of the $BaSO_4$ value at the 2.5 μ point and falls off at shorter wave lengths. Surprisingly, the reflectance was actually slightly less at 2.5 μ showing the high performance of the $BaSO_4$ at the longer wavelengths. In contrast, the MgO is seen to be almost 20% deficient, relatively, at 2.5 μ, and although considerably better at shorter wavelengths, is at least 3-4% deficient over the entire range. The $BaSO_4$ is clearly a very superior reflecting material over the .2-2.5 μ range and, for practical purposes, may be considered as a 100% reflector over this region. Combined with the Cu standards, this allowed direct absolute measurements of R over the entire spectral region of interest. T measurements were essentially unaffected by these standards changes.

Although this standards switch made measurements and calculations much easier and more accurate, coming in the middle of the program it created a significant problem. Since the earlier data was based on MgO, comparison with later results required data conversion which was tedious in view of the enormous quantities of data being generated. In addition, performance criteria changed somewhat during the program so that actual design goals changed with time. For example, the reflectivity goal for retrofit windows was increased from .8 (at 10 μ) at the beginning of the program to .85 (emissivity .15) later.

The use of MgO also caused some confusion since it was believed to overstate R at 2.5 μ by 10% rather than 20% (see Figure 3). All samples were not measured at long IR wavelengths due to limited spectrometer availability. However, there was a reliable direct correlation for good IR reflecting materials between the 10 μ reflectivity and the 2.5 μ reflectivity. The data for most samples therefore only had to be taken up to 2.5 μ as long as the values there were essentially absolute based on good standards. This technique was well established by the end of the program and was verified by extensive

cross-checking.

Curves based on both MgO and $BaSO_4$ appear in this report and where necessary the differences are discussed. These differences are particularly evident where the samples were followed over long periods of time. Results in this section are organized into six categories including Office Windows (OW), Office Window Retrofits (OWR), Residential Windows (RW), Residential Window Retrofits (RWR), Long Wavelength Infrared, and Glued Samples (plastic glued to glass). Although Section 4 specifically covers weathering results, many of the samples presented in this section were followed with time for various reasons.

The following symbolism has been used throughout this report:

Cal.	≡	calibration curve (usually set for nominal 100% at 0.55 μ for .35-.8 μ range, 1.5 μ for 0.5-2.5 μ range, and 10 μ for long wavelength IR ranges.
Cal.'	≡	calibration curve for .35-.8 μ range when it is plotted on same graph as 0.5-2.5 μ range.
S	≡	standard or uncoated substrate curve
R	≡	reflectivity measured from deposited film side
r	≡	reflectivity measured from substrate side.
T	≡	transmission measured from deposited film side.
t	≡	transmission measured from substrate side.
Curve #	≡	either sample # or legend # corresponding to sample # (e.g. 124 or 4 ≡ 124, S ≡ standard); if both reflectivity and transmission are on one set of curves, the curve number is suffixed accordingly (e.g. 124R or SR, 124T or ST); no designation is used if sample is obvious (e.g. R curve for sample 124 only).

'	≡	.35-.8 μ (lower scale on abscissa) range when both spectral ranges are on one set of curves.
Bs	≡	brass
P	≡	polyester (thickness in brackets, e.g. .001", Type 442 unless otherwise specified)
F	≡	teflon FEP
PR	≡	polypropylene
G	≡	glass
Al	≡	commercial Al solar control film - older type

As a rough rule of thumb, for the metals used, an R value of .75 at 2.5 μ translates to greater than .85 at 10 μ, and an R value of .9 at 2.5 μ translates to greater than .95 at 2.5 μ. These are for absolute values at all wavelengths. For the older curves based on MgO standards, the 2.5 μ values must be decreased by 20% before this comparison can be made. This is difficult for the OW and OWR cases where the 2.5 μ values were relatively (to MgO) greater than 100%. In these cases the original design was based on general curve shapes and known relationships to the 10 μ values. However, for the more important final designs, the curves are all in absolute values based on $BaSO_4$ and Cu standards and no conversions are necessary.

Interestingly, particularly for RW and RWR designs, 10 μ R values of .65-.70 can be achieved with 2.5 μ values in the .4 range which gives almost no solar absorption (because of curve shape vs. solar spectrum curve shape) "in the deposited layer". A medium efficiency heat mirror design having maximum solar transmission is therefore a possible alternative design to higher efficiency-lower transmission designs. Such medium efficiency designs are essentially colorless for practical purposes.

3.2 Office Windows (OW)

At the end of the previous program a sample set of office windows was made on PPG solarbronze (3/16" thick) substrates using the Cu-SiO_2 system. The PPG glass used is strongly absorbing and was used to provide a direct comparison in terms of energy conservation with the standard PPG solarcool glass. It was recognized that the use of such absorbing glass would result in insufficient light transmission for normal working conditions without internal lighting but this glass was representative of that being produced by industry. Much improved overall glass performance (with outside reflecting layer) could be achieved with a less absorbing substrate glass while still retaining its advantages (primarily less reflection inside).

The results of this sample set were duplicated at the beginning of the present program and extended to the Ag-SiO_2 and Bs-SiO_2 systems using the same SiO_2 thicknesses. Basic performance results for these combinations were similar to the Cu-SiO_2 results with some variation in color characteristics.

Figs. 5-8 show the R & T curves for the Ag-SiO_2 system using MgO standards. The threshold for transition to higher reflectivities is approximately .7 μ (Fig. 5) with R tapering off to 15-40% at lower wavelengths (Fig. 7). Overall transmissions (Fig. 6) are quite low with the visible transmissions (Fig. 8) being below that desired for reasonable intensity levels without internal lighting. Transmission is higher than the Cu-SiO_2 system at the blue end because of the lower blue absorption. Coloring for this set was considerably different, and in general less intense, than for the Cu-SiO_2 sample sets. This is due to the neutral characteristic of the Ag reflecting layer vs. the relatively intense red of the Cu. The colors for the different samples are:

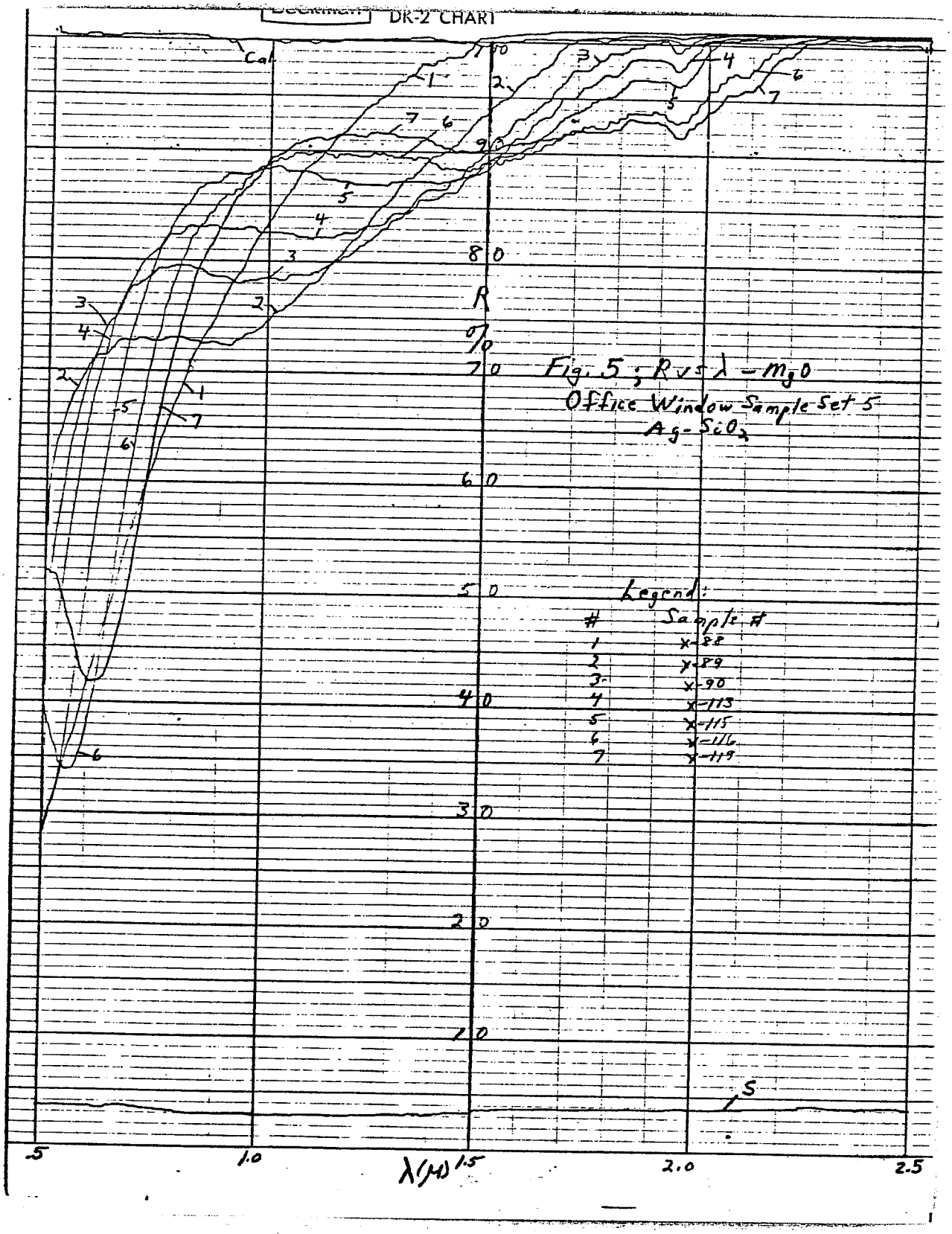

Fig. 5; R vs λ – m_gO
Office Window Sample Set 5
Ag-SiO_2

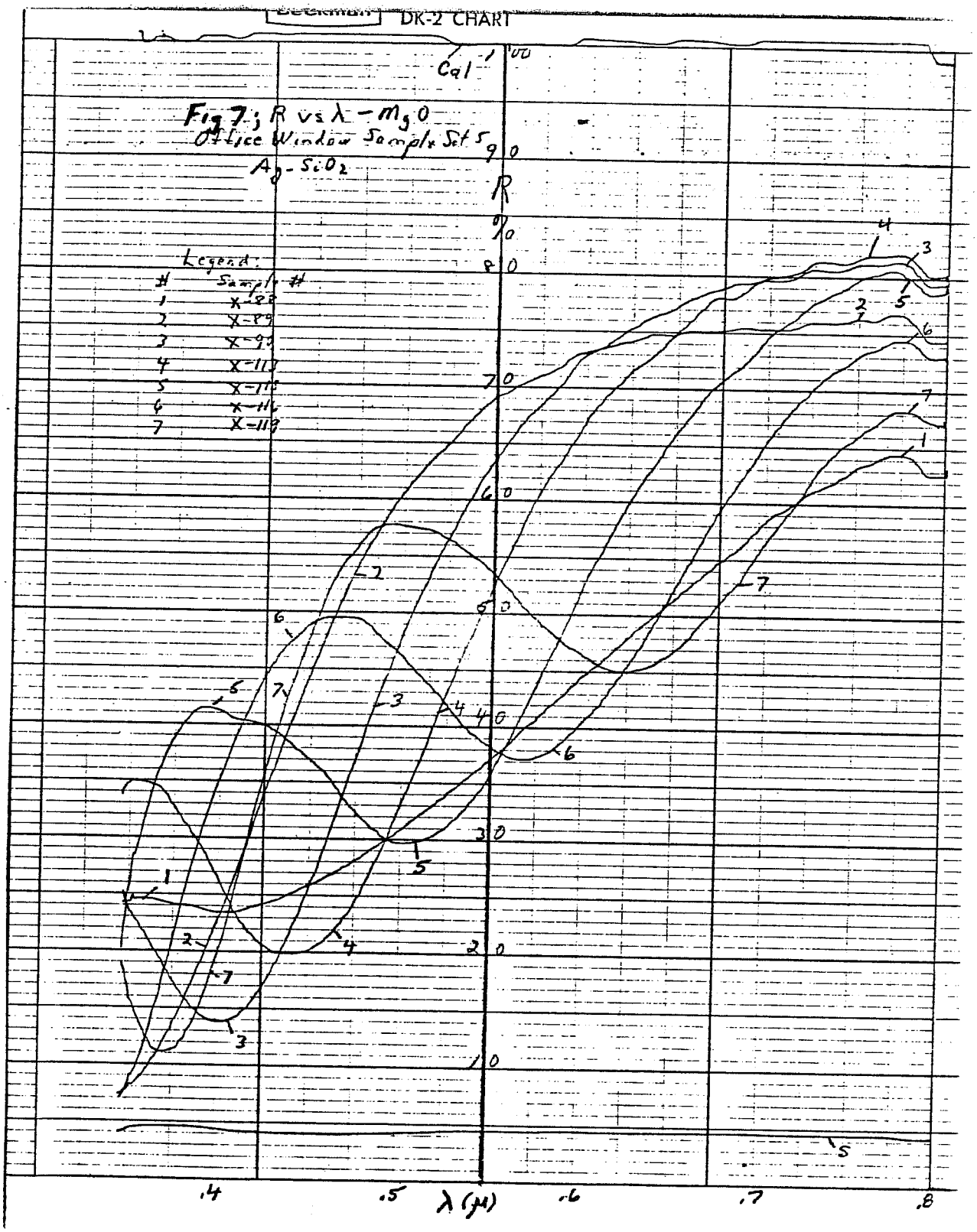
DK-2 CHART
Cal
Fig 7; R vs λ – mg 0
Office Window Samples Set 5
Ag - SiO2
R
%
Legend:
Sample
1 X-
2 X-
3 X-
4 X-
5 X-
6 X-
7 X-
100
90
80
70
60
50
40
30
20
10
.4
.5
.6
.7
.8
λ (μ)

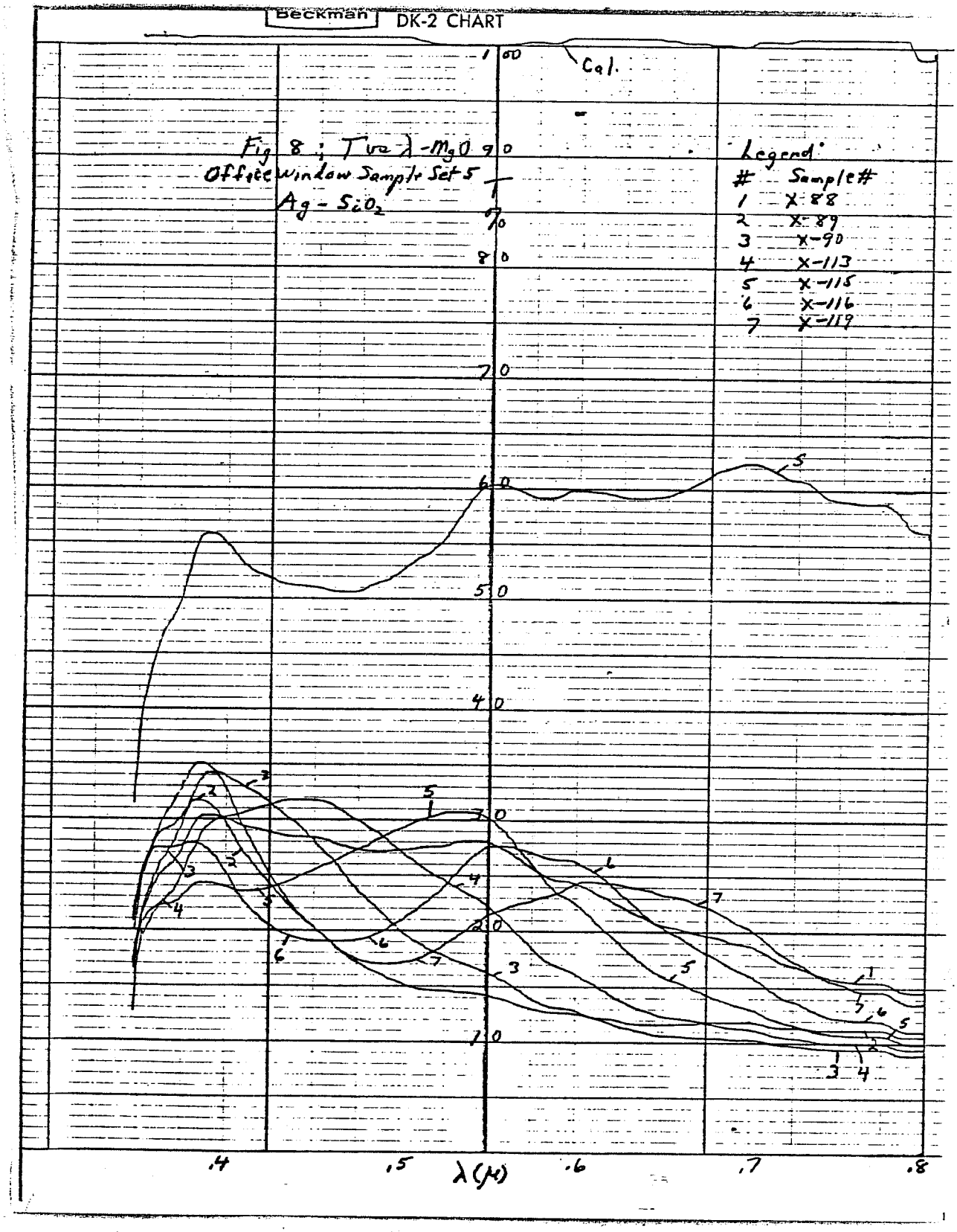
Beckman DK-2 CHART
Cal.
Fig 8 ; T vs λ - MgO
Office window Sample Set 5
Ag - SiO2
Legend
Sample#
1 X-88
2 X-89
3 X-90
4 X-113
5 X-115
6 X-116
7 X-119
100
90
80
70
60
50
40
30
20
10
%
.4
.5
.6
.7
.8
λ (μ)

Sample #	Curve #	External Color	Transmitted Color
X-88	1	Light tan neutral	Med. tan gray
X-89	2	Light tan gold	Med. purple gray
X-90	3	Greenish yellow gold	Med. purple gray
X-113	4	Tan gold	Med blue gray
X-115	5	Light copper tan	Med. green brown
X-116	6	Very light yellowish neutral	Med. brown
X-119	7	Yellowish neutral	Med. reddish tan

Characteristics for a similar sample set using the Bs-SiO_2 system are shown in Figs. 9-11. In general, these curves are similar to those of the other sample sets. Coloring for this set was slightly different than for the Cu-SiO_2 system, being somewhat less red and slightly less intense. For comparison to the above Ag-SiO_2 results, the colors at the same SiO_2 thicknesses are:

Sample #	Curve #	External Color	Transmitted Color
X-137	7	Tan melon	Med. yellow brown
X-146	6	Tan neutral	Med. gray brown
X-149	9	Yellow gold	Med. gray
X-150	0	Tan gold	Med. yellowish gray
X-151	1	Tan copper	Med. yellowish gray
X-152	2	Light violet	Med. Yellowish brown
X-153	3	Yellowish neutral	Med. brown

Another set was made with Cu-SiO_2 on PPG solargray (1/4" thick) substrates with similar although slightly different (color) results. Other possibilities, such as gold for the metal layer, in general will give colors which are basically the same as one of the above systems (e.g. gold-same as brass) although the reflectivity performance might be different.

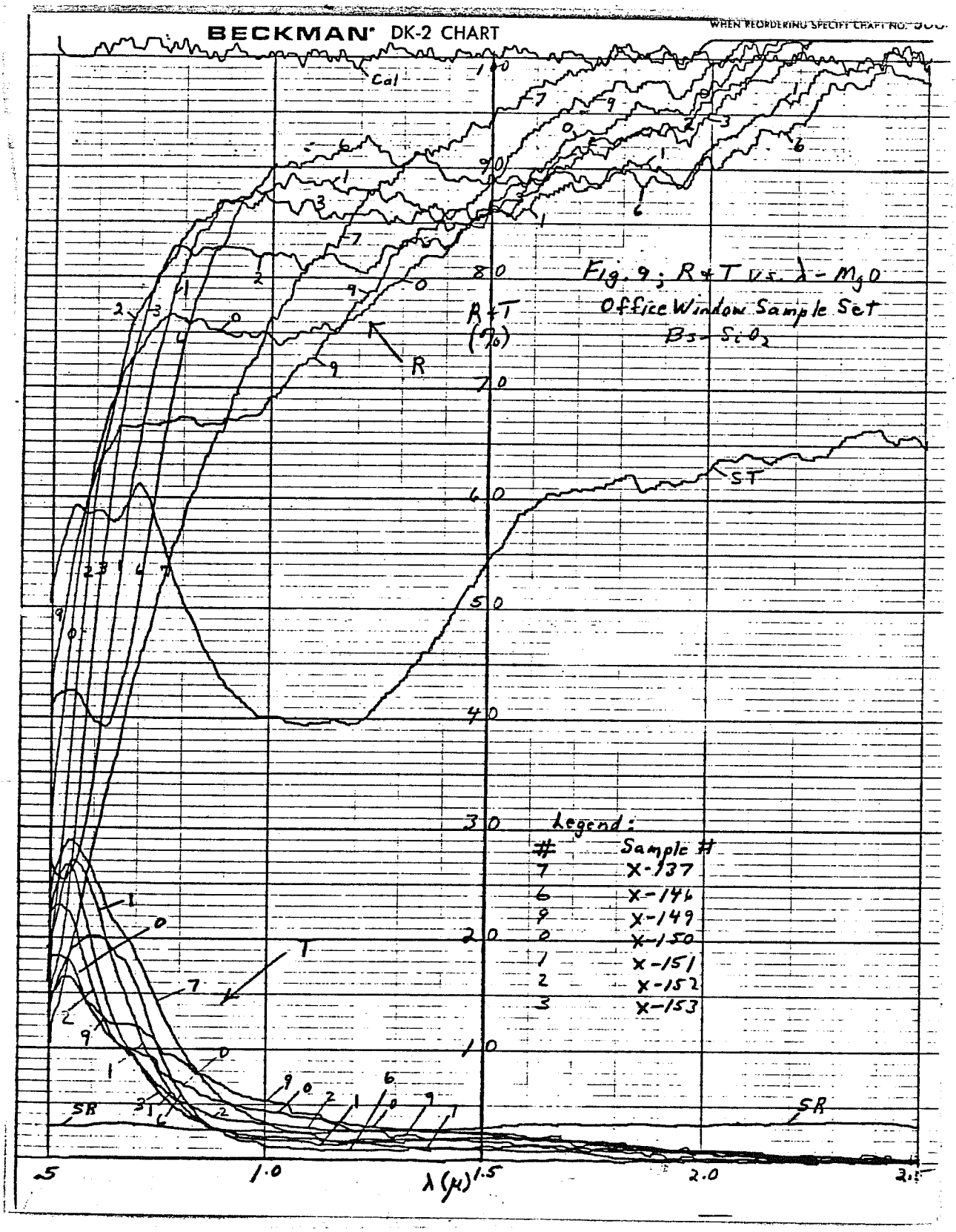
BECKMAN DK-2 CHART
Cal
R
ST
SR
SR
R+T (%)
λ (μ)
.5
1.0
1.5
2.0
Fig. 9; R+T vs. λ - MgO
Office Window Sample Set
Bs - Sc θ2
Legend:
Sample
7 X-137
6 X-146
9 X-149
0 X-150
1 X-151
2 X-152
3 X-153

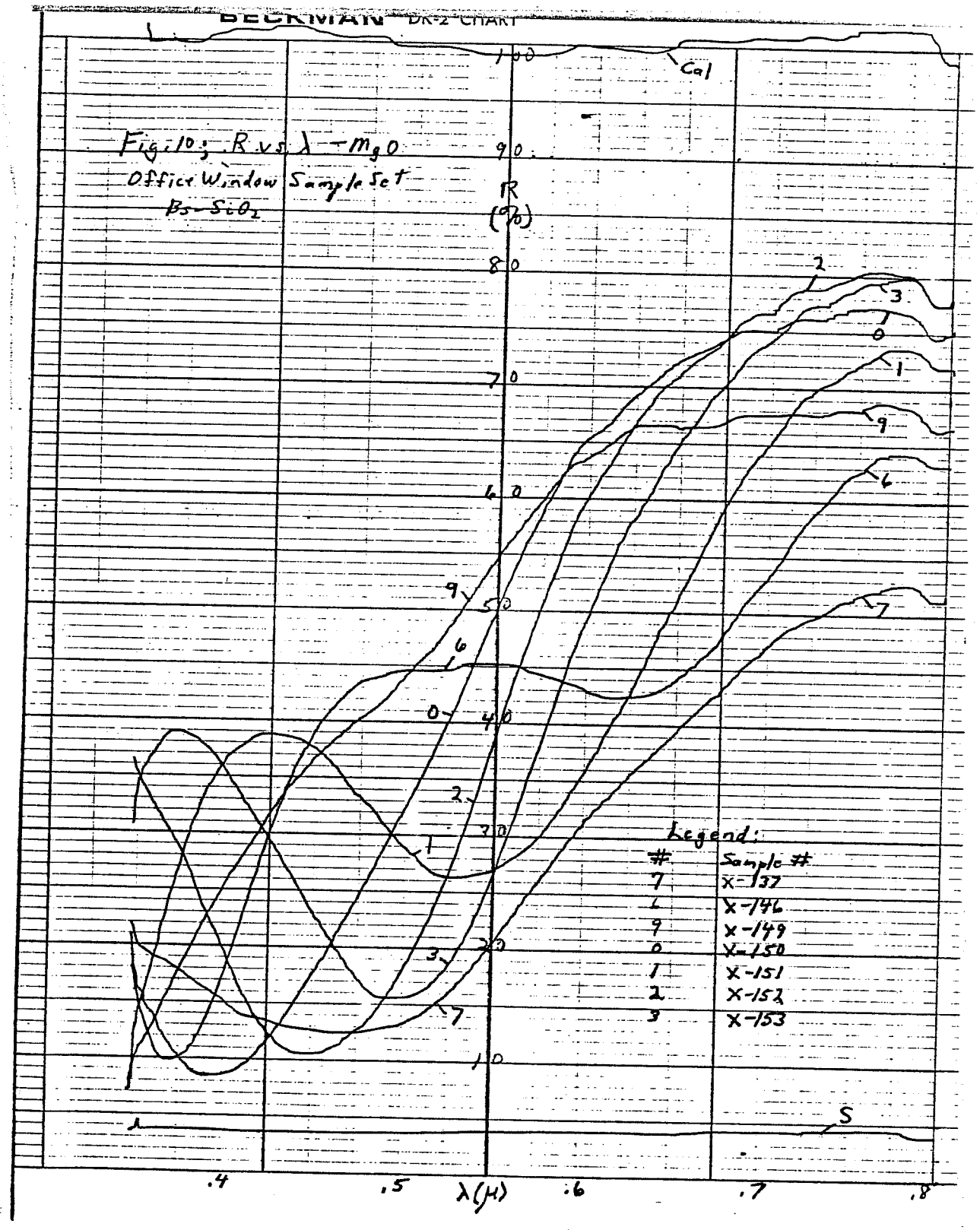
BECKMAN DK-2 CHART
Cal
Fig. 10: R vs λ - MgO
Office Window Sample Set
P_2-SiO_2
R (%)
100
90
80
70
60
50
40
30
20
10
λ
S
.4
.5
λ(μ)
.6
.7
.8
Legend:
Sample
7 X-137
6 X-146
9 X-149
0 X-150
1 X-151
2 X-152
3 X-153

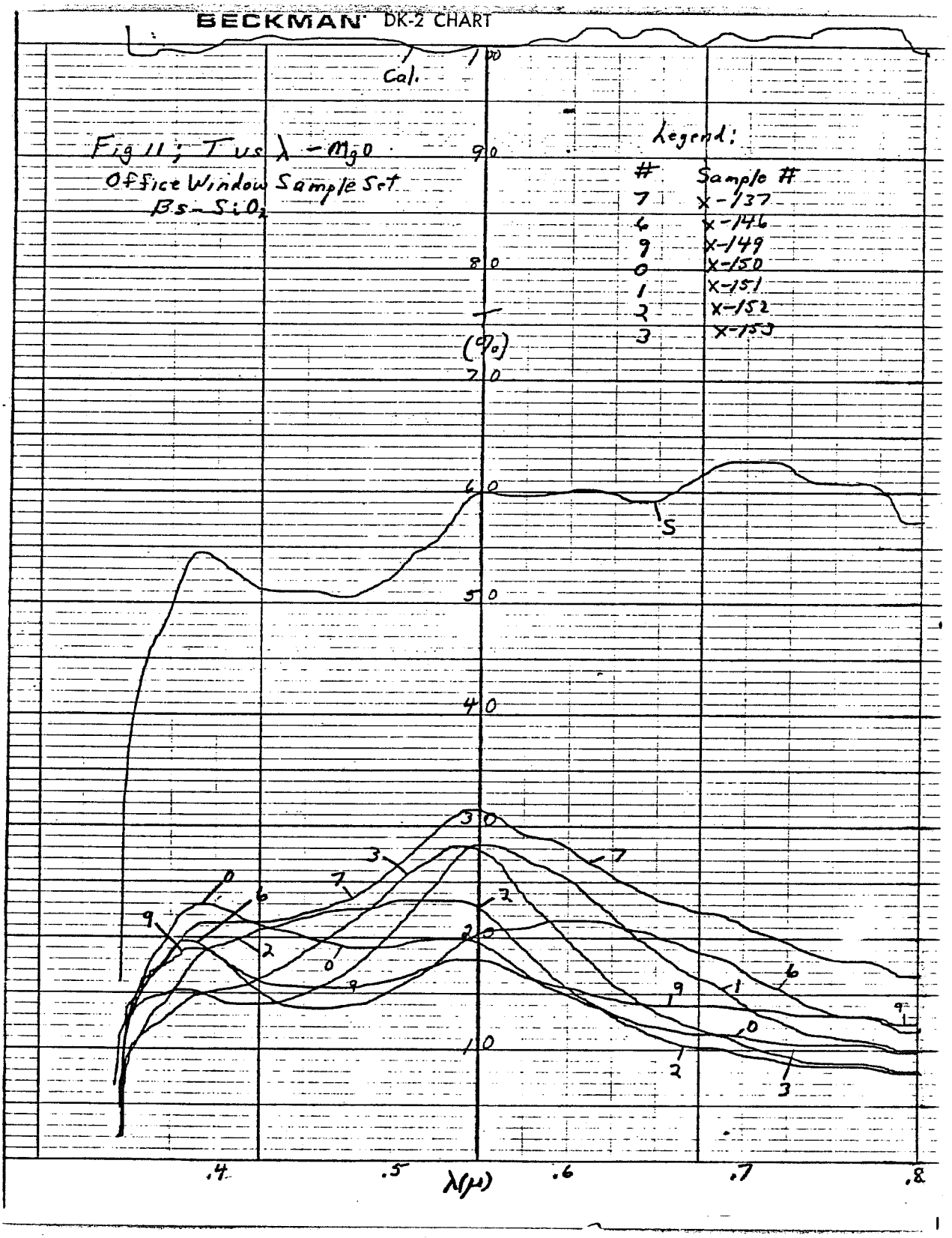
BECKMAN DK-2 CHART
Cal.
Fig 11; T vs λ - MgO
Office Window Sample Set
Bs - SiO2
Legend:
Sample
7 X-137
6 X-146
9 X-149
0 X-150
1 X-151
2 X-152
3 X-153
(%)
100
90
80
70
60
50
40
30
20
10
S
.4
.5
λ(μ)
.6
.7
.8

Certain potential problems became apparent, especially on Cu based samples, when these sample sets were allowed to sit around the laboratory for 1 1/2 - 2 years. Some small (1/64 - 1/8" diameter) clear spots became apparent on some of the samples which at first glance were attributed to corrosion through pinholes. However, the spots seemed to be self-limiting in size and occurred on thick as well as thin oxide samples. In addition, it was known from long-term harsh weatherometer studies (Section 5) that corrosion does not proceed from full penetration scratches deliberately introduced in the deposited layer. Finally similar samples made on PPG solarbronze substrates 4 years earlier using the exact same deposition conditions did not show this effect in any of thirty different samples. The latter, however, were cleaned with ultrasonic solvent techniques followed by plasma etching while the program samples, which were primarily for color demonstration, were only solvent cleaned. It was apparent from this and other related evidence that these spots were almost certainly due to chemical reaction of the deposited metal layer with foreign material left on the glass substrate after cleaning. Presumably application of the reflecting layers to fresh glass during production would not show this effect. Samples in other program areas, particularly on plastics, usually did not show this effect.

Subsequent activity on office windows was primarily restricted to retrofit configurations, with occasional use of glass substrates for comparison. Figs. 12 and 13 give R & T curves for one of the latter made using the Ag-Al_2O_3 combination on clear window glass. This sample has excellent near IR reflectivity with a value of .87 (MgO standard -.82 vs. $BaSO_4$) at 1 μ and approximately .95 ($BaSO_4$ -known from curve shape) at 2.5 μ. The visible transmission is quite good and the color as viewed from the inside is a medium light neutral blue-gray. This type of sample has not shown any evidence to date of the spotting phenomenon noted above.

Characteristics for other deposited material combinations may be inferred from those obtained for office window retrofits (Section 3.3). Any characteristic that can be achieved on plastic can be achieved on glass with the only difference being that due to the difference in substrate absorption.

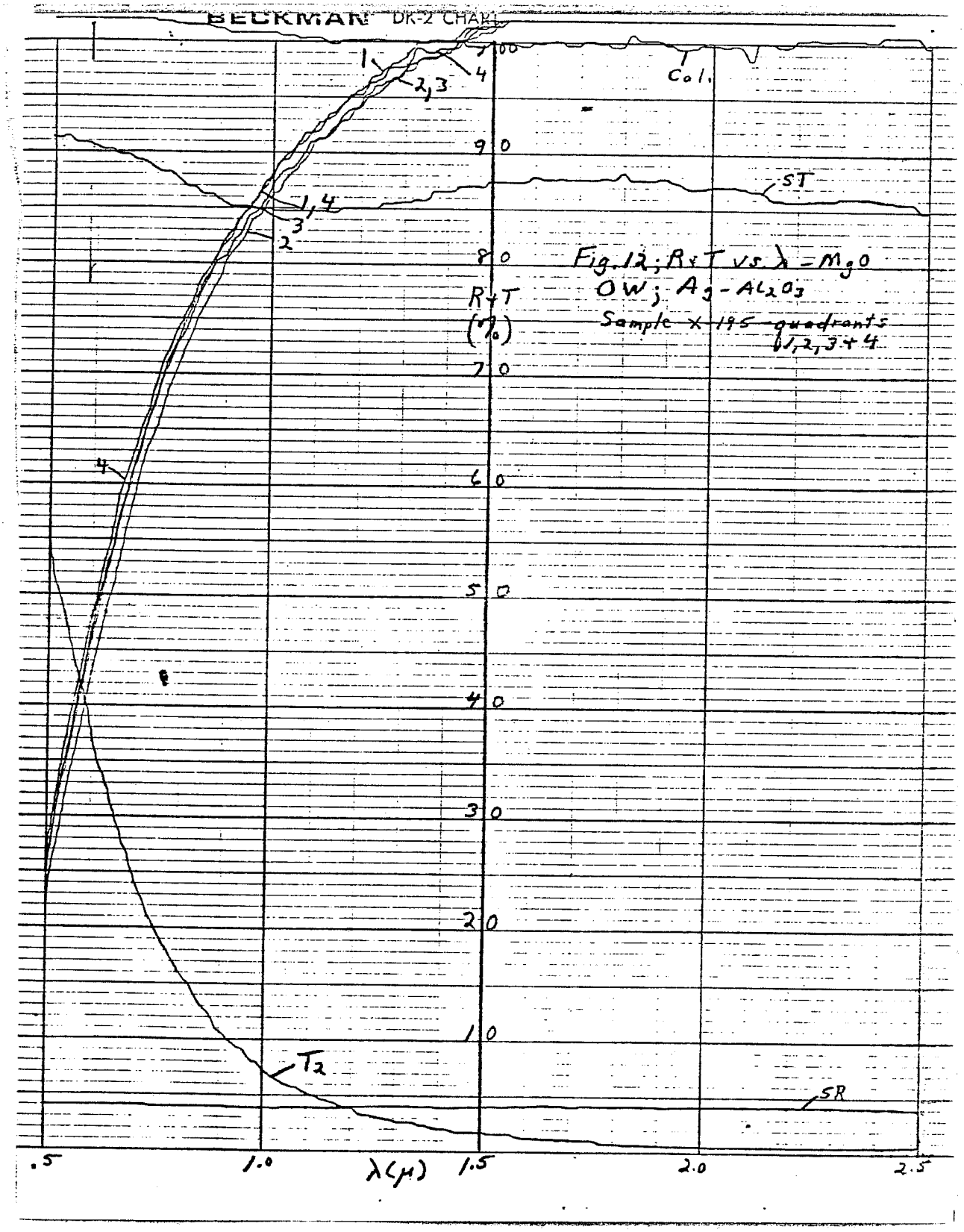

Fig. 12; R+T vs λ = MgO OW; Ag - Al2O3 Sample ~~x 195 quadrants~~ 1,2,3+4

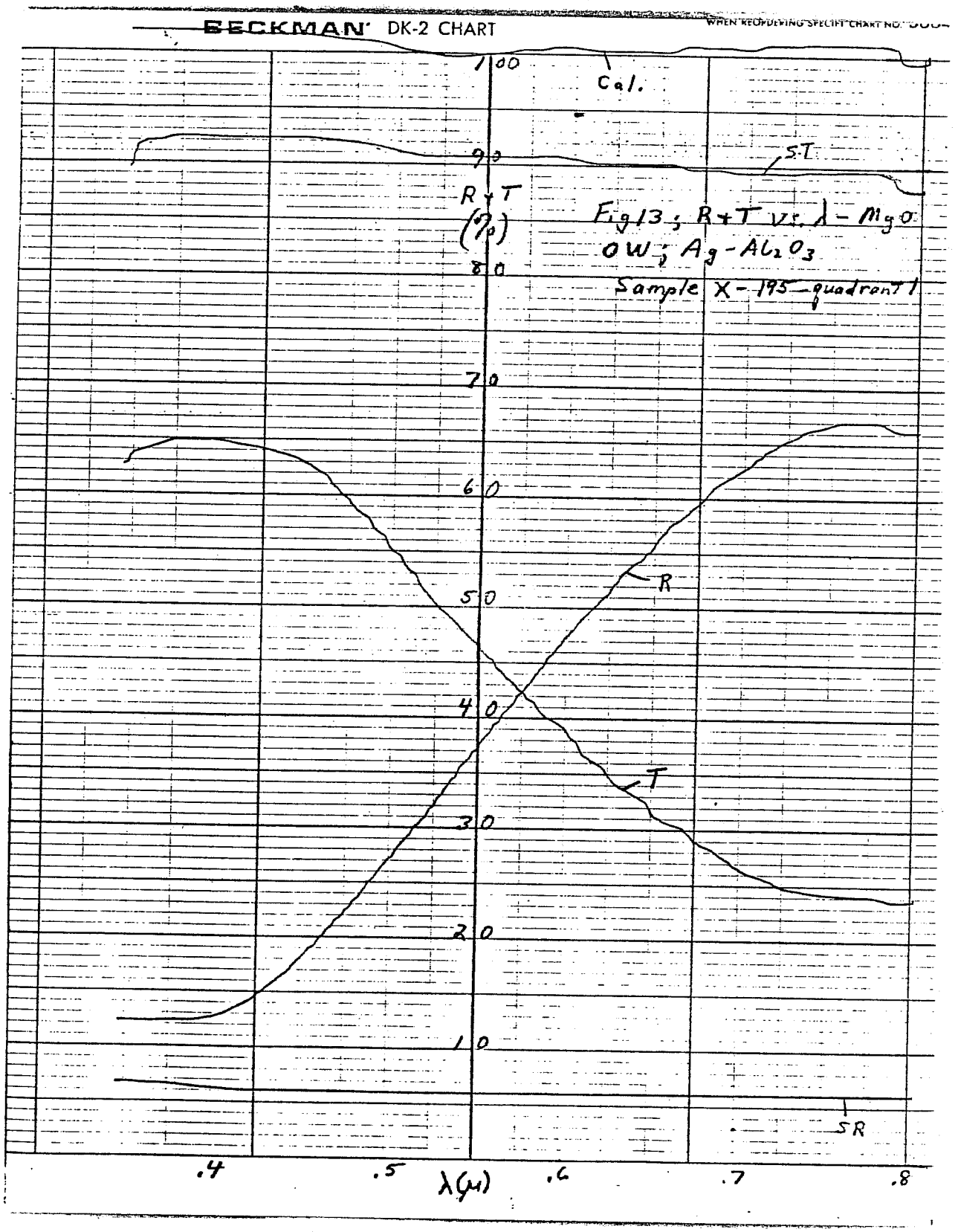
BECKMAN DK-2 CHART
Cal.
S.T
R + T
(%)
Fig 13; R+T vs. λ - MgO
OW; Ag - Al2O3
Sample X-195 quadrant 1
100
90
80
70
60
50
40
30
20
10
R
T
SR
.4
.5
λ(μ)
.6
.7
.8

3.3 Office Window Retrofits (OWR)

It was decided part way through the program that pure Cu as a reflecting layer displayed severe interaction effects with potential substrate impurities or residual foreign material. There was also some evidence that it might be chemically interacting with the oxide overcoats over long periods of time. Except as a convenient (from target viewpoint) test material it was therefore rejected from further consideration leaving brass and silver as the only two alternatives being actively investigated. The OWR results presented in this section involve Bs-SiO_2, Ag-SiO_2, Bs-Al_2O_3 and Ag-Al_2O_3 on polyester and teflon FEP substrates.

Although proprietary KCI methods of changing material compositions were known to prevent long term degradation of retrofit structures, and were being used on RWRs (Section 3.5), they were considered unneccessary for OWRs early in the program. Long term observation showed a gradual decrease in R performance (overall, not localized, no degradation observable by eye) to a lower but acceptable and apparently stable level. Compensation for this partial performance drop could be made by increasing the initial R values by about 10% with a corresponding decrease in T. Alternately, the OWR materials could be modified to those used for RWRs and this was done at the end of the program. The following data shows this progression in method.

Figures 14-30 present some of the more important results including some time related data. Initial studies of Bs-SiO_2 on P (.004"-Figs. 14-15) show a steady decrease in R from 0 time to 385 days. Curve 5 was taken with $BaSO_4$ standards, while the others were taken with MgO. The expected difference between the values using these different standards is 11% at 1.5 μ so that a value of .87 would be expected for R with no degradation. The actual value was .77. Although some changes occur due to spectrometer modification, overhaul etc., this difference of 10% absolute is well outside of spectrometer variations which usually run 1-3%.

Performance for the older type commercial Al solar control film vs MgO is also shown in Figs. 14 and 15. Performance vs. $BaSO_4$ is given for reference in Figs. 27-30. The IR reflectivity of this Bs-SiO_2 system is still

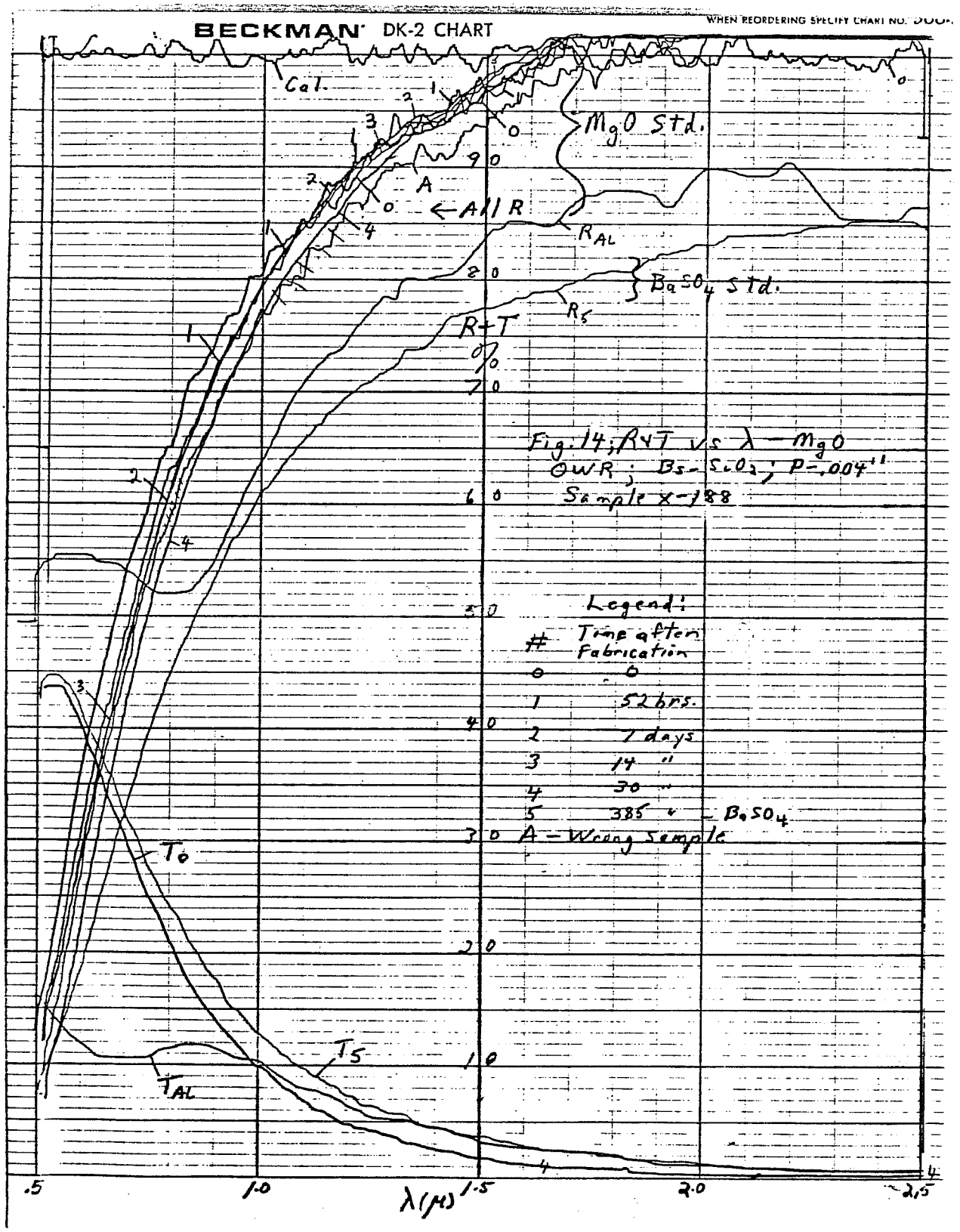
BECKMAN DK-2 CHART
WHEN REORDERING SPECIFY CHART NO.
Cal.
MgO Std.
A
← Air
R
R_{AL}
R_S
$BaSO_4$ Std.
R+T
%
Fig. 14; R+T vs λ — MgO
OWR; Bs - SiO_2; P=.004"
Sample X-188
Legend:
Time after Fabrication
0 0
1 52 hrs.
2 7 days
3 14 "
4 30 "
5 385 " - $BaSO_4$
A - Wrong Sample
T_0
T_5
T_{AL}
.5
1.0
1.5
2.0
2.5
λ(μ)

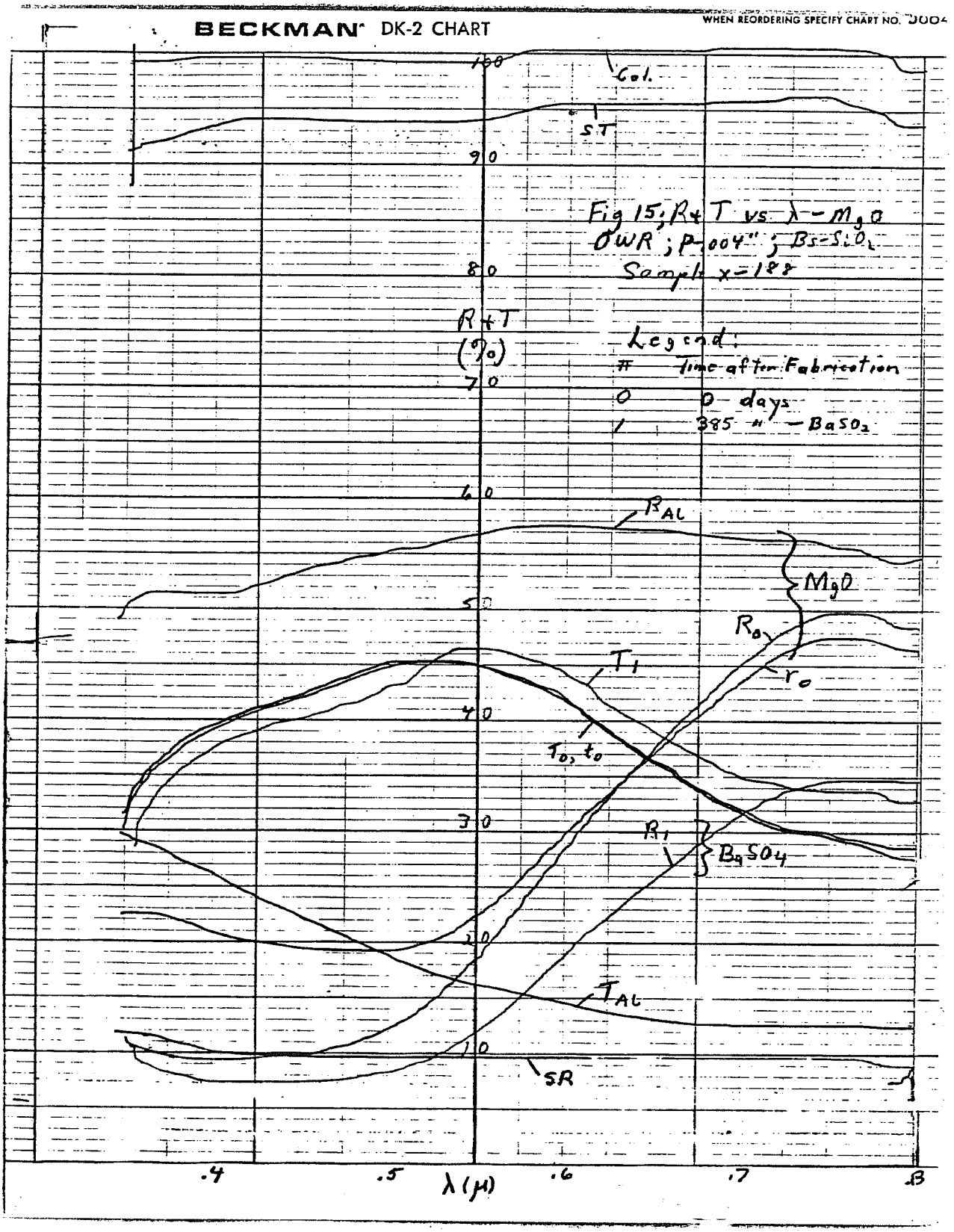
BECKMAN DK-2 CHART
WHEN REORDERING SPECIFY CHART NO. 3004
Col.
ST
Fig 15; R+T vs λ -- MgO
OWR ; P-004" ; Bs-SiO2
Sample x=188
R+T
(%)
Legend:
time after Fabrication
0 0 days
1 385 " -BaSO4
RAL
MgO
R0
T1
r0
T0, t0
R1
BaSO4
TAL
SR
100
90
80
70
60
50
40
30
20
10
.4
.5
λ(μ)
.6
.7
.8

better after one year than that of the Al film. From Fig. 15 it is apparent that the visible T is more than twice that of the alumized film, with a slight increase as R decreases. Changes in R are apparent in the visible region before the IR region, as evidenced by the relatively large change in R (e.g. at .7 μ, 13% absolute vs. expected 1%). Changes in visible R values with time are a good indicator of film stability. This particular system was rated unsatisfactory for long term service although it might be adequate if stabilized at the values shown.

A similar OWR on FEP, as shown in Figs 16-17, gave slightly lower values of R for the same metal layer, with very similar T values. Degradation with time (Fig. 16) was considerably less than for the P substrate. This sample had data taken vs. Cu as well as MgO and the R curve vs. Cu is seen to be down roughly 2% after 1 year. $BaSO_4$ results after 1 year vs. the original MgO curve show a somewhat greater fall-off with an R (1.5 μ) of .79 vs. the non-degraded .83. This is just outside of spectrometer variations over a 1 year period of time but the increase in T indicates that it is a real decrease in R. The values for reflectivity through the substrate (r) in Fig. 16 show the effect of absorption in the substrate and give expected performance for the deposit side glued to the window. This system is more stable than that on P substrates and is probably commercially useable, especially for deposited film to glass configurations.

A similar set of samples was made for Bs-SiO_2 on FEP using the same Bs layer but a SiO_2 layer only half as thick. In this case, as shown in Fig. 18, the R degradation over the same period ot time was somewhat greater (.775 vs. non-degraded .84 at 1.5 μ) but still better than the P substrate case. The change in R is apparently continuous but probably limiting since R_7 and R_6 are close (.775 at 372 days vs. .80 at 58 days).

The results for Ag-SiO_2 were essentially the reverse. On P substrates (Figs. 19-20) there was very little if any degradation after 200 days, although the slight T increase in the visible may mean that the slight shift in R in the visible is real. On FEP (Figs. 21-22) R decreases 6% at 1.5 μ

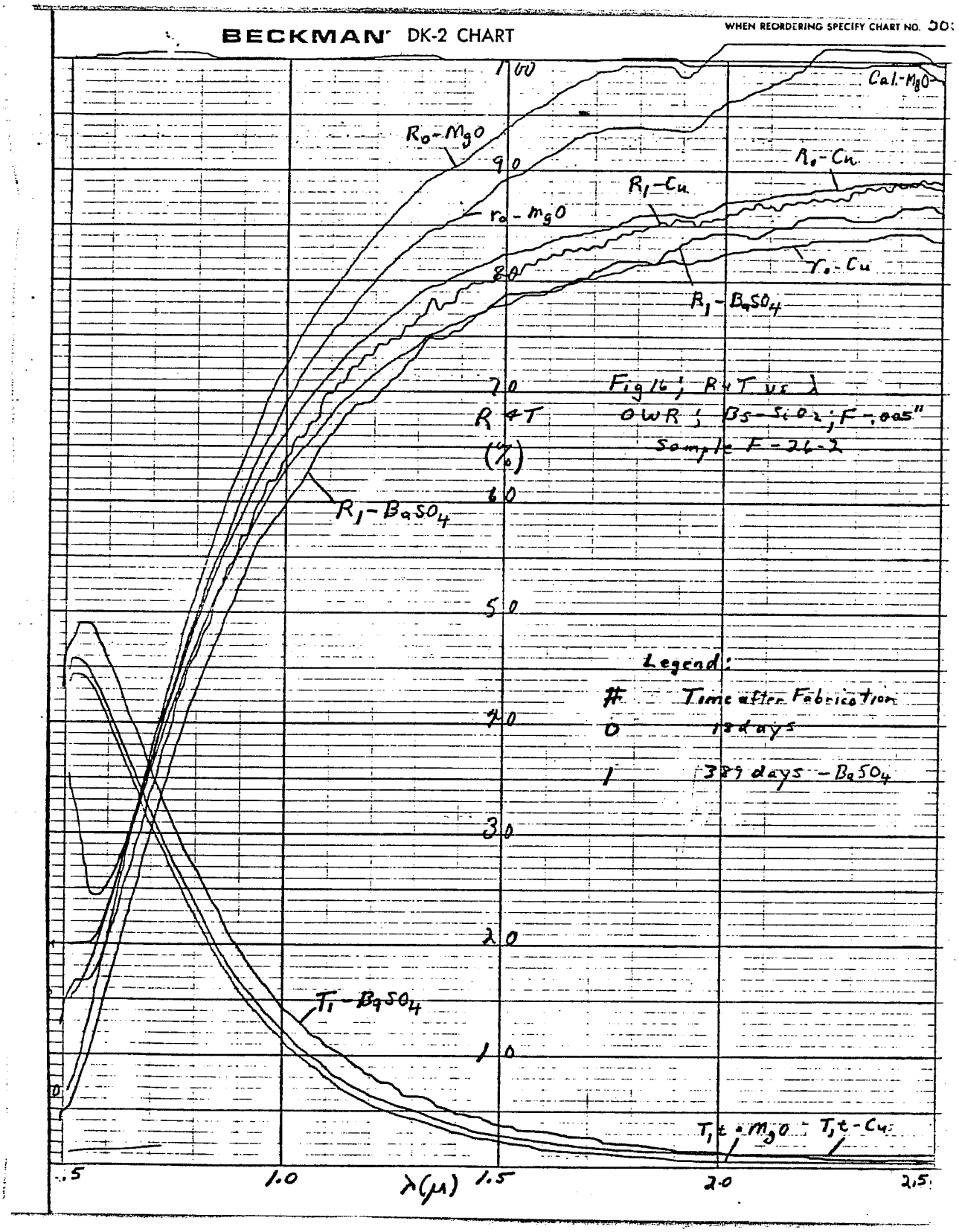
BECKMAN DK-2 CHART
WHEN REORDERING SPECIFY CHART NO. 30
Cal.-MgO
R₀-MgO
R₀-Cu
R₁-Cu
r₀-MgO
r₀-Cu
R₁-BaSO₄
R₁-BaSO₄
R+T (%)
Fig 16; R+T vs λ
OWR; Bs-SiO₂; F-.005"
Sample F-26-2
Legend:
Time after Fabrication
0 18 days
1 389 days - BaSO₄
T₁-BaSO₄
T,t-MgO
T,t-Cu
λ(μ)
.5
1.0
1.5
2.0
2.5

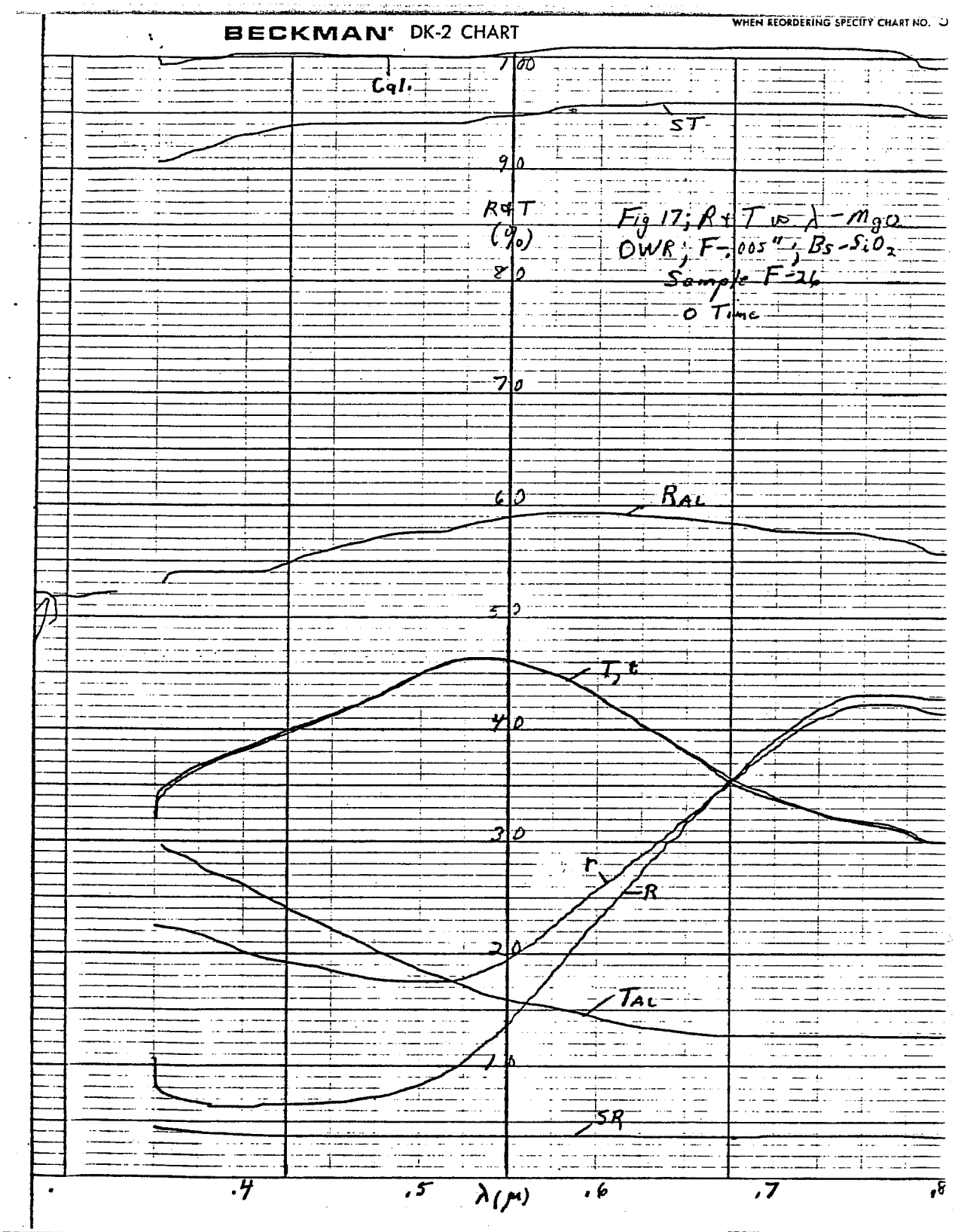
BECKMAN DK-2 CHART
WHEN REORDERING SPECIFY CHART NO.
Cal.
ST
R&T (%)
100
90
80
70
60
50
40
30
20
10
Fig 17; R + T vs λ - MgO
OWR; F-.005", Bs-SiO2
Sample F-26
0 Time
RAL
T, t
r
R
TAL
SR
.4
.5
λ(μ)
.6
.7
.8

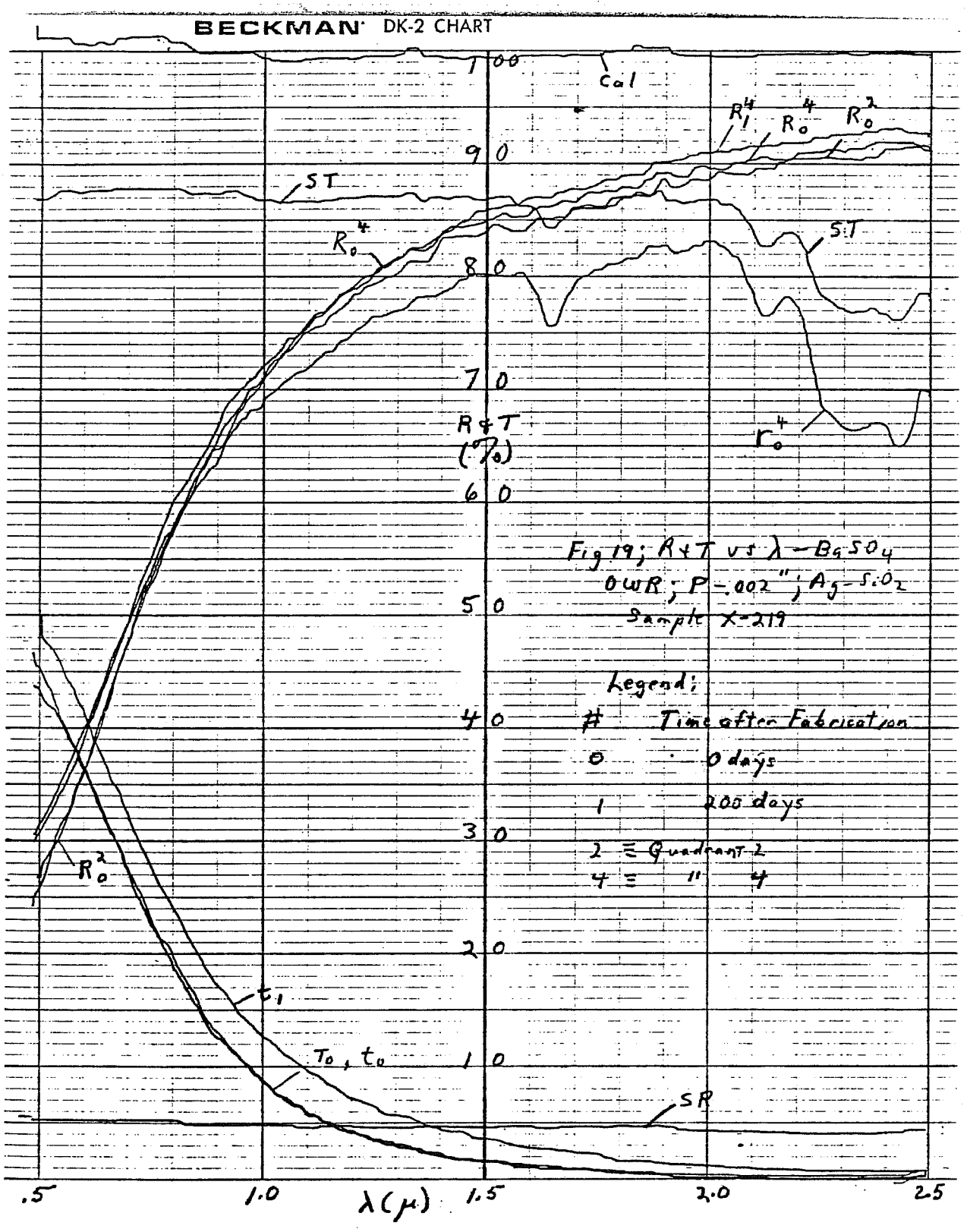
BECKMAN DK-2 CHART
100
90
80
70
60
50
40
30
20
10
R & T (%)
Cal
ST
ST
R_1^4
R_0^4
R_0^2
R_0^4
r_0^4
R_0^2
T_1
T_0, t_0
SR
.5
1.0
1.5
2.0
2.5
λ(μ)
Fig 19; R+T vs λ - BaSO4
OWR; P = .002"; Ag - SiO2
Sample X-219
Legend;
Time after Fabrication
0 0 days
1 200 days
2 ≡ Quadrant 2
4 = " 4

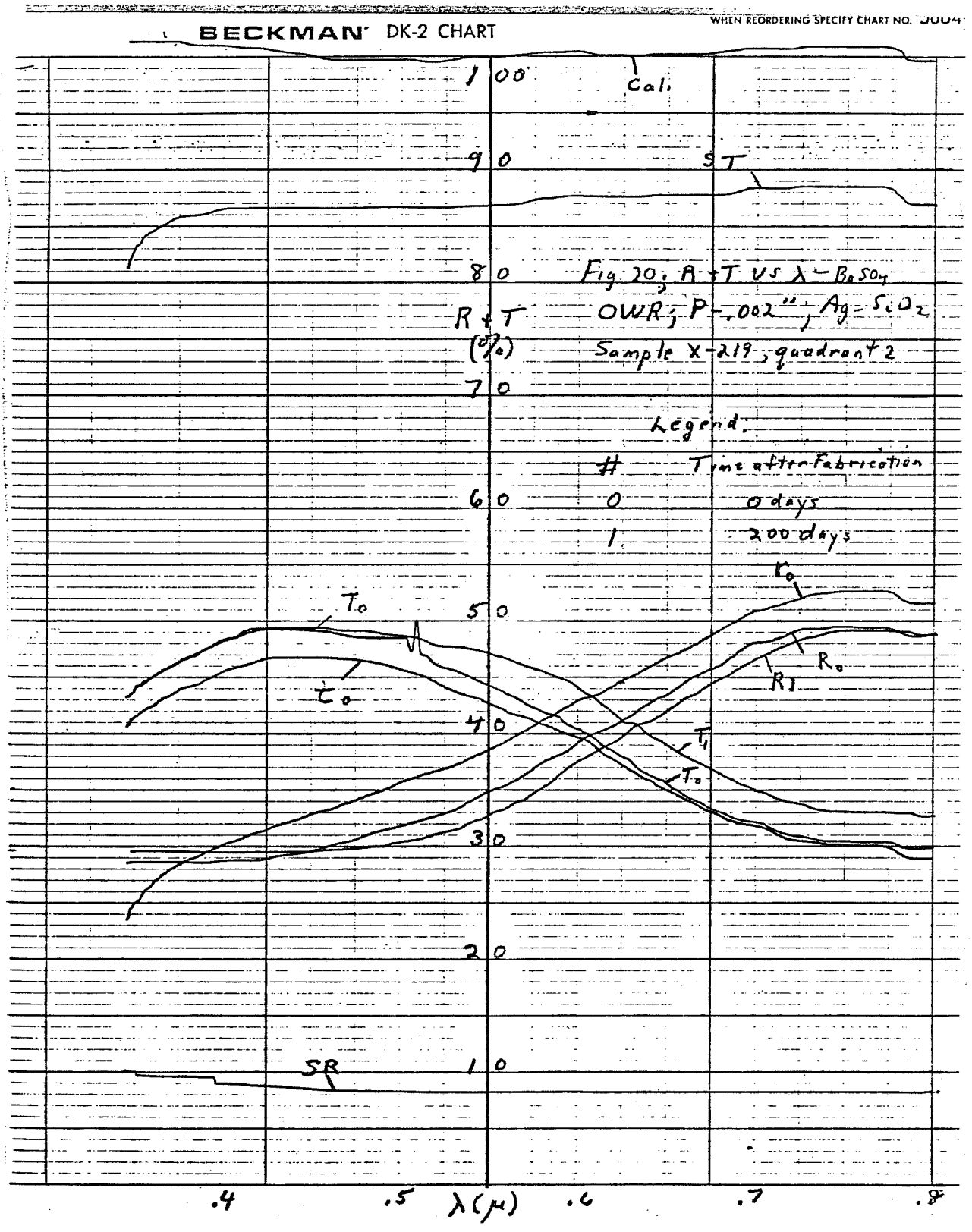
BECKMAN DK-2 CHART
WHEN REORDERING SPECIFY CHART NO. 3004
100
90
80
70
60
50
40
30
20
10
R+T (%)
Cal.
ST
SR
Fig. 20; R+T vs λ-BaSO4
OWR; P-.002", Ag-SiO2
Sample X-219, quadrant 2
Legend:
Time after Fabrication
0 0 days
1 200 days
T0
t0
r0
R0
R1
T1
T0
.4
.5
λ(μ)
.6
.7
.8

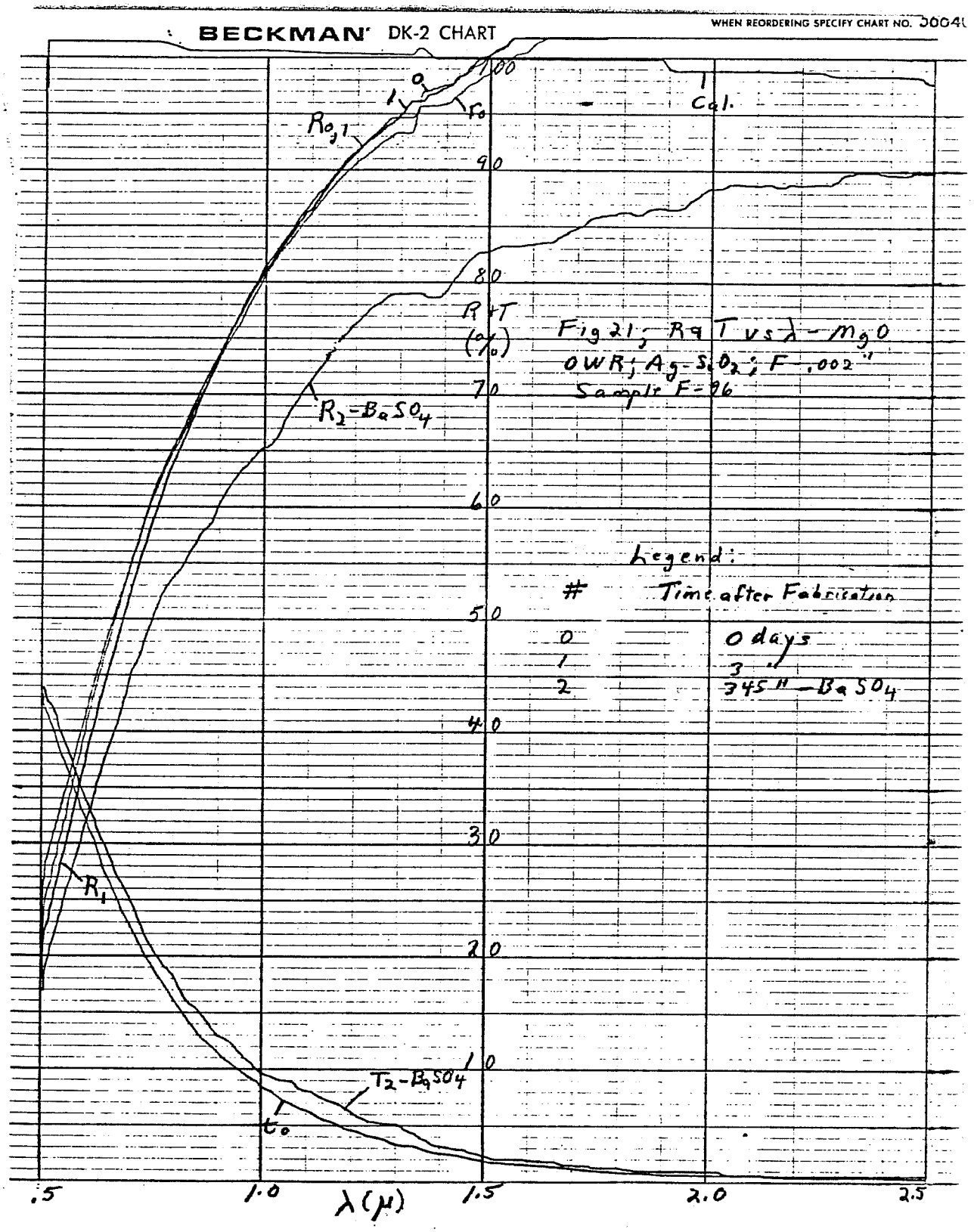
BECKMAN DK-2 CHART
WHEN REORDERING SPECIFY CHART NO. 30041
100
90
80
70
60
50
40
30
20
10
R+T (%)
.5
1.0
1.5
2.0
2.5
λ(μ)
Cal.
$R_{0,1}$
r_0
$R_2 = BaSO_4$
R_1
$T_2 - BaSO_4$
t_0
Fig 21; R+T vs λ - MgO
OWR; Ag-SiO2; F=.002"
Sample F=96
Legend:
Time after Fabrication
0 0 days
1
2 345 H - BaSO4

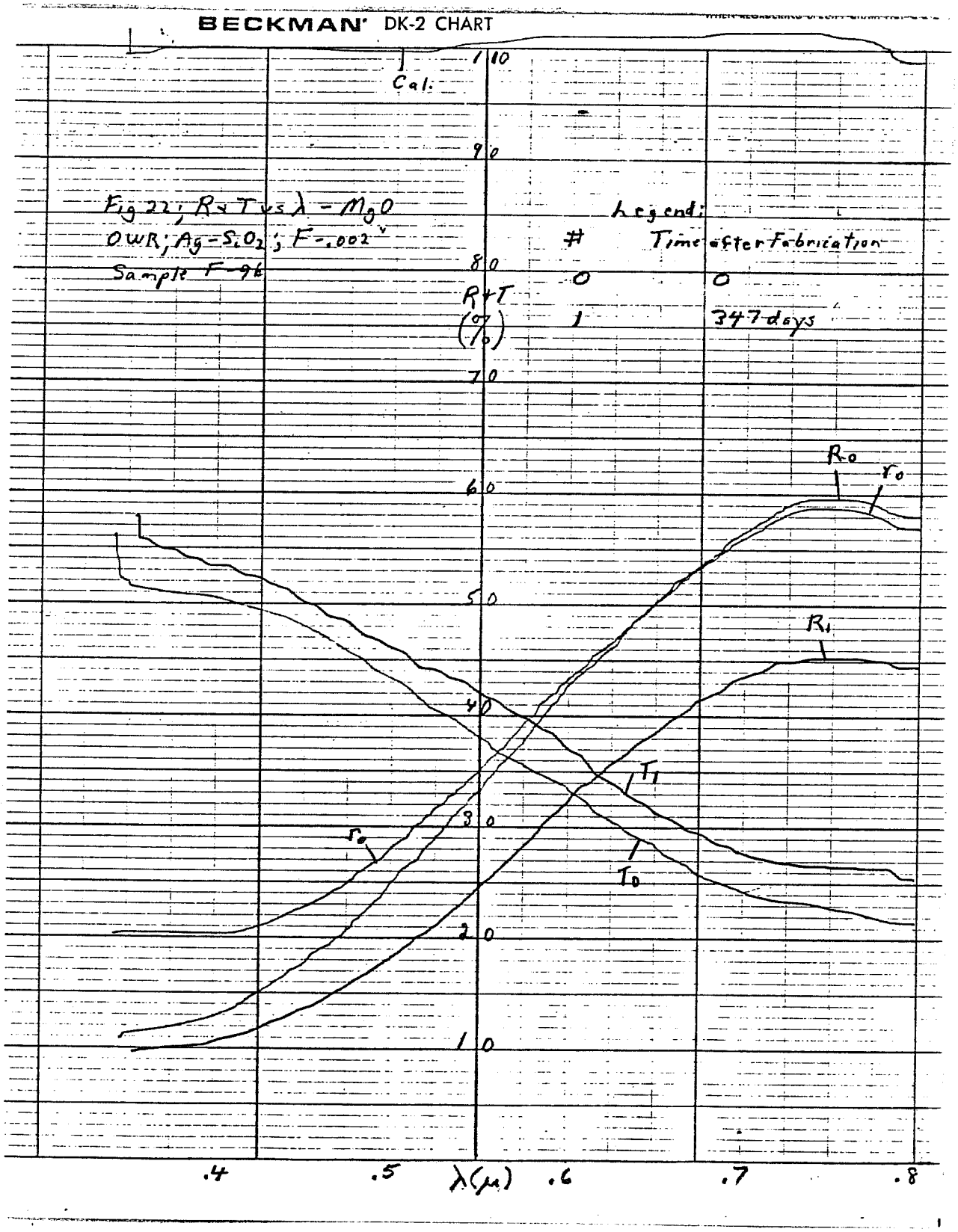
BECKMAN DK-2 CHART
Cal.
Fig 22; R+T vs λ = MgO
OWR; Ag-SiO2; F-.002"
Sample F-96
Legend:
Time after Fabrication
0 0
1 347 days
R+T (%)
10
90
80
70
60
50
40
30
20
10
R0
r0
R1
T1
r1
T0
.4
.5
λ(μ)
.6
.7
.8

(. 83 vs. . 89 non-degraded) and substantially in the visible after 345 days. All curves for the P case use $BaSO_4$ standards while those for FEP use MgO and $BaSO_4$. In general, the R and T characteristics are very acceptable for both substrates. It is important to note that the FEP samples when glued with the deposited side to the glass, are extremely stable (see Section 3. 7).

Results for the Ag-Al_2O_3 system are given in Figs. 23-24 for P substrates and Figs. 25-26 for FEP substrates. Although these, and other, representative curves have the thickness of the substrate specified, there was no difference in R value results for different substrate thicknesses within experimental limitations. Differences in T values were strictly a function of absorption in the substrate material. Figs. 23 and 24 give complete performance with R, r, R_{Al} and T values. This combination does not show any appreciable degradation with time. The slight decrease in R in the visible after 34 days is close to normal spectrometer variations (note: original calibration curve is high) and had not changed after an additional half year. Other similar samples show little, if any, degradation after 9 months. The R curves in the near infrared show the clear superiority over the conventional Al reflecting layer while the T curves indicate more than twice as much transmitted visible light. The R superiority is maintained throughout the entire IR region where the metal-dielectric OWR films have continuous very high values. The near IR reflectivity can be increased significantly (e. g. to . 85 at 1 μ) while only decreasing visible T by roughly 10%. For some applications this could be desirable.

The FEP substrate results (Figs. 25-26) are very similar. The slight visible shifts are in close ageeement with those observed for the P substrates which indicates a small spectrometer or standard shift over the period since both sets of curves were taken at the same time. (The spectrometer is particularly sensitive to changes in the. 7-. 8 μ region because of inadequate energy on the slit except for perfect adjustment. The visible curves are considered accurate only for the . 35-. 7 μ region). Since this visible variation is quite small, the difference in R values for the 1-2. 5 μ range must be considered anomalous and also indicates spectrometer or measurement

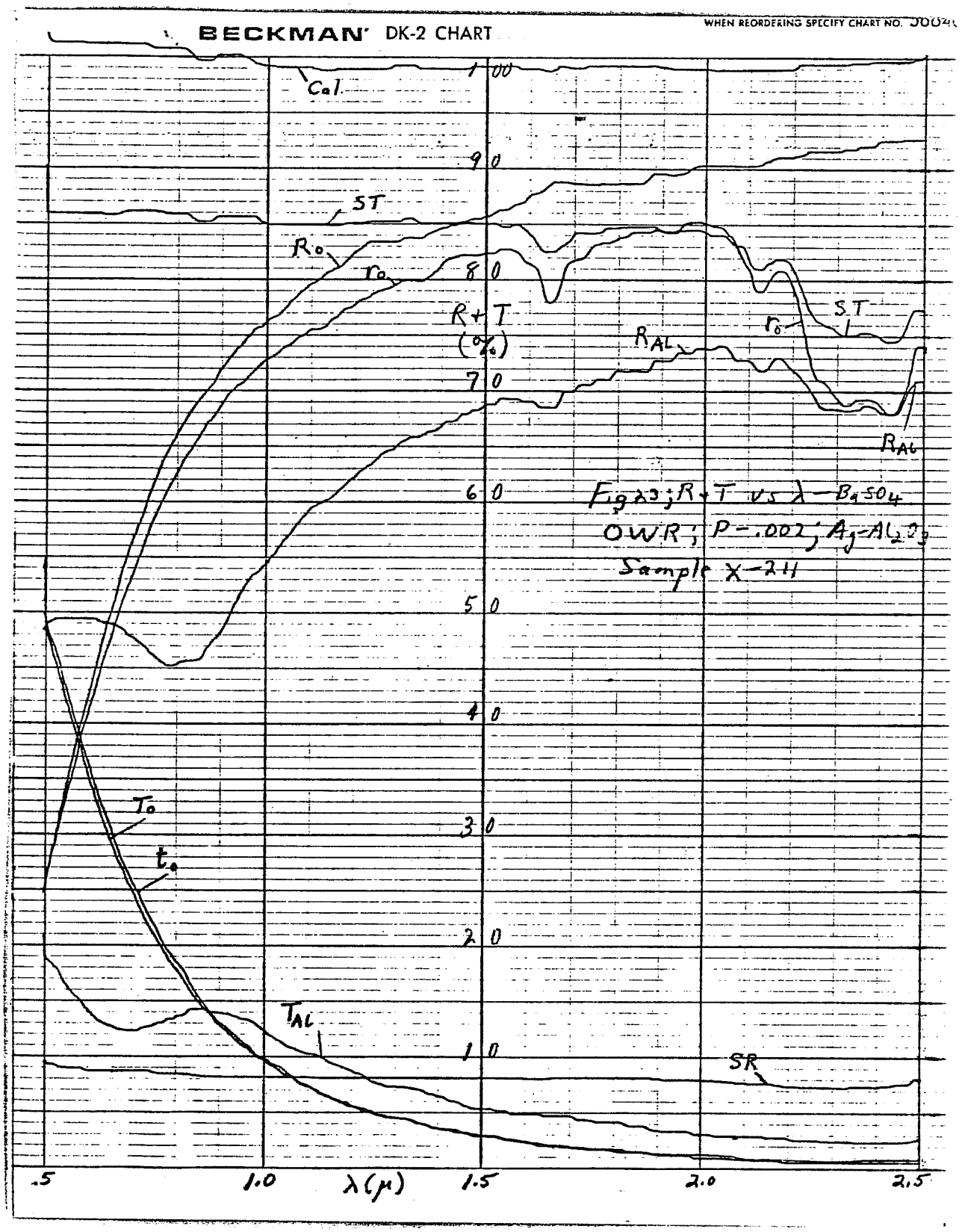
BECKMAN DK-2 CHART
WHEN REORDERING SPECIFY CHART NO. 30024
Cal.
100
90
ST
R_o
r_o
80
R+T (%)
R_{AL}
r_o
S.T
70
R_{AL}
60
Fig 23; R+T vs λ — $BaSO_4$
OWR; P=.002; Al_2O_3
Sample X-211
50
40
T_o
t_o
30
20
T_{AL}
10
SR
.5
1.0
λ(μ)
1.5
2.0
2.5

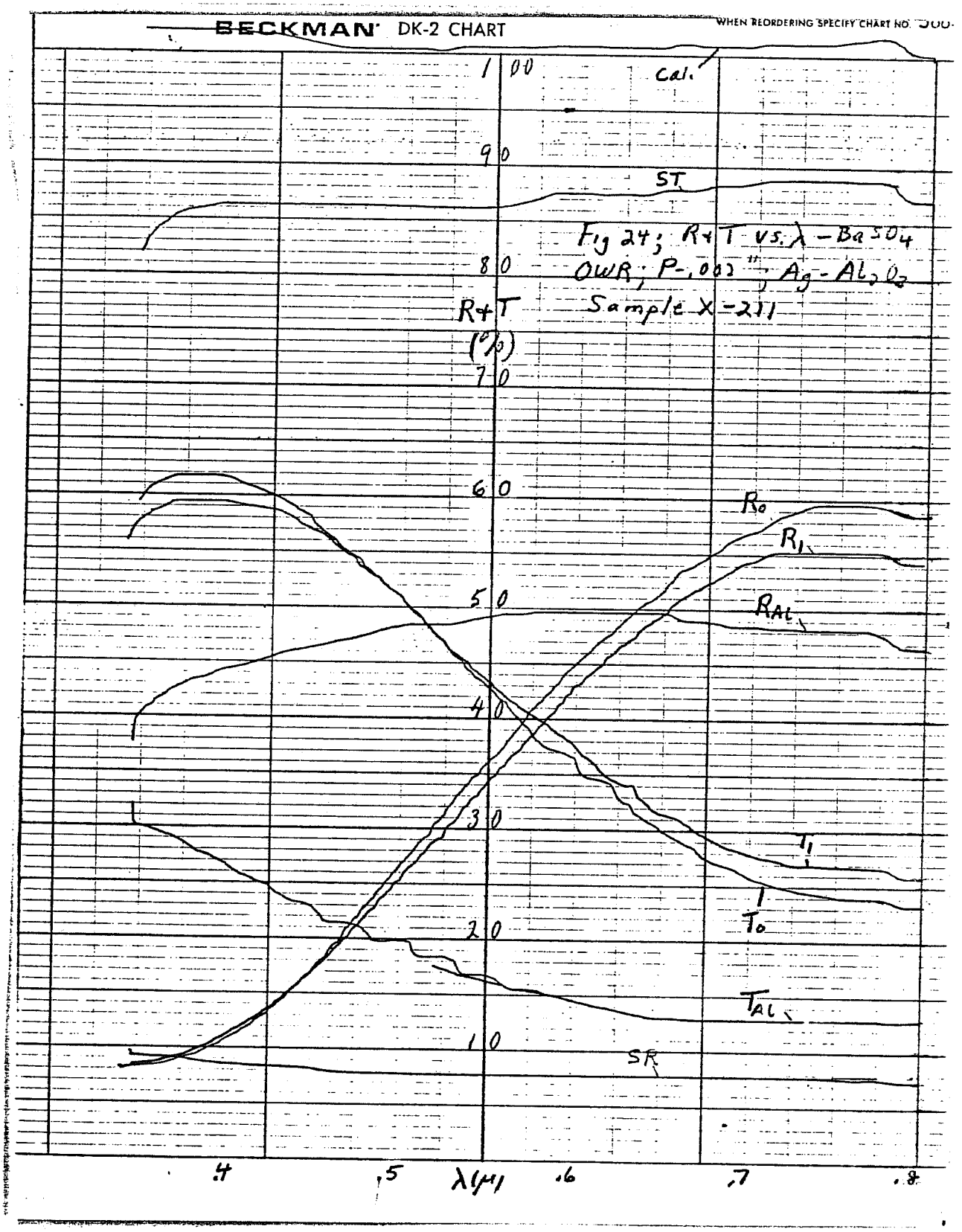
BECKMAN DK-2 CHART
WHEN REORDERING SPECIFY CHART NO.
100
Cal.
90
ST
Fig 24; R+T vs. λ - BaSO4
OWR; P-.003" - Ag - Al2O3
Sample X-211
80
R+T
(%)
70
60
50
40
30
20
10
R0
R1
RAl
T1
T0
TAl
SR
.4
.5
λ(μ)
.6
.7
.8

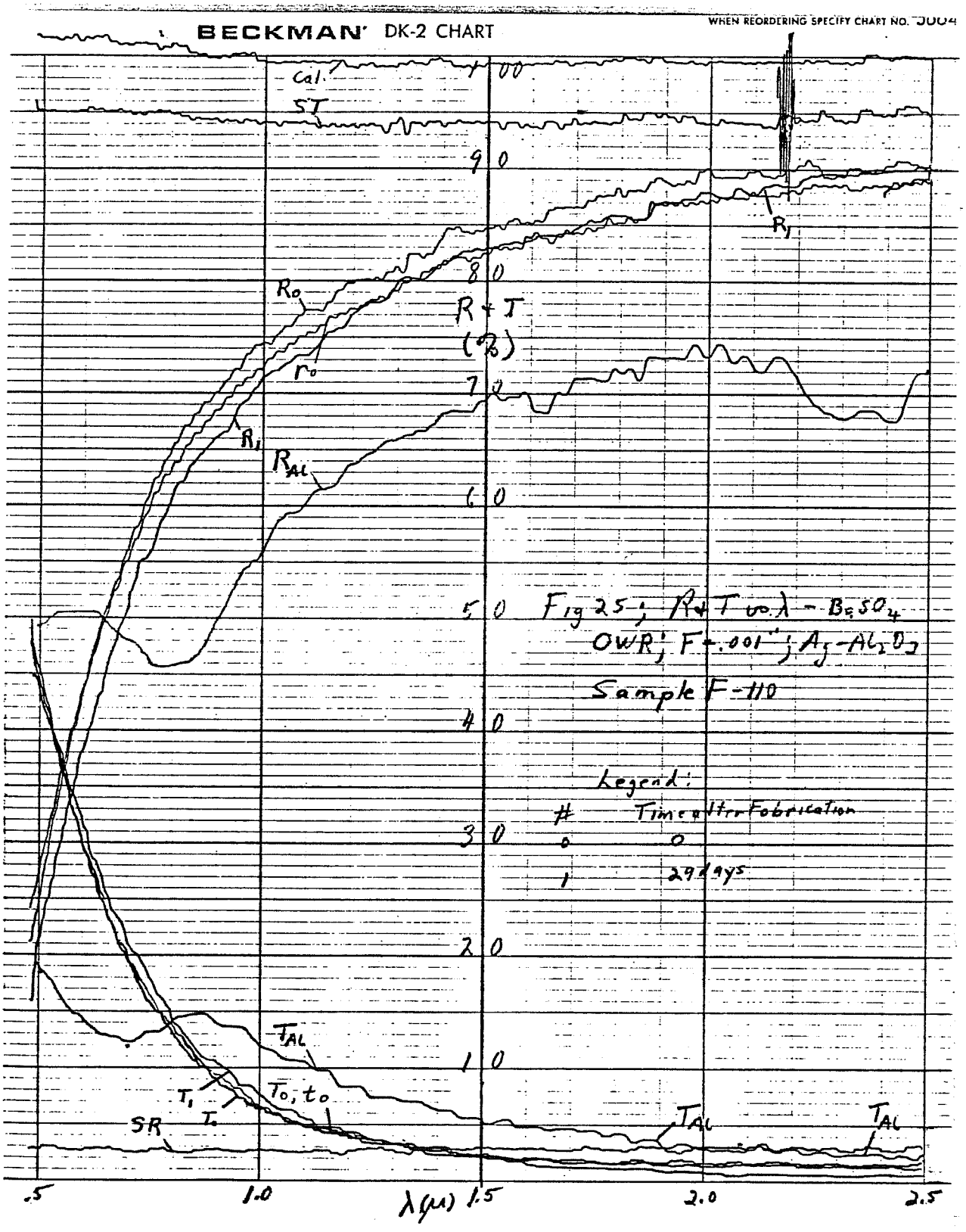
BECKMAN DK-2 CHART
WHEN REORDERING SPECIFY CHART NO. 3004
Cal.
ST
100
90
80
70
60
50
40
30
20
10
R + T (%)
R_o
r_o
R_i
R_{AL}
R_f
T_{AL}
T_i
T_o
t_o
SR
T_{AL}
T_{AL}
Fig 25; R+T vs λ - B_2SO_4
OWR; F=.001"; A_f-Al_2O_3
Sample F-110
Legend:
Time after Fabrication
0 0
1 29 days
.5
1.0
λ(μ) 1.5
2.0
2.5

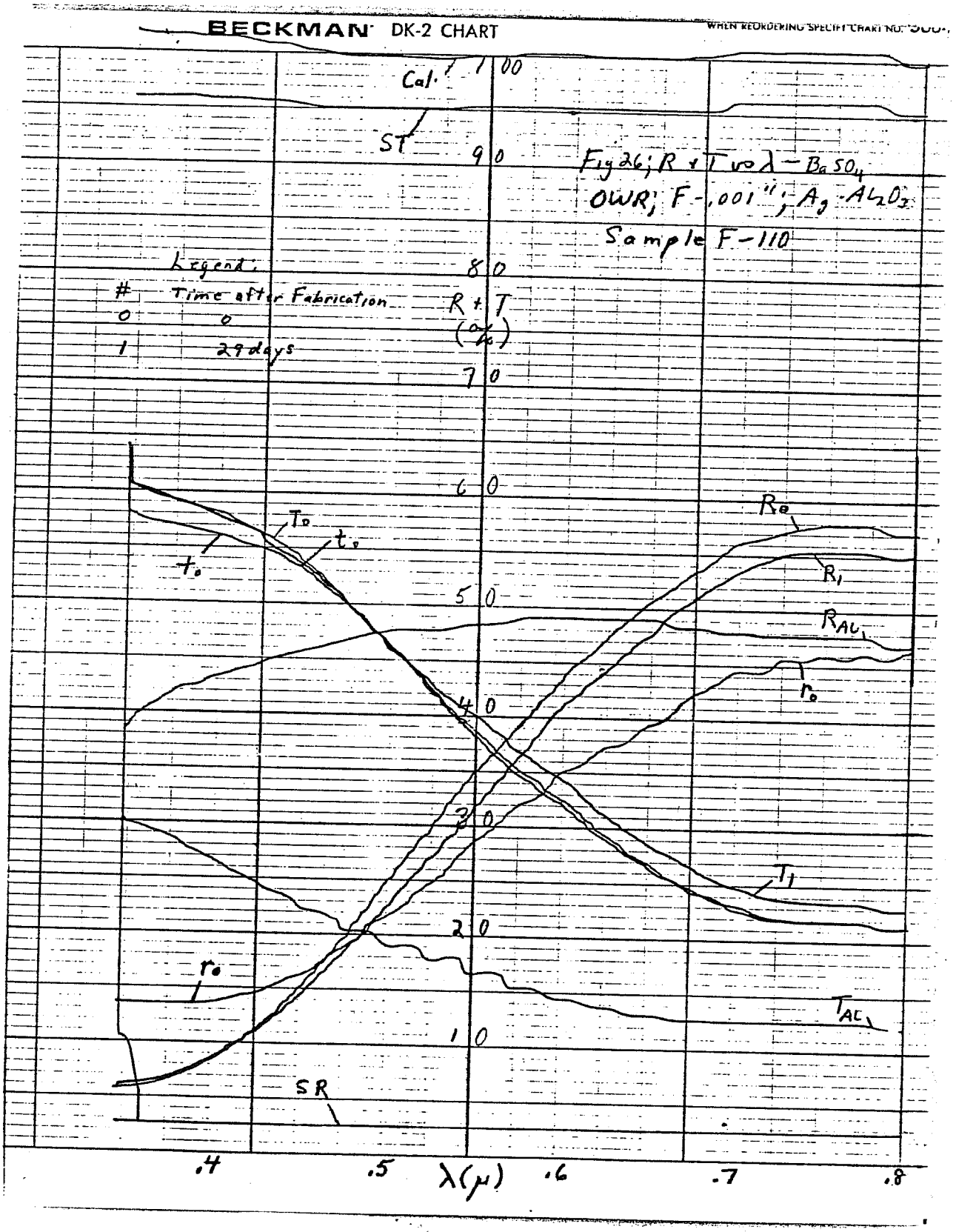
BECKMAN DK-2 CHART
Cal.
ST
100
90
80
70
60
50
40
30
20
10
Fig 26; R + T vs λ – BaSO4
OWR; F-.001"; Ag-Al2O3
Sample F-110
Legend:
Time after Fabrication
0 0
1 29 days
R + T (%)
T0
t0
t1
R0
R1
RAL
r0
T1
TAL
SR
.4
.5
λ(μ)
.6
.7
.8

variation. Again, subsequent measurements after 9 months indicate little if any, real degradation. Visible T values are somewhat less than for P substrates due to the fact that slightly more metal must be used to obtain similar R values. Average T values for both substrates are similar to those obtained with the Ag-SiO_2 combination.

The Ag-Al_2O_3 combination looks very good on both P and FEP substrates and is considered an excellent commercial combination. All final demonstration samples were made with this system. The Ag-SiO_2 system, however, is a very close second choice and may actually be preferable in production.

The final system studied was Bs-Al_2O_3 with typical results shown in Figs 27-30. These samples were made after the results were obtained on Bs-SiO_2 and, because of the degradation observed in that case, the standard RWR processing was used. Because of this change, the visible T values were somewhat lower on the average, with the FEP sample being significantly lower. R values were similar. There was little, if any, change in the P substrate sample (Figs. 27-28) after 41 days and subsequent quick checks (R at 1.5 μ) showed little change after 5 months. The FEP samples (Figs. 29-30) showed a greater change in the visible R values. Since the visible T values are abnormally low, it is now believed that these FEP samples were improperly processed. Since the Bs-Al_2O_3 system is not being actively pursued for retrofit applications, these investigations have not been repeated.

Additional elapsed time is required to determine long term stability of the latter samples. It should be emphasized, however, that gluing studies show Cu based systems to be very stable when the deposited side is glued to the glass.

The results as presented here, plus post-program results, especially on polypropylene substrates, indicate that the requirements for all possible window configurations (Section 1) can be met with the present method. Additional results and samples are discussed under weathering (Section 4) and demonstration results (Section 5).

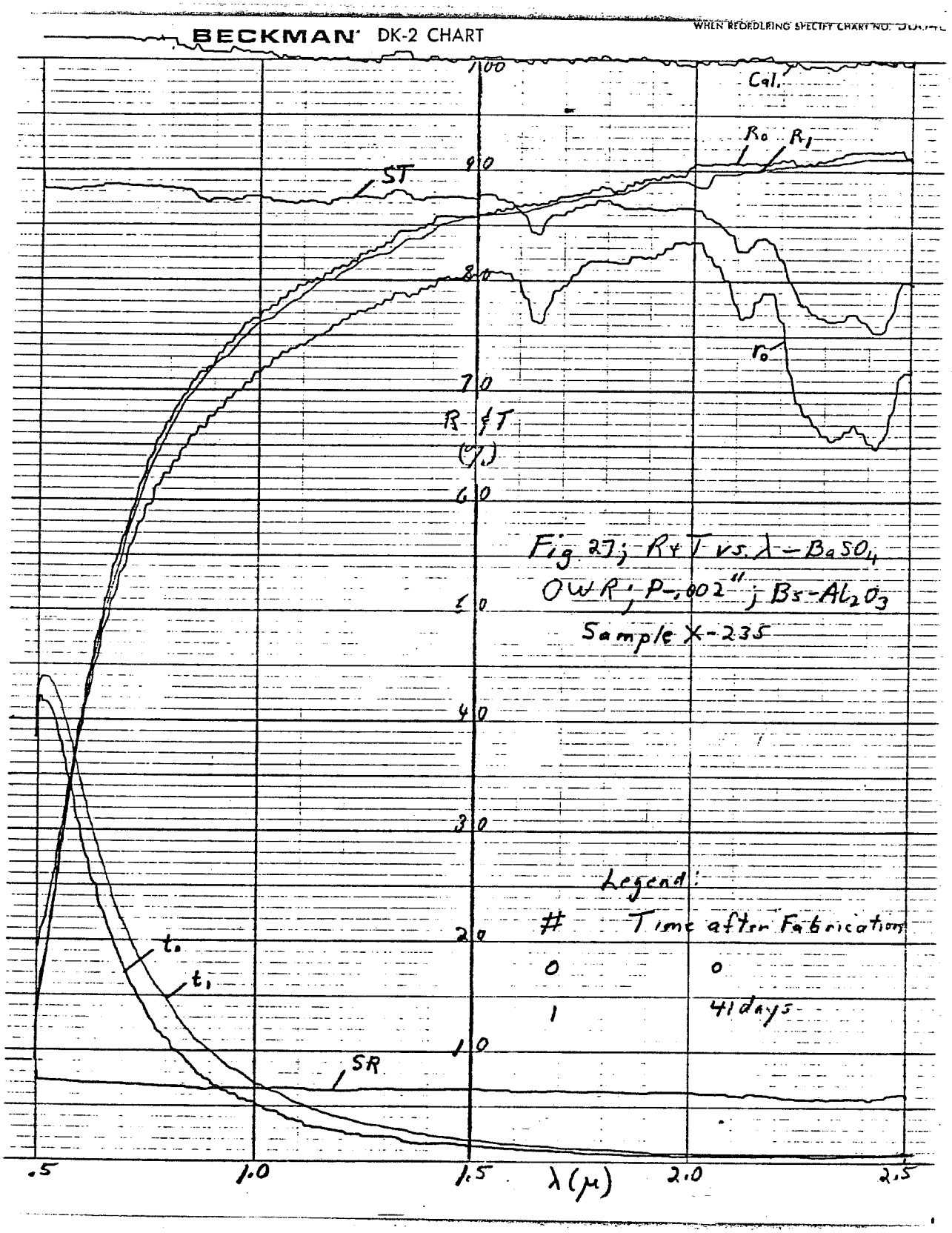
BECKMAN DK-2 CHART
WHEN REORDERING SPECIFY CHART NO.
100
90
80
70
60
50
40
30
20
10
Cal.
R_o
R_1
ST
r_o
R & T (%)
SR
t_o
t_1
.5
1.0
1.5
2.0
2.5
λ(μ)
Fig 27; R+T vs. λ - $BaSO_4$
OWR; P-.002"; Bs-Al_2O_3
Sample X-235
Legend:
Time after Fabrication
0 0
1 41 days

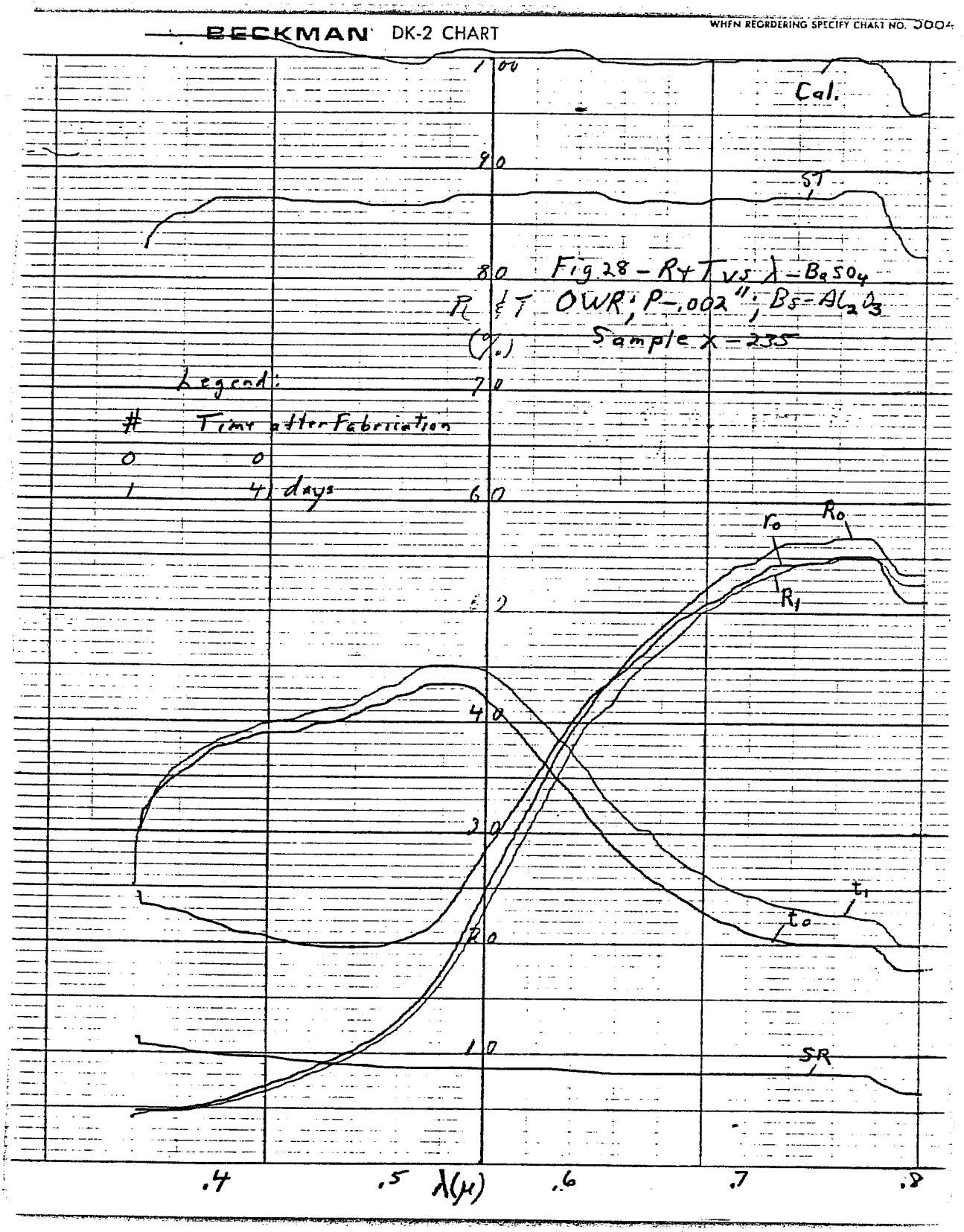
BECKMAN DK-2 CHART
WHEN REORDERING SPECIFY CHART NO. 3004
Cal.
ST
SR
Fig 28 - R+T vs λ - BaSO4
R & T OWR; P-.002"; Bs-Al2O3
Sample x=235
(%)
Legend:
Time after Fabrication
0 0
1 4) days
100
90
80
70
60
40
30
20
10
R0
r0
R1
t1
t0
.4
.5
λ(μ)
.6
.7
.8

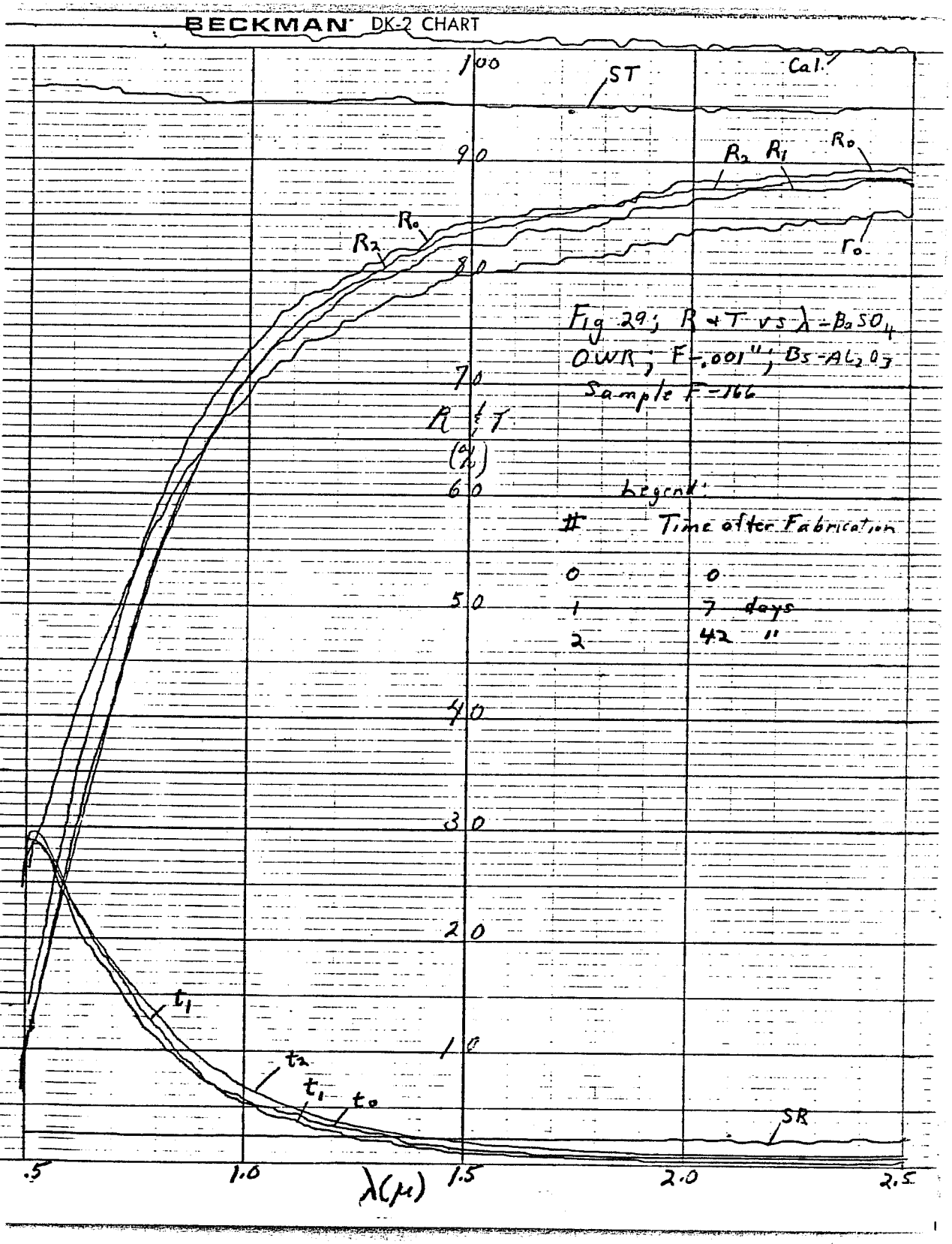
BECKMAN DK-2 CHART
100
90
80
70
60
50
40
30
20
10
ST
Cal.
R₂ R₁ R₀
R₀
R₂
r₀
Fig 29; R+T vs λ - BaSO₄
OWR; F-.001"; Bs-Al₂O₃
Sample F-166
R & T
(%)
Legend:
Time after Fabrication
0 0
1 7 days
2 42 "
t₁
t₂
t₁
t₀
SR
.5
1.0
1.5
2.0
2.5
λ(μ)

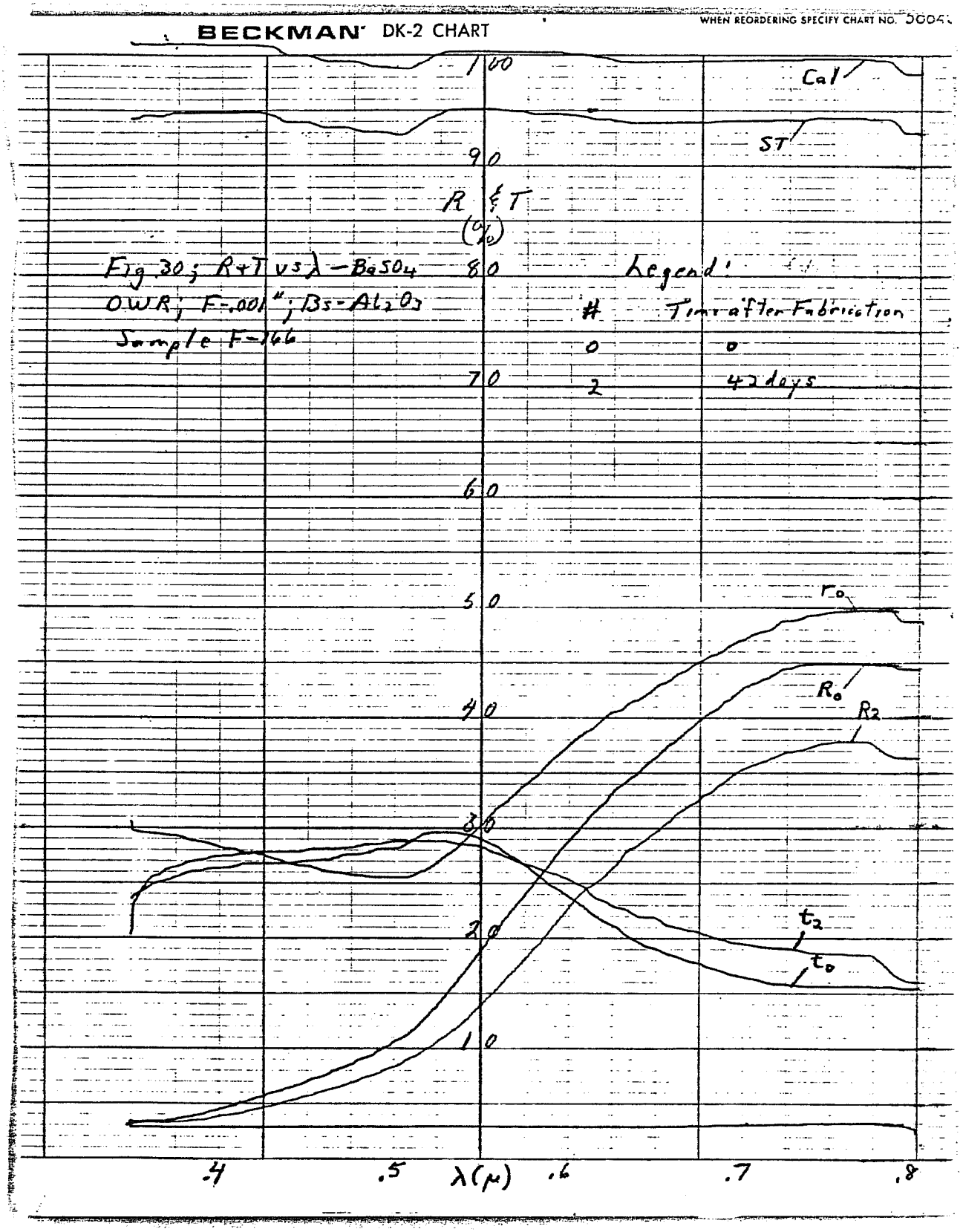
BECKMAN DK-2 CHART
WHEN REORDERING SPECIFY CHART NO. 5004
100
90
80
70
60
50
40
30
20
10
R & T (%)
Cal
ST
Fig 30; R+T vs λ - BaSO4
OWR; F=.001"; Bs=Al2O3
Sample F-166
Legend:
Time after Fabrication
0 0
2 42 days
r0
R0
R2
t2
t0
.4
.5
λ(μ)
.6
.7
.8

3.4 Residential Windows (RW)

While all metal-dielectric combinations have been tried for RWs at one time or another, only certain systems were used during this contract and this more or less only for spot checks. The results presented here include Cu-SiO_2, Bs-SiO_2, Ag-SiO_2, Ag-Al_2O_3 and Al-Al_2O_3. These are representative of almost any system that might be tried.

Although studied extensively under the previous program, the Cu-SiO_2 system was repeated since it was initially considered to be the test vehicle. Fig. 31 shows the basic R curves obtained with varying values of metal thickness and the same SiO_2 thickness. Curves for all four quadrants (sample X-35 non-uniform) of a 4" x 4" glass sample are shown for most cases. In essence the curves can be precisely altered to provide any desired near-infrared values of R while keeping visible R quite low. This is true of all Cu or Ag based metal-dielectric systems. The curves are vs. MgO standards so that a real window by present standards would have a 2.5μ R value slightly greater than sample X-34.

For Cu based systems, Bs is preferred over pure Cu because of its much better stability. An example is given in Figs. 32-35 which give the characteristics for a Bs-SiO_2 sample made relatively early in the program. Because of this, the R value at 2.5μ is lower than present values. Comparison of Figs. 32 and 33 after 432 days with Figs. 34 and 35 for zero time shows very little change. After an additional 6 months there was still essentially no change in characteristics and no visual change in appearance (Note: Complete curves are only taken at predetermined times but quick checks at 2.5μ are made frequently).

This system is very promising for residential windows although probably inferior to the Bs-Al_2O_3 system (see weathering results - Section 5). There are potential Bs-substrate interactions which can cause defects after an extended period of time if the glass is not properly cleaned, but these have been shown to be avoidable under proper fabrication conditions and should not exist for new glass. It is interesting to note that some samples which deteriorate under weatherometer conditions including solar illumination, rain and elevated tempera-

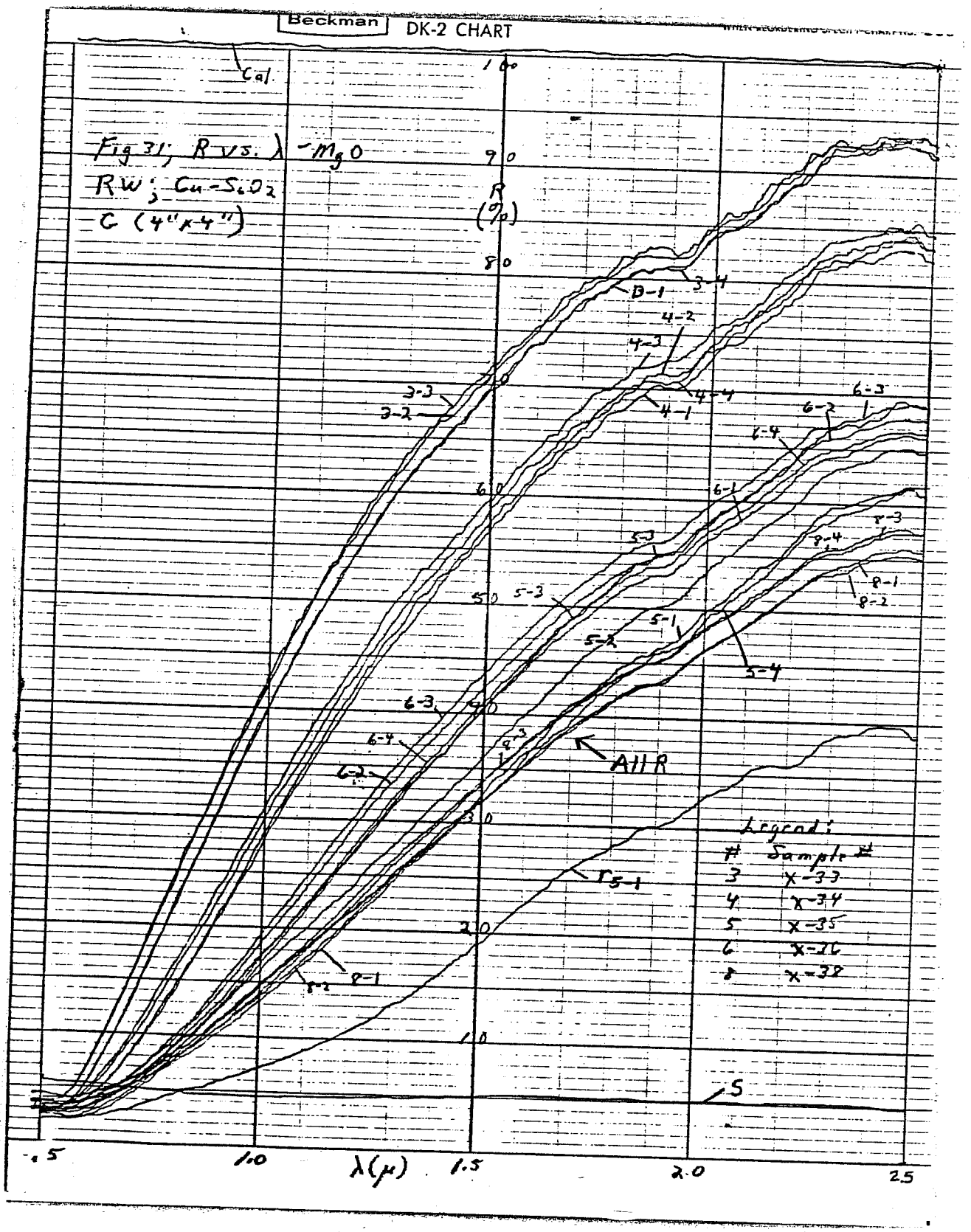
Beckman DK-2 CHART
Cal.
Fig 31; R vs. λ - MgO
RW; Cu-SiO2
C (4"x4")
R (%)
100
90
80
70
60
50
40
30
20
10
B-1
3-4
4-2
4-3
4-4
4-1
3-3
3-2
6-3
6-2
6-4
6-1
5-3
5-4
5-1
5-2
8-3
8-4
8-1
8-2
All R
R5-1
S
.5
1.0
λ(μ)
1.5
2.0
2.5
Legend:
Sample
3 X-33
4 X-34
5 X-35
6 X-26
8 X-32

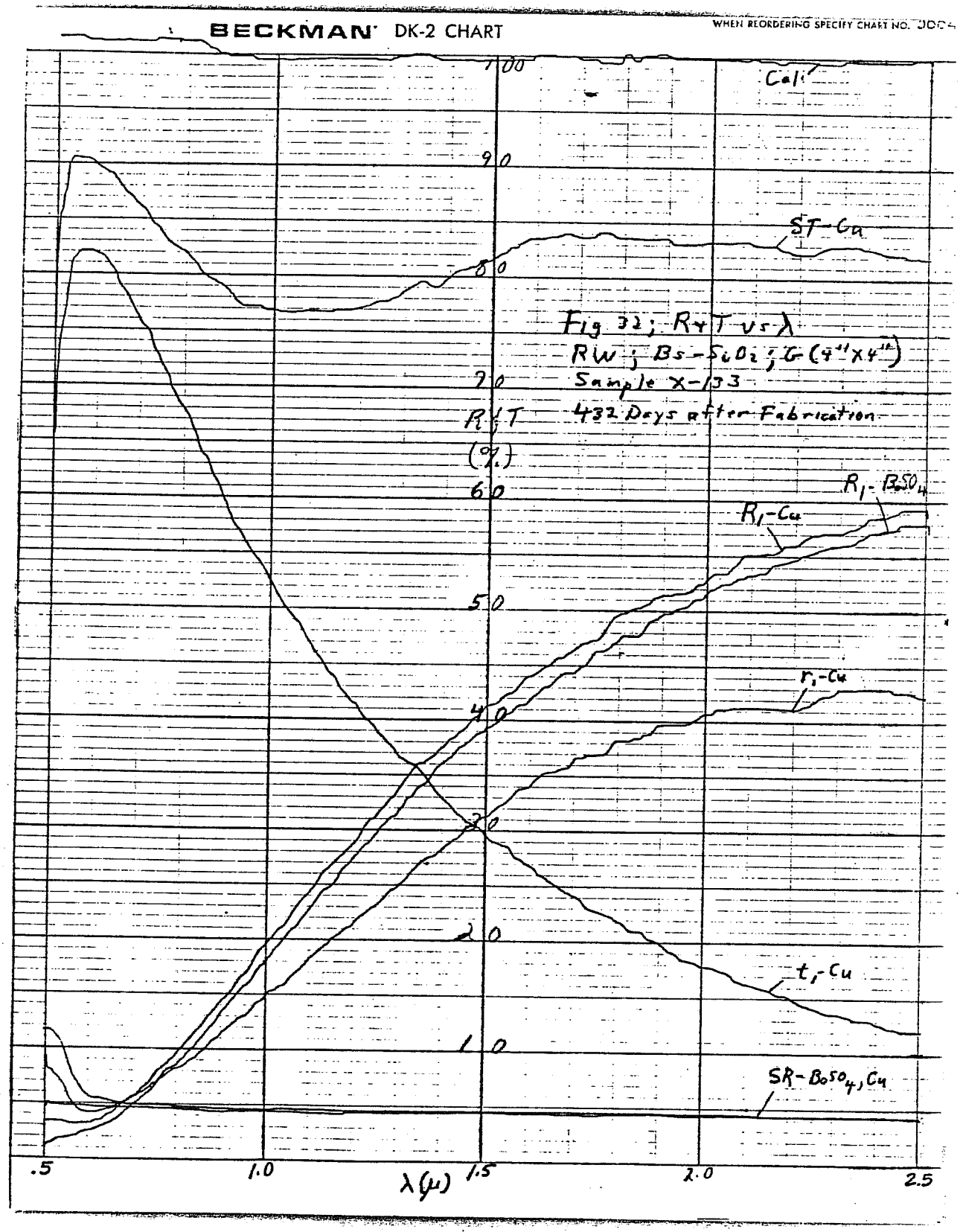
BECKMAN DK-2 CHART
WHEN REORDERING SPECIFY CHART NO. 10024
100
90
80
70
60
50
40
30
20
10
R+T (%)
Cal
ST-Cu
Fig 32; R+T vs λ
RW; Bs-SiO2; G (4"x4")
Sample X-133
432 Days after Fabrication
R1-BaSO4
R1-Cu
r1-Cu
t1-Cu
SR-BaSO4, Cu
.5
1.0
1.5
2.0
2.5
λ(μ)

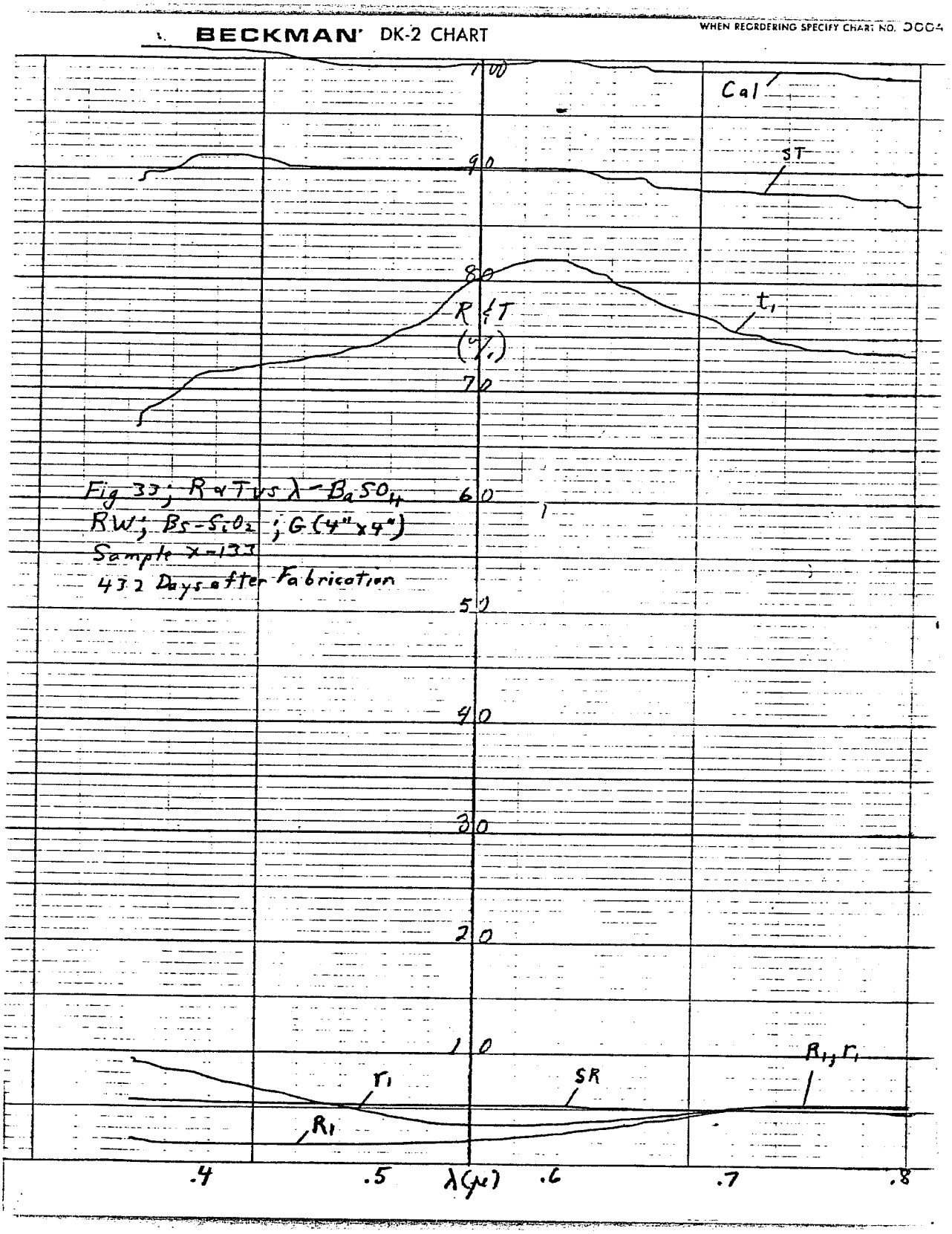
BECKMAN DK-2 CHART
WHEN REORDERING SPECIFY CHART NO. 3004
100
90
80
70
60
50
40
30
20
10
Cal
ST
R & T (%)
t1
Fig 33; R+T vs λ - Ba SO4
RW; Bs-Si02 ; G (4" x 4")
Sample x-133
432 Days after Fabrication
r1
SR
R1
R1, r1
.4
.5
λ(μ)
.6
.7
.8

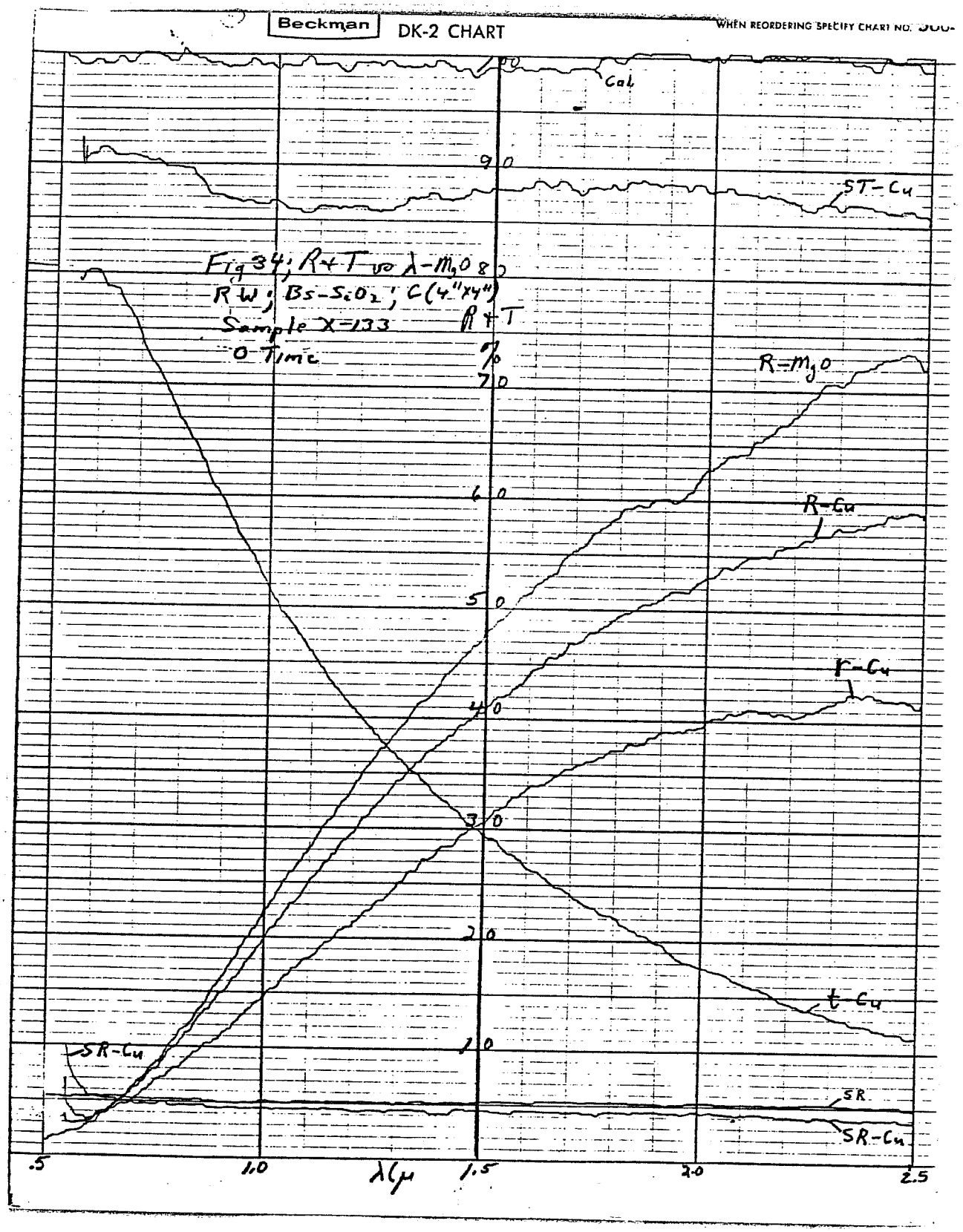
Beckman
DK-2 CHART
WHEN REORDERING SPECIFY CHART NO.
Cal
ST-Cu
Fig 34; R+T vs λ-M3O8
RW; Bs-SiO2; C(4"x4")
Sample X-133
0 Time
R+T
%
R-M3O
R-Cu
T-Cu
t-Cu
SR-Cu
SR
SR-Cu
9 0
8 0
7 0
6 0
5 0
4 0
3 0
2 0
1 0
.5
1.0
λ(μ
1.5
2.0
2.5

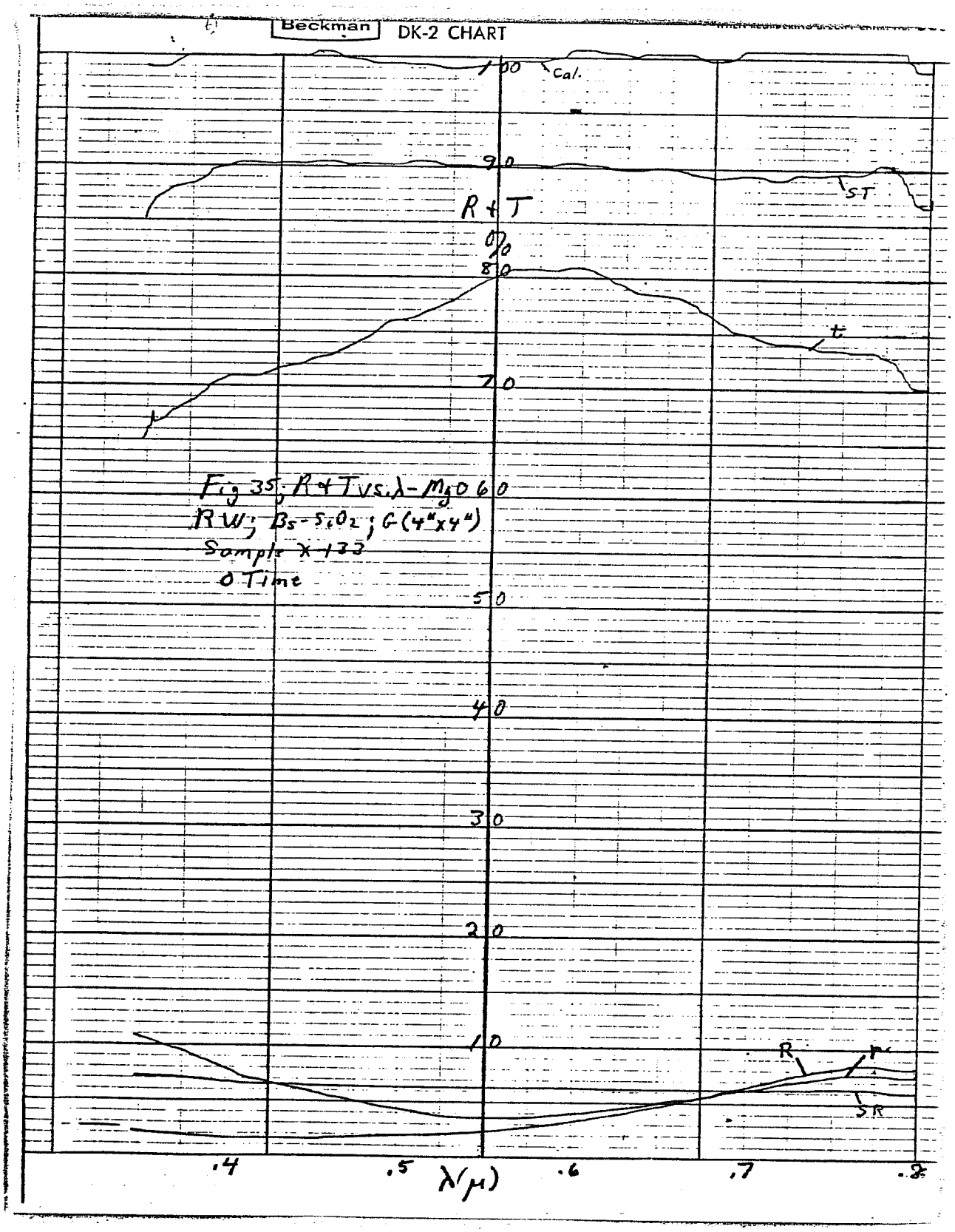

Fig 35; R+T vs. λ - MgO 60
RW; Bs - SiO2; G (4"x4")
Sample X-133
0 Time

tures, degrade under ambient laboratory conditions after equivalent real elapsed times. This is particularly true for Cu based systems and implies that the mechanism is not light or oxygen (corrosion) induced, but may be due to something more complex such as direct chemical interaction with the substrate, overcoat, or contaminants.

General performance for the Ag-SiO_2 system is shown in Figs. 36-39 with Figs. 36-37 giving performance measured from the front or deposit side and 38-39 from the back or substrate side. Again, any level of reflectivity at 2.5μ is readily achieved and can be used to accurately control window performance. Since this is MgO data, a real window by present standards would have a characteristic with a slightly higher reflectivity than sample X-73. Transmission in the visible as shown in Fig. 38, is similar to that achieved with the Bs-SiO_2 system but runs higher at the blue end where the Cu absorbs. This T curve is for sample X-76 which was near the established reflectivity curve for the older, longer wavelength standard reflectivity (.8 at 10μ). Present values would run a few percent less.

As shown in Fig. 38, reflectivity through the glass is considerably less, primarily due to absorption during the two light passes. Visible T, as shown in Fig. 39, is essentially identical to the front side T. Reflectivity in the visible for a real window design is usually about 8% . This is important since it shows that most of the light that is not being transmitted is being absorbed in the glass and can be partly transmitted to the interior by conduction/convection or by reradiation. The same argument applies for the near IR energy (see Fig. 38), particularly in the region from .7 - 1.5μ where the solar spectrum is still relatively intense. Measurements at other laboratories[1] have established that this transfer of absorbed energy to the interior does indeed occur.

Results for a more recent Ag based system, using an Al_2O_3 overcoat are shown in Figs. 40-41 (Note: The downturn in the Cal. and T value at .77μ is

---

(1) Prof. T. Johnson, Dept. of Architecture, MIT, private conversation.

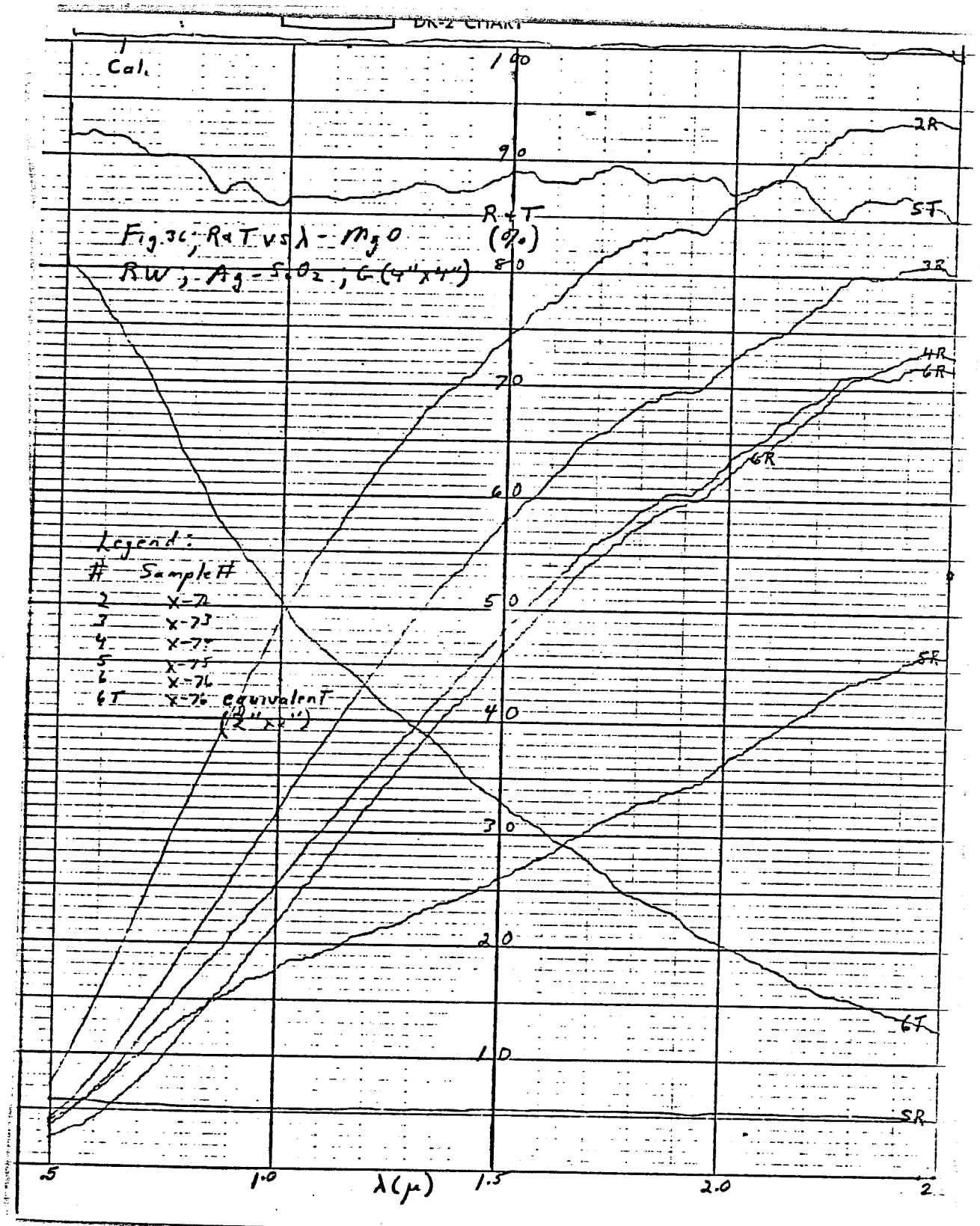
DR-2 CHART
Cal.
100
90
80
70
60
50
40
30
20
10
R+T (%)
2R
5T
3R
4R
6R
6R
5R
6T
5R
Fig. 3c; R+T vs λ - MgO
RW; - Ag - SiO2 ; G (4"x4")
Legend:
Sample
2 X-72
3 X-73
4 X-74
5 X-75
6 X-76
6T X-76 equivalent (2"x2")
.5
1.0
λ(μ)
1.5
2.0
2

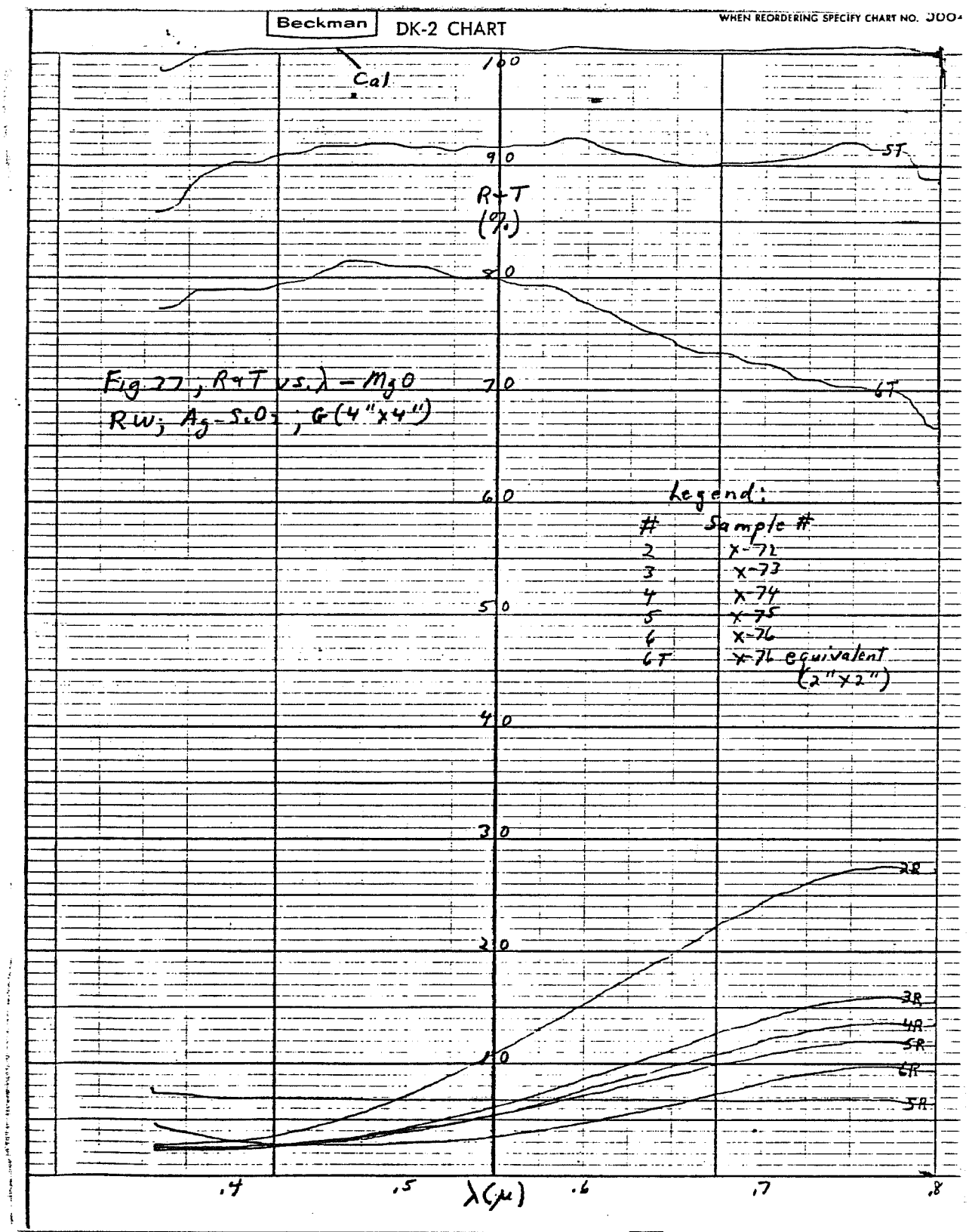
Beckman
DK-2 CHART
WHEN REORDERING SPECIFY CHART NO. 3004
Cal
100
90
80
70
60
50
40
30
20
10
R+T
(%)
ST
6T
Fig 27; R+T vs. λ = MgO
RW; Ag-SiO2; G(4"x4")
Legend:
Sample
2 x-72
3 x-73
4 x-74
5 x-75
6 x-76
6T x-76 equivalent (2"x2")
2R
3R
4R
5R
6R
5R
.4
.5
λ(μ)
.6
.7
.8

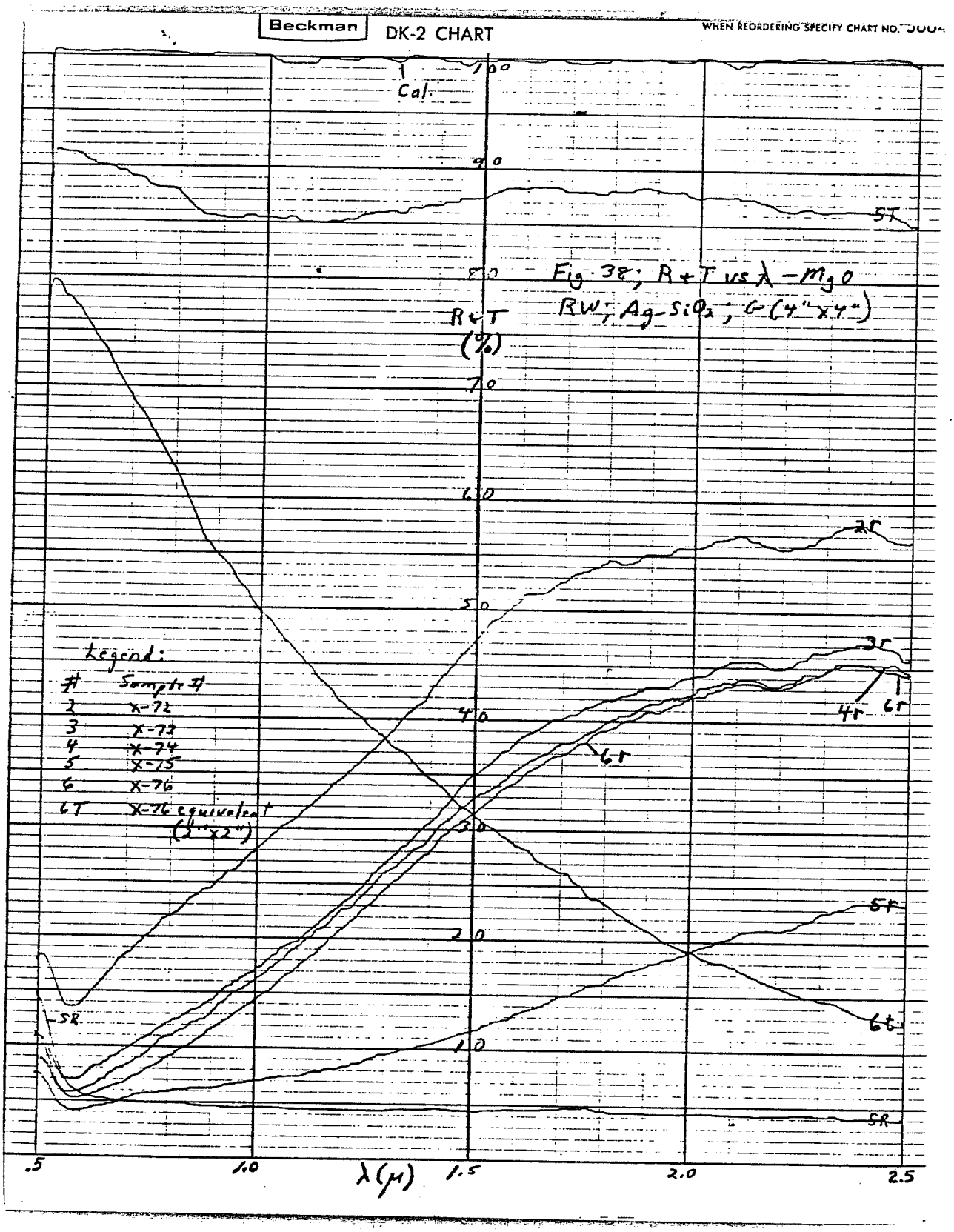
Beckman
DK-2 CHART
WHEN REORDERING SPECIFY CHART NO.
Cal.
100
90
80
70
60
50
40
30
20
10
R+T
(%)
5T
2r
3r
4r
6r
5r
6t
5R
Fig. 38; R+T vs λ - MgO
RW; Ag-SiO2; G (4" x 4")
Legend:
Sample
2 X-72
3 X-73
4 X-74
5 X-75
6 X-76
6T X-76 equivalent (2" x 2")
.5
1.0
λ(μ)
1.5
2.0
2.5

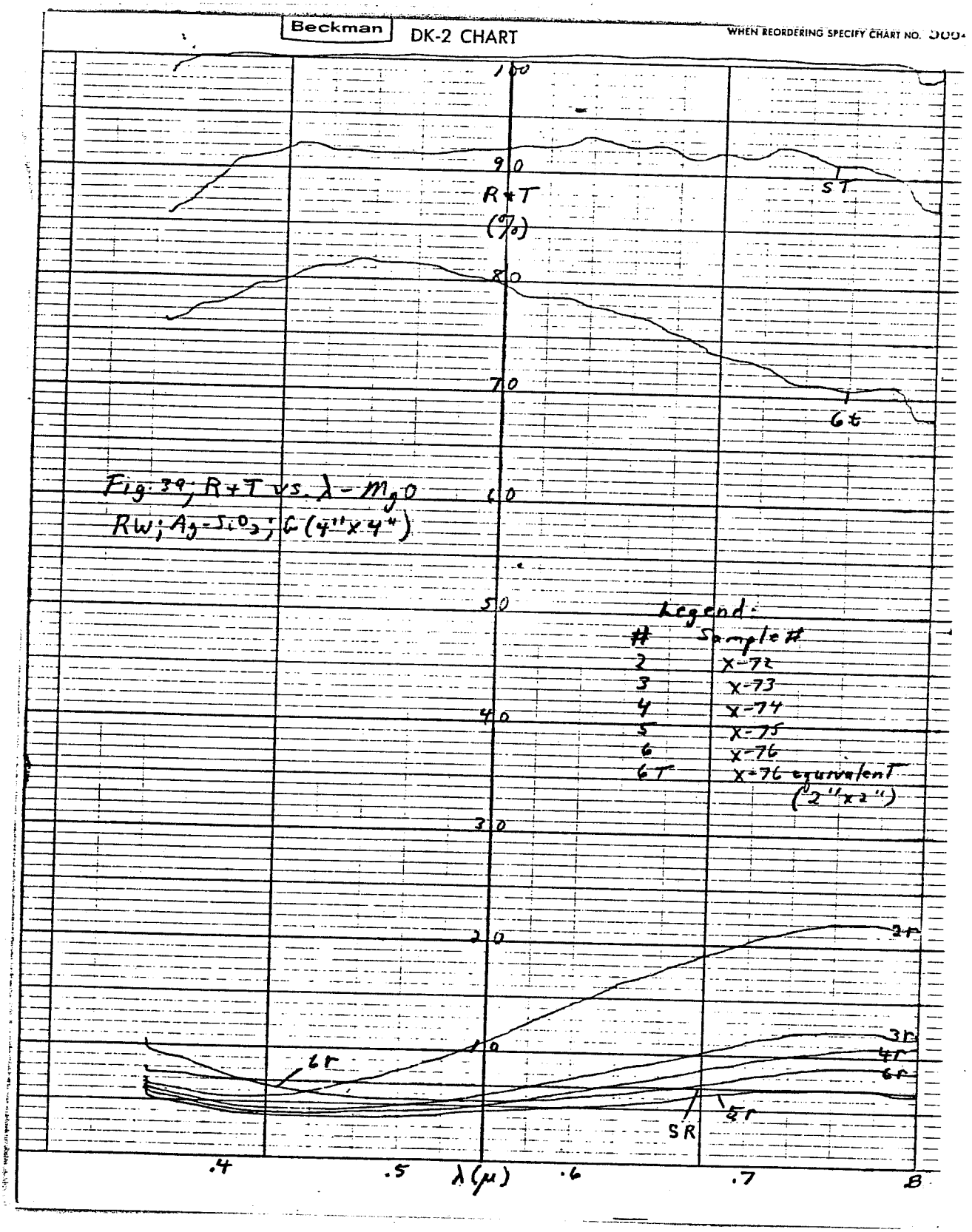
Beckman
DK-2 CHART
WHEN REORDERING SPECIFY CHART NO. 3004
100
90
80
70
60
50
40
30
20
10
R+T
(%)
ST
6t
Fig. 39; R+T vs. λ - MgO
RW; Ag-SiO2; G (4" x 4")
Legend:
Sample
2 X-72
3 X-73
4 X-74
5 X-75
6 X-76
6T X-76 equivalent
(2" x 2")
3r
3r
4r
6r
6r
4r
SR
.4
.5
λ(μ)
.6
.7
.8

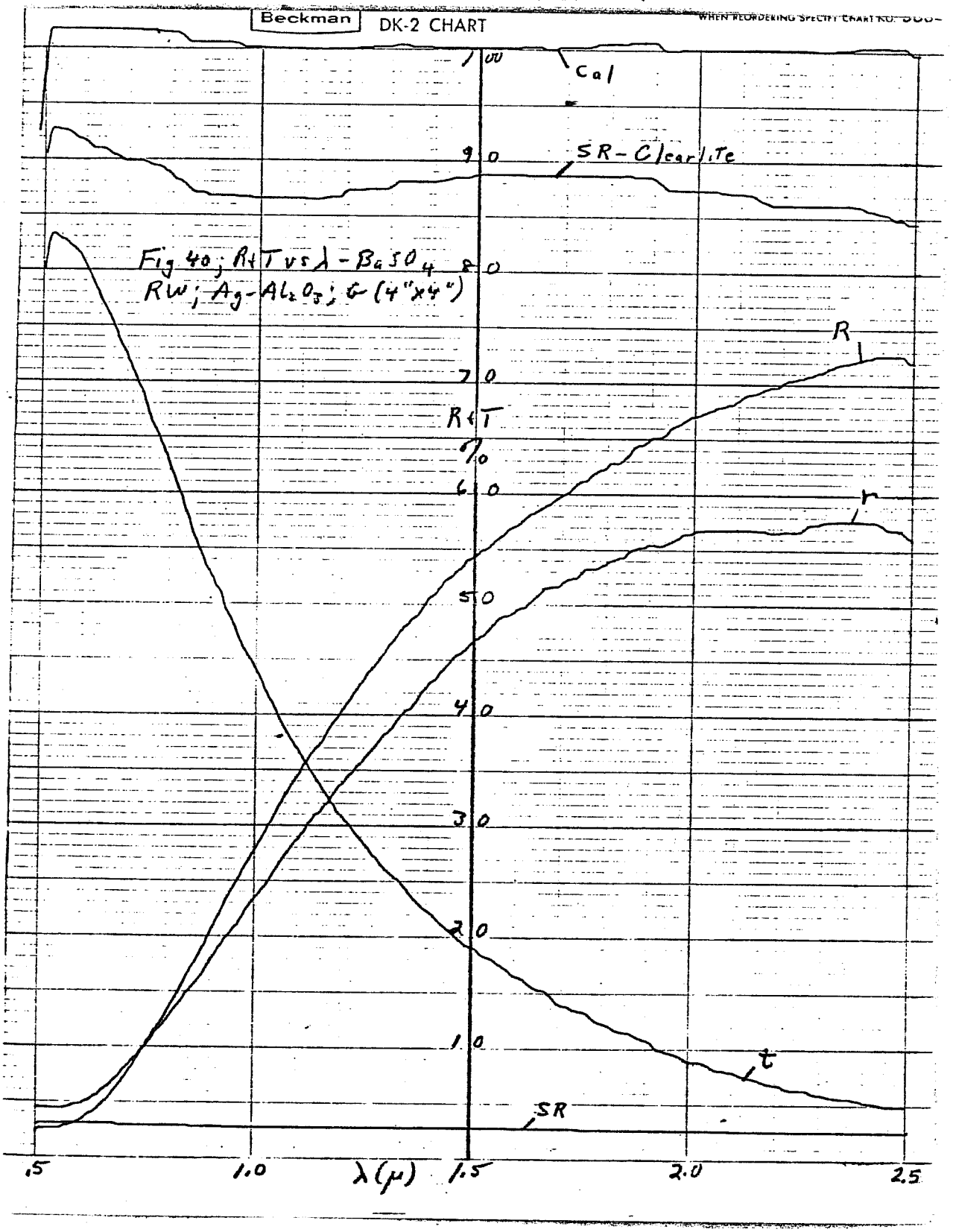
Beckman
DK-2 CHART
100
Cal
90
SR - Clear Lite
80
Fig 40; R+T vs λ - BaSO4
RW; Ag-Al2O3; G (4"x4")
70
R
R+T
%
60
r
50
40
30
20
10
t
SR
.5
1.0
λ(μ)
1.5
2.0
2.5

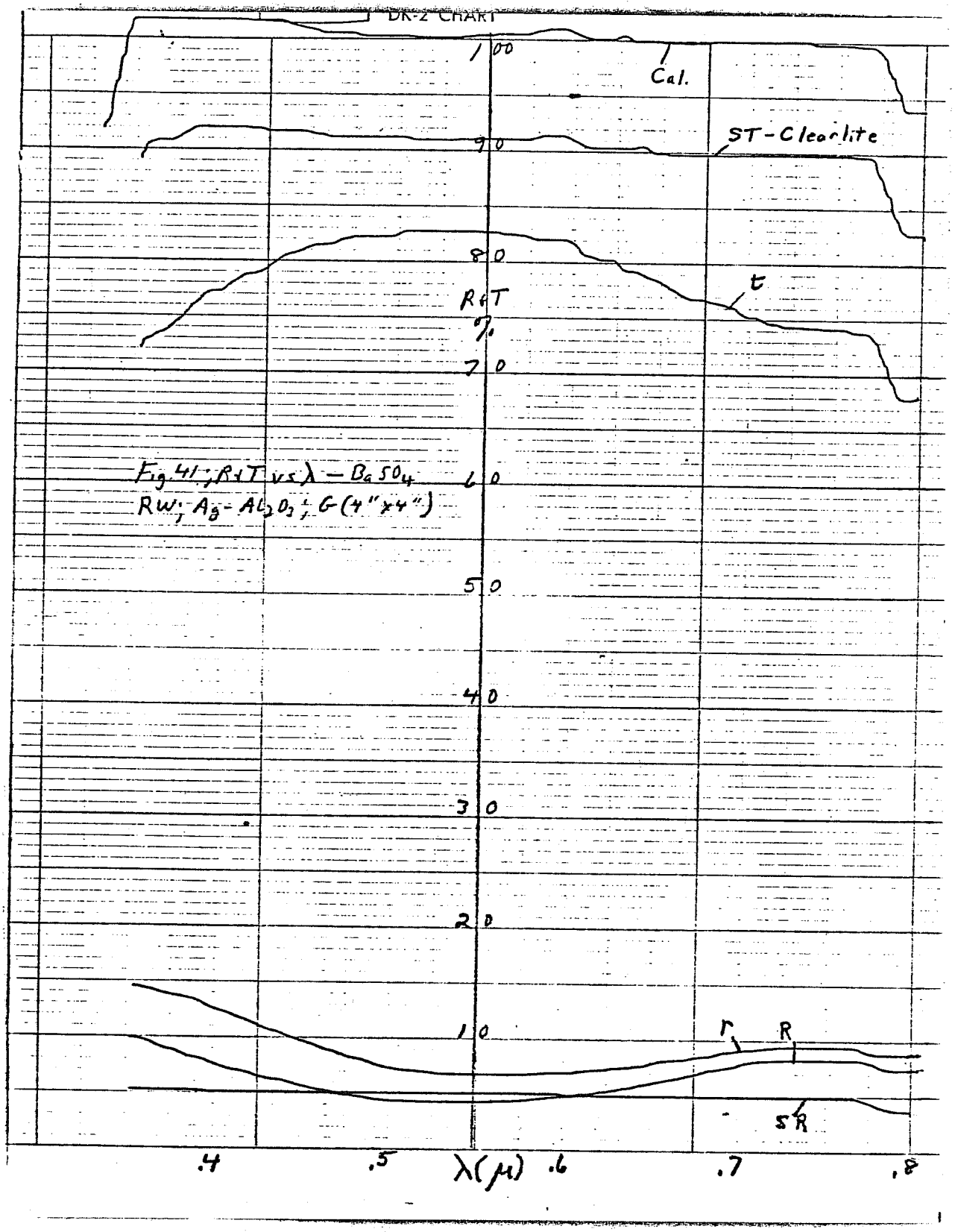

Fig. 41 ; R+T vs λ — $BaSO_4$
RW ; Al_2O_3 ; G (4" x 4")

an anomaly of the spectrometer due to inadequate energy on the slit). In contrast to the previous RW curves, these curves were taken vs. $BaSO_4$ standards and are to present design values. The most obvious difference is that for an R (2.5μ) value of 72-73%, the visible T values are actually higher than those of, for example, sample X-76 (see Figs. 36-37) which has an R (2.5μ) value which is 20% less. This Ag-Al_2O_3 combination also appears to have superior weatherability compared to the Ag-SiO_2 system which has evidenced stress problems. Although further weathering testing is required since this system was tried near the end of the program, it is by present results quite attractive and presents a viable alternative to the Bs based systems.

In order to compare with the type of performance achievable with the more conventional Al based solar control films, the Al-Al_2O_3 combination was tried near the end of the program. As shown in Figs. 42-43, with the R (2.5μ) value set at 73-74%, the visible T values were very low, averaging less than 40%. This is consistent with the commercial solar control films which have an average visible T of less than 20% for higher R values. Clearly the Al based systems are unsuitable for the present type of application. The lack of performance on glass also rules out any potential use on plastic.

In general, no additional work is required to develop a suitable metal-dielectric combination for RW applications. The Bs-Al_2O_3 system, although not studied specifically here, was studied as part of the previous program and is being followed in the weathering studies. Because of the latter, it is considered to be the best system, followed by Bs-SiO_2 and/or Ag-Al_2O_3. If weathering results turn out favorably, the Ag-Al_2O_3 system would be the optimum system.

3.5 Residential Window Retrofits (RWR)

Although only a minor area at the beginning of the program, this area was increasingly emphasized as the program progressed, as an area in which a near term major contribution to energy conservation could be made. Investigations became quite extensive and included the Cu-SiO_2, Bs-SiO_2, Ag-SiO_2, BsAl_2O_3 Ag-Al_2O_3 and Al-Al_2O_3 combinations on polyester and FEP substrates. In

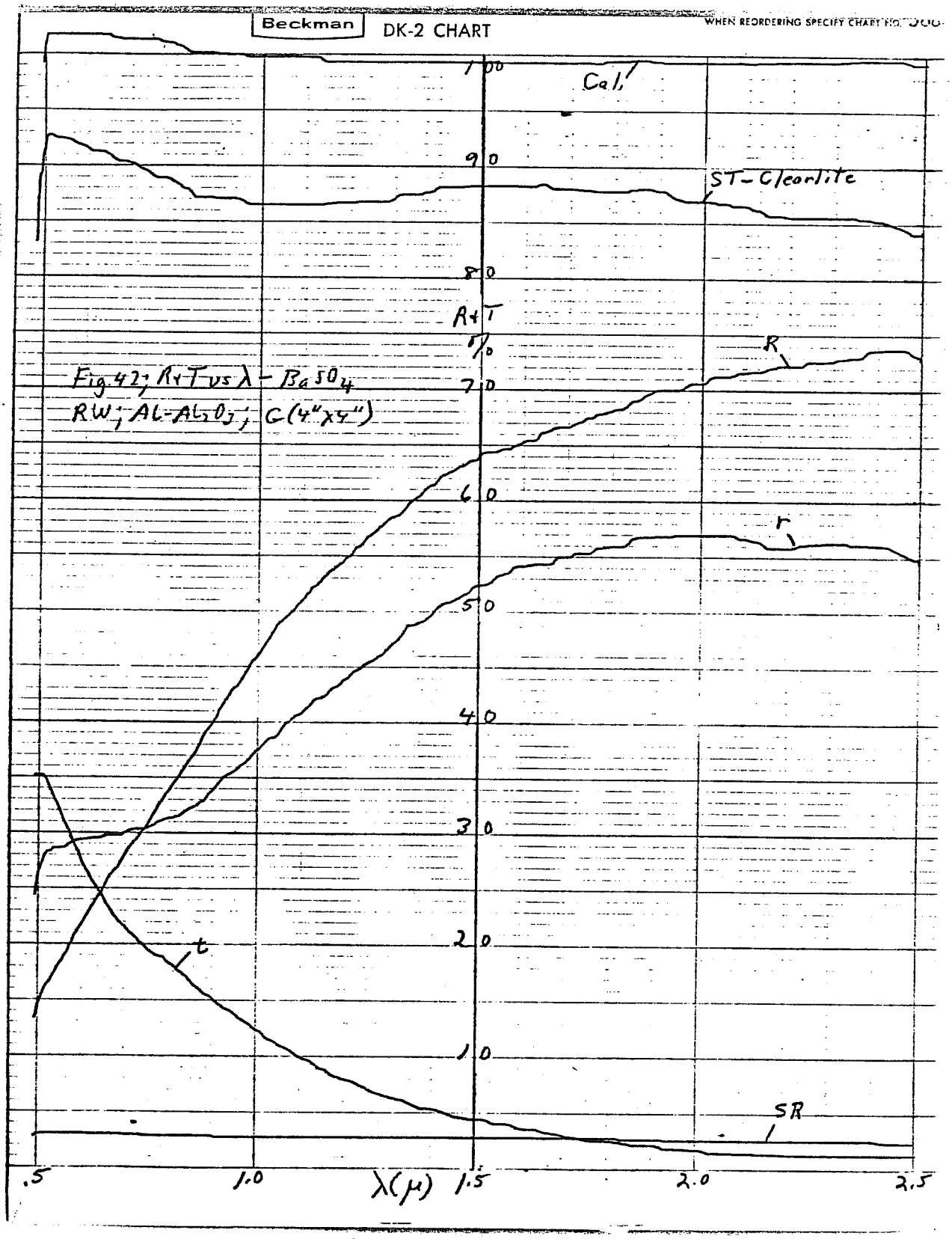
Beckman
DK-2 CHART
WHEN REORDERING SPECIFY CHART NO.
Cal.
ST-Clearlite
R
r
t
SR
R+T
%
100
90
80
70
60
50
40
30
20
10
.5
1.0
1.5
2.0
2.5
λ(μ)
Fig. 42; R+T vs λ - BaSO4
RW; Al-Al2O3; C(4"x4")

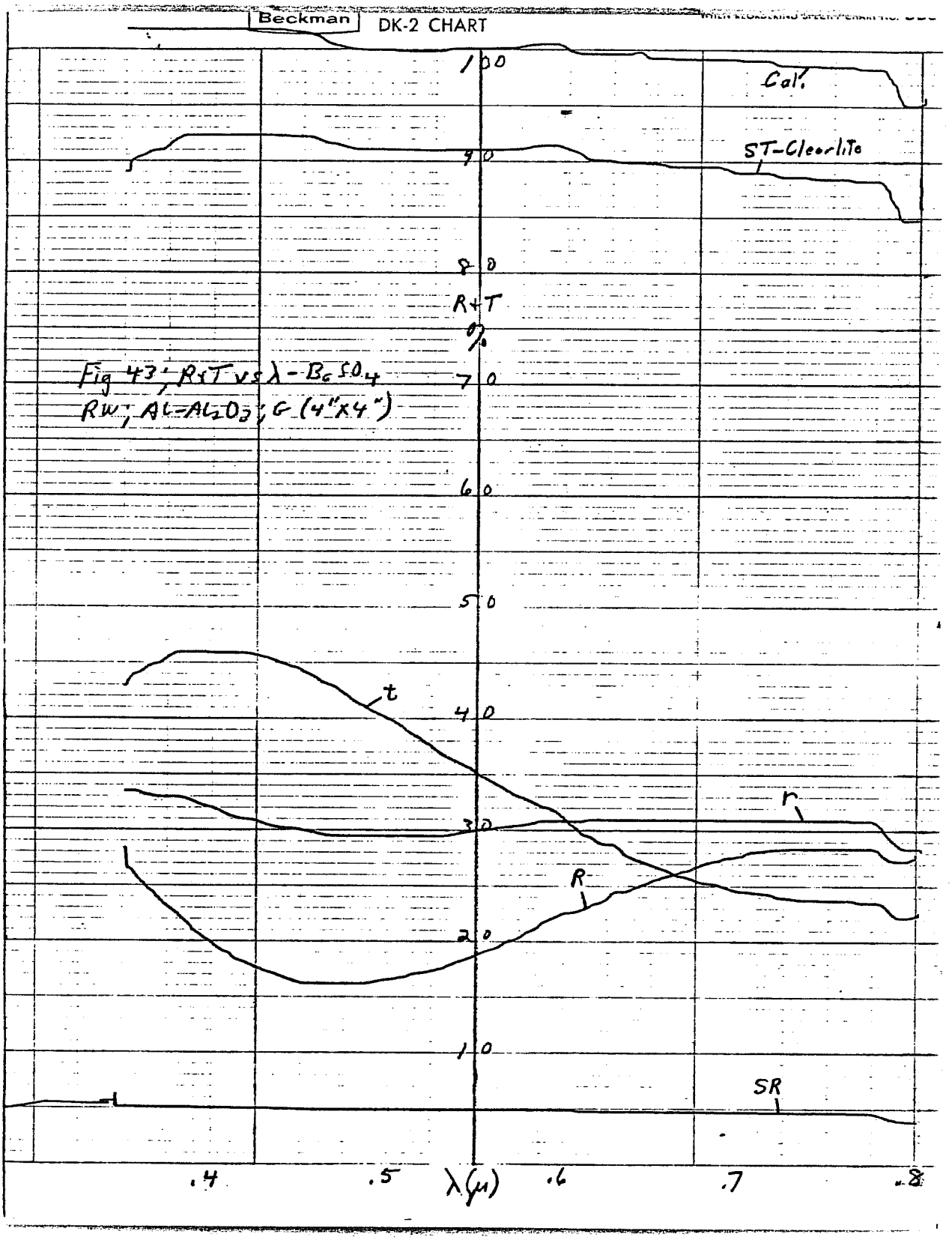

Fig 43; R+T vs λ - $BaSO_4$
RW; Al=Al_2O_3; G (4"x4")

addition, some post program efforts were applied to polypropylene substrates (see Section 6).

The Cu-SiO_2 combination shown in Fig. 44 shows a continuous degradation of R with time. A subsequent set of runs using an improved oxide deposition technique, improved the stability, as shown in Fig. 45, but did not cure the problem. This combination has been eliminated from consideration.

In contrast, the Bs-SiO_2 system, when fully developed, was found to be very stable. As evident in Fig. 46, this combination showed essentially zero degradation with time on polyester substrates. More complete data is given for another sample (X-186) in Figs. 47-50. This particular sample (X-186) was made with a slightly low R (2.5μ) value but had the more critical visible data taken vs. time. The visible T is essentially the same after 405 days (Fig. 49) as it was at zero time (Fig. 50). Within minor variations this is a very stable system.

Bs-SiO_2 on FEP for RWR parameters decreased with time slightly faster than did the equivalent OWRs (Figs. 16-18). Although probably usable in configurations in which the deposit side is glued to the window, overall they were considered unattractive for further development.

Ag-SiO_2 on P resulted in a very attractive combination. Figs. 51-54 show a low R value early sample (X-106). After 639 days of ambient exposure, this sample was identical to the zero time values for practical purposes. As discussed in Section 5, this system is also very resistant to common household solvents etc. and in general is a prime candidate for commercialization.

When applied to FEP substrates, Ag-SiO_2, although being as stable as on P substrates, in general had inferior characteristics. In particular, visible T values (Fig. 56) averaged considerably lower since additional metal had to be deposited to achieve the same R (2.5μ) values (Fig. 55). Characteristics for commercial solar control film have been plotted on these curves in order to show the general differences in design for the different film functions. Although having the same R (2.5μ) value, the very near 1 R (.7 - 1.5μ) and visible R values are much lower for the RWR samples. Solar T is therefore much higher as desired for a heating season residential window. This difference

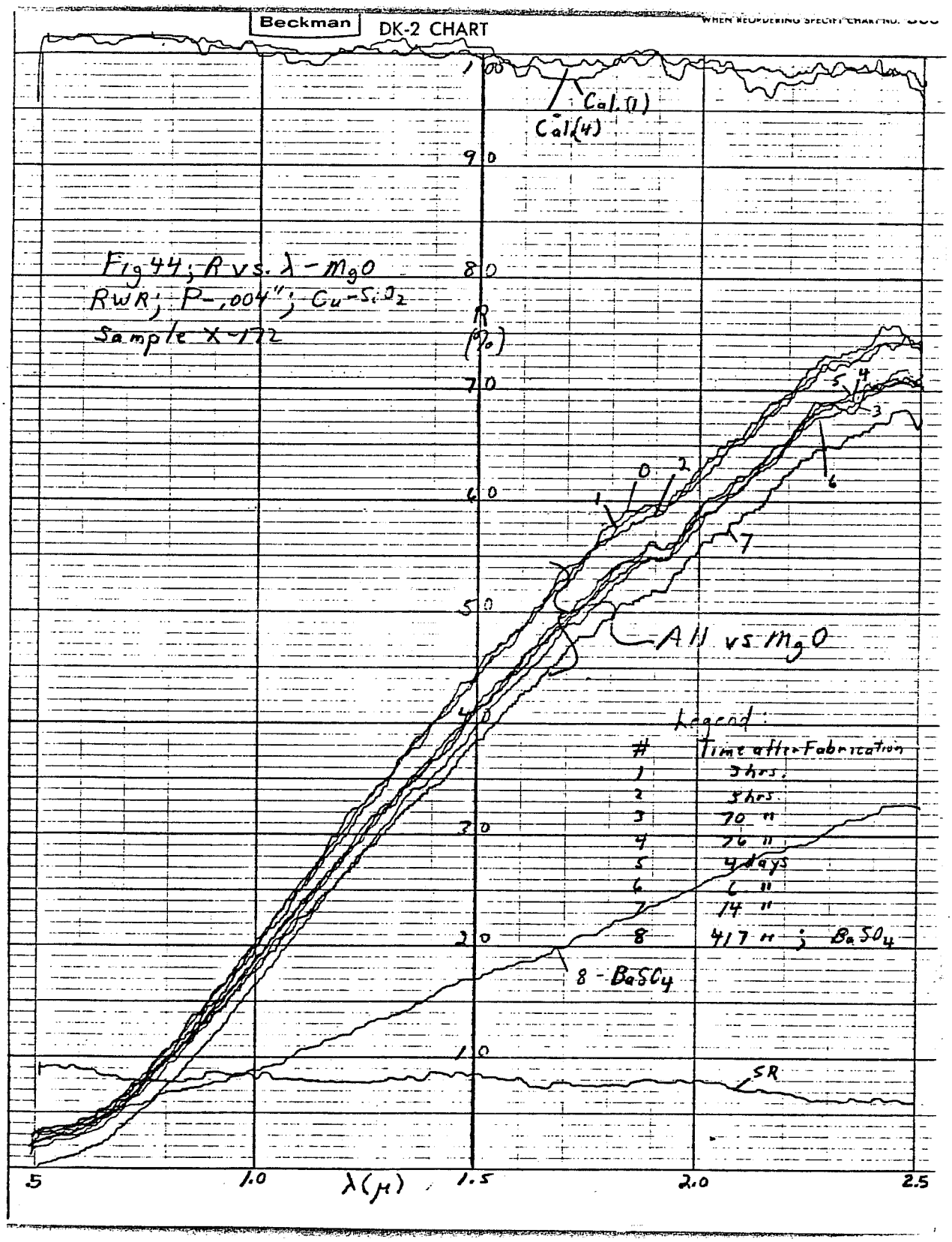
Beckman
DK-2 CHART
Cal.(1)
Cal(4)
Fig 44; R vs. λ - MgO
RWR; P-.004"; Cu-SiO2
Sample X-172
R (%)
100
90
80
70
60
50
40
30
20
10
1
2
3
4
5
6
7
8
Al vs MgO
Legend:
Time after Fabrication
1 3 hrs.
2 5 hrs.
3 70 "
4 76 "
5 4 days
6 6 "
7 14 "
8 417 "; BaSO4
8 - BaSO4
SR
.5
1.0
λ(μ)
1.5
2.0
2.5

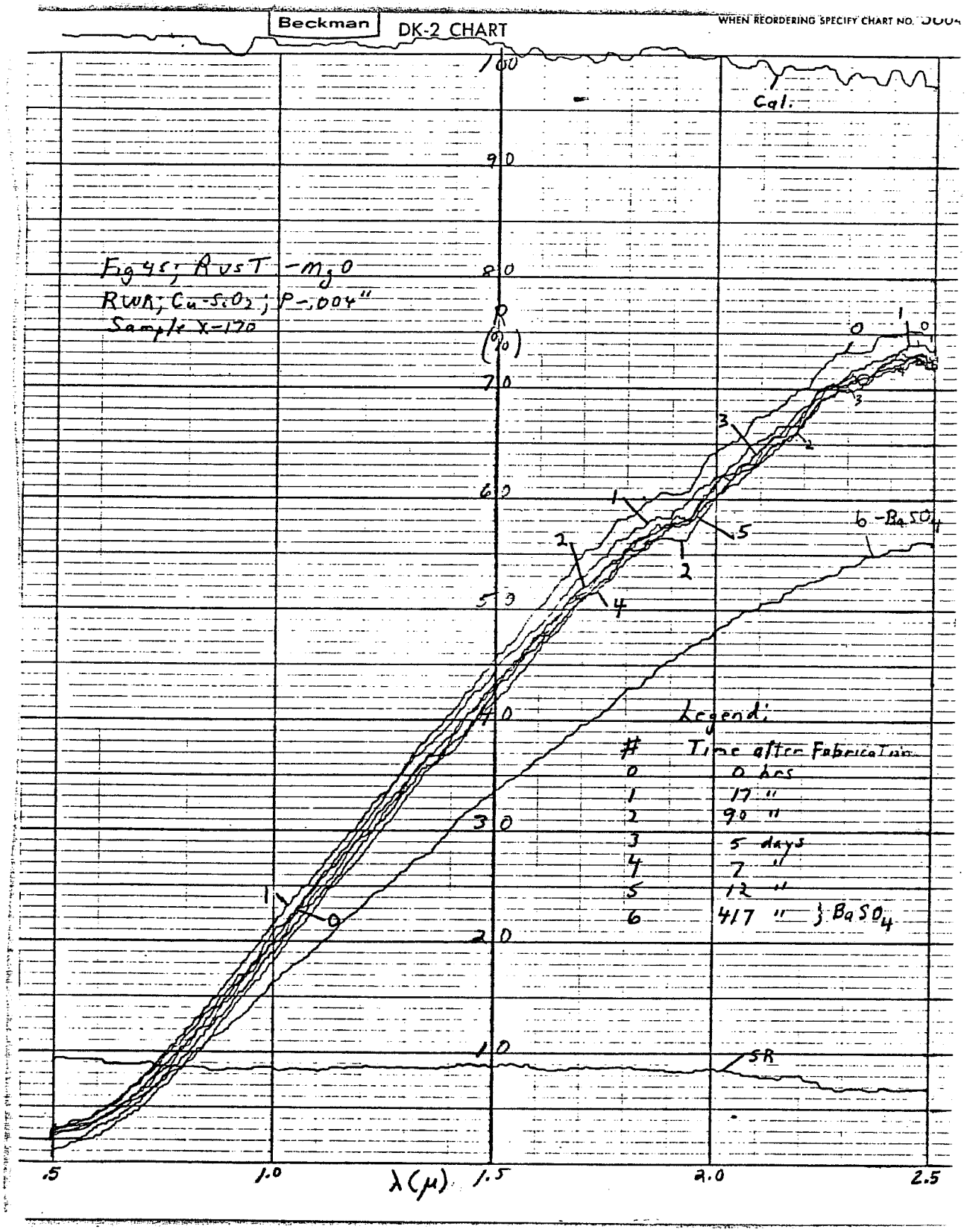
Beckman
DK-2 CHART
WHEN REORDERING SPECIFY CHART NO.
Cal.
Fig 45; R vs T - mgO
RWR; Cu-5.02; P-.004"
Sample X-170
R (%)
100
90
80
70
60
50
40
30
20
10
.5
1.0
λ(μ)
1.5
2.0
2.5
b-BaSO4
SR
Legend:
Time after Fabrication
0 0 hrs
1 17 "
2 90 "
3 5 days
4 7 "
5 12 "
6 417 " + BaSO4

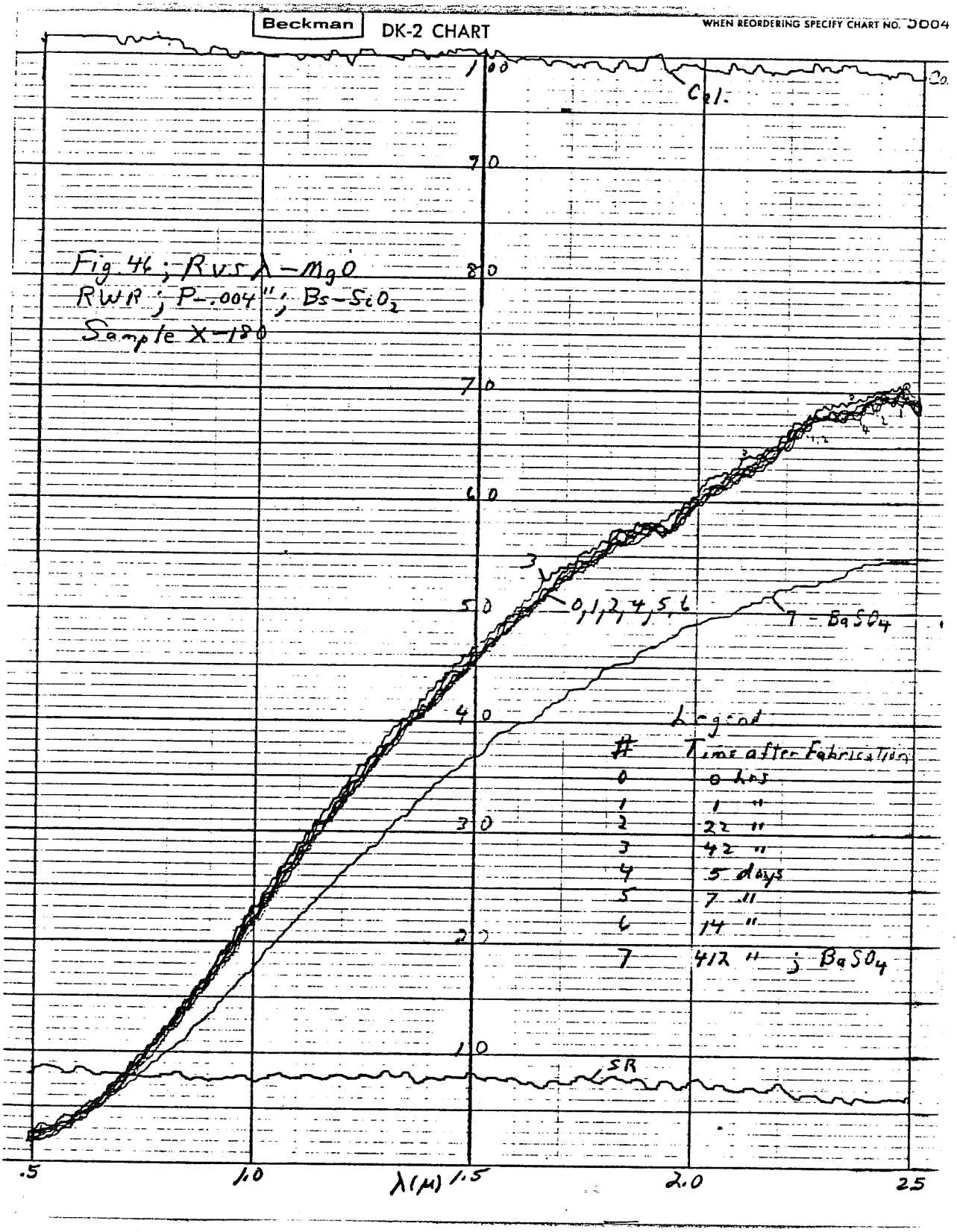
Beckman
DK-2 CHART
WHEN REORDERING SPECIFY CHART NO. 3004
Fig. 46; R vs λ – MgO
RWR; P–.004"; Bs–SiO2
Sample X-180
Ref.
0,1,2,4,5,6
7 = BaSO4
Legend
Time after Fabrication
0 0 hrs
1 1 "
2 22 "
3 42 "
4 5 days
5 7 "
6 14 "
7 412 "; BaSO4
SR
100
90
80
70
60
50
40
30
20
10
.5
1.0
λ(μ) 1.5
2.0
2.5

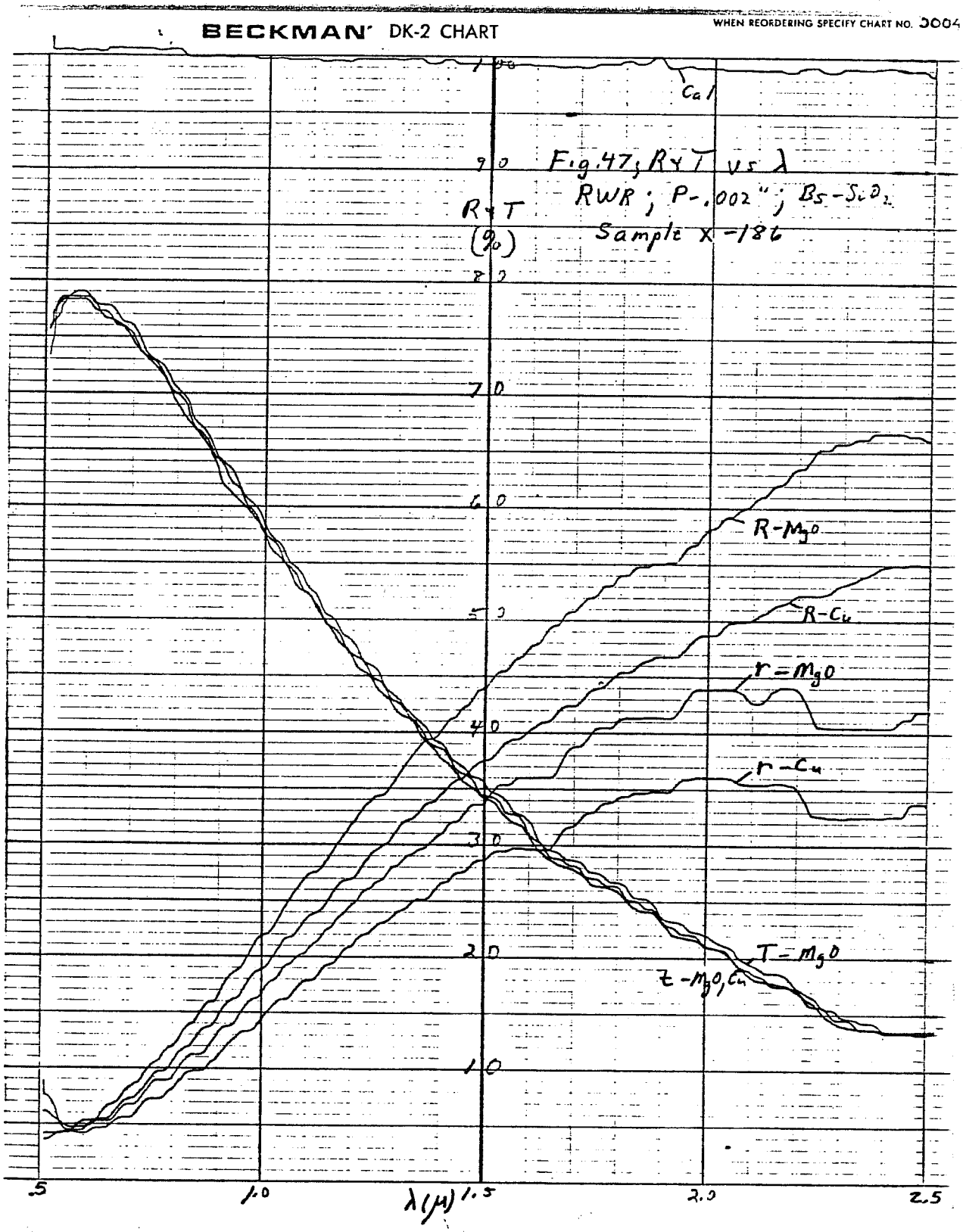
BECKMAN DK-2 CHART
WHEN REORDERING SPECIFY CHART NO. 3004
Cal
Fig. 47; R+T vs λ
RWR ; P-.002" ; Bs-SiO2
Sample X-186
R+T
(%)
100
90
80
70
60
50
40
30
20
10
R-MgO
R-Cu
r-MgO
r-Cu
T-MgO
t-MgO,Cu
.5
1.0
λ(μ) 1.5
2.0
2.5

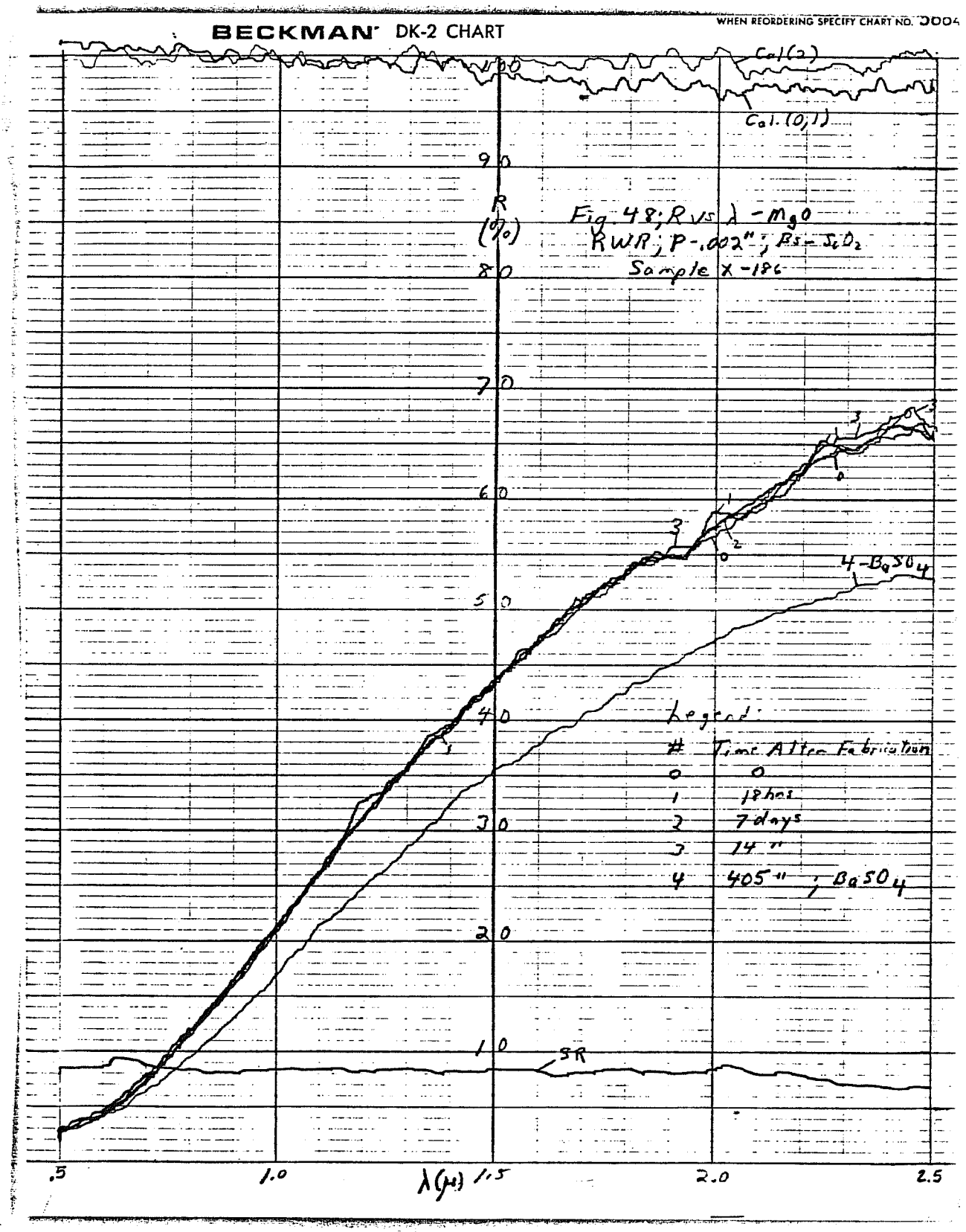
BECKMAN DK-2 CHART
WHEN REORDERING SPECIFY CHART NO. 3004
Cal(2)
Cal. (0,1)
R (%)
Fig. 48; R vs λ - MgO
RWR; P-.002"; Bs - Si O2
Sample X-186
100
90
80
70
60
50
40
30
20
10
3
0
1
2
4-BaSO4
Legend:
Time After Fabrication
0 0
1 18 hrs
2 7 days
3 14 "
4 405 " ; BaSO4
SR
.5
1.0
λ(μ) 1.5
2.0
2.5

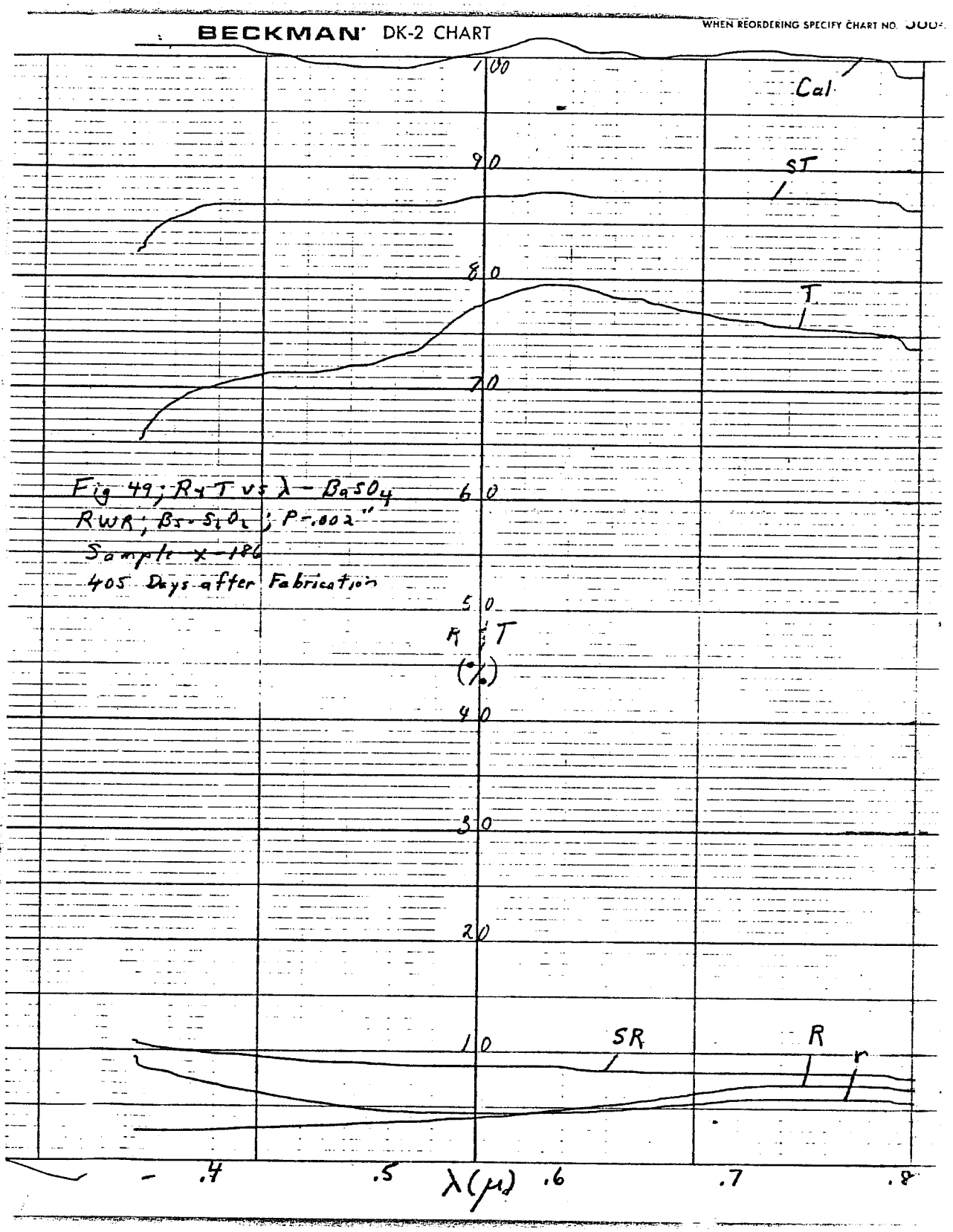
BECKMAN DK-2 CHART
WHEN REORDERING SPECIFY CHART NO.
100
90
80
70
60
50
40
30
20
10
Cal
ST
T
SR
R
r
Fig 49; R+T vs λ - BaSO4
RWR; B5-S10L; P-.002"
Sample x-186
405 Days after Fabrication
R+T (%)
.4
.5
λ(μ)
.6
.7
.8

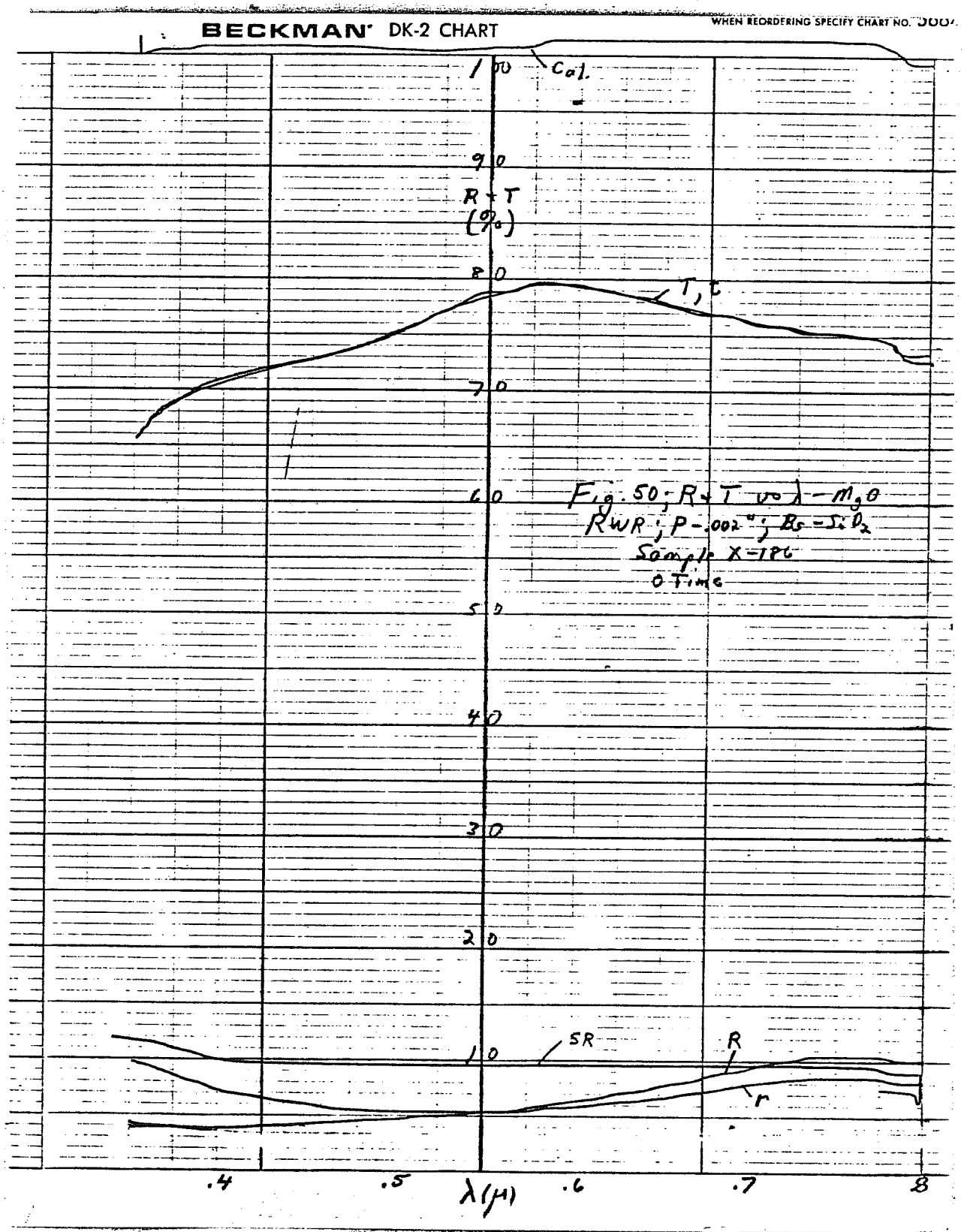
BECKMAN DK-2 CHART
WHEN REORDERING SPECIFY CHART NO. 3004
100
Cal.
90
R+T
(%)
80
T, t
70
60
Fig. 50; R+T vs λ - MgO
RWR; P-.002"; Bs-SiO2
Sample X-186
0 Time
50
40
30
20
10
SR
R
r
.4
.5
λ(μ)
.6
.7
.8

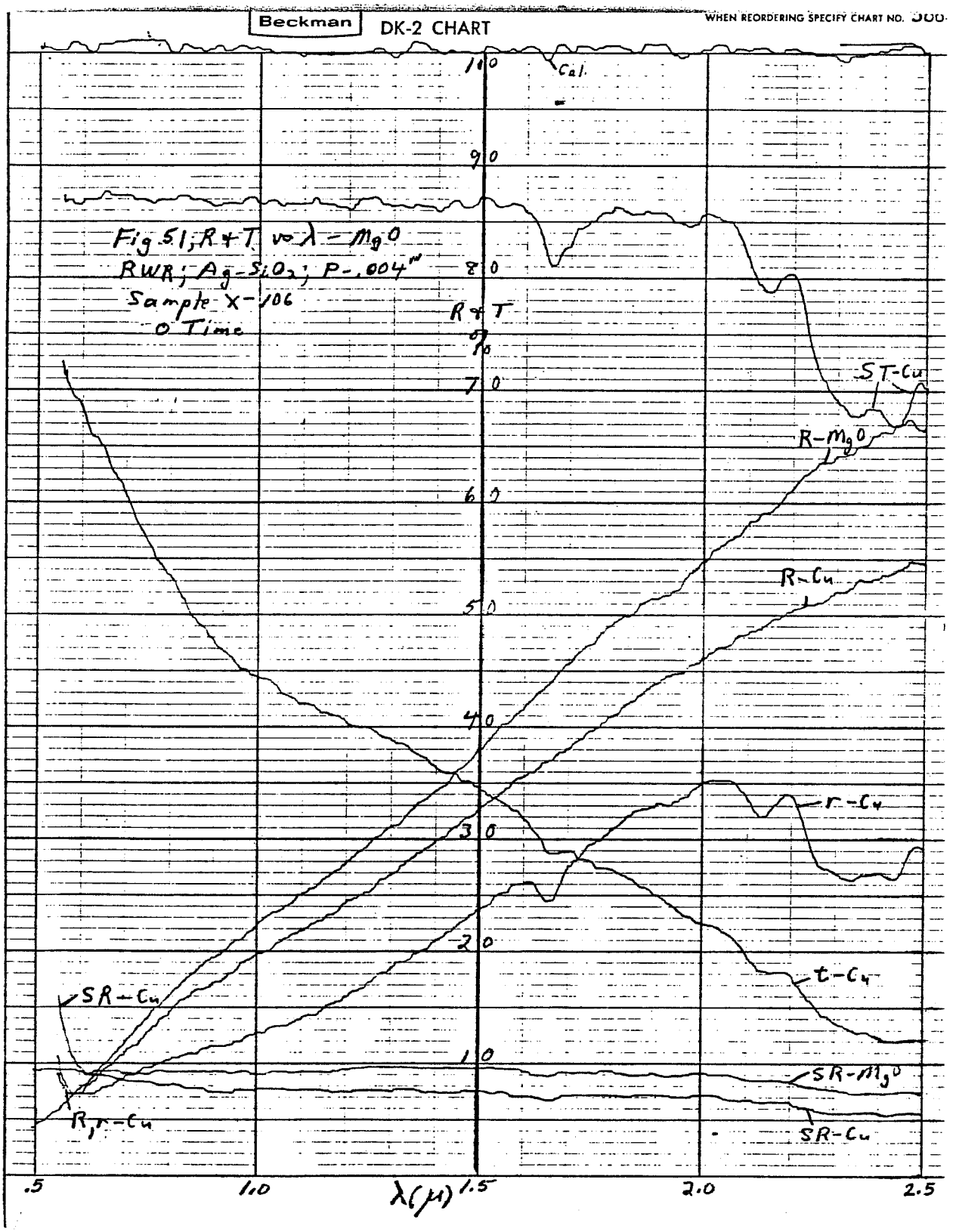
Beckman
DK-2 CHART
WHEN REORDERING SPECIFY CHART NO. 300
Cal.
Fig 51; R+T vs λ = MgO
RWR; Ag-SiO2; P-.004"
Sample X-106
0 Time
R+T
%
110
90
80
70
60
50
40
30
20
10
ST-Cu
R-MgO
R-Cu
r-Cu
t-Cu
SR-Cu
SR-MgO
R,r-Cu
SR-Cu
.5
1.0
λ(μ)
1.5
2.0
2.5

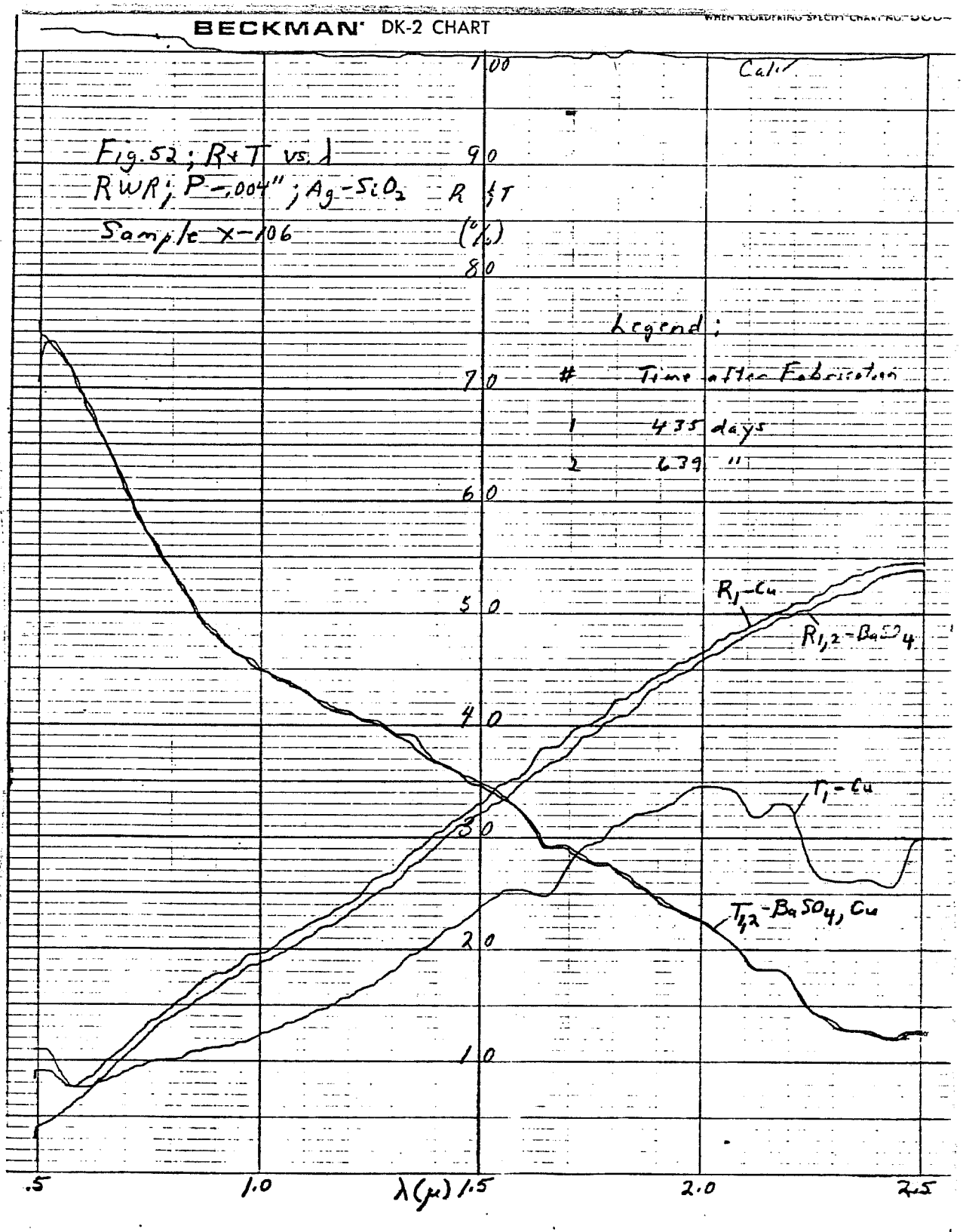
BECKMAN DK-2 CHART
Fig. 52; R+T vs. λ
RWR; P=.004"; Ag-SiO2
Sample X-106
R & T (%)
100
90
80
70
60
50
40
30
20
10
Legend;
Time after Fabrication
1 435 days
2 639 "
R1-Cu
R1,2-BaSO4
T1-Cu
T1,2-BaSO4, Cu
.5
1.0
λ(μ) 1.5
2.0
2.5

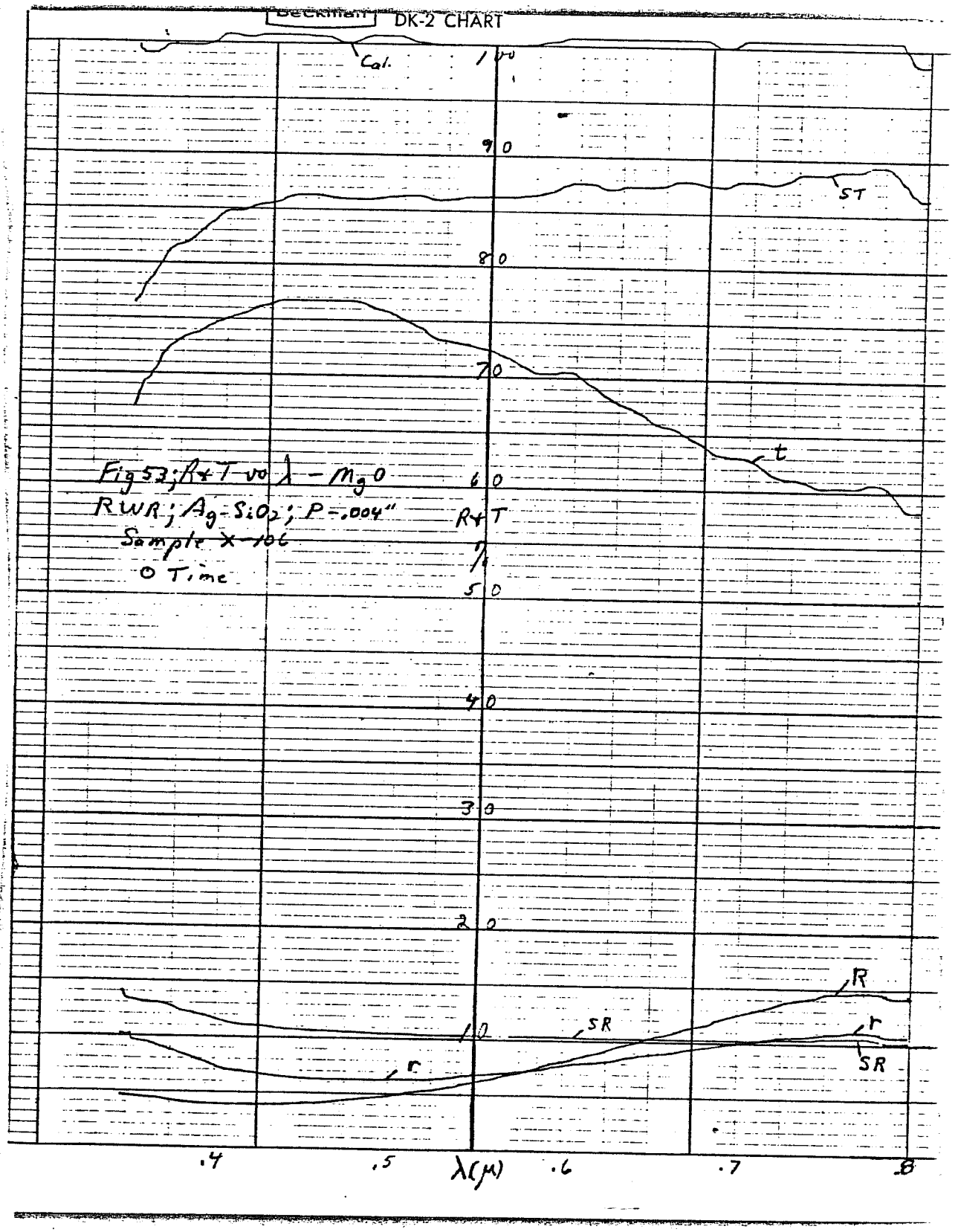

Fig 53; R+T vs λ - MgO
RWR; Ag-SiO2; P=.004"
Sample X-106
O Time

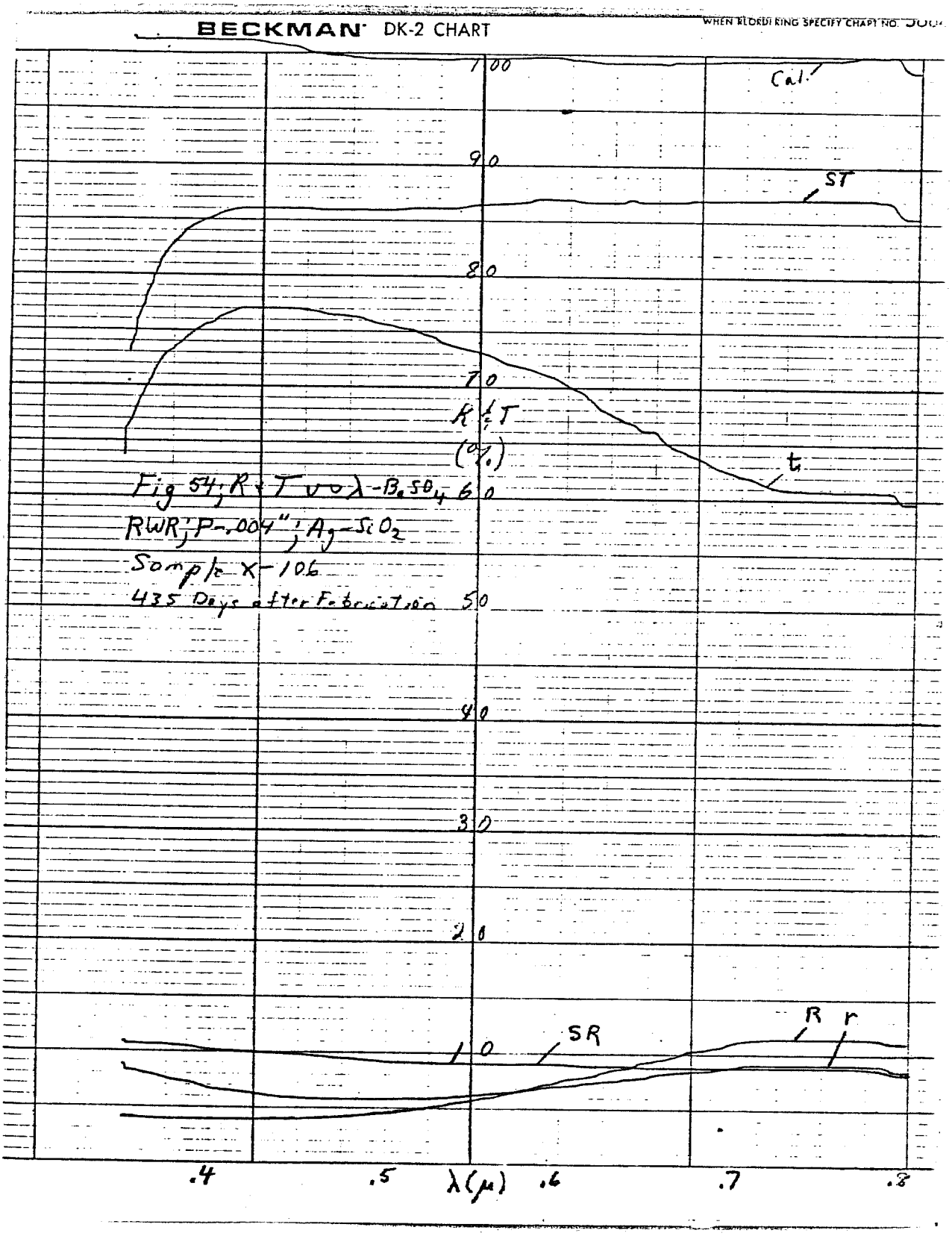
BECKMAN DK-2 CHART
WHEN RECORDING SPECIFY CHART NO. 30
100
90
80
70
60
50
40
30
20
10
Cal.
ST
R & T (%)
t
SR
R
r
Fig 54; R + T vs λ - B2O3 6
RWR; P-.004"; Ag-SiO2
Sample X-106
435 Days after Fabrication
.4
.5
λ(μ)
.6
.7
.8

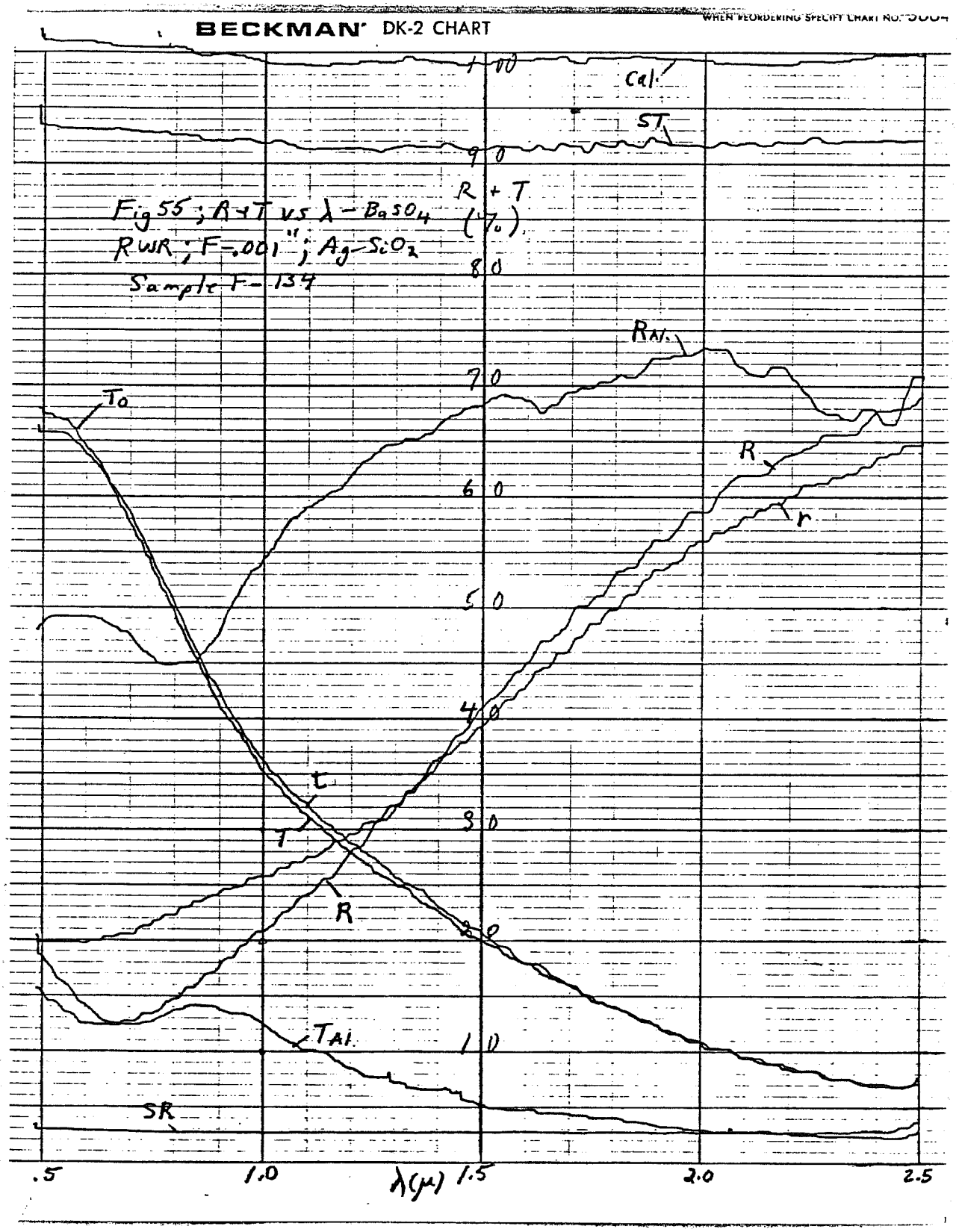
BECKMAN DK-2 CHART
Cal.
ST
R + T (%)
Fig 55 ; R+T vs λ - BaSO4
RWR ; F=.001" ; Ag-SiO2
Sample F-134
RAl.
To
R
r
T
R
TAl.
SR
.5
1.0
λ(μ)
1.5
2.0
2.5

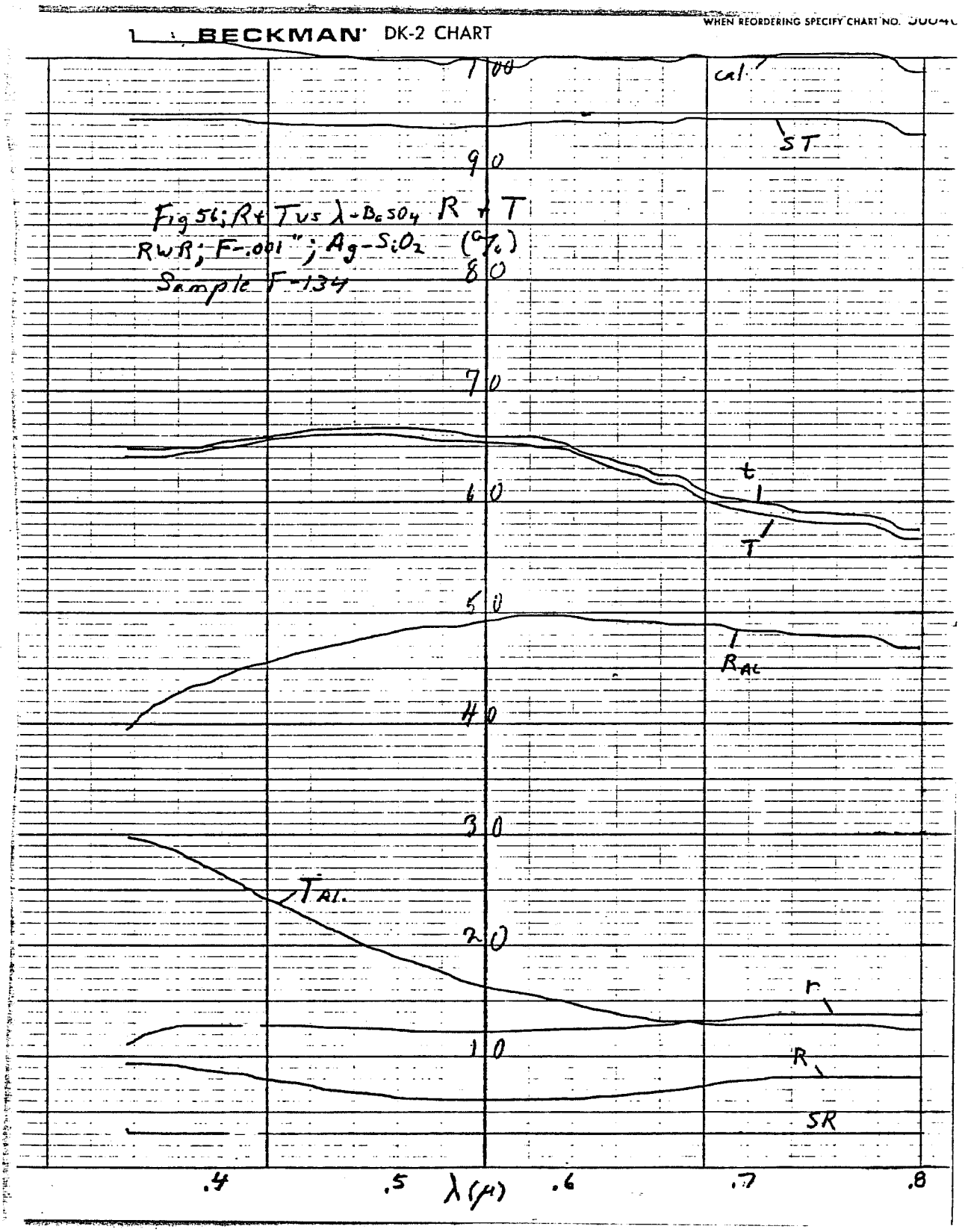
BECKMAN DK-2 CHART
WHEN REORDERING SPECIFY CHART NO.
100
90
80
70
60
50
40
30
20
10
cal.
ST
Fig 56; R+T vs λ - BaSO4 R + T
RWB; F-.001"; Ag-SiO2 (%)
Sample F-134
t
T
RAL
TAL.
r
R
SR
.4
.5
λ(μ)
.6
.7
.8

is, of course, much more pronounced for the higher transmission RWR configurations (e.g. Ag-Al_2O_3 - Fig. 62). OWRs, on the other hand, as seen previously have characteristics yielding higher very near IR reflectivities while maintaining lower visible R values and higher visible T values.

Bs-Al_2O_3 on P (Figs. 57-58) yields an apparently stable structure but the visible T values are surprisingly low compared to those for the Bs-SiO_2 system. Comparision of these low T values with other combinations, in particular Bs-Al_2O_3 on FEP (Figs. 59-60) which should have lower T values but doesn't, implies something was wrong during fabrication of these samples. The problem can only be pinpointed by making additional samples. Since the Bs-SiO_2 system is quite stable etc. and cheaper to produce, no further effort is planned on this combination.

When applied to FEP, Bs-Al_2O_3 resulted in a somewhat less stable structure (Figs. 59-60) than on P. This combination has been deferred in favor of alternate combinations.

Ag-Al_2O_3 on P or FEP results in a favorable combination. Curves are shown in Figs. 61-62 for three slightly different variations around the normal R (2.5μ) value. Although sample X-209 has a slightly smaller amount of metal (since R 2.5μ is lower), samples X-212 and X-213 have higher average visible T values due to oxide overcoats roughtly 50% thicker. In production the extra transmission has to be weighed against the cost of depositing the extra Al_2O_3. These samples showed no ambient degradation after 10 months and the combination is considered very viable for production. All delivered demonstration sample for the roller system (Section 6) used Ag-Al_2O_3.

On FEP (Fig. 63-64), the Ag-Al_2O_3 is believed to be stable although the samples are not subject to as many time related measurements due to their tendency to wrinkle on handling. This wrinkling makes reflectivity measurements quite difficult. Although individual measurements on different samples indicate slight changes (e.g. R in Fig. 63) the overall indication is stability (Note: R relatively unchanged in Fig. 63). Some samples have been set aside after only a preliminary zero time measurement (R at 2.5μ) and will be remeasured after one year. In any event, the use of FEP for RWRs with deposited coating glued

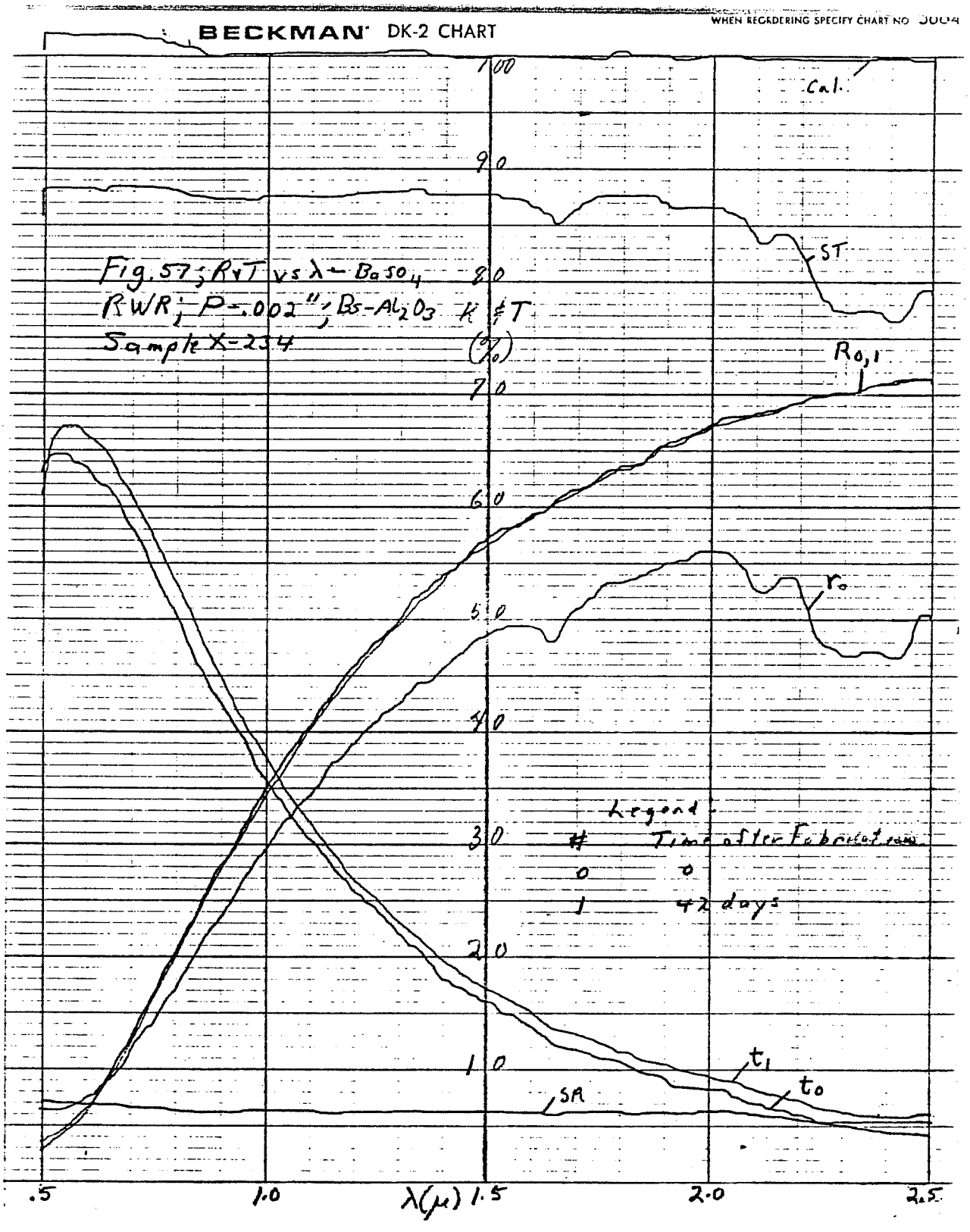
BECKMAN DK-2 CHART
WHEN REORDERING SPECIFY CHART NO 30084
Fig. 57; RvT vs λ - BaSO4
RWR; P=.002"; Bs-Al2O3 K & T
Sample X-234
100
90
80
70
60
50
40
30
20
10
(%)
Cal.
ST
R0,1
r0
t1
t0
SR
Legend
Time after Fabrication
0 0
1 42 days
.5
1.0
λ(μ) 1.5
2.0
2.5

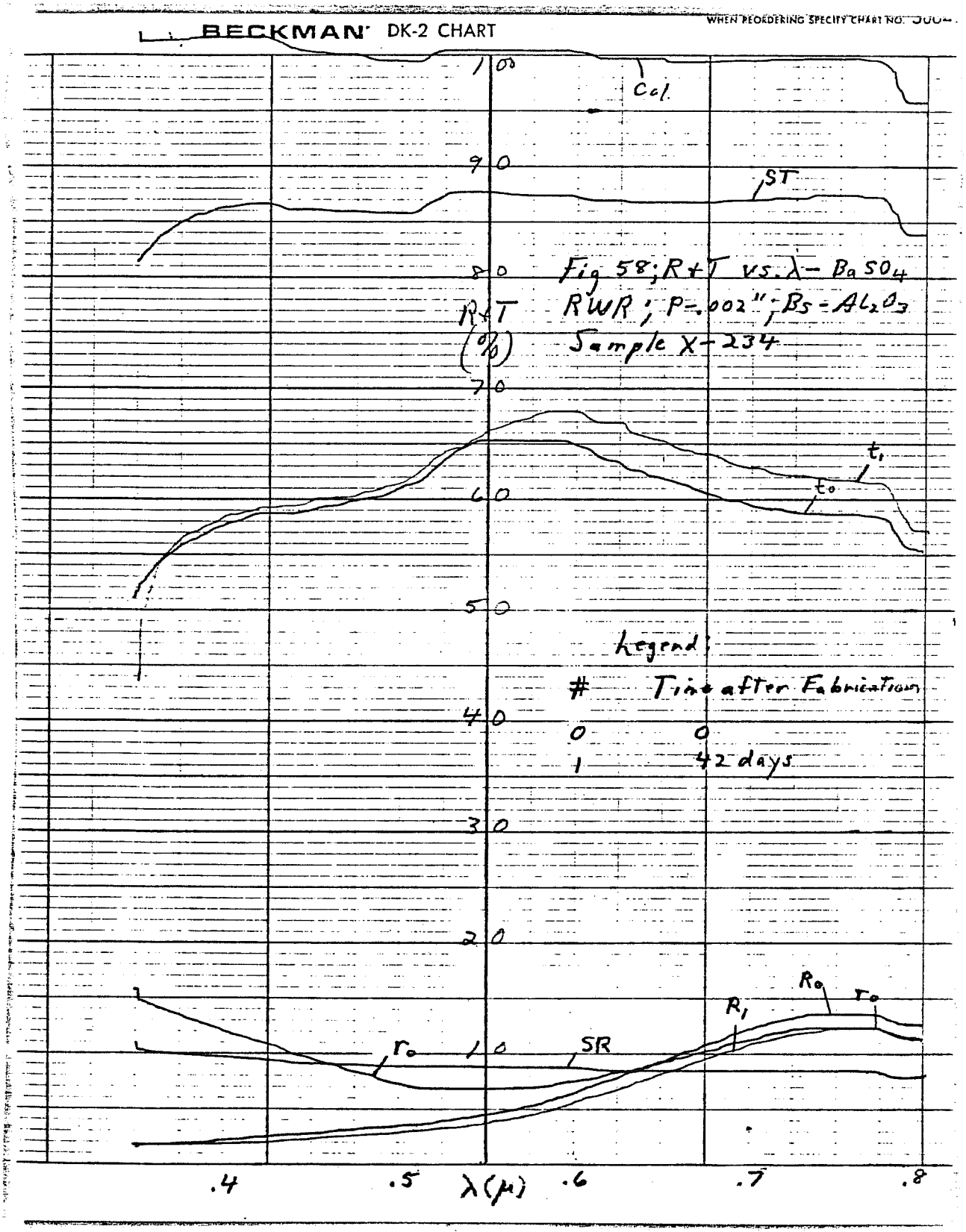
BECKMAN DK-2 CHART
WHEN REORDERING SPECIFY CHART NO. 5004
100
90
80
70
60
50
40
30
20
10
Cal.
ST
R+T (%)
Fig 58; R+T vs. λ - BaSO4
RWR; P=.002"; Bs = Al2O3
Sample X-234
t1
t0
Legend:
Time after Fabrication
0 0
1 42 days
R0
r0
R1
r0
SR
.4
.5
λ(μ)
.6
.7
.8

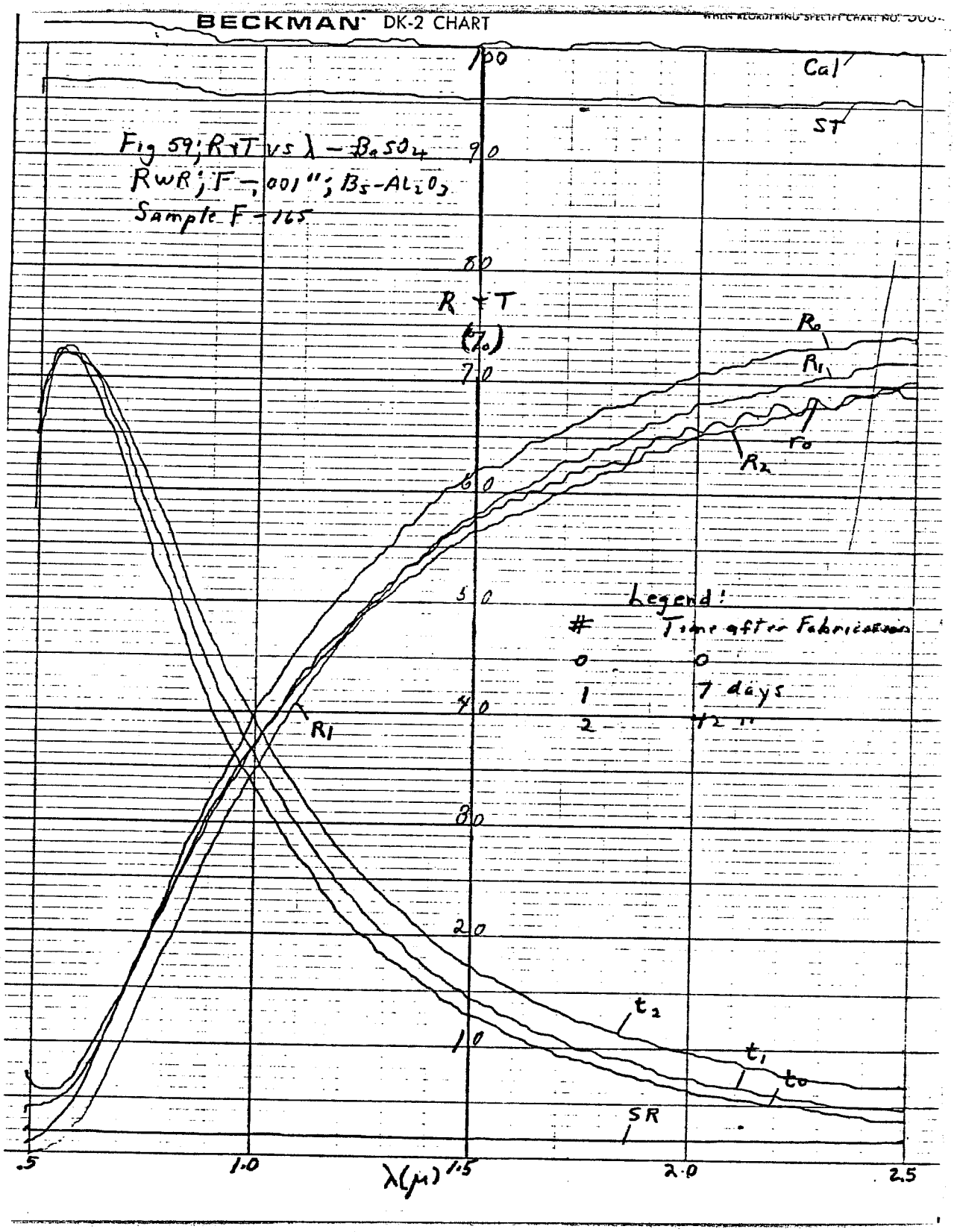
BECKMAN DK-2 CHART
Cal
ST
Fig 59; R+T vs λ – $BaSO_4$
RwR; F – .001"; $Bs-Al_2O_3$
Sample F-165
100
90
80
R + T
(%)
70
60
50
40
30
20
10
R_0
R_1
R_2
F_0
R_1
Legend:
Time after Fabrication
0 0
1 7 days
2 12 "
t_2
t_1
t_0
SR
.5
1.0
λ(μ) 1.5
2.0
2.5

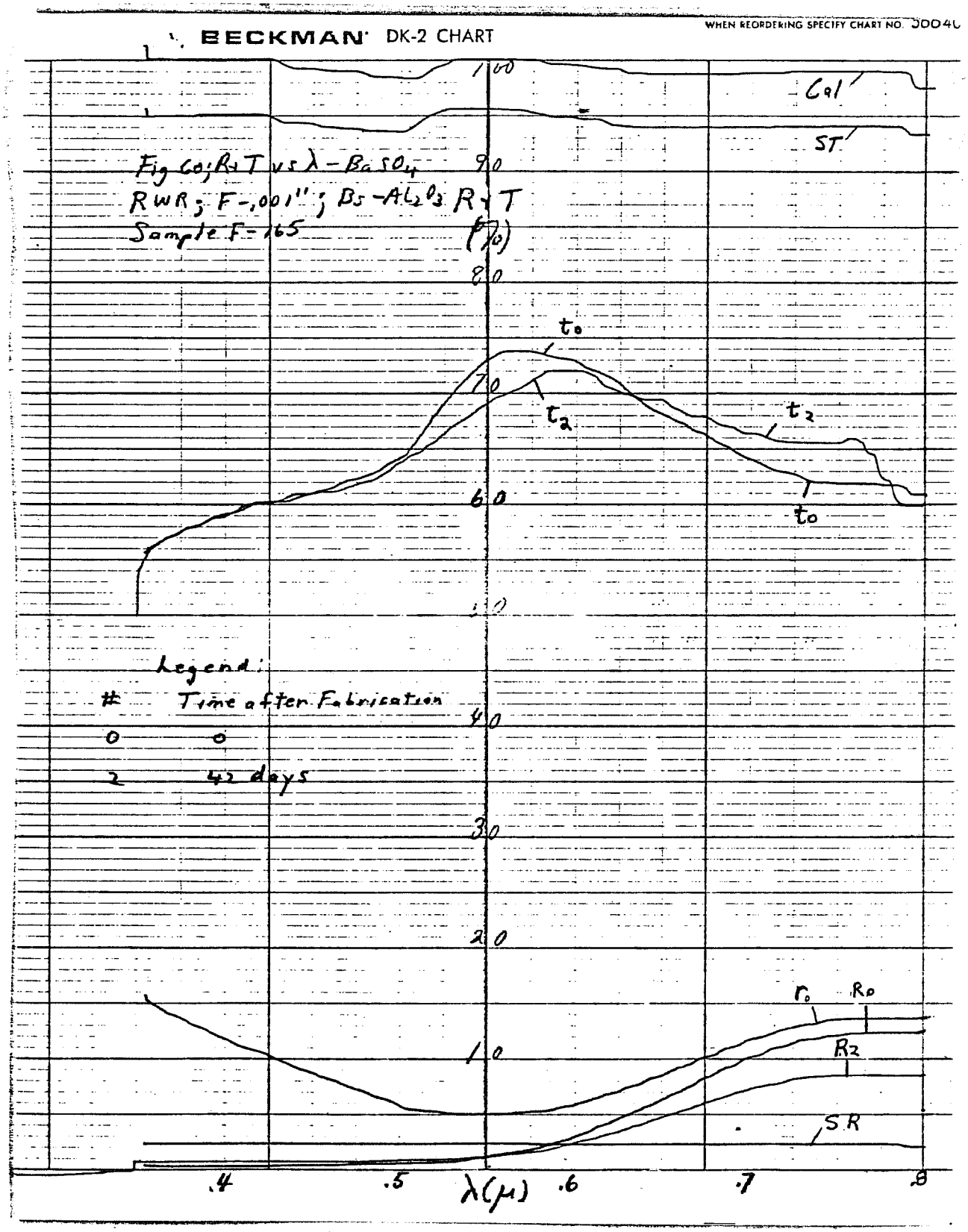
BECKMAN DK-2 CHART
WHEN REORDERING SPECIFY CHART NO. 30040
Col
ST
Fig 60; R+T vs λ - BaSO4
RWR; F-.001"; B5 - Al2O3 R+T
Sample F-165
(%)
100
90
80
70
60
40
30
20
10
t0
t2
t2
t0
Legend:
Time after Fabrication
0 0
2 42 days
r0
R0
R2
SR
.4
.5
λ(μ)
.6
.7
.8

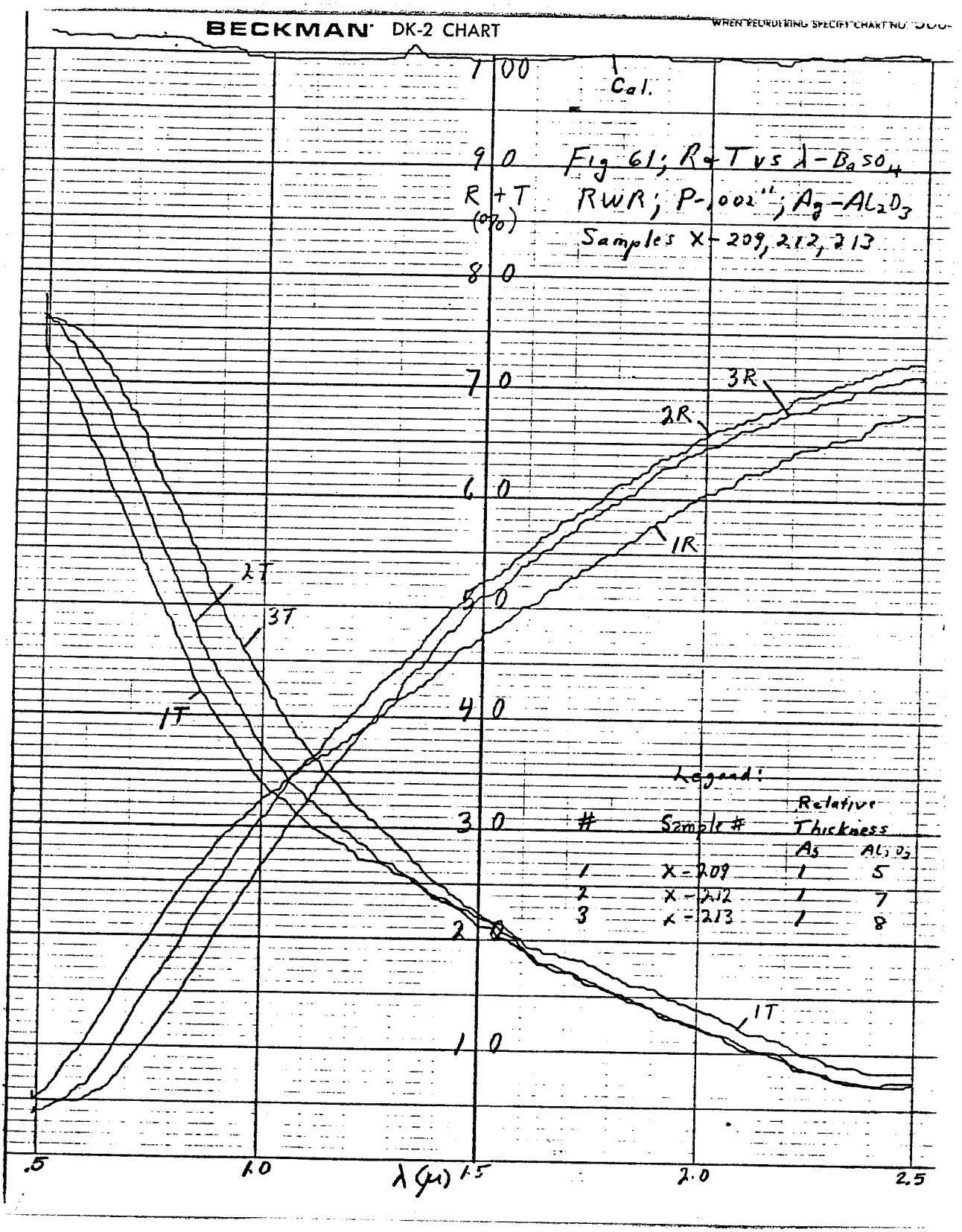
BECKMAN DK-2 CHART
Cal.
Fig 61; R+T vs λ - BaSO4
RWR; P-.002"; Ag - AL2O3
Samples X-209, 212, 213
R+T (%)
100
90
80
70
60
50
40
30
20
10
3R
2R
1R
2T
3T
1T
Legend:
Sample # Relative Thickness As AL2O3
1 X-209 1 5
2 X-212 1 7
3 X-213 1 8
.5
1.0
λ (μ) 1.5
2.0
2.5

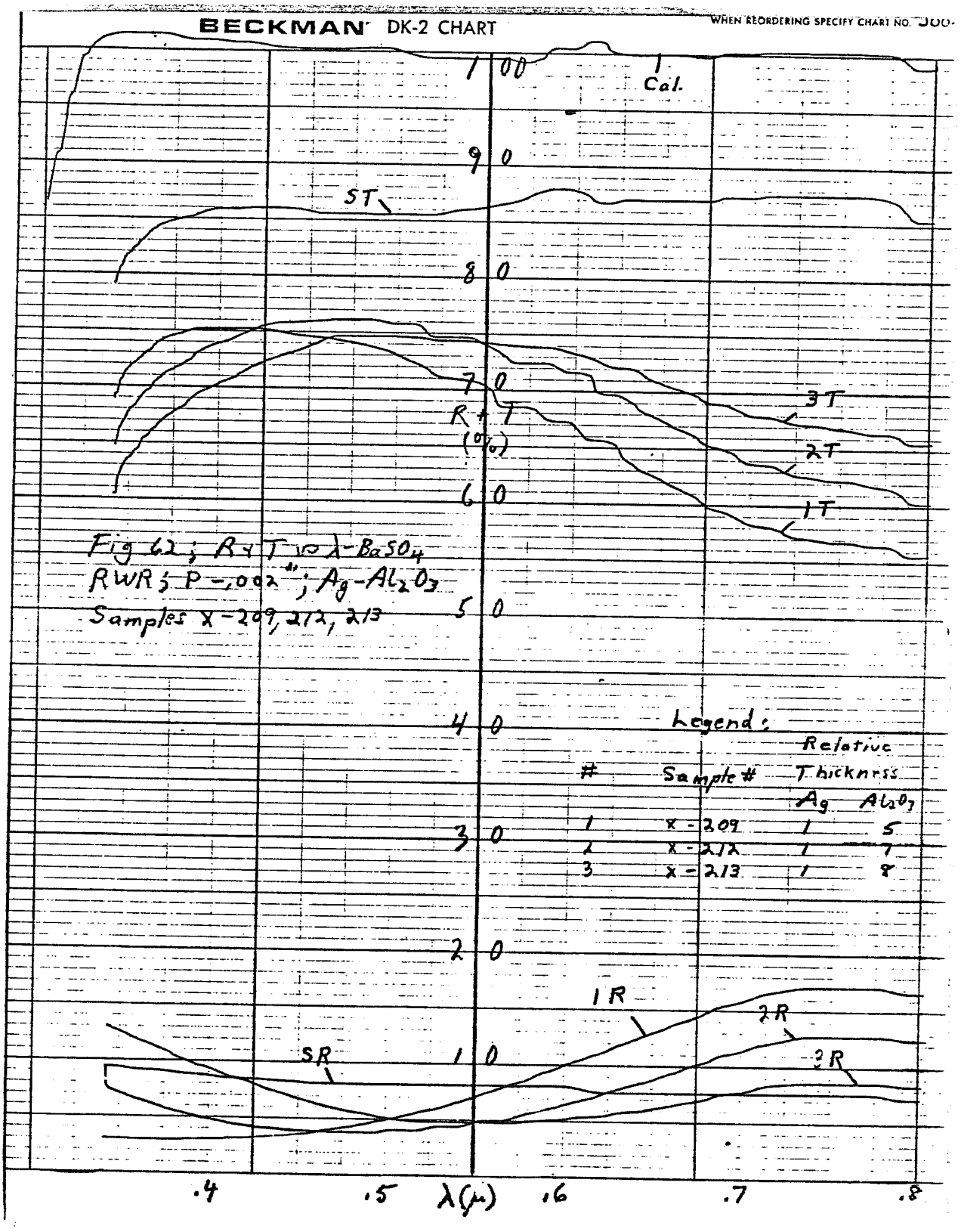
BECKMAN DK-2 CHART
WHEN REORDERING SPECIFY CHART NO. 300-
100
Cal.
90
ST
80
70
R + T
(%)
3T
2T
1T
60
50
40
30
20
10
1R
2R
3R
SR
.4
.5
λ(μ)
.6
.7
.8
Fig 62; R+T vs λ-BaSO4
RWR; P-.002"; Ag-Al2O3
Samples X-209, 212, 213
Legend:
Sample # Relative Thickness Ag Al2O3
1 X-209 1 5
2 X-212 1 7
3 X-213 1 8

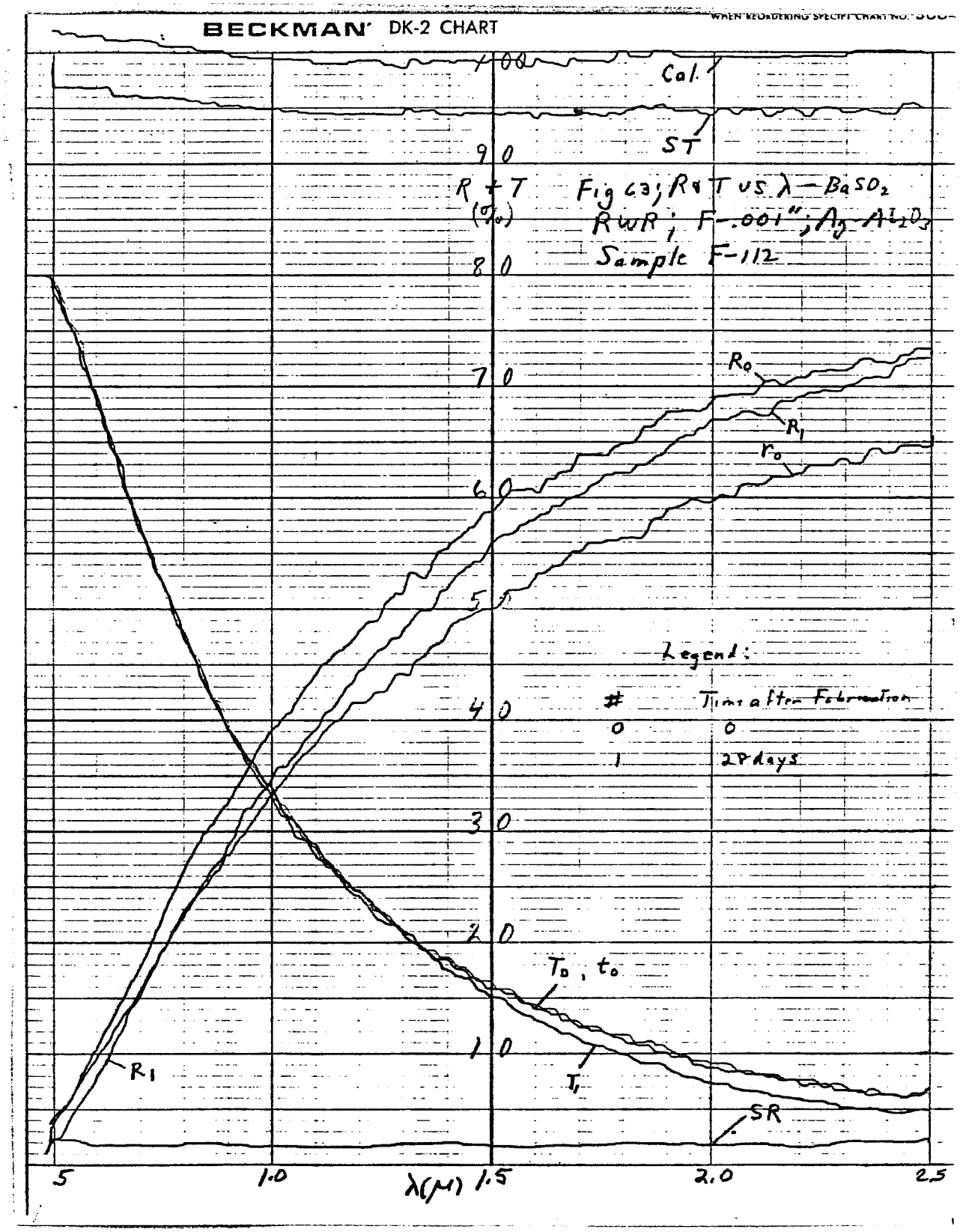
BECKMAN DK-2 CHART
Cal.
ST
R + T
(%)
Fig 23; R+T vs λ — BaSO4
RwR; F-.001"; Ag-Al2O3
Sample F-112
R0
R1
r0
Legend:
Time after Fabrication
0 0
1 28 days
TD, t0
T1
R1
SR
100
90
80
70
60
50
40
30
20
10
.5
1.0
1.5
2.0
2.5
λ(μ)

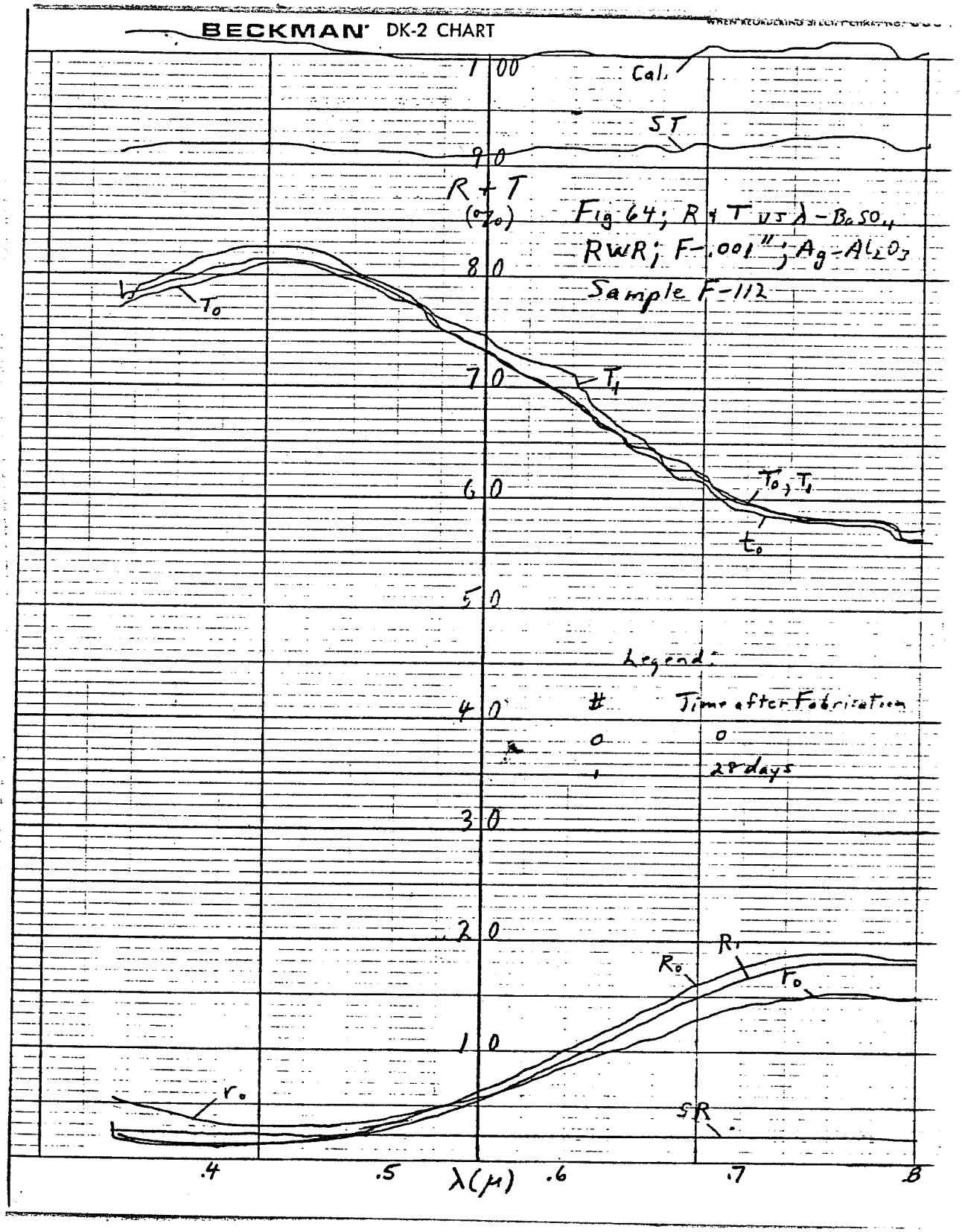
BECKMAN DK-2 CHART
100
Cal.
ST
90
R + T
(%)
80
70
60
50
40
30
20
10
Fig 64; R + T vs λ - BaSO4
RWR; F-.001"; Ag-Al2O3
Sample F-112
T0
T1
T0, T1
t0
Legend:
Time after Fabrication
0 0
28 days
R1
R0
r0
SR
.4
.5
λ(μ)
.6
.7
.8

to window configuration has been deferred in favor of other possible combinations.

One final check was made on the potential use of Al. Figs. 65-66 give the characteristics for an RWR sample using Al-Al_2O_3 on P. Even for a slightly low R value at 2.5μ (Fig. 65), the visible T values are impossibly low. It is quite clear that the characteristics developed for OW and RW applications under this program cannot be achieved with Al as the reflecting material. It is also clear that the necessary values and stability can be achieved with Bs-SiO_2, Ag-SiO_2 or Ag-Al_2O_3.

3.6 Long Wavelength Infrared

Although there were a great many samples generated during the program, it was only possible to take full long wavelength IR measurements for selected ones. The instruments used for the measurements (Perkin-Elmer 337) was in constant use and only limited time was available. It was, however, quickly established that the R values at 10μ were clearly indicative of the entire curve shape from 2.5 to 10μ and up and for fast measurement or for spot checks, the 10μ values were used. After the program was over, some time was obtained on a new Perkin-Elmer 283B instrument which was used primarily to measure 10μ values on a large selection of glued samples (i.e. plastic retrofits glued to glass substrates). The measured values on these later glued films (Section 5) ran higher than most of the unglued films or early glued films which were subject to poor technique.

Severe difficulties were encountered in obtaining reliable data in these longer wavelength measurements, particularly for FEP substrates. The specular reflectance attachment for the spectrometer required such critical angular positioning that only the glass substrate standard gave 100% reproducible results. Any folds, dents etc. in the plastic films, no matter how minor, frequently caused large changes in R. To alleviate the problem for unglued samples, and to prevent noise (in the form of ambient light) from reaching the detector through the film, all measurements were made with the plastic films backed in

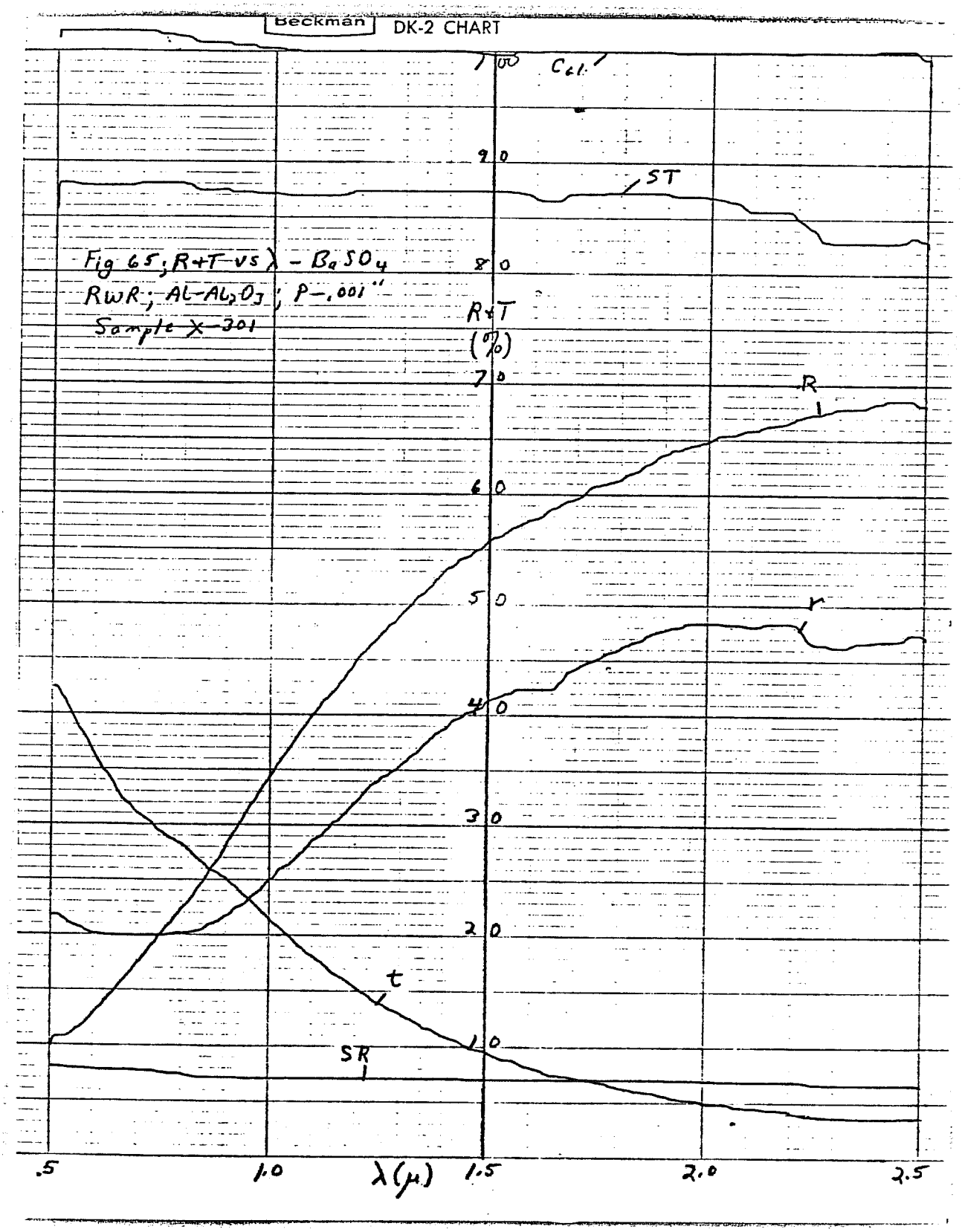
Beckman DK-2 CHART
Cal.
100
90
ST
Fig 65; R+T vs λ - BaSO4
RwR; Al-Al2O3; P-.001"
Sample X-301
80
R+T
(%)
70
R
60
50
r
40
30
20
t
10
SR
.5
1.0
λ(μ)
1.5
2.0
2.5

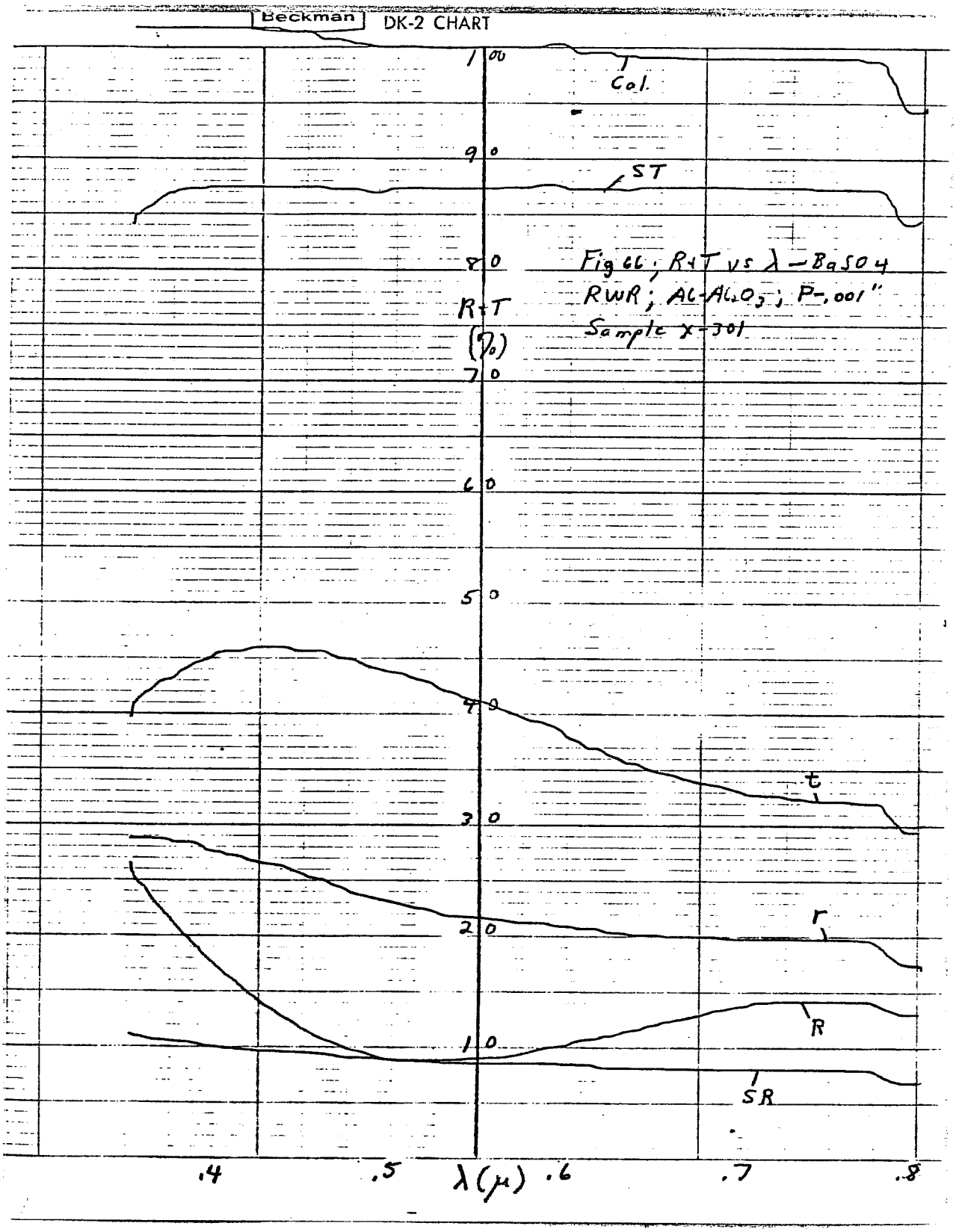
Beckman DK-2 CHART
100
90
80
70
60
50
40
30
20
10
R+T (%)
Col.
ST
t
r
R
SR
.4
.5
λ(μ)
.6
.7
.8
Fig 66; R+T vs λ – BaSO4
RWR; Al-Al2O3; P-.001"
Sample x-301

the holder by a sheet of glass, painted flat black. For easy to measure samples, the glass backed results were identical to the non-backed ones.

For reference, Fig. 67 gives the curve for the reflectivity calibration standard (KCI coated Cu on glass) used for all 2.5 - 25μ measurements (repeated on each graph). This standard is known, from previous measurements at MIT Lincoln Labs, to be 98-100% reflecting in this wavelength region. Also shown is the 7.5 - 25μ T curve for the .002" P film used for some of the P samples discussed in this section. Other standard T curves are given, as applicable, in subsequent graphs.

Figs. 68-69 show the results for some of the later films ($Ag-Al_2O_3$) glued on glass substrates using water soluble adhesive (furnished by Transilwrap). Curves are shown for P substrate samples with the polyester side glued to the glass (X-267, X-268, and X-270) and for PR (polypropylene - .001") with the deposit side glued to the glass (PR7-1 and PR10-4) and with the deposit side away from the glass (PR7-2 and PR10-2).

P substrate OWR samples (X-268 and X-270) have smooth reflectivity curve with values increasing from .9 at 2.5μ to .97 at 10μ and beyond. The PR substrate OWR sample (PR7-2) has a similar curve and a value of .95 at 10μ.

The P substrate RWR sample (X-267) has a smooth reflectivity increase from .71 at 2.5μ to .85 at 10μ. Results for PR10-2 are essentially identical.

The PR samples with the deposit side glued to the glass, still have very substantial reflectivities for the longer I R radiation because of the very high I R transmission of the PR substrate. The latter (furnished by Transilwrap). is optically quite clear and defect free compared to most PR material and is considered optically adequate for retrofit window use. The average values of reflectivity over the 2.5-25 μ range are approximately .75-.8 for the OWR (PR7-1) and .65 - .7 for the RWR (PR10-4). This PR material therefore has sufficient transmission to allow its use for insulating (i.e. thermal mirror) purposes in a configuration (deposit side to the glass) that gives maximum physical protection to the deposited material.

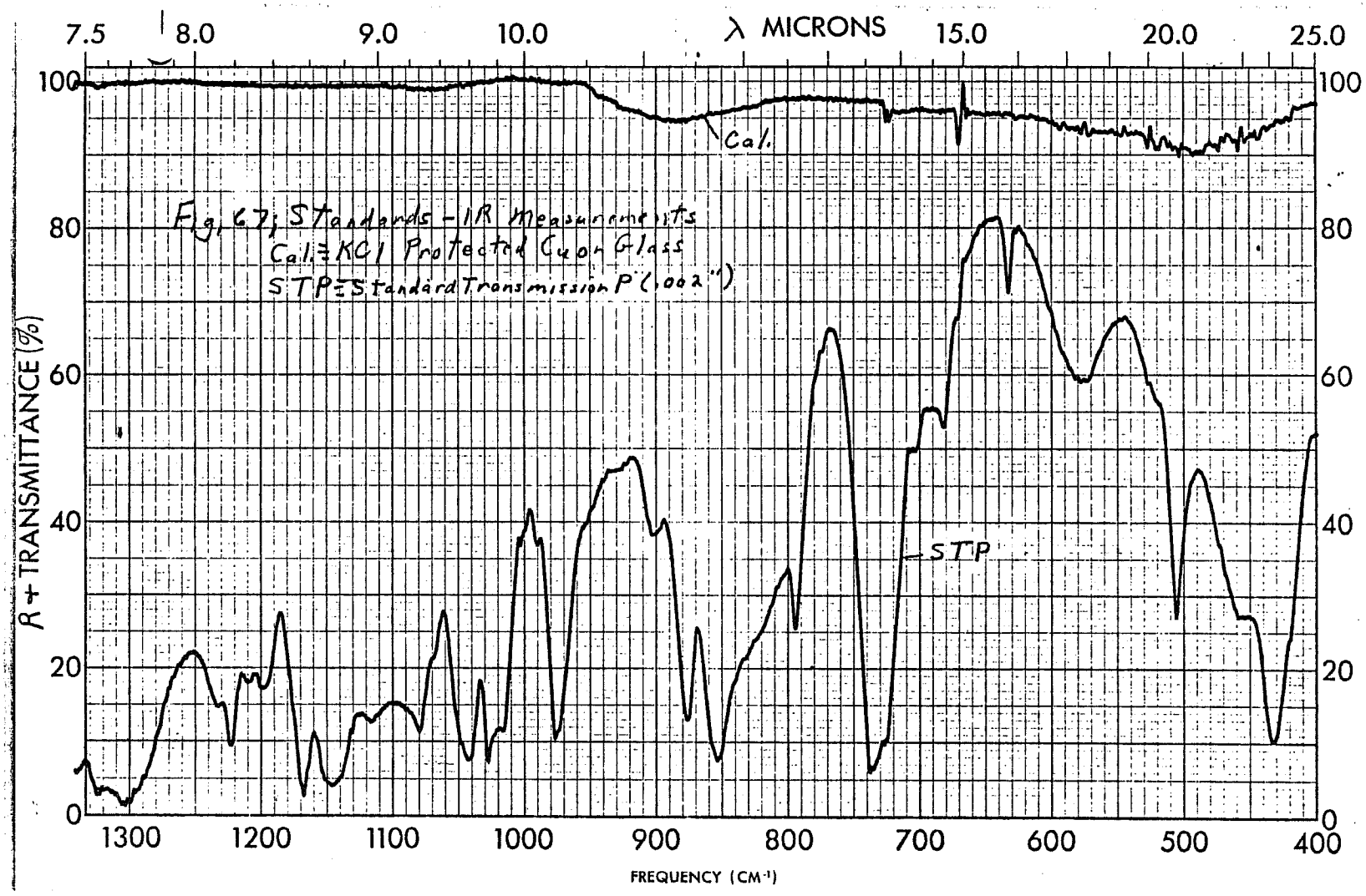

Fig. 67; Standards - IR Measurements
Cal. = KCl Protected Cu on Glass
STP = Standard Transmission P (.002")

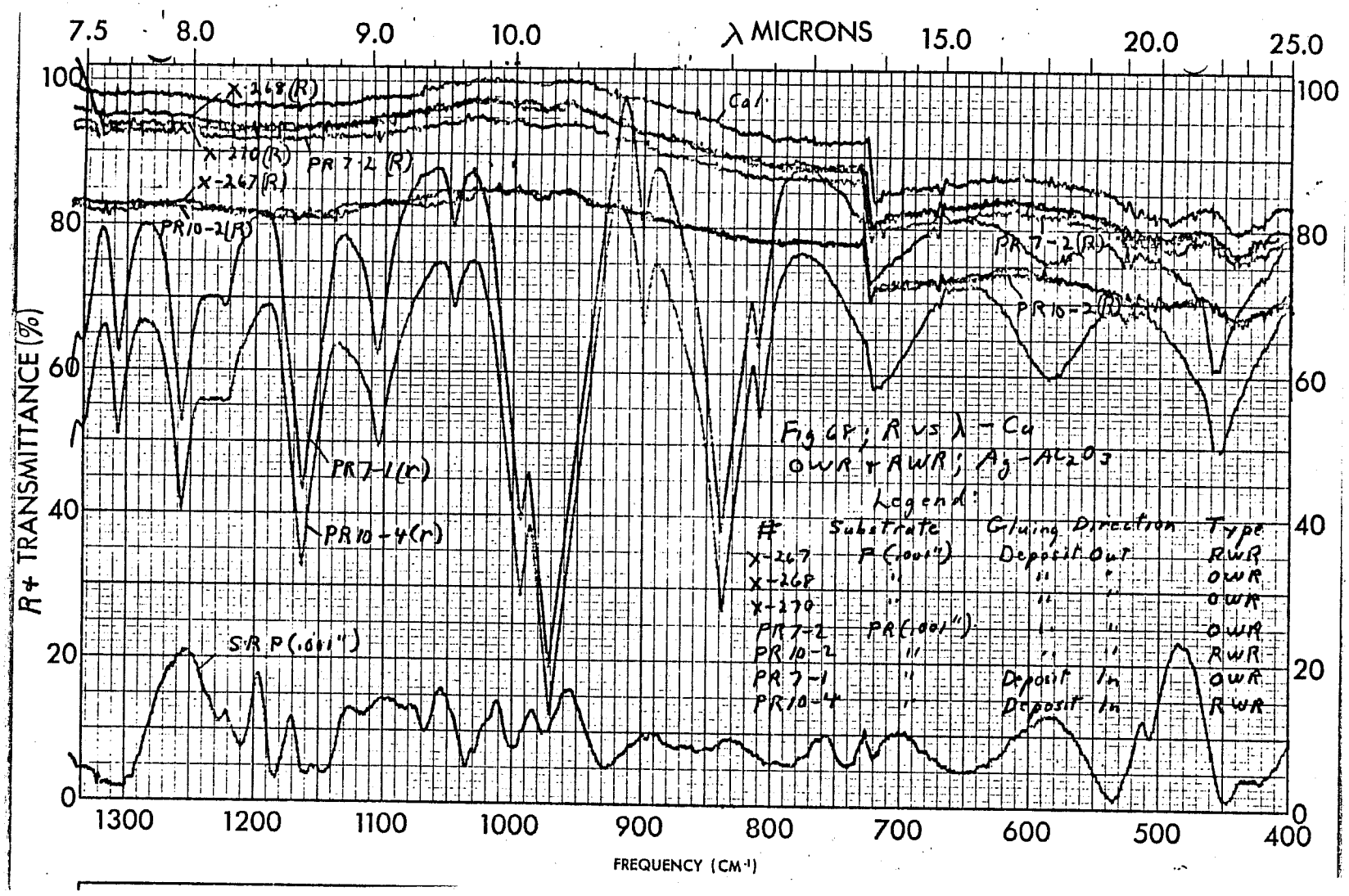
7.5
8.0
9.0
10.0
λ MICRONS
15.0
20.0
25.0
100
80
60
40
20
0
R+ TRANSMITTANCE (%)
X-268 (R)
X-270 (R)
X-267 (R)
PR 7-2 (R)
PR10-2(R)
Cal.
PR 7-2 (R)
PR10-2(R)
PR7-1(r)
PR10-4(r)
S-R P(.001")
Fig 6F; R vs λ - Ca
OWR + RWR; Ag-Al2O3
Legend:
Substrate Gluing Direction Type
X-267 P(.001") Deposit Out RWR
X-268 " " " OWR
X-270 " " " OWR
PR 7-2 PR(.001") " " OWR
PR 10-2 " " " RWR
PR 7-1 " Deposit In OWR
PR10-4 " Deposit In RWR
1300
1200
1100
1000
900
800
700
600
500
400
FREQUENCY (CM-1)

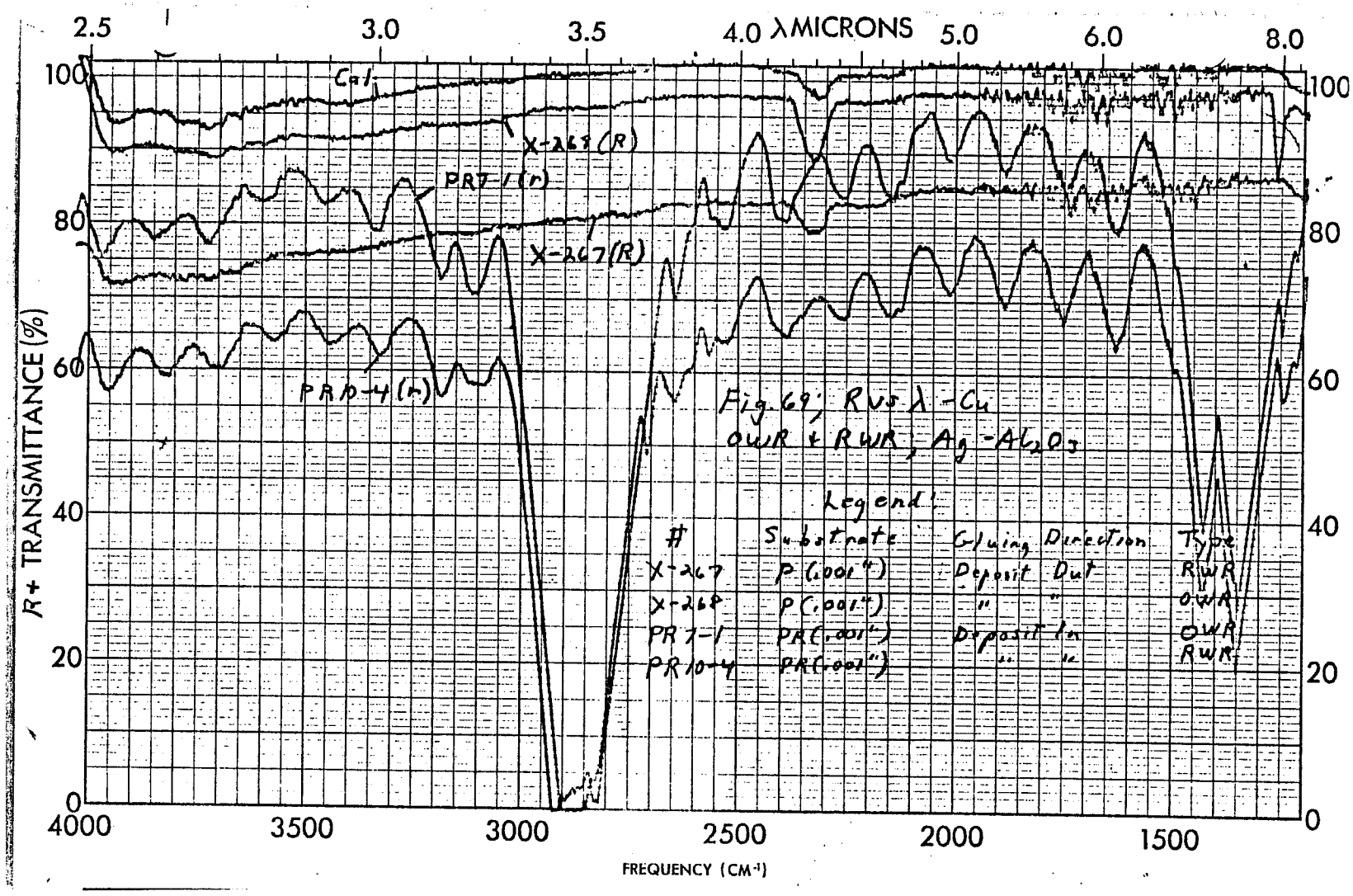
2.5
3.0
3.5
4.0 λ MICRONS
5.0
6.0
8.0
100
80
60
40
20
0
Cu
X-268 (R)
PRT-1 (R)
X-267 (R)
PR 10-4 (R)
R+ TRANSMITTANCE (%)
4000
3500
3000
2500
2000
1500
FREQUENCY (CM⁻¹)
Fig. 69; R vs λ - Cu
OWR & RWR, Ag - Al2O3
Legend
Substrate Gluing Direction Type
X-267 P (.001") Deposit Out RWR
X-268 P (.001") " OWR
PR 1-1 PRC(.001") Deposit In OWR
PR 10-4 PRC(.001") " " RWR

This additional protection is gained at the expense of reduced insulating performance. However, in the case of the OWR, the cooling season performance will actually be improved over that of the deposit side away from glass configuration (for inside attachment) because of higher R values for solar radiation. The potential UV degradation is under investigation (Section 3.7) and at present does not appear to be a problem.

Comparative performance for Bs-Al_2O_3 coated films (i.e. not glued) on P substrates are given in Figs. 70-71. The 10μ R values are .96 for the OWR (X-235) and .81 for the RWR (X-234). The latter slightly low value is almost certainly due to difficulties in keeping the sample at the correct angle since the value for the OWR case is similar to that achieved for Ag-Al_2O_3. Some variation was also observed in the measurements (Fig. 71) taken in two different quadrants of X-235, probably also due to angular variations.

Also shown in Figs. 70-71 are the R values from the substrate side. The values, though low, are large enough to warrant an evaluation of thin (.0005") P substrates for deposit side flued to window OWR configurations. Such samples were made after completion of this program, but have not yet been characterized at longer wavelengths.

Curves and values for other combinations (e.g. Ag-SiO_2, Bs-SiO_2) are essentially identical to the above. Sufficient data has been obtained over many samples to clearly demonstrate that the values of R at 2.5μ for the Bs and Ag based systems directly indicate the values to be expected at 10μ. Many experimental samples were therefore measured only up to 2.5μ. At the end of the program, however, many glued samples on glass were assembled and characterized (Section 5). These samples essentially gave 10μ R values >.85 for RWRs and >.95 for OWRs.

Comparative transmission curves were made on selected samples as shown in Figs. 72-73. The former shows very little difference for the Ag-Al_2O_3, Ag-SiO_2 and Bs-Al_2O_3 systems for RWRs (F-109, F-138 and F-165, respectively) in the 7.5 - 25μ region (Fig. 72) while T for the OWR case (F-167, Bs-Al_2O_3) is slightly lower. Measured values for FEP (F-165) and P (X-234) samples were similar in the 2.5 - 8μ region (Fig. 73) with a steady decrease as wavelength increases.

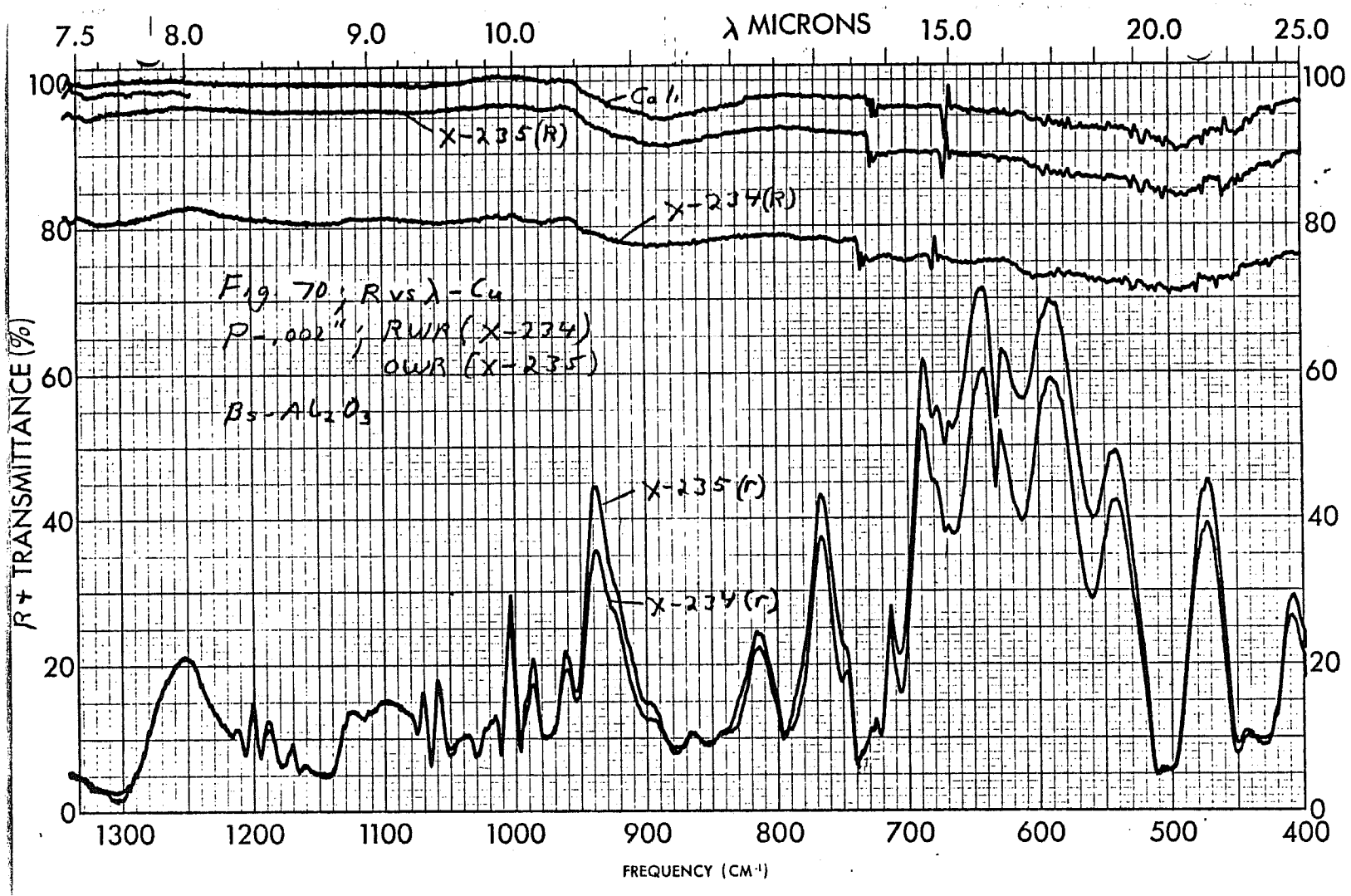
7.5
8.0
9.0
10.0
λ MICRONS
15.0
20.0
25.0
100
80
60
40
20
0
R+ TRANSMITTANCE (%)
Ca 1
X-235(R)
X-234(R)
Fig. 70: R vs λ - C4
P ~ .002"; RWR (X-234)
OWR (X-235)
β3-Al2O3
X-235 (r)
X-234 (r)
1300
1200
1100
1000
900
800
700
600
500
400
FREQUENCY (CM-1)

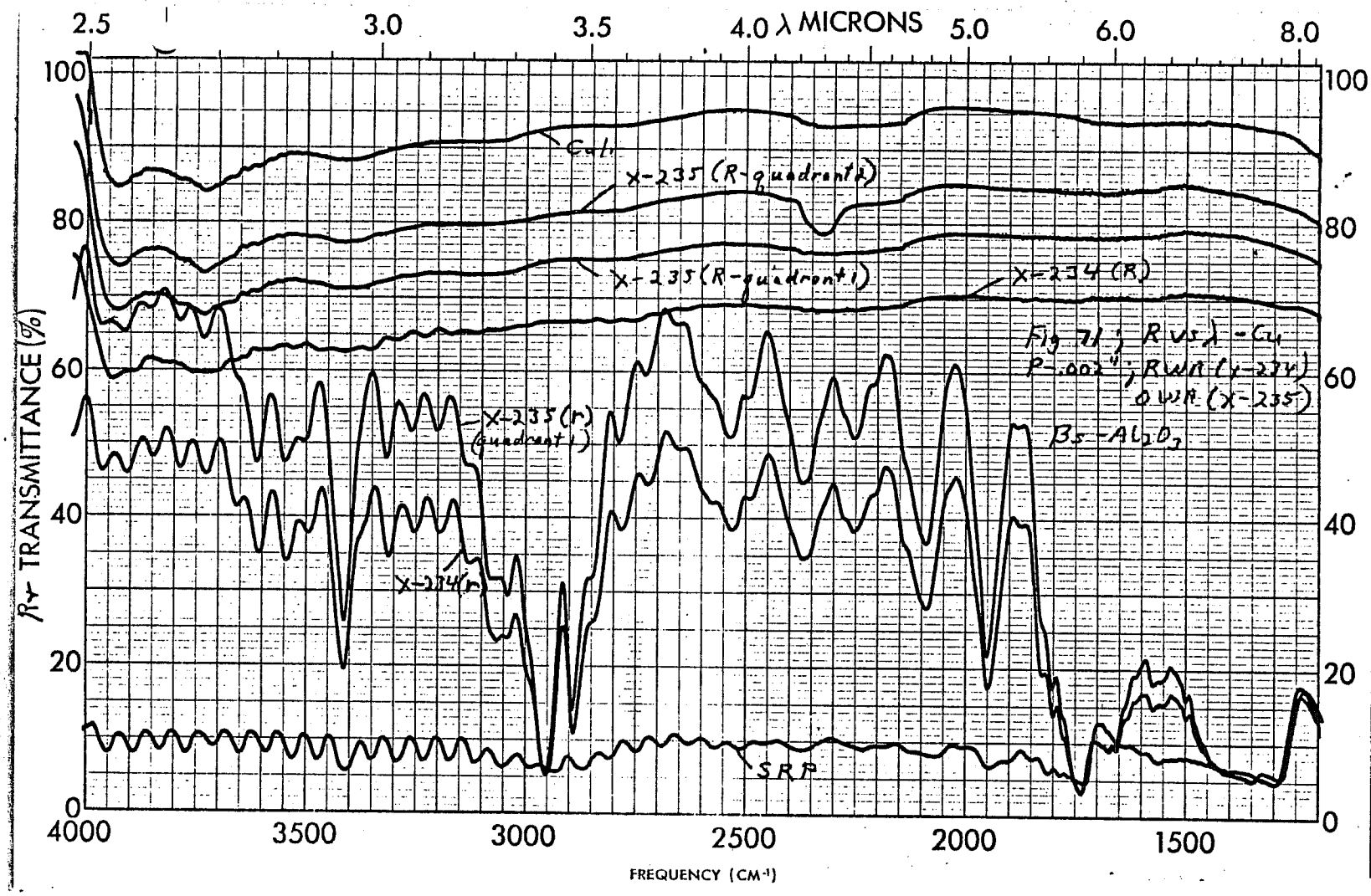
2.5
3.0
3.5
4.0 λ MICRONS
5.0
6.0
8.0
100
80
60
40
20
0
Rr TRANSMITTANCE (%)
4000
3500
3000
2500
2000
1500
FREQUENCY (CM⁻¹)
Cu
X-235 (R-quadrant 2)
X-235 (R-quadrant 1)
X-234 (R)
X-235 (r) (quadrant 1)
X-234 (r)
SRP
Fig 71; R vs λ - Cu
P-.002"; RWR (X-234)
RWR (X-235)
Bs - Al2O3

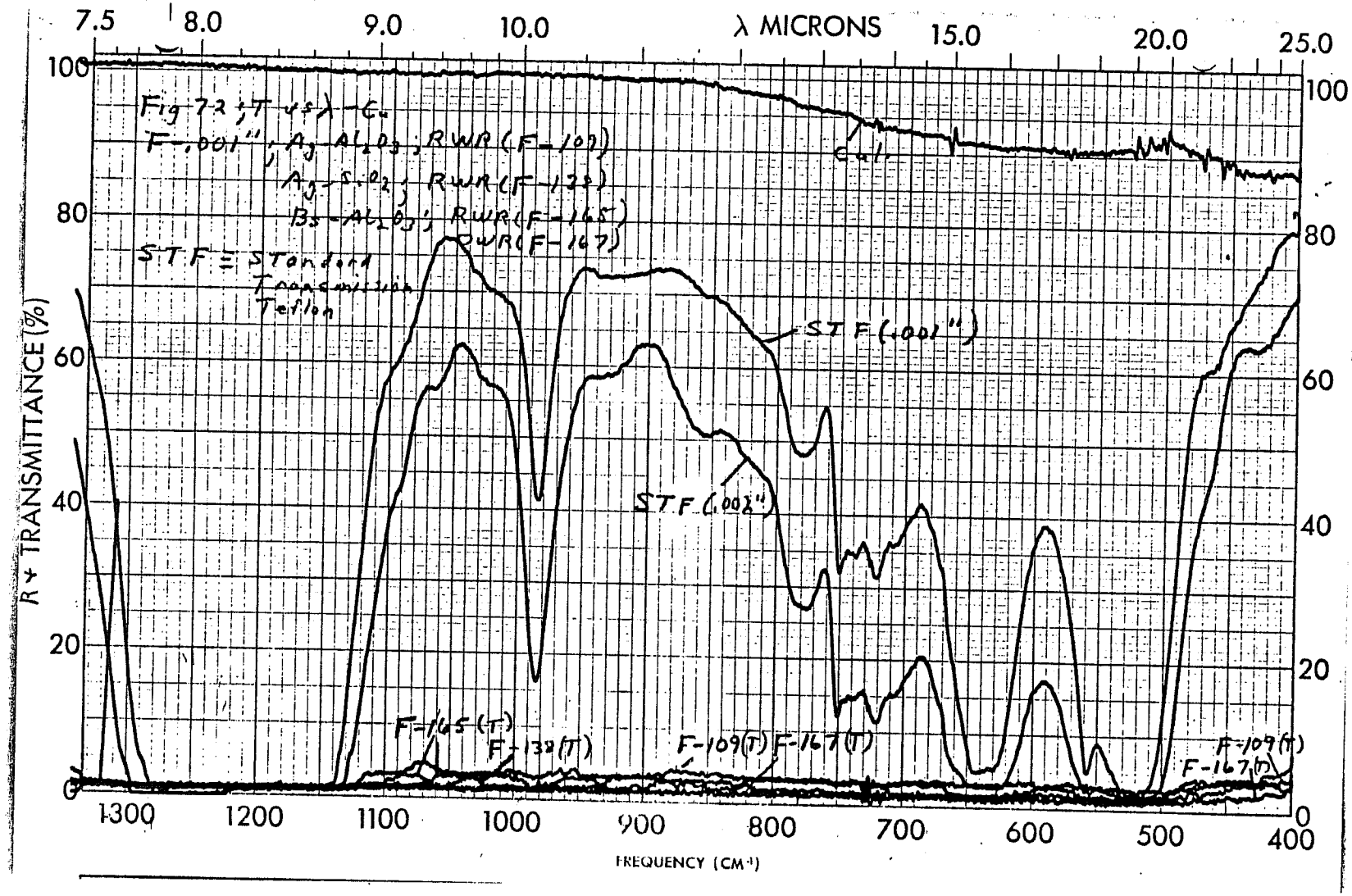
7.5
8.0
9.0
10.0
λ MICRONS
15.0
20.0
25.0
100
80
60
40
20
0
R + TRANSMITTANCE (%)
Fig 7-2 ; T vs λ - Cu
F-.001" ; Ag - Al2O3 ; RWR (F-109)
Ag - SiO2 ; RWR (F-132)
Bs - Al2O3 ; RWR (F-165)
RWR (F-167)
STF = Standard Transmission Teflon
Cu
STF (.001")
STF (.002")
F-165 (T)
F-132 (T)
F-109 (T)
F-167 (T)
1300
1200
1100
1000
900
800
700
600
500
400
FREQUENCY (CM-1)

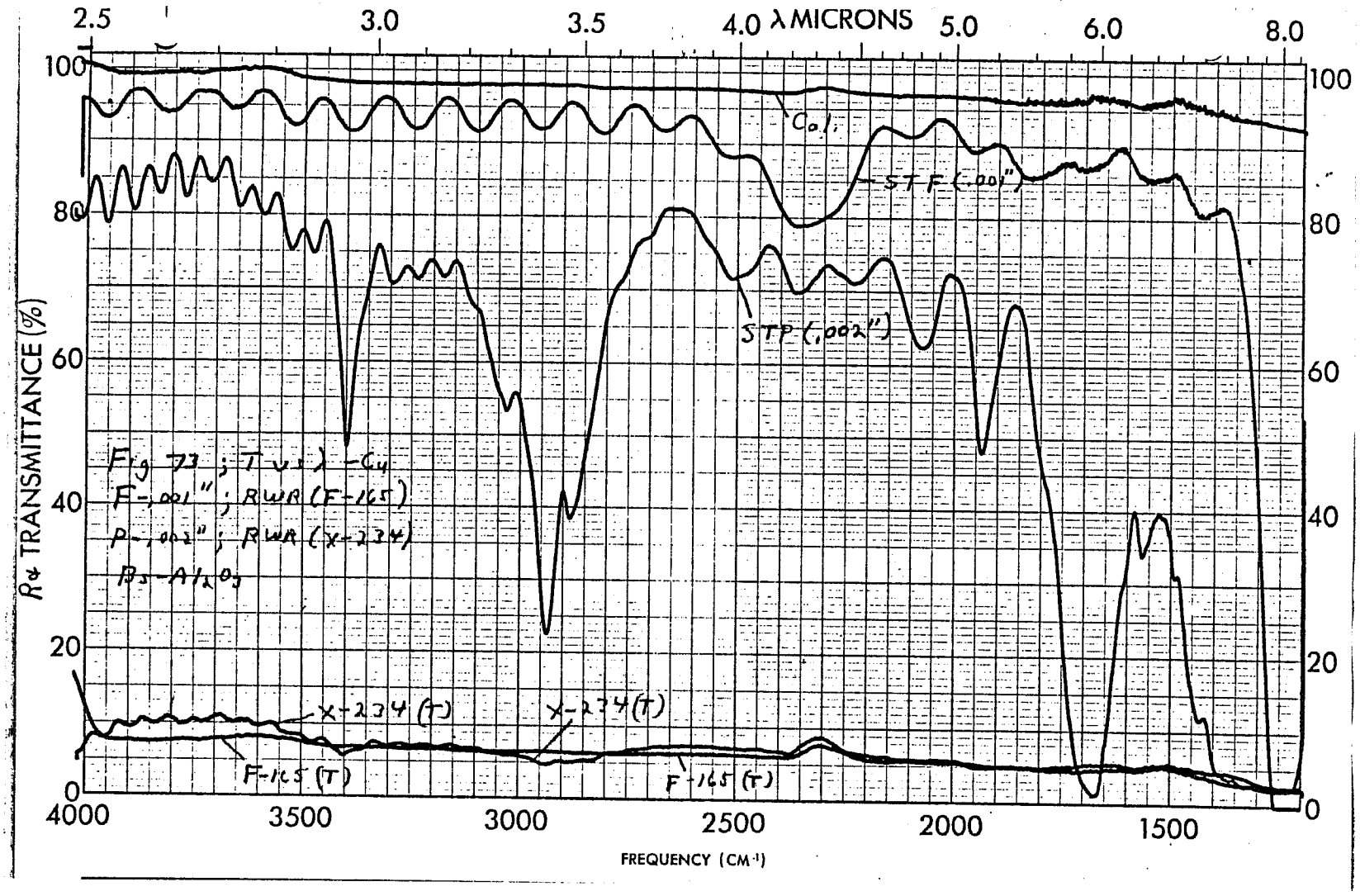
2.5
3.0
3.5
4.0 λ MICRONS
5.0
6.0
8.0
100
80
60
40
20
0
% TRANSMITTANCE (%)
Col.
STF (.001")
STP (.002")
Fig 73 ; T vs λ - C4
F-.001" ; RWR (F-165)
P-.002" ; RWR (X-234)
B3-A12O3
X-234 (T)
X-234 (T)
F-165 (T)
F-165 (T)
4000
3500
3000
2500
2000
1500
FREQUENCY (CM-1)

Figs. 74-75 give performance curves for the Ag-SiO_2 system on FEP substrates demonstrating one of the potential problems of this substrate material. Fig. 74 gives results for well-handled films (F-114 and F-115) and for similar but previously unhandled films (F-138 and F-141). While the 10μ R values for the latter are roughly equivalent (very difficult to measure) to P substrate values, those for the well-handled films are seriously degraded. This effect is clearly due to extensive wrinkling of the soft FEP material resulting in decreased measured R. Actual R may, in fact, be quite a bit higher.

R values through the substrate for the well-handled films were also seriously degraded (Fig. 74) although the low R values are partly due to the .002" thickness. In contrast, films on .001" thick substrates which had been handled previously (Fig. 75) gave higher but still inadequate R values through the substrate. Optical performance of the PR substrate samples (Figs. 68-69) is clearly superior to FEP for deposit side to glass configurations. However, stability of the PR system is still under investigation.

3.7 Gluing Samples

Many of the results presented in this section could be appropriately classed under weathering studies. They are included here since they were conducted as part of the materials studies to evaluate potential attachment problems, rather than as specific weathering tests after attachment.

Extensive R and T data were generated on glued polyester and FEP samples. For these earlier investigations pressure sensitive glue was used with the films being applied to ordinary window glass with a plastic roller. Although many more samples were processed, the more limited results presented here are representative of overall performance. In general the results are very favorable and indicate that long term stability and performance under real operating conditions should be quite acceptable.

It should be noted that all of the earlier glued samples were made with films which were on the low side of acceptable R values. This was done deliberately since the onset of acceptable R values occurs over a fairly narrow

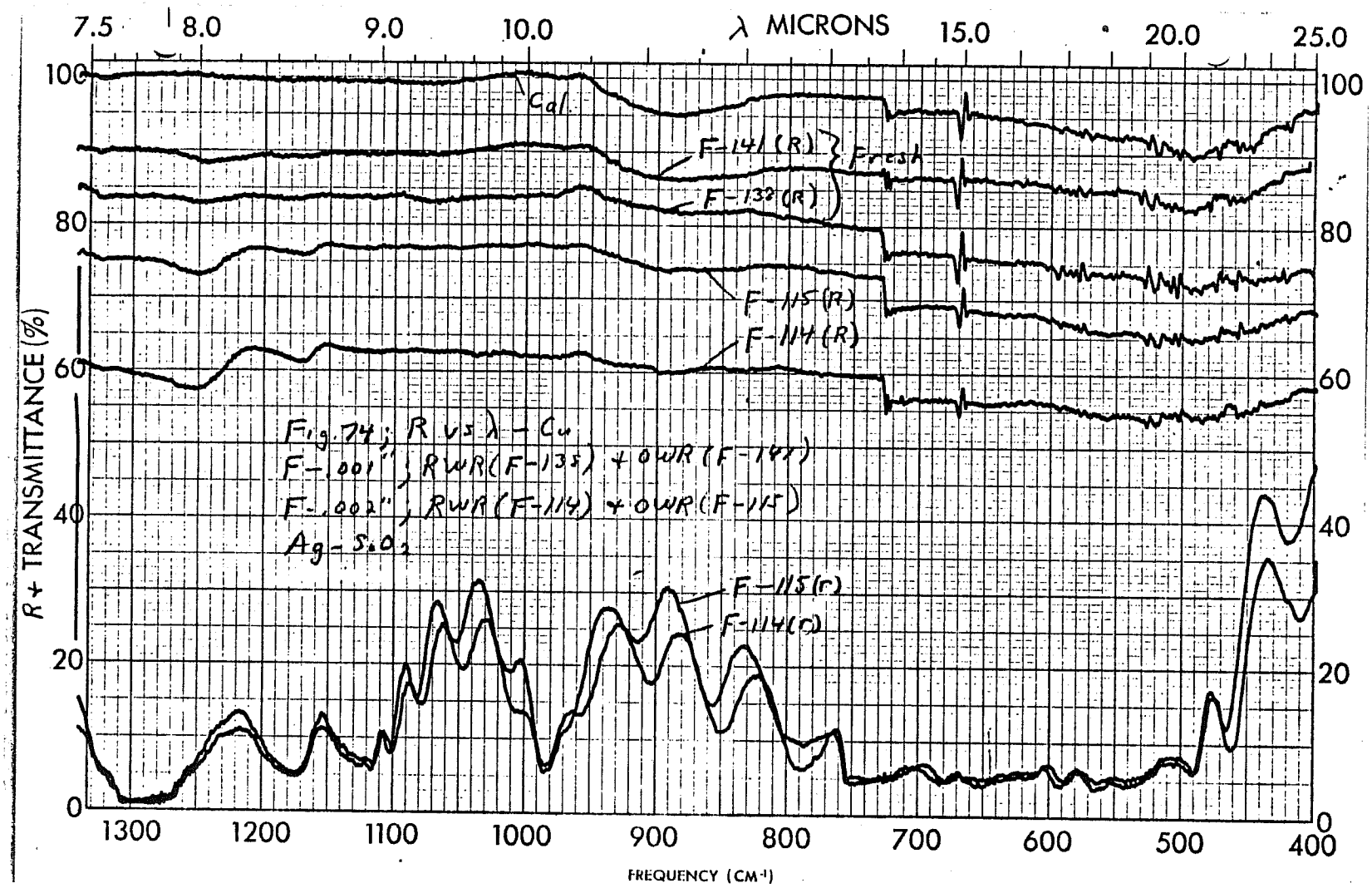
7.5
8.0
9.0
10.0
λ MICRONS
15.0
20.0
25.0
100
80
60
40
20
0
R + TRANSMITTANCE (%)
Cal.
F-141 (R)
F-132 (R)
F-115 (R)
F-114 (R)
Fresh
Fig. 74; R vs λ - Cu
F-.001"; RWR(F-135) + OWR(F-141)
F-.002"; RWR(F-114) + OWR(F-115)
Ag - 5.0 Å
F-115 (r)
F-114 (r)
1300
1200
1100
1000
900
800
700
600
500
400
FREQUENCY (CM-1)

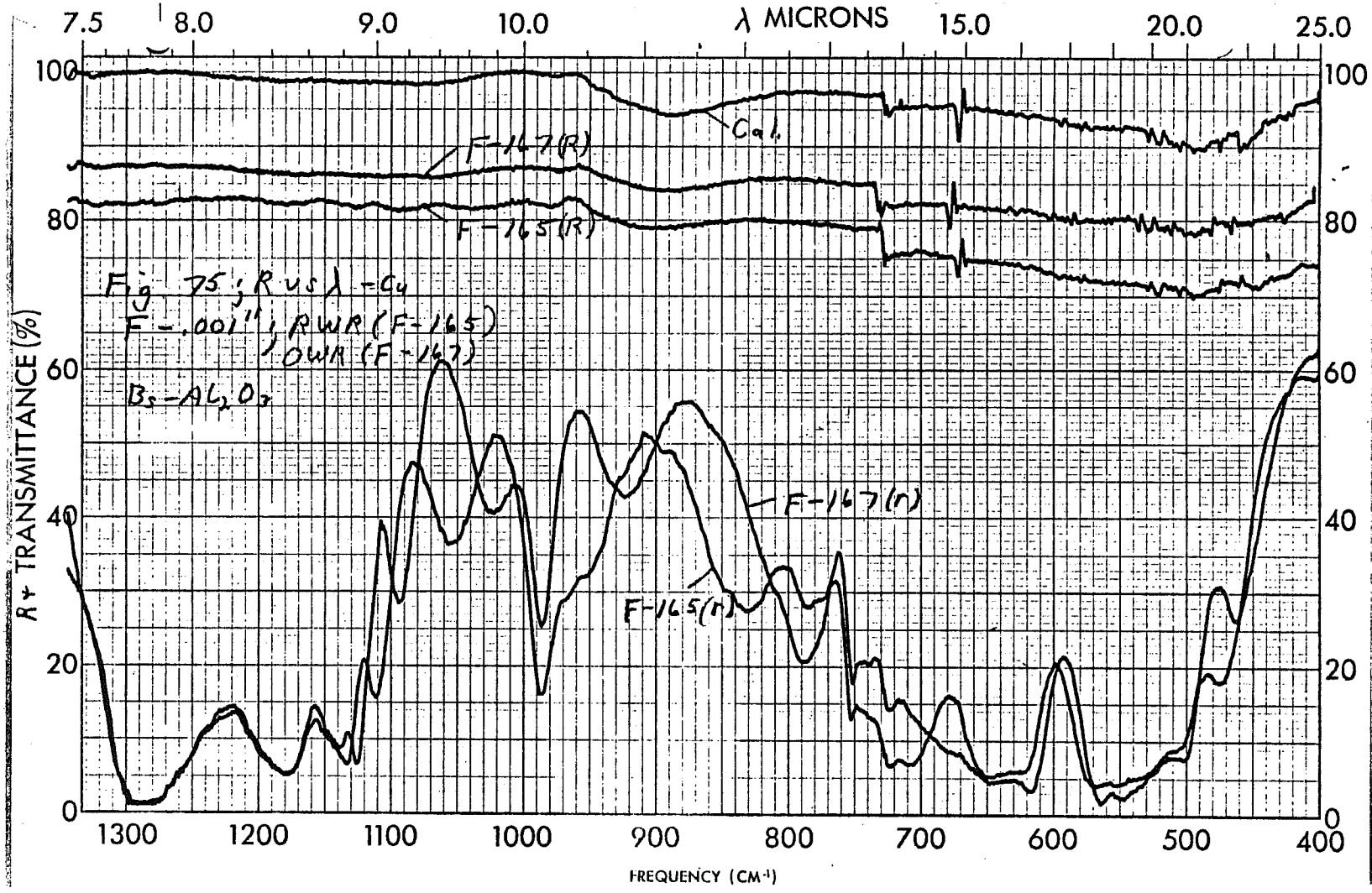
7.5
8.0
9.0
10.0
λ MICRONS
15.0
20.0
25.0
100
80
60
40
20
0
R+ TRANSMITTANCE (%)
Cal.
F-167(R)
F-165(R)
Fig 75; R vs λ - Cu
F - .001"; RWR (F-165)
OWR (F-167)
B2 - Al2 O3
F-167(T)
F-165(T)
1300
1200
1100
1000
900
800
700
600
500
400
FREQUENCY (CM-1)

band of film thicknesses and it was felt that using films at the low end of the scale would accentuate degradation effects. In addition, these samples were also made under the earlier criteria using MgO standards, and therefore were designed for lower R (2.5μ) values. The results, as presented, are independent of these considerations except that curves have been taken vs. both MgO and $BaSO_4$ standards because of the elapsed time. With the added complexity of the many curves, this means that great care must be taken in evaluating the data.

There was also a significant spread in the data for any given sample depending on precisely how the sample was oriented during measurement. This was primarily due to changes resulting from gluing since these samples were relatively small (2" x 2") and the films themselves were very uniform. Fig. 80 (sample F-41-1) gives an indication of the level of change that could be made by position of the sample in the spectrophotometer. At the 12 week reading curves were taken for r (through plastic substrate) at the two extreme reading positions (5-1 and 5-h). Since the samples were normally inserted roughly on center, the variation in most cases was much less than this but it does account for small discrepancies.

Figs. 76-77 give R and T data for two polyester substrate samples using the Bs-SiO_2 (Fig. 76, sample X-186-3) and Ag-SiO_2 (Fig. 77, sample X-124-1) systems. These samples were glued with the deposit side away from the glass as they would be in a real installation. After 585 days of ambient environment, washing (ammonia water and solvents) and handling on a laboratory basis, there is no change, either visual or measured, in either of these samples. The basic systems are clearly stable and degradation is more likely to occur from scratching, solvent or ambient gases.

The curves for reflectivity through the glass (r) are representative, although slightly lower, of the response of these glued configurations to solar illumination from the outside. Most of the incident light is transmitted. Most of that which is not is absorbed in the glass or glue and is partly reradiated or conducted towards the inside of the building.

Results for samples on FEP substrates using Bs-SiO_2 and Ag-SiO_2 are given in Figs. 78-81. All of the samples shown were glued with the deposit side to the glass. The Bs-SiO_2 system for an OWR (Fig. 78, sample F-26-1)

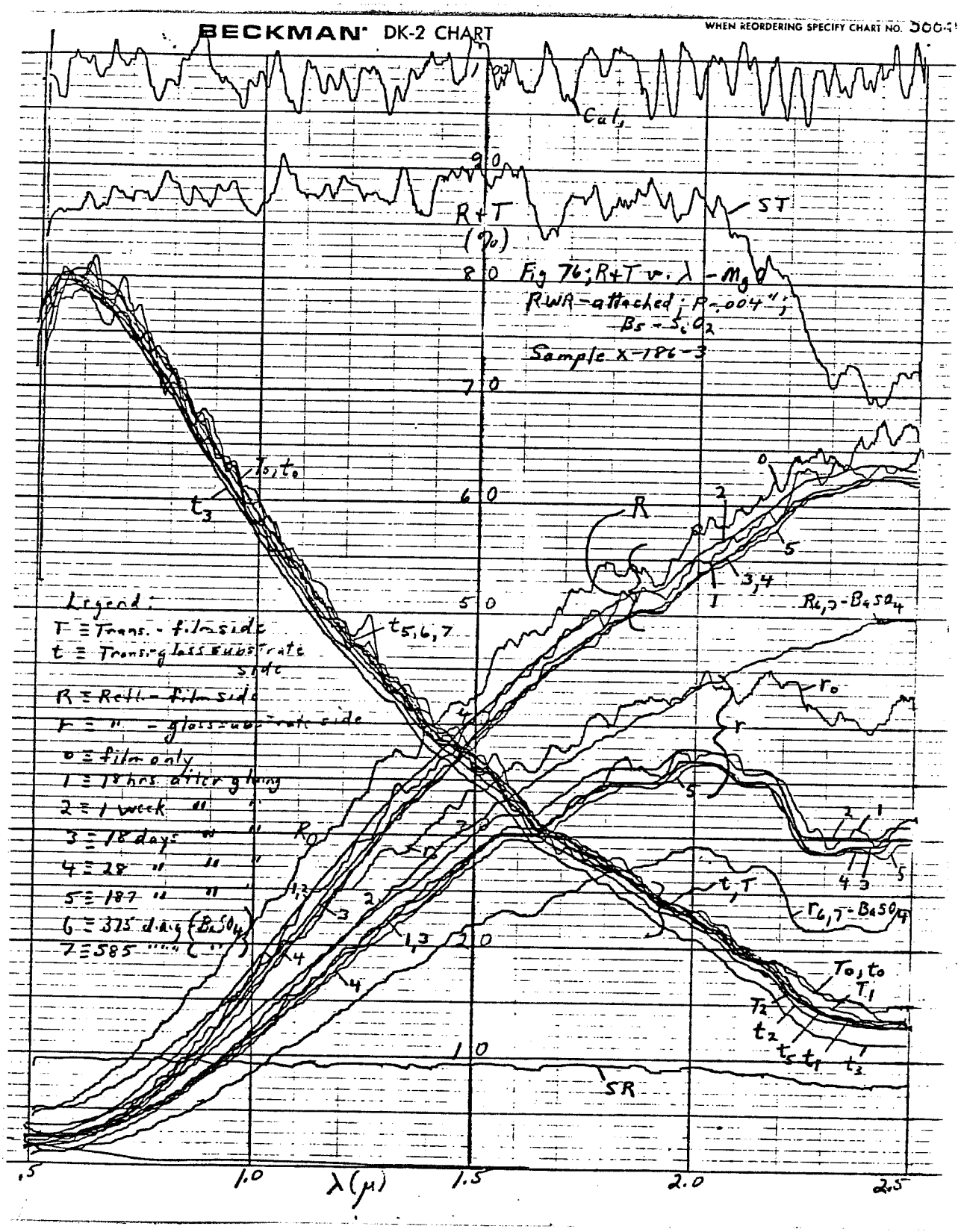
BECKMAN DK-2 CHART
WHEN REORDERING SPECIFY CHART NO. 300-4
Cal.
R+T
(%)
ST
SR
Fig 76; R+T v. λ - MgO
RWA-attached; P=.004";
Bs - Sio2
Sample X-186-3
Legend:
T ≡ Trans. - film side
t ≡ Trans. - glass substrate side
R ≡ Refl. - film side
r ≡ " - glass substrate side
0 ≡ film only
1 ≡ 18 hrs. after glazing
2 ≡ 1 week "
3 ≡ 18 days "
4 ≡ 28 "
5 ≡ 187 "
6 ≡ 375 days (BaSO4)
7 ≡ 585 " " "
λ(μ)
.5
1.0
1.5
2.0
2.5
90
80
70
60
50
40
30
20
10

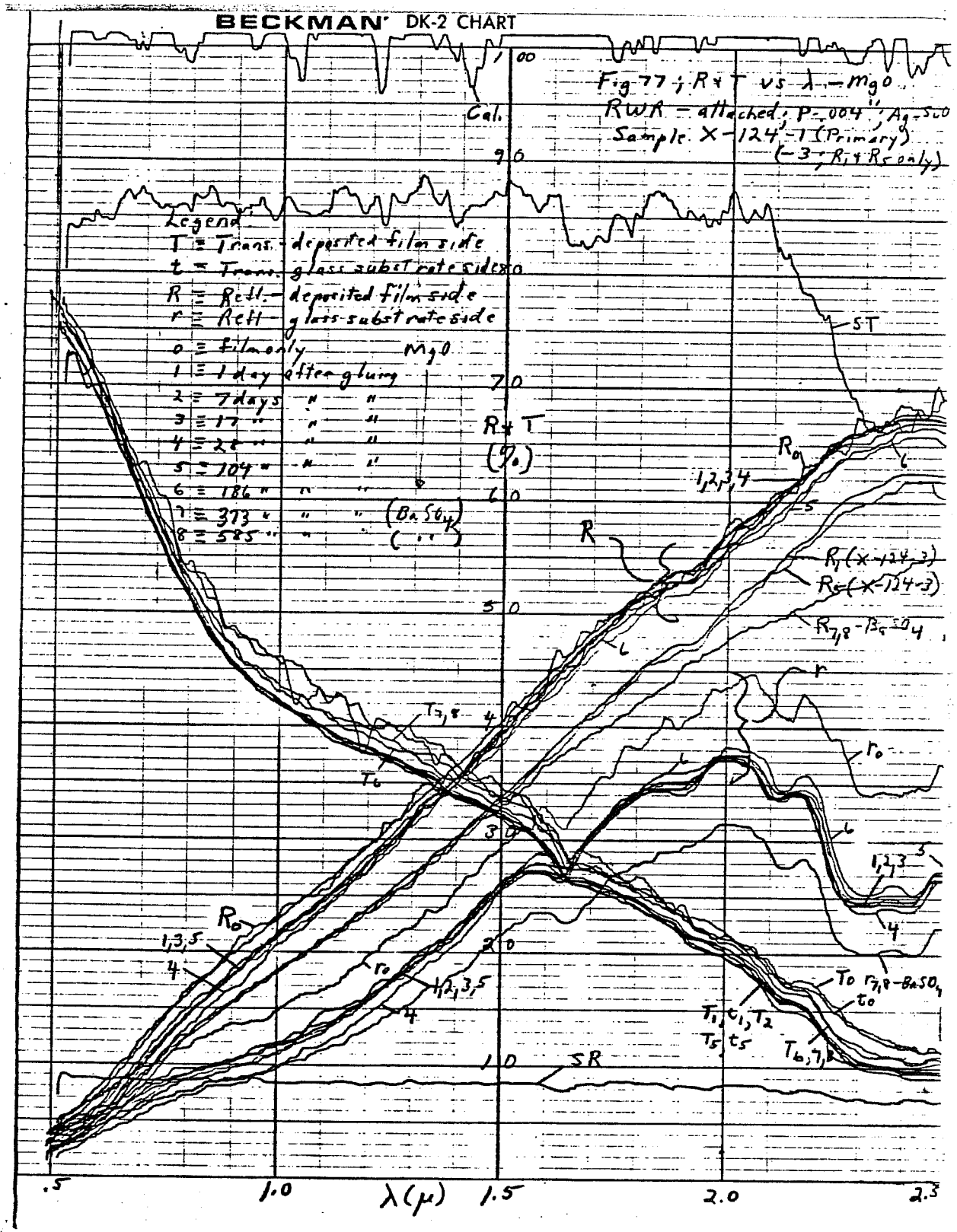
BECKMAN DK-2 CHART
Fig 77 ; R + T vs λ - MgO
RWR - attached ; P-.004" ; Ag-500
Sample X-124'-1 (Primary)
(-3 ; R + R only)
Cal.
Legend:
T = Trans. - deposited film side
t = Trans. - glass substrate side
R = Refl. - deposited film side
r = Refl - glass substrate side
0 = film only
1 = 1 day after gluing
2 = 7 days " "
3 = 17 " " "
4 = 28 " " "
5 = 104 " " "
6 = 186 " " "
7 = 373 " " "
8 = 585 " " "
MgO
(BaSO4)
(" ")
R + T (%)
100
90
80
70
60
50
40
30
20
10
ST
SR
R0
1,2,3,4
5
R
R1 (X-124-3)
R8 (X-124-3)
R7,8 - BaSO4
T1,8
T6
r0
1,2,3
4
1,3,5
T0 r7,8 - BaSO4
t0
T1, t1, T2
T5 t5
T6,7,8
.5
1.0
λ(μ)
1.5
2.0
2.3

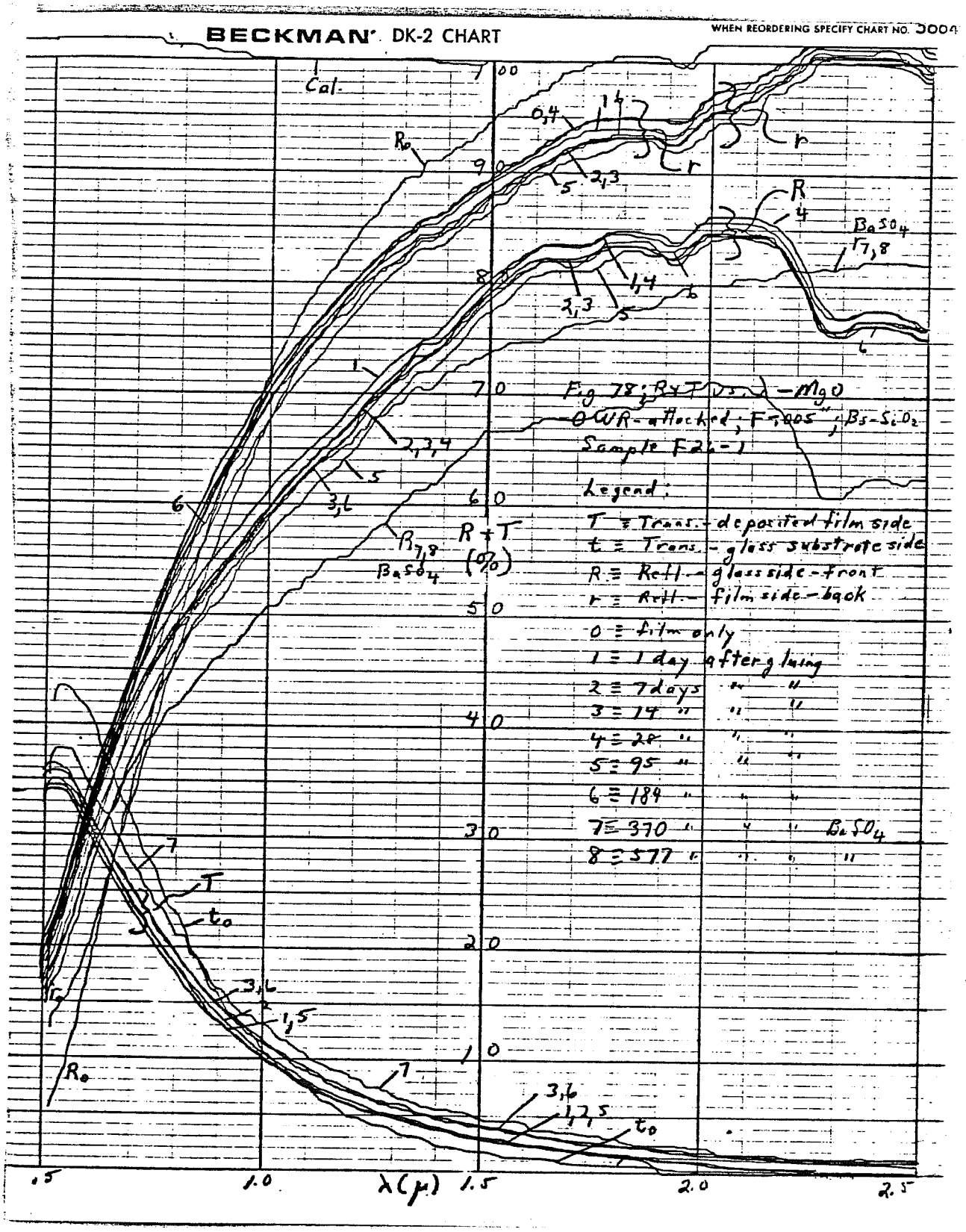
BECKMAN DK-2 CHART
WHEN REORDERING SPECIFY CHART NO. 3004
Cal.
100
90
80
70
60
50
40
30
20
10
R+T (%)
.5
1.0
λ(μ)
1.5
2.0
2.5
Fig 78; R+T vs. λ — MgO
OWR - attacked; F-005; Bs-SiO2
Sample F24-1
Legend:
T = Trans. - deposited film side
t = Trans. - glass substrate side
R = Refl. - glass side - front
r = Refl. - film side - back
0 = film only
1 = 1 day after gluing
2 = 7 days " "
3 = 14 " "
4 = 28 " "
5 = 95 " "
6 = 184 " "
7 = 370 " " " BaSO4
8 = 577 " " "
BaSO4
Ro
To
to

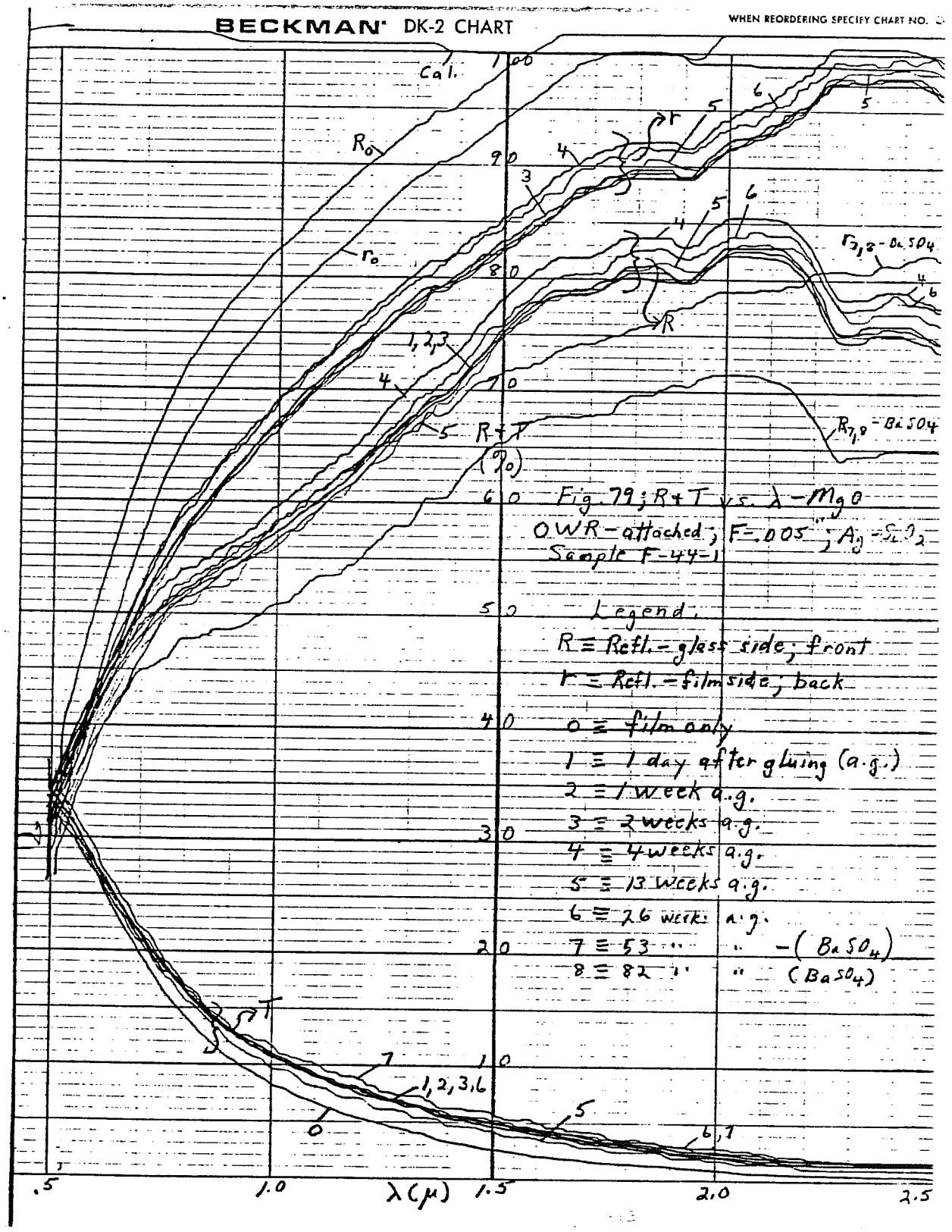
BECKMAN DK-2 CHART
WHEN REORDERING SPECIFY CHART NO.
Cal.
R_0
r_0
$r_{7,8}$ - $BaSO_4$
$R_{7,8}$ - $BaSO_4$
R
r
R+T (%)
100
90
80
70
60
50
40
30
20
10
0
.5
1.0
1.5
2.0
2.5
λ(μ)
Fig. 79; R+T vs. λ - MgO
OWR - attached; F=.005"; Ag - SiO_2
Sample F-44-1
Legend:
R = Refl. - glass side; front
r = Refl. - film side; back
0 = film only
1 = 1 day after gluing (a.g.)
2 = 1 week a.g.
3 = 2 weeks a.g.
4 = 4 weeks a.g.
5 = 13 weeks a.g.
6 = 26 weeks a.g.
7 = 53 " " - ($BaSO_4$)
8 = 82 " " ($BaSO_4$)

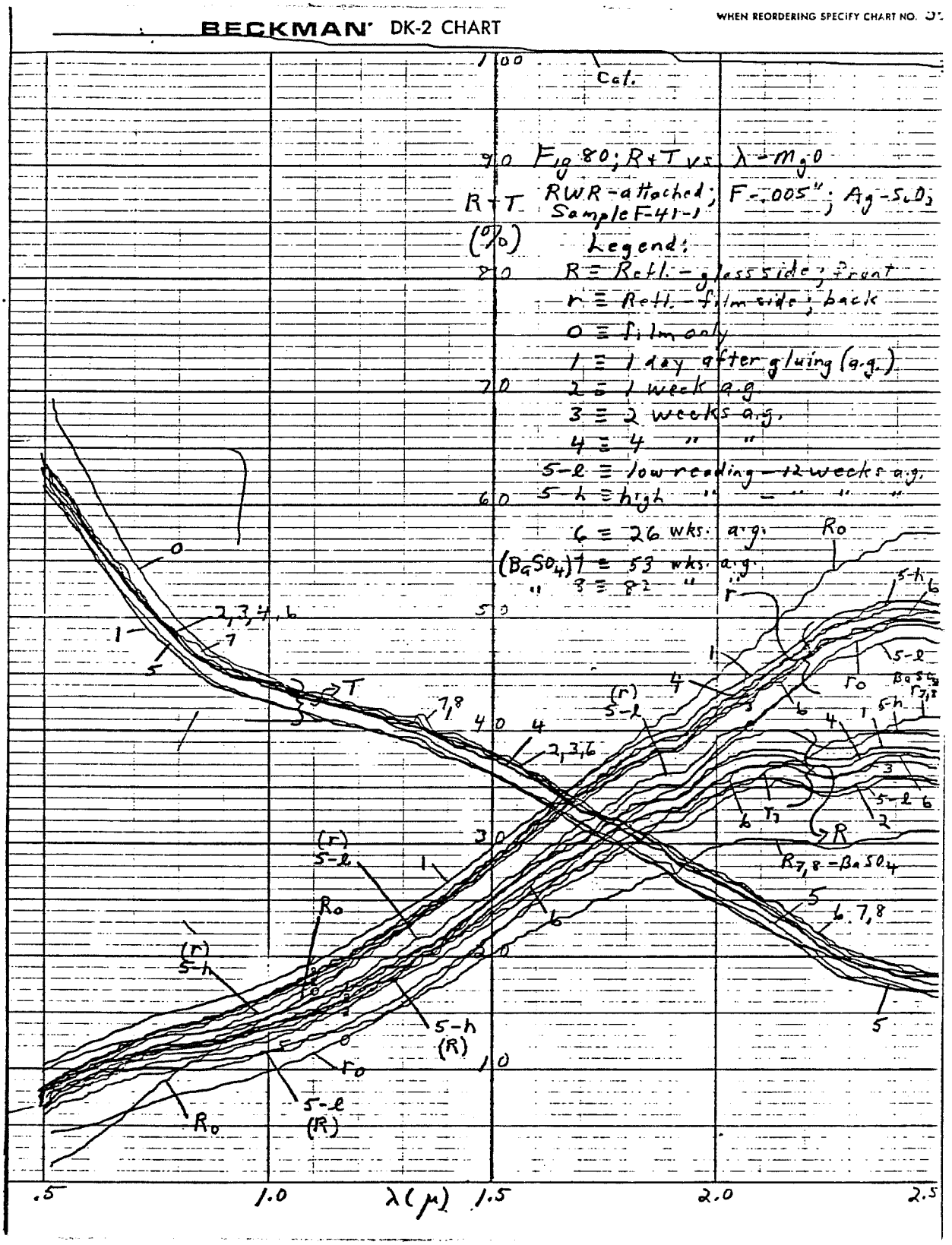
BECKMAN DK-2 CHART
WHEN REORDERING SPECIFY CHART NO.
Cal.
Fig 80; R+T vs λ - M.g.O
RWR-attached; F-.005"; Ag-SiO2
Sample F-41-1
R+T (%)
Legend:
R ≡ Refl. - glass side; front
r ≡ Refl. - film side; back
0 ≡ film only
1 ≡ 1 day after gluing (a.g.)
2 ≡ 1 week a.g.
3 ≡ 2 weeks a.g.
4 ≡ 4 " "
5-l ≡ low reading - 12 weeks a.g.
5-h ≡ high " - " " "
6 ≡ 26 wks. a.g.
(BaSO4) 7 ≡ 53 wks. a.g.
" 8 ≡ 82 "
100
90
80
70
60
50
40
30
20
10
.5
1.0
λ(μ)
1.5
2.0
2.5
T
R
Ro
ro
(r) 5-l
(r) 5-h
5-h (R)
5-l (R)
R7,8 - BaSO4
6,7,8
2,3,4,6
7,8

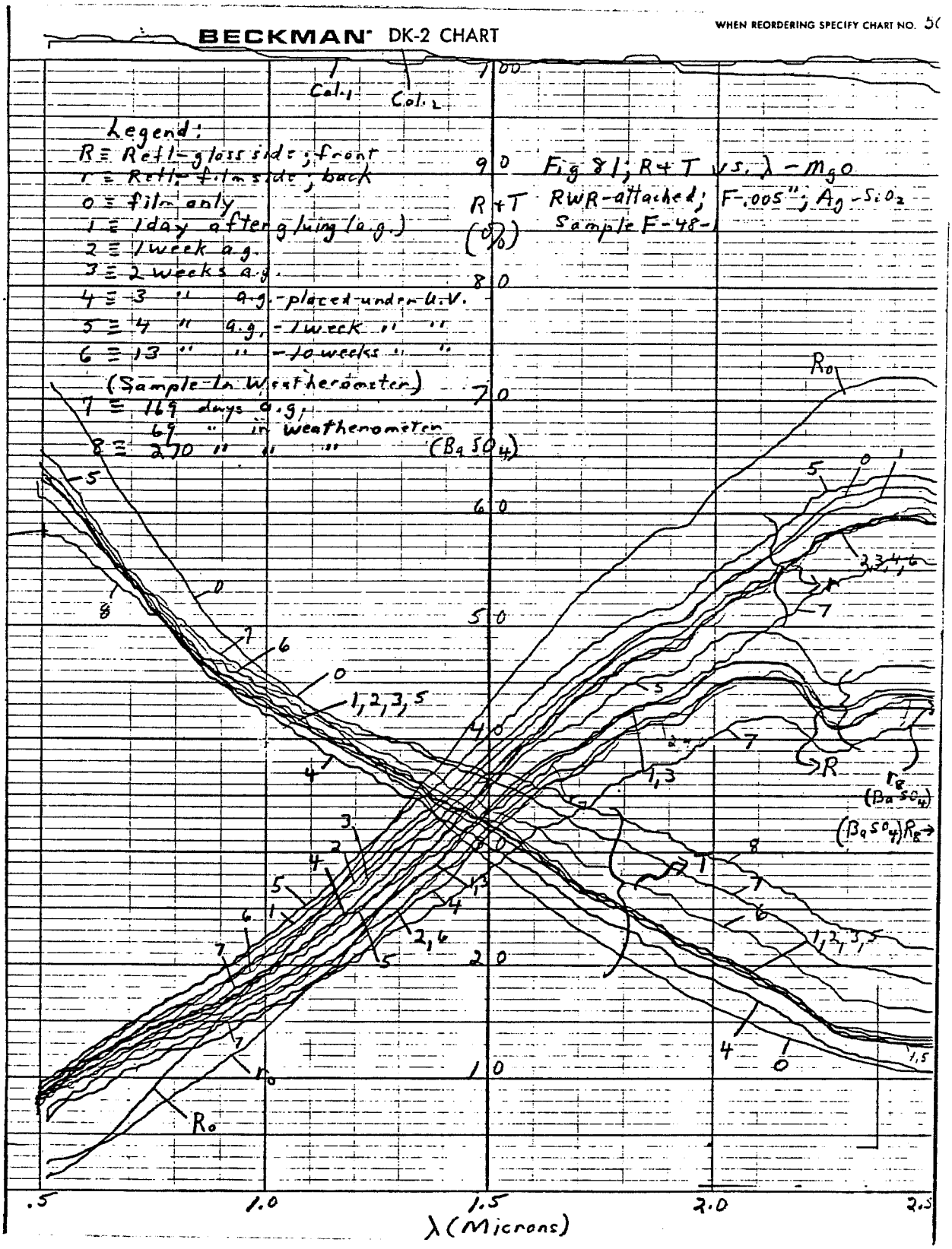
BECKMAN DK-2 CHART
WHEN REORDERING SPECIFY CHART NO. 5(
Col. 1
Col. 2
Legend:
R ≡ Refl-gloss side; front
r = Refl-film side; back
0 ≡ film only
1 ≡ 1day after glazing (a.g.)
2 ≡ 1week a.g.
3 ≡ 2 weeks a.g.
4 ≡ 3 " a.g.-placed under U.V.
5 ≡ 4 " a.g. - 1week " "
6 ≡ 13 " " - 10 weeks " "
(Sample-In Weatherometer)
7 ≡ 169 days a.g.;
69 " in weathenometer
8 ≡ 270 " " "
Fig 81; R+T vs. λ - MgO
RWR-attached; F-.005"; Ag - SiO2
Sample F-48-
R+T (%)
100
90
80
70
60
50
40
30
20
10
(Ba SO4)
Ro
ro
R
rg (Ba SO4)
(Ba SO4) Rg
.5
1.0
1.5
2.0
2.5
λ (Microns)

shows no degradation with time after 577 days. Note that the initial value of r before gluing (r_o) is roughly comparable to the value after gluing. In general, this was true, but as seen in Fig. 79, improper gluing methods resulted in degradation in r during gluing even though r was from the substrate side.

This type of configuration is especially adapted for application to the outside of an office window in a southern climate where only cooling is required. The FEP substrate is exposed to the atmosphere and protects the deposited film. This type of FEP film is essentially inert to atmospheric attack and these window configurations could reasonably be expected to last for 20 years or more. Performance loss due to some slight absorption of the incident solar illumination in the FEP substrate before and after reflection (r vs. R), is more than compensated for by the outside mounting which prevents absorption in the glass. Energy absorbed on the FEP film can only reach the inside by conduction/convection since reradiated energy will be reflected to the outside by the deposited reflecting film.

The Ag-SiO_2 system on FEP (Fig. 79, sample F-44-1) used a slightly different gluing method (less diluting solvent) and showed a substantial change in r after gluing. This must be due to some effect of the glue on the deposited film reflectivity (perhaps due to stress) since both R and r suffered greater relative reductions than sample F-26-1. Stability of the final configuration, however, is comparable and excellent.

Comparable results for FEP substrate RWR samples using the Ag-SiO_2 system are given in Figs. 80-81. Sample F-41-1 (Fig. 80) shows no degradation in r on gluing and no changes with time. Although this system was originally considered for a deposit-glued-to-glass configuration, it has been rejected in favor of PR substrates or P substrates with the deposit side away from the glass (i.e. facing room interior).

Additional information over that given for sample F-41-1 is given in Fig. 81 for sample F-48-1. This sample was subjected to a variety of tests including gluing, UV testing and weatherometer testing. After gluing, the sample was left under a Hg black light at a distance of 6" with the FEP side facing the lamp. After a period of 10 weeks, equivalent to 20 years solar UV exposure,

there was absolutely no change in appearance, performance or bonding. The sample was then placed in the KCI weatherometer(Section 4) and after 270 days had degraded to .32 and .43 for R and r respectively vs. non-degraded values of .35 and .48 (MgO converted to $BaSO_2$). Considering the severe conditions of the weatherometer and its potential effect on the glue, this performance is considered extremely good and predicts good long term stability for RWR films attached in this manner.

Due to its better transmission in the far IR, PR has been investigated for such configurations. The primary disadvantage is its apparent susceptibility to UV degradation. Since these RWR films will be mounted on the inside of the window, the UV solar illumination must first pass through the glass. Using KCI bonding techniques, a more recent RWR sample having Ag-Al_2O_3 on PR was glued to glass (deposit to glass) using water soluble glue. The sample was then left under a Hg lamp for continuous intense UV irradiation (hitting glass side first). After 11 weeks, equivalent to more than 20 years of AM2 solar UV, there was no change in visual or measured characteristics of the sample.

Optical characteristics are shown in Figs. 82-84 vs. time. Because of its high transparency, the performance in the visible (Fig. 83) and near IR (Fig. 82) is quite similar in the two directions. Very little change, if any, has occurred under the intense UV irradiation. For this sample data was also taken in the near UV (Fig. 84) and again no change has occurred after 11 weeks. The sample has been left under the lamp for continued evaluation.

The overall picture presented by this data is that all of the various desired configurations (Section 1) can be obtained with KCI films glued to glass (see also Section 5).

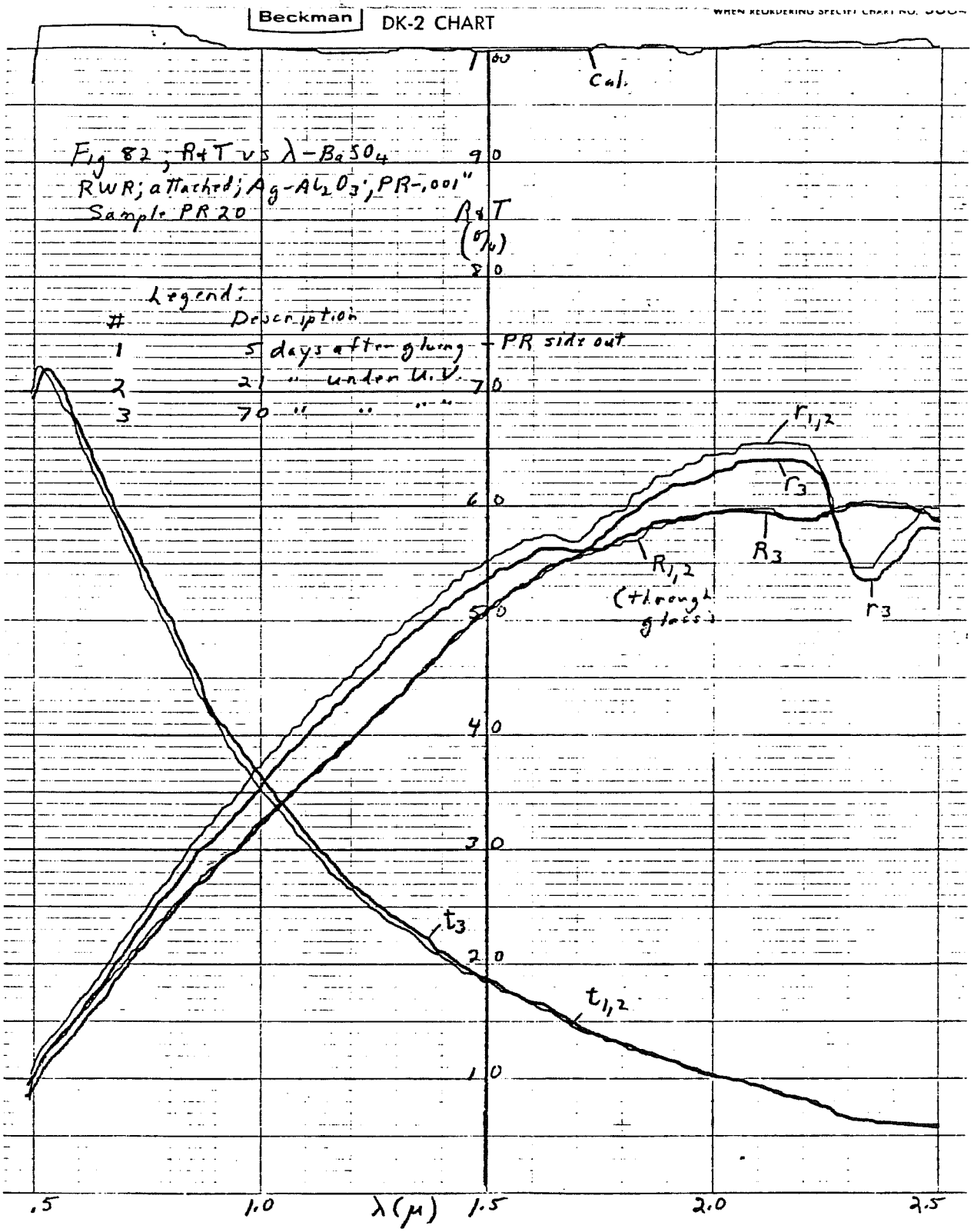
Beckman
DK-2 CHART
Cal.
Fig 82; R+T vs λ - BaSO4
RWR; attached; Ag-Al2O3; PR-.001"
Sample PR 20
R+T (%)
Legend:
Description
1 5 days after glazing - PR side out
2 21 " under U.V.
3 70 " " "
r1,2
r3
R3
R1,2 (+through glass)
r3
t3
t1,2
.5
1.0
λ(μ)
1.5
2.0
2.5

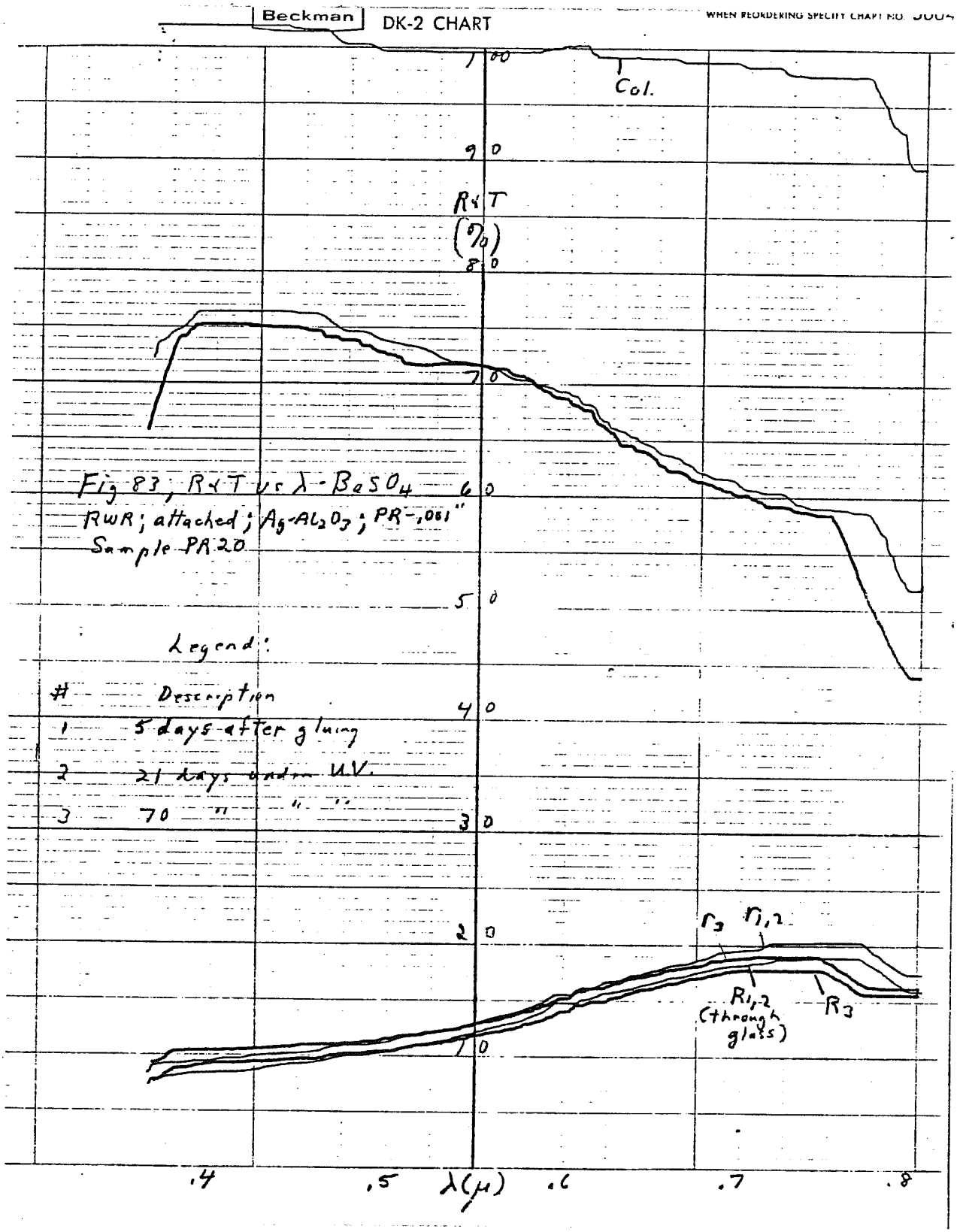
Beckman DK-2 CHART
WHEN REORDERING SPECIFY CHART NO. 3004
100
Col.
90
R+T
(%)
80
70
60
50
40
30
20
10
Fig 83; R+T vs λ - BaSO4
RWR; attached; Ag-Al2O3; PR-.081"
Sample PR 20
Legend:
Description
1 5 days after gluing
2 21 days under UV.
3 70 " " "
r3
r1,2
R1,2 (through glass)
R3
.4
.5
λ(μ)
.6
.7
.8

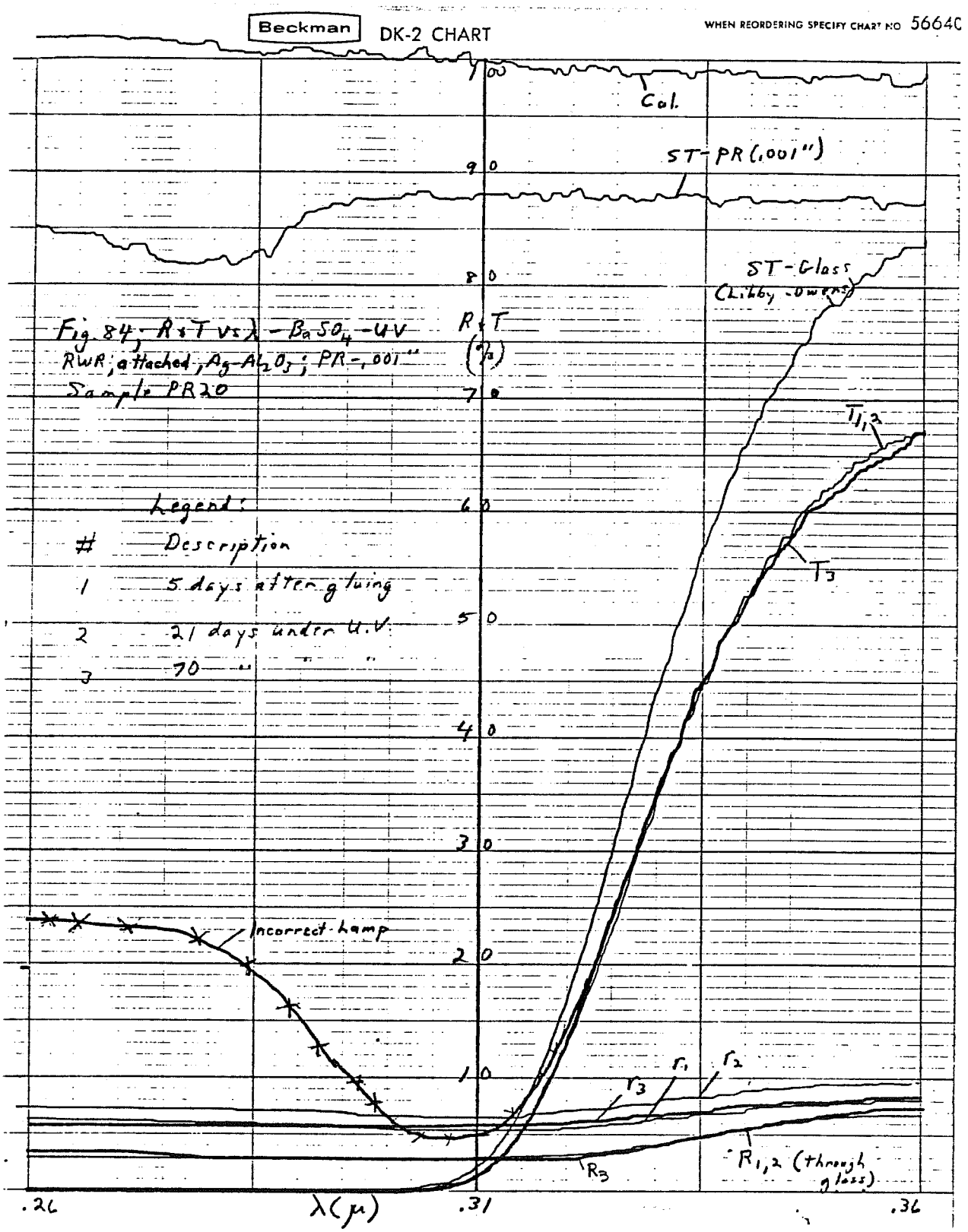
Beckman
DK-2 CHART
WHEN REORDERING SPECIFY CHART NO 56640
Col.
ST-PR(.001")
ST-Glass
(2.66y - 0 wks)
Fig. 84; R & T vs λ - BaSO4 - UV
RWR; attached, Ag-Al2O3; PR-.001"
Sample PR20
R & T
(%)
Legend:
Description
1 5 days after coating
2 21 days under U.V.
3 70 " " "
T1,2
T3
Incorrect lamp
r1
r2
r3
R3
R1,2 (through glass)
.26
λ(μ)
.31
.36

4 Weathering Studies

The best way to test the stability and general weathering characteristics of these high performance solar control windows is somewhat open to question. Testing under real conditions is, for obvious reasons, difficult and very time consuming. Accelerated testing methods tend to introduce extraneous factors which can negatively affect performance but which are really artifacts of the testing and would not exist in real life. KCI has chosen to use a combination of methods including long term general exposure to ambient environment plus handling and washing etc., accelerated weatherometer testing, which is particularly suitable for glass substrates (OWs and RWs), and deliberate exposure to potentially harsh environments or chance factors such as solvents, paint thinners, harsh cleaners, abrasives etc. The latter are more important to the plastic substrate forms (OWRs and RWRs) particularly for configurations where they are bonded with the deposited layer exposed.

The previous section on materials covered some weathering aspects such as long term ambient degradation, some UV testing, and resistance to change during and after gluing. Additional data along these lines is included in this and the next section (Demonstration Program). Also included in this section are typical weatherometer and solvent test data. The data generated under this program are very extensive and those given here were selected to present the more important results.

An extensive study was started under the previous program to evaluate long term exposure and washing effects, particularly on glass substrates. This study has been continued without break through the present program and has been expanded to include plastic substrates as necessary. The reader is referred to the previous report (LBL-7825) for details of the weatherometer and wash cycle program. In essence, the washing consisted of 20 years equivalent industrial cleaning (120 washes - 1 every 2 months) using ammonia water and squeegee techniques. For plastic substrates the squeegee was replaced with a soft cloth or, in most cases, with conventional laboratory size kleenex (Scott Soft-Cote disposable wipers). The coated plastic substrates

were quite easy to clean for most contaminants such as fingerprints. For deposit side to window configurations, it is the plastic itself which is cleaned and, for these cases, minute scratches over a period of time are the most likely cause of performance loss.

It has been rather convincingly determined that scratches, per se, are not likely to affect the performance of either glass substrate or plastic substrate films. Scratches deliberately introduced through the coating on glass substrate samples inserted in the weatherometer have in no cases resulted in undercutting or oxidation of the metal film after a period of 2 1/2 years real elapsed time (15 years equivalent - 8 hours sun and 20 minutes rain each day - temperature 64°C or higher). No patterns of any type attributable to oxidation of the coating on plastic substrate samples resulting from scratches has been observed. Degradation modes, when they have occurred, are more likely to result from long term reflecting film - overcoat interactions.

The weatherometer basically consists of three 1500 watt G. E. tungsten halogen floodlamps (2000 hour lifetime) mounted at one end of a 3' x 3' x 3 1/2' Al enclosure. Samples are mounted on a 30" x 32" area on a door at the far end and are illuminated continuously at 2.1 - 2.8 suns (Air Mass 2 - terrestrial). Since the system runs continuously, each day is equivalent to approximately 6-8 days at 1 sun for 8 hours. A rain cycle of 20 minute occurs every 4 hours. Sample temperatures are roughly 64°C during the sun cycle and 23°C during the rain cycle. The rain is sprayed on the samples at the elevated temperatures producing a very severe test environment. Before introduction of a cooling fan, many of the samples were subjected to 180°C temperatures during the sun cycle but this caused highly corrosive Al compounds to form.

In general, weatherometer results have been used to complement the metal-dielectric material studies (Section 3) in choosing the combinations for development. At the present time, various systems still look viable. Final choices will be made on the basis of additional weathering data plus economic factors.

At the beginning of the program, the Cu-SiO_2 combination was believed to be stable and was chosen as the test vehicle for the demonstration samples. Longer term studies showed that the Cu systems had some basic chemical interaction problems with the overcoat which were greatly reduced by going to Bs and eliminated with Al_2O_3 as the overcoat.

The general problem with the Cu-SiO_2 system is demonstrated by the time related characteristics of the OWR color sample set shown in Figs. 85-91. Figs. 85, 88 and 90 give the characteristics after 13 months ambient exposure and Figs. 86, 87, 89 and 91 are for zero time. Fig. 85 has both R and T characteristics (.5 - 2.5μ) to complement Figs. 86 and 87. These samples were made to duplicate the colors of the sample sets made on glass (Section 3.2) and did an excellent job of duplicating the external coloring. The substrate material used was originally thought to be P (.004") but was later found to be an acetate. Various thicknesses were used for the SiO_2 overcoat with a 2:1 variation.

After 23 months, the samples were visually unaltered, without corrosion or coloring changes. The spectrometer measurements after 13 months (Figs. 85, 88, 90) when compared to the zero time values (Figs. 86, 87, 89, 91) showed a small decrease in R and corresponding increase in T. The R change is particulary evident in the visible (cp. Figs. 88 and 89) but is still quite clear at 1.5μ (note standards difference). These changes took place for all samples and were not related to oxide overcoat thicknesses. Although there were some relative curve shifts, these were within experimental variation, or, in some cases, were balanced by relative shifts in the other direction (i.e. vs. oxide thickness) for other sample pairs.

This general R fall-off may be stabilized at the new lower values and additional measurements will be made to check this at the end of 2 years. These results, combined with others discussed previously, definitely indicated that there were problems with the Cu-SiO_2 system which would not be cured by going to thicker dielectric layers and it was therefore completely rejected as a test vehicle. Because it was not quite clear at the time that the Bs based

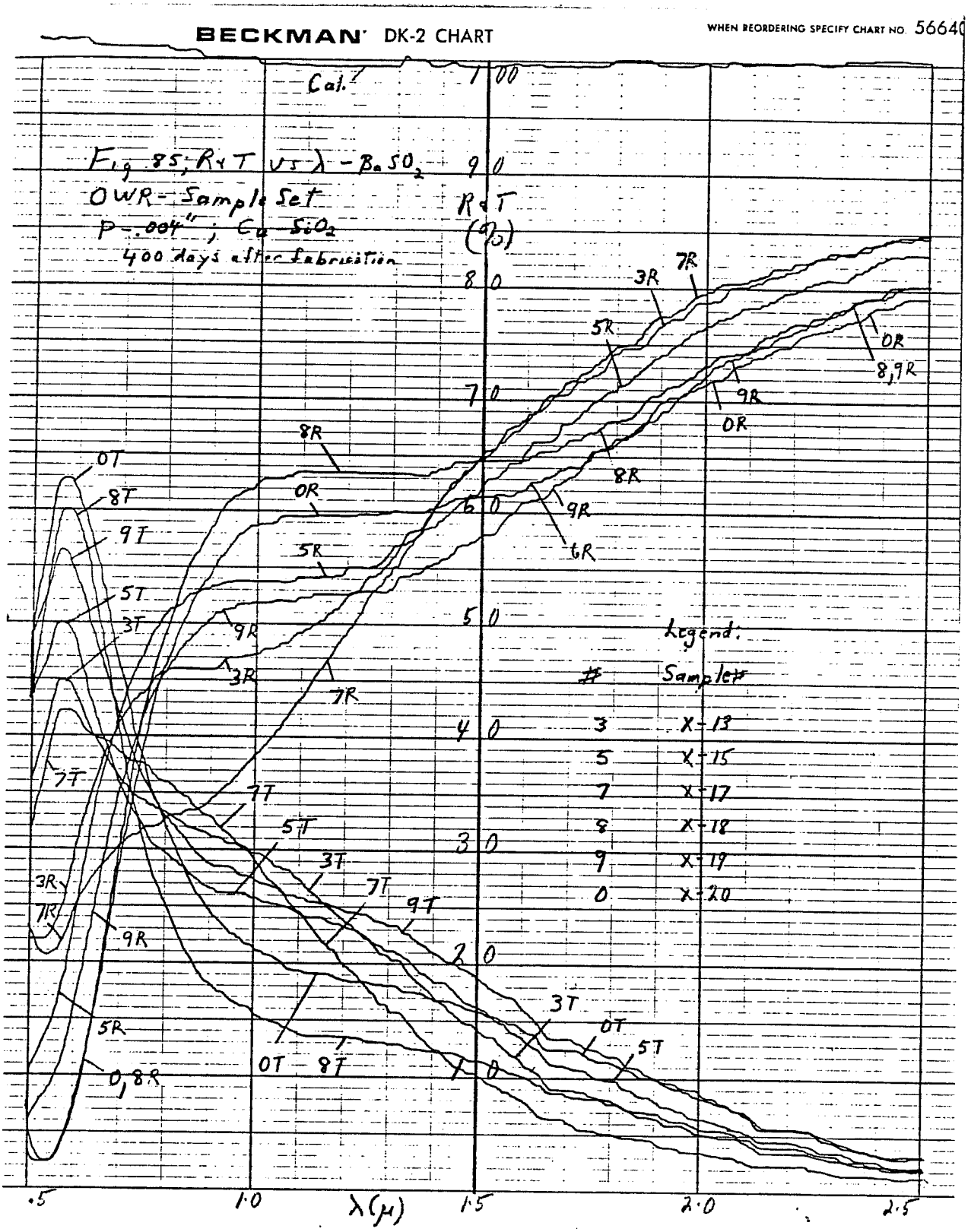
BECKMAN DK-2 CHART
WHEN REORDERING SPECIFY CHART NO. 56640
Cal.
Fig 85; R+T vs λ - Ba SO2
OWR - Sample Set
P - .004"; Ca SiO2
400 days after fabrication
R+T (%)
100
90
80
70
60
50
40
30
20
10
0
λ(μ)
.5
1.0
1.5
2.0
2.5
Legend:
Sample#
3 X-13
5 X-15
7 X-17
8 X-18
9 X-19
0 X-20
0T
8T
9T
5T
3T
7T
3R
7R
9R
5R
0,8R
OR
8R
6R
0T - 8T

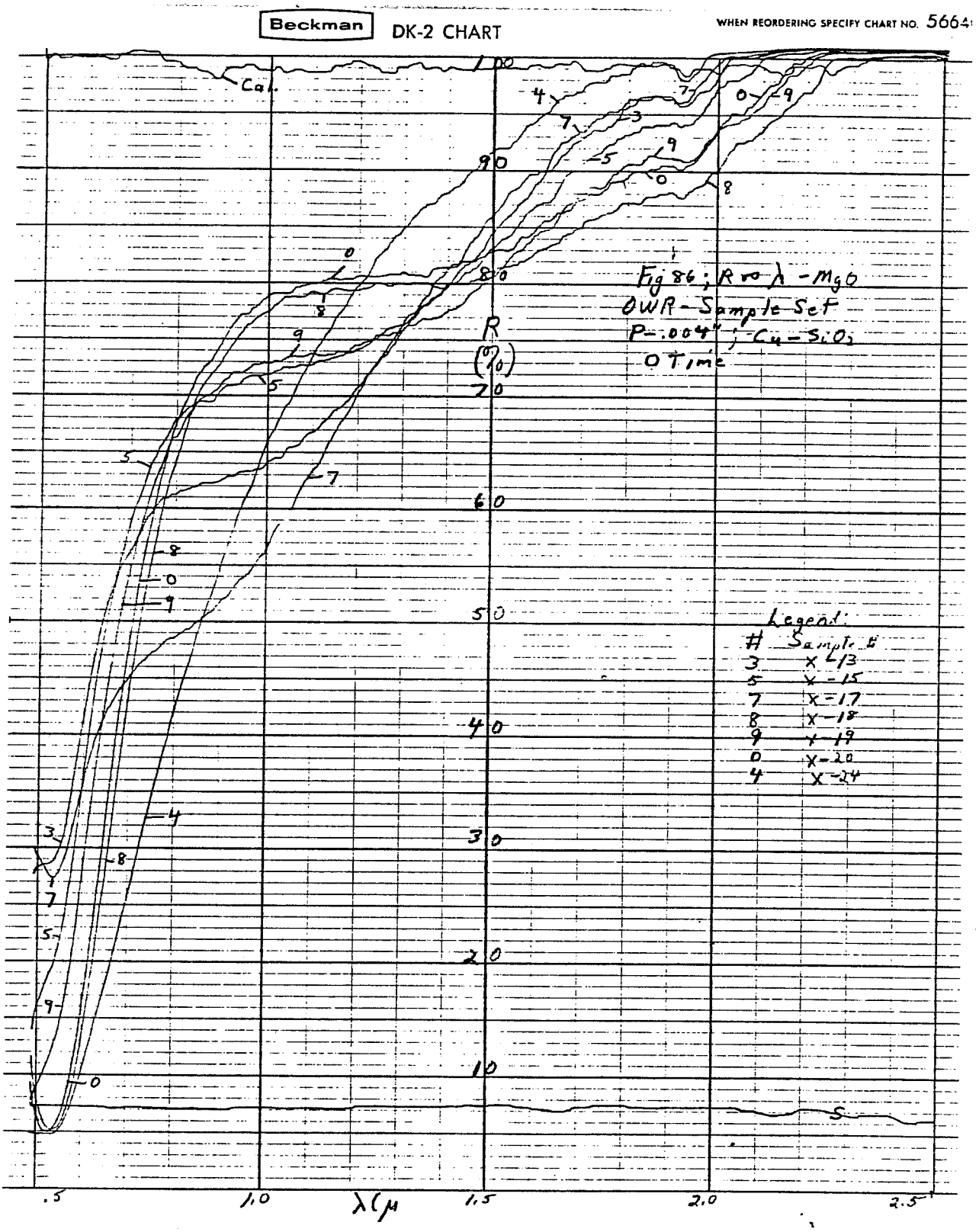
Beckman
DK-2 CHART
WHEN REORDERING SPECIFY CHART NO. 5664
Cal.
Fig 86; R vs λ - MgO
OWR - Sample Set
P=.004" ; C4 = SiO2
0 Time
R (%)
λ (μ
.5
1.0
1.5
2.0
2.5
Legend:
Sample
3 x-13
5 x-15
7 x-17
8 x-18
9 x-19
0 x-20
4 x-24

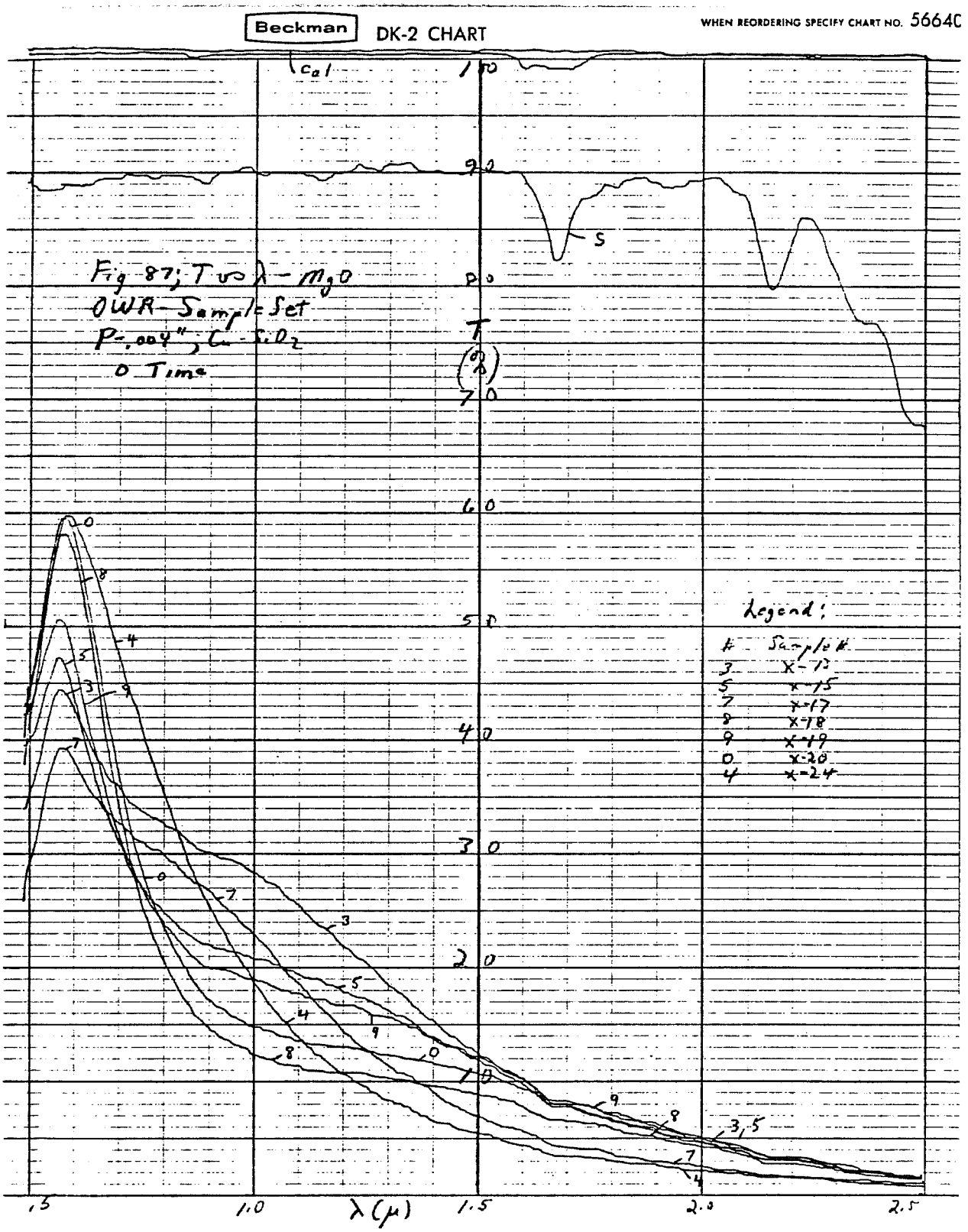
Beckman
DK-2 CHART
WHEN REORDERING SPECIFY CHART NO. 56640
Cal
100
90
80
70
60
50
40
30
20
10
T (%)
S
Fig 87; Tvo λ - MgO
OWR - Sample Set
P=.004"; Cu - SiO2
0 Time
Legend:
Sample
3 X-13
5 X-15
7 X-17
8 X-18
9 X-19
0 X-20
4 X-24
1.5
1.0
λ (μ)
1.5
2.0
2.5

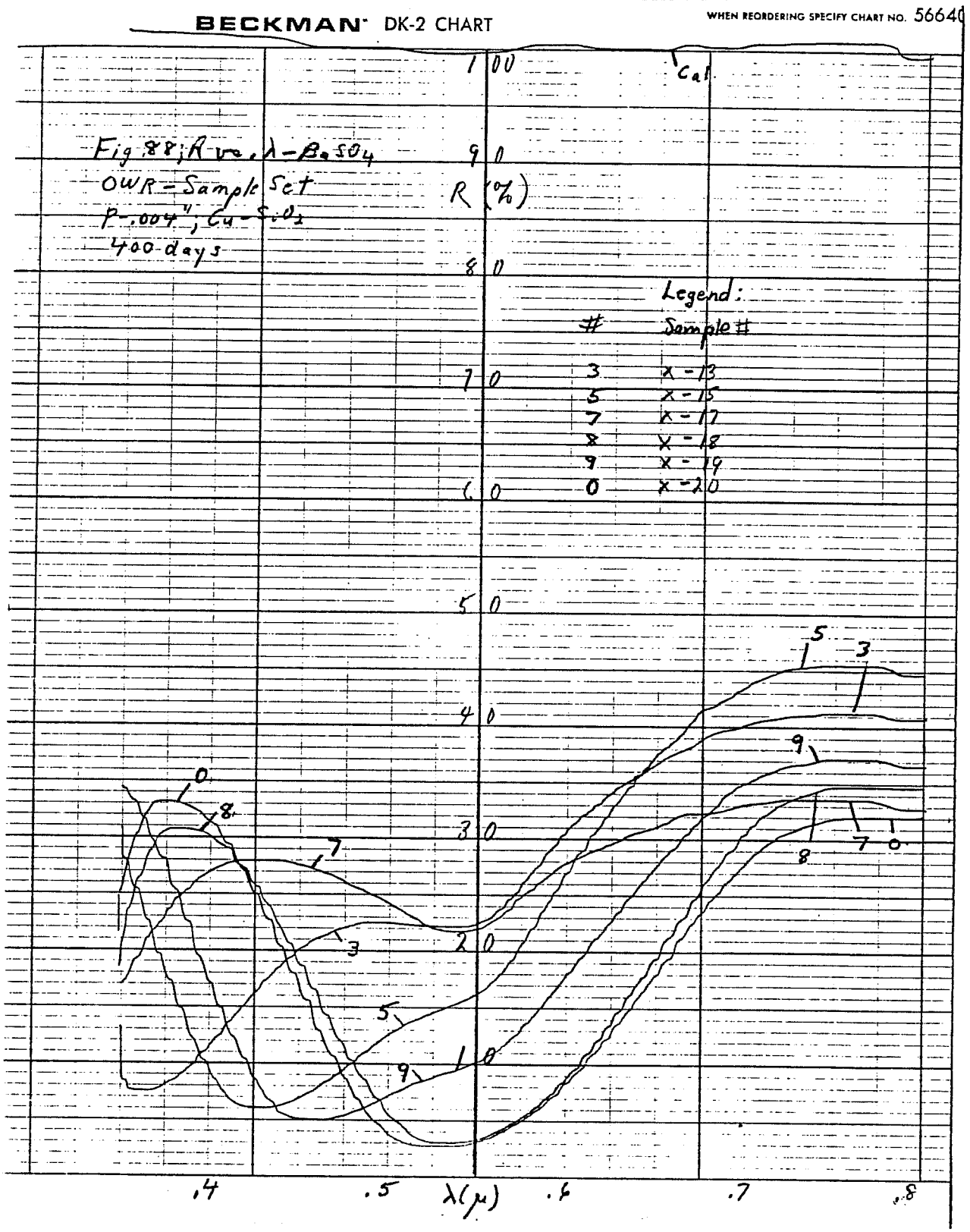
BECKMAN DK-2 CHART
WHEN REORDERING SPECIFY CHART NO. 56640
Cal.
Fig. 88; R vs. λ - Ba_2SO_4
OWR - Sample Set
p-.004"; C_4 - S_iO_2
400 days
R (%)
100
90
80
70
60
50
40
30
20
10
Legend:
Sample
3 x - 13
5 x - 15
7 x - 17
8 x - 18
9 x - 19
0 x - 20
.4
.5
λ(μ)
.6
.7
.8

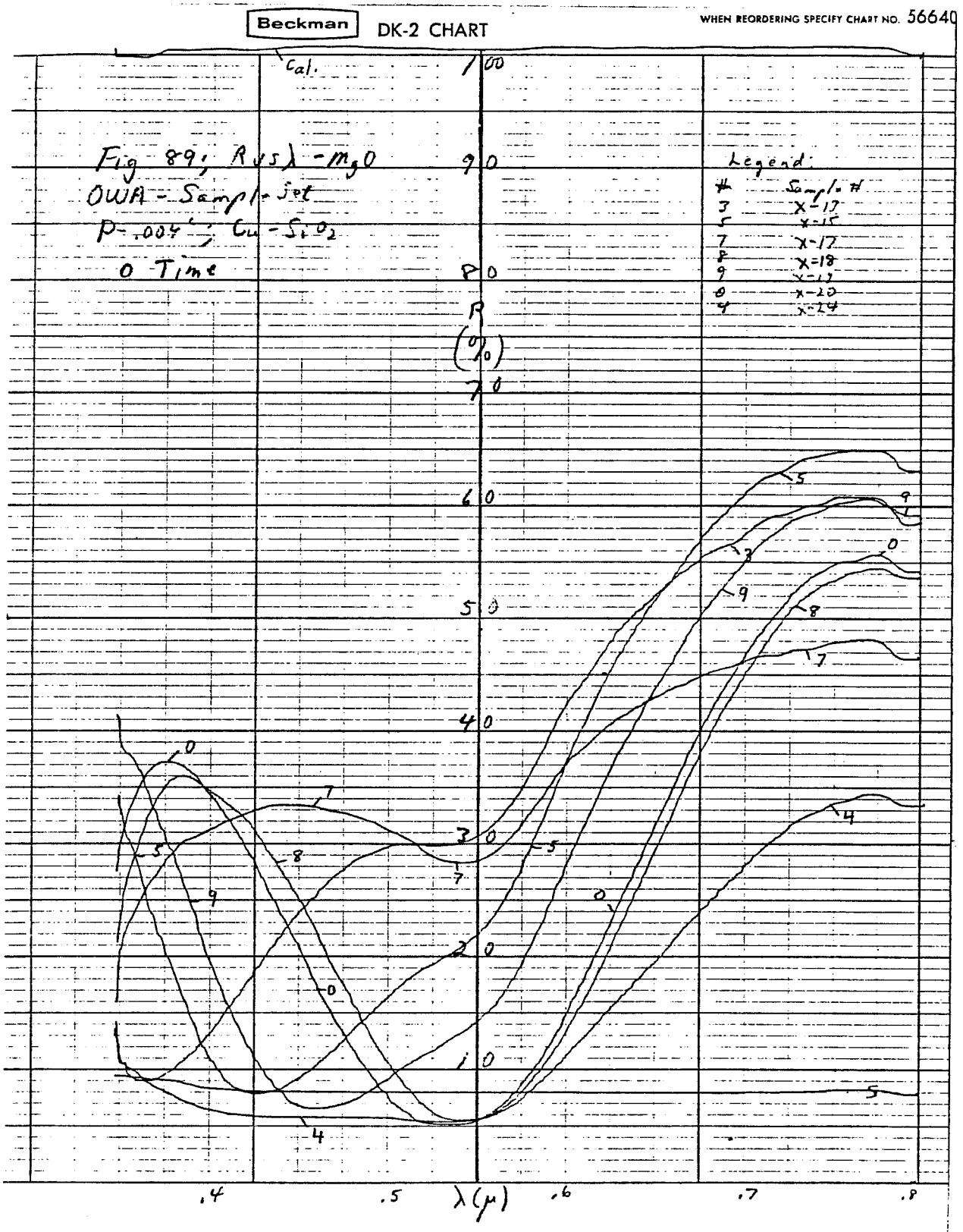
Beckman
DK-2 CHART
WHEN REORDERING SPECIFY CHART NO. 56640
Cal.
Fig 89; R vs λ - MgO
OWA - Sample set
P-.004"; Cu - SiO2
0 Time
Legend:
Sample
3 X-17
5 X-15
7 X-17
8 X-18
9 X-19
0 X-20
4 X-24
R (%)
100
90
80
70
60
50
40
30
20
10
.4
.5
.6
.7
.8
λ(μ)

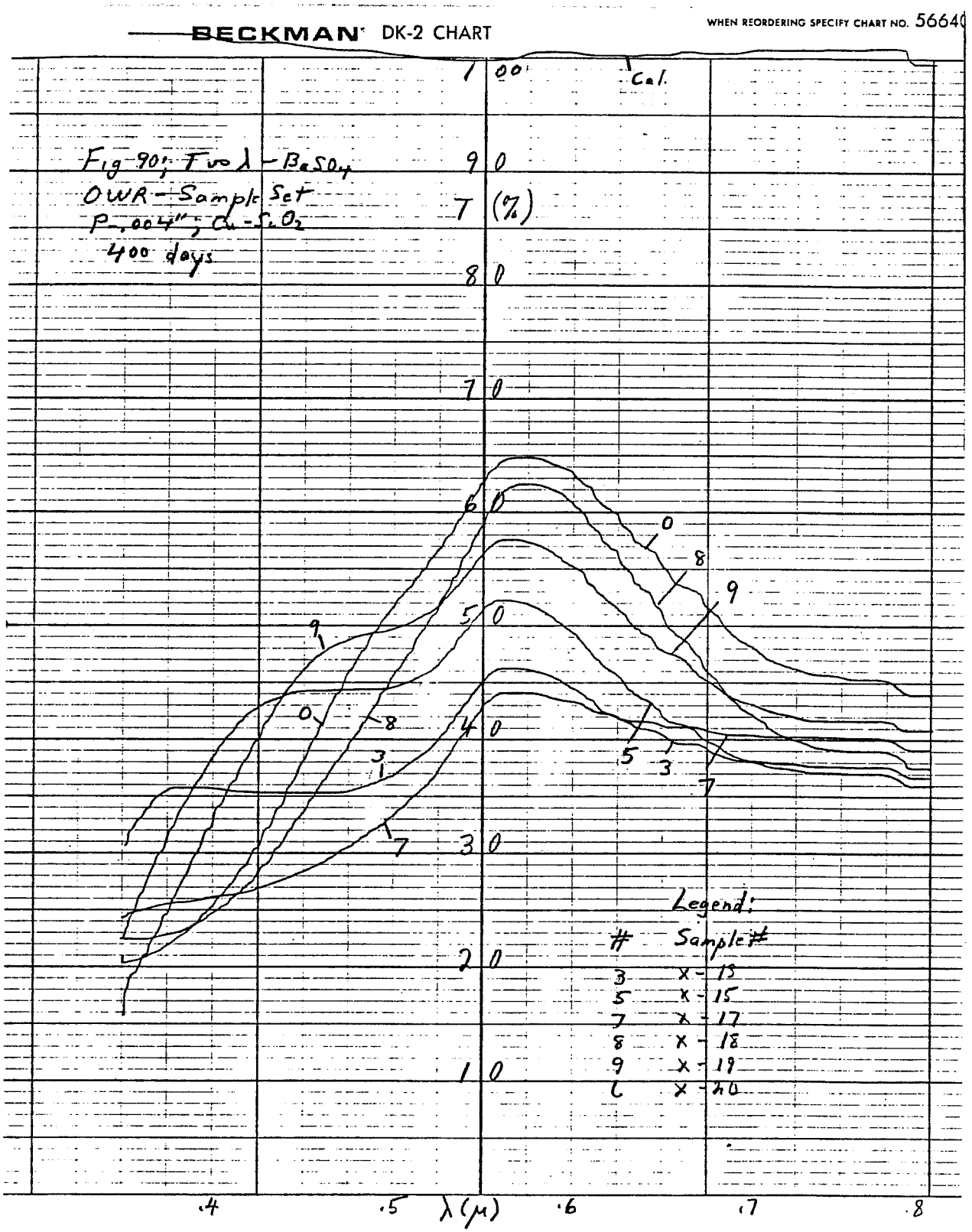
BECKMAN DK-2 CHART
WHEN REORDERING SPECIFY CHART NO. 56640
Fig 90; T vs λ - BaSO4
OWR - Sample Set
P-.004"; Cu-S.O2
400 days
100
Cal.
90
T (%)
80
70
60
50
40
30
20
10
.4
.5
λ (μ)
.6
.7
.8
Legend:
Sample
3 X - 13
5 X - 15
7 X - 17
8 X - 18
9 X - 19
C X - 20

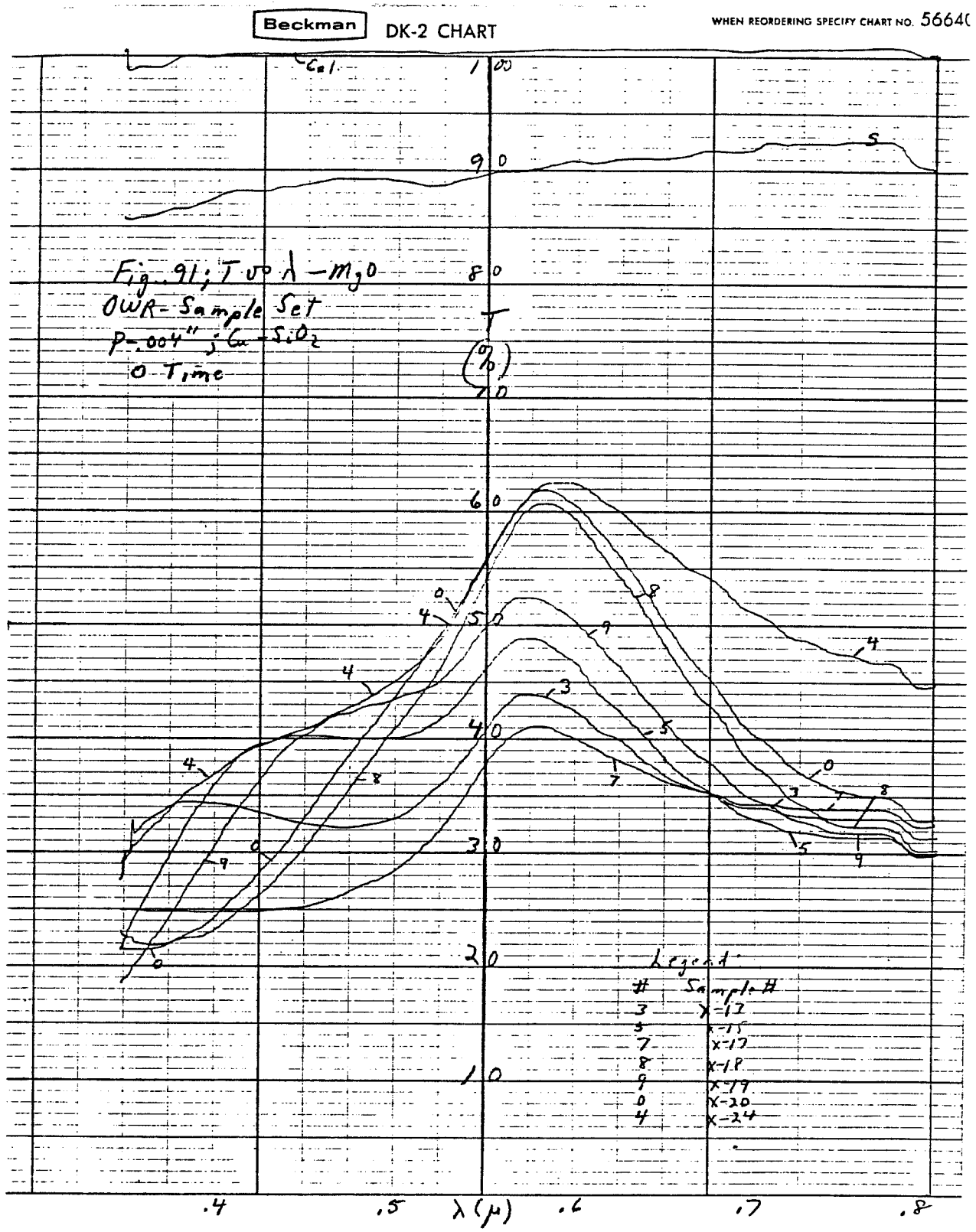
Beckman
DK-2 CHART
WHEN REORDERING SPECIFY CHART NO. 56640
Cal.
100
90
80
70
60
50
40
30
20
10
T (%)
Fig. 91; T vs λ - MgO
OWR - Sample Set
P-.004" ; Ca - SiO2
0 Time
.4
.5
λ (μ)
.6
.7
.8
Legend
Sample
3 X-12
5 X-15
7 X-17
8 X-18
9 X-19
0 X-20
4 X-24

systems could obviate the Cu problems, Ag was substituted for the demonstration samples. Also Al_2O_3 was used to replace SiO_2 because of the latter's uncertain role in the Cu degradation process. The final demonstration samples (Section 5) were therefore made with Ag-Al_2O_3.

For original equipment configurations (OW and RW) the weatherometer data has been quite useful in determining the best system. Because of the original very severe high temperature (180°C) environment and the continuing severe environment, KCI feels that any samples which retain their characteristics are very likely to withstand all normal conditions for many years (goal - 20 years). Samples which show more degradation are not necessarily eliminated but those that pass should certainly be favored.

The metal-dielectric systems covered under this program are the only ones of interest here although others have been investigated. Of the latter, the Al-Al_2O_3 combination is of special interest since Al is used in conventional solar control films. This system stands up very well to the present weatherometer conditions, as do some others (e.g. Ni-SiO_2, Mo-SiO_2) but the characteristics needed for high performance windows cannot be achieved with Al. This conclusion has been tested many times and many ways both on glass and plastic substrates.

With Cu eliminated, the rest can be divided into Bs based and Ag based systems. Both of the Bs combinations (Bs-SiO_2 and Bs-Al_2O_3) were attacked by the initial very high temperature environment with the Al_2O_3 coatings, in particular, being etched along drip lines due to hydrated alumina compounds (no other damage). At the lower temperature (64°C) these etch effects discontinued. The Bs-SiO_2 system has continued to degrade overall with time at a slow rate, but it is unfortunately not clear whether this degradation would have occurred without the original very high temperature testing (steam dissolves SiO_2).

The Bs-Al_2O_3 system, on the other hand, has shown very little degradation under the lower temperature environment. Figs. 92-97 give comparative data at 426 days (Figs. 92 and 95), 261 days (Figs. 93 and 96) and

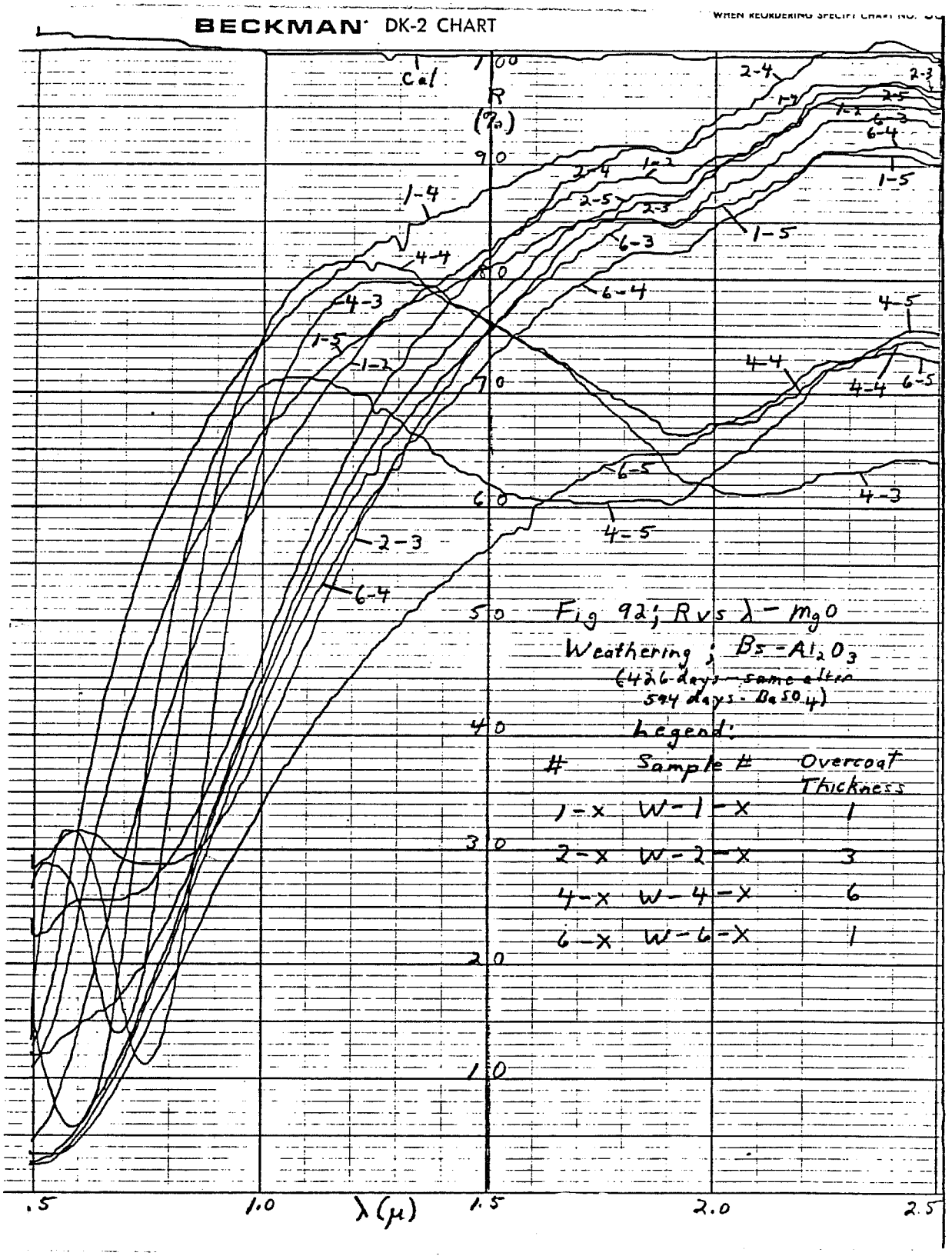
BECKMAN DK-2 CHART
Cal
R (%)
100
90
80
70
60
50
40
30
20
10
.5
1.0
λ (μ)
1.5
2.0
2.5
1-4
4-4
4-3
1-5
1-2
2-3
6-4
2-4
1-3
2-5
6-3
4-5
6-5
Fig 92; R vs λ - MgO
Weathering; Bs = Al2O3
(426 days - same effect
524 days - BaSO4)
Legend:
Sample # Overcoat Thickness
1-x W-1-x 1
2-x W-2-x 3
4-x W-4-x 6
6-x W-6-x 1

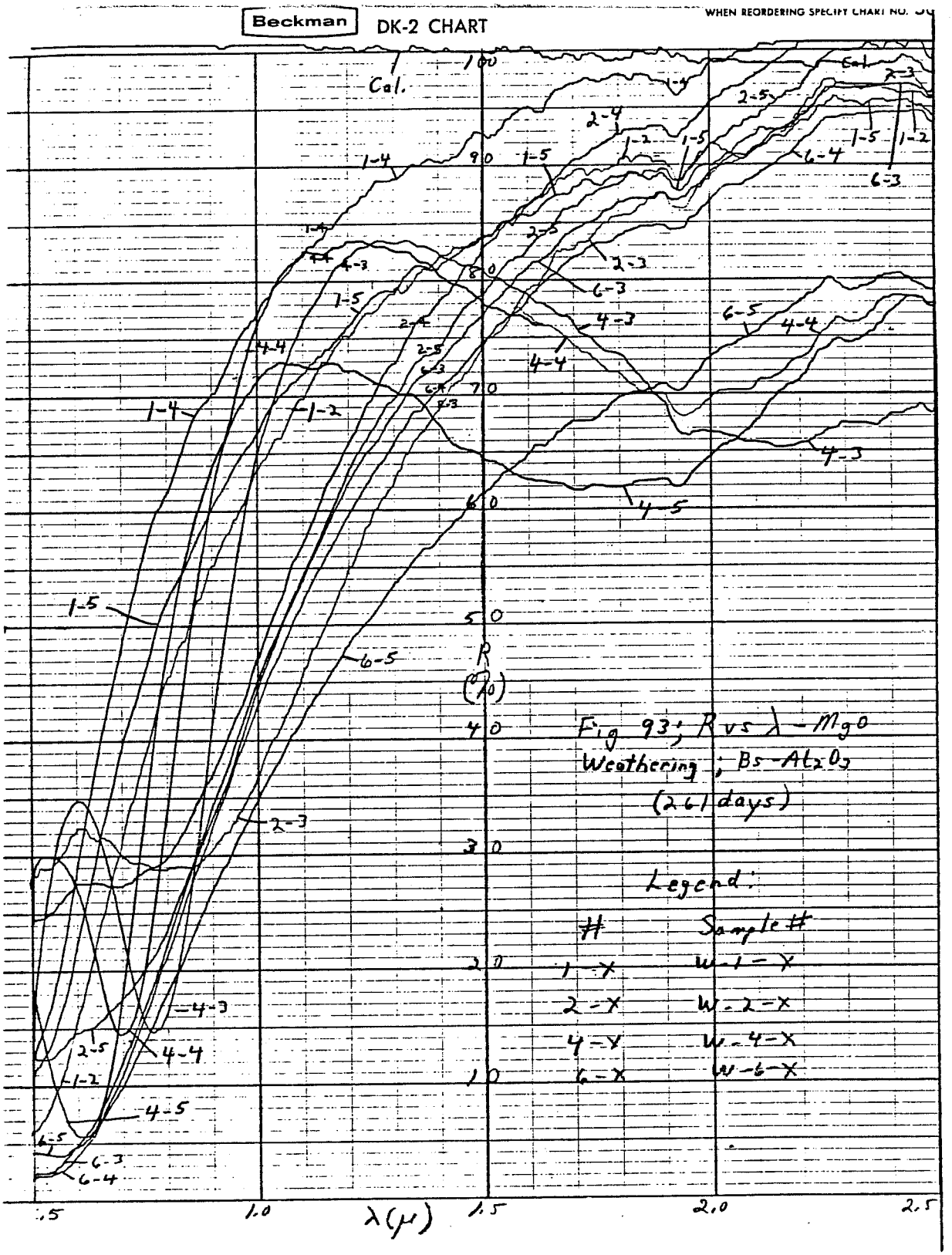
Beckman
DK-2 CHART
WHEN REORDERING SPECIFY CHART NO.
Col.
100
90
80
70
60
50
40
30
20
10
R
(%)
.5
1.0
λ(μ)
1.5
2.0
2.5
1-4
1-2
1-5
6-5
2-3
4-3
2-5
4-4
4-5
6-3
6-4
2-4
6-1
Fig 93; R vs λ - MgO
Weathering; Bs-Al2O3
(261 days)
Legend:
Sample
1-X W-1-X
2-X W-2-X
4-X W-4-X
6-X W-6-X

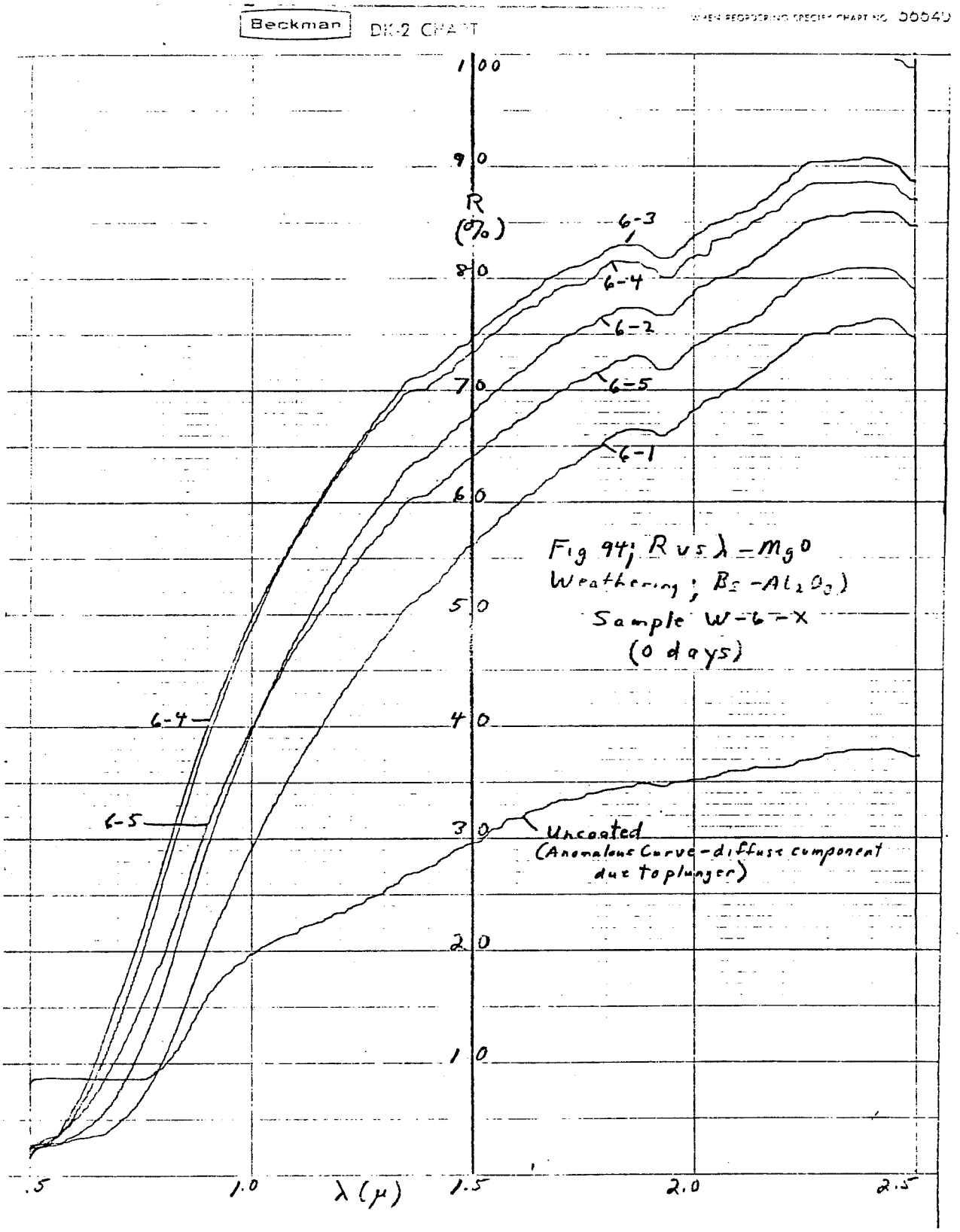

Fig 94; R vs λ – MgO
Weathering; (B_2-Al_2O_3)
Sample W-6-X
(0 days)

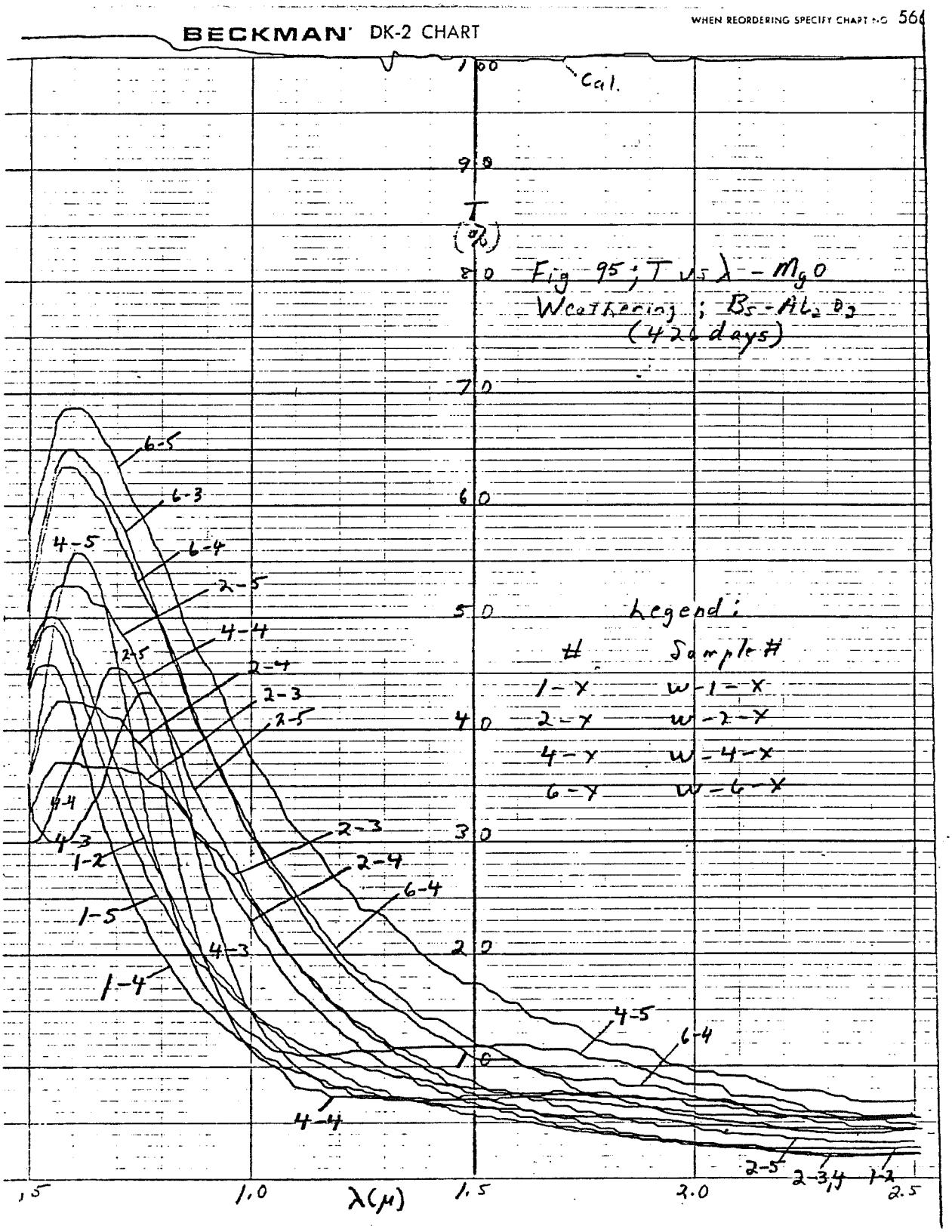
BECKMAN DK-2 CHART
WHEN REORDERING SPECIFY CHART NO. 566
100
Cal.
90
T
(%)
80
70
60
50
40
30
20
10
Fig 95; T vs λ - MgO
Weathering; B5-Al2O3
(426 days)
Legend:
Sample
1-x w-1-x
2-x w-2-x
4-x w-4-x
6-x w-6-x
6-5
6-3
4-5
6-4
2-5
4-4
2-4
2-3
2-5
4-4
4-3
1-2
2-3
2-4
6-4
1-5
4-3
1-4
4-5
6-4
4-4
2-5
2-3,4
1-2
.5
1.0
λ(μ)
1.5
2.0
2.5

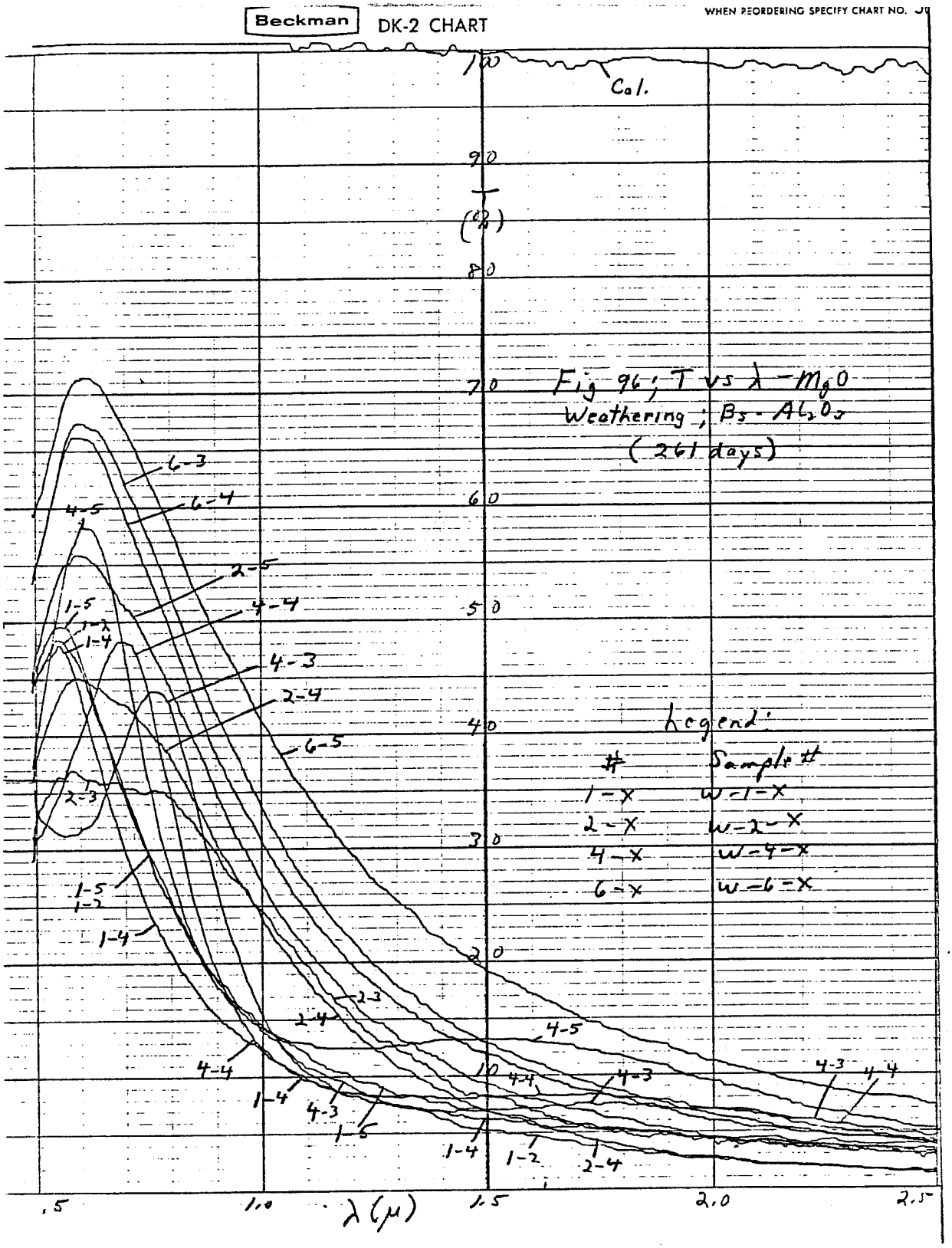
Beckman
DK-2 CHART
WHEN REORDERING SPECIFY CHART NO.
Cal.
100
90
80
70
60
50
40
30
20
10
T (%)
Fig 96; T vs λ - MgO
Weathering; B5 - Al2O3
(261 days)
Legend:
Sample
1-x w-1-x
2-x w-2-x
4-x w-4-x
6-x w-6-x
.5
1.0
1.5
2.0
2.5
λ (μ)

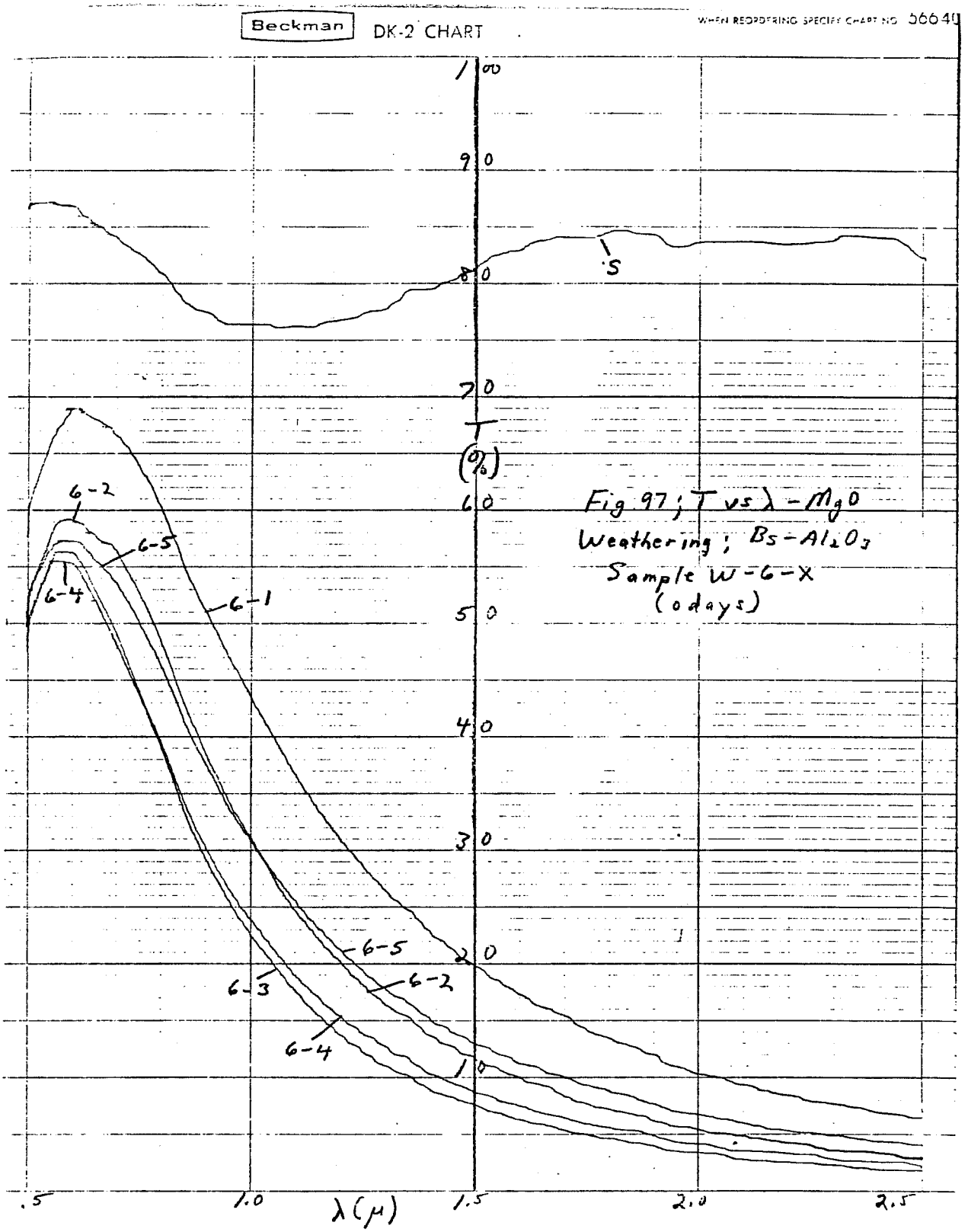
Beckman
DK-2 CHART
WHEN REORDERING SPECIFY CHART NO 56640
100
90
80
70
T
(%)
60
50
40
30
20
10
S
6-2
6-5
6-4
6-1
6-5
6-3
6-2
6-4
.5
1.0
λ(μ)
1.5
2.0
2.5
Fig 97; T vs λ - MgO
Weathering; Bs - Al2O3
Sample W-6-X
(0 days)

zero time (Figs. 94 and 97). For zero time only one set of curves (sample 6) are given since the other results are similar and sample 6 had the thinnest oxide overcoat. The curves for 426 days and 261 days should be viewed with the knowledge that there was a systematic 1-2% decrease for all 426 day measurements over most of the spectrum with the decrease being slightly greater at the 2.5μ. This decrease was due to the MgO standards problem discussed earlier. The 261 day R curves are noticeably higher than the zero time values indicating that they may be anomalously high. The 426 day values are, in fact, very close to the zero time values and indicate no change has occurred except for the very high temperature etch lines. Sample 6-5 is an exception but this particular sample was severly attacked under the original 180°C temperatures condition since it was directly in the path of water run-off. Visually there are no changes in these samples in the unetched areas.

Spot checks made of the R curves at the end of 594 days also indicated no change. The T curves were also essentially unaffected between the 261 and 426 day points. Both of the latter give higher T values than at zero time but this is primarliy due to the fact that the open areas due to the etch lines cannot be avoided in the T measurements. The 426 day T values also show the systematic 1-2% change relative to the 261 day values (rather than expected increase based on R data).

Sample 6-1, which has a deliberate diagonal scratch through its coating, is not checked for R and T but looks excellent and shows absolutely no sign of undercutting oxidation due to the scratch. These samples, which have been in the system since the beginning, at the end of 594 days had seen the equivalent (3500+ cycles) of thermally cycling from 23°C to 64°C (or higher) every day for about 10 years with an equivalent sun exposure of 12 years with the sun shining for 8 hours every day and rain nearly once a day on the windows at their highest temperature. Visual observation at the end of 960 days, or 19 years solar equivalent, still showed no change. These samples were also washed 120 times or 20 years industrial equivalent. They have therefore been subjected to very severe test conditions which speaks very well for the Bs-Al_2O_3

system which has stood up remarkably once the original 180° C test condition was relieved.

Results for the Ag-SiO_2 system on glass have been very interesting. For a period of roughly half a year in the weatherometer (64° C temperature only) there were essentially no changes in the test samples, either visual or measured. At the end of 1 year there was a severe reduction in R and corresponding increase in T. Physically the coatings began to show microscopic to macroscopic sized cracks etc. in patterns which were almost certainly stress related (rectilinear) rather than corrosion (evidenced by fading) related. Increases in T were roughly comparable to increases in the "open" area of the samples due to cracking and resulting spallation. Where the coating was intact, the physical appearance and reflectivity were essentially unchanged from the original condition. No comparable effect has been seen on plastic substrate samples.

The most interesting observation was that this degradation was apparently not a strong function of overcoat thickness. Samples with overcoats 6-7 times as thick as other samples degraded as much, or more, than the thinner overcoat samples. In contrast, samples with very thick Ag layers (normal mirror level) did not degrade in the same manner, even with thin oxide coatings. The thickness and character of the reflecting layer is therefore clearly an important factor in any thermal stress effects since the Ag underlayer samples were clearly the most susceptible to such effects.

In order to reduce stress effects due to the low thermal expansion SiO_2, samples were made with the Ag-Al_2O_3 combination and inserted in the weatherometer. As shown in Fig. 98, there was no change in R (2.5μ) at the end of 261 days nor was there any visual change (Note: measurements of R and T made in 2 quadrants of sample at 261 days; quadrant 2 only at zero time). Considerably more time will be needed to fully evaluate this system for original equipment use.

Much of the time spent on life testing of plastic substrates was concerned with solvent tests using distilled water, ammonia water (made with tap

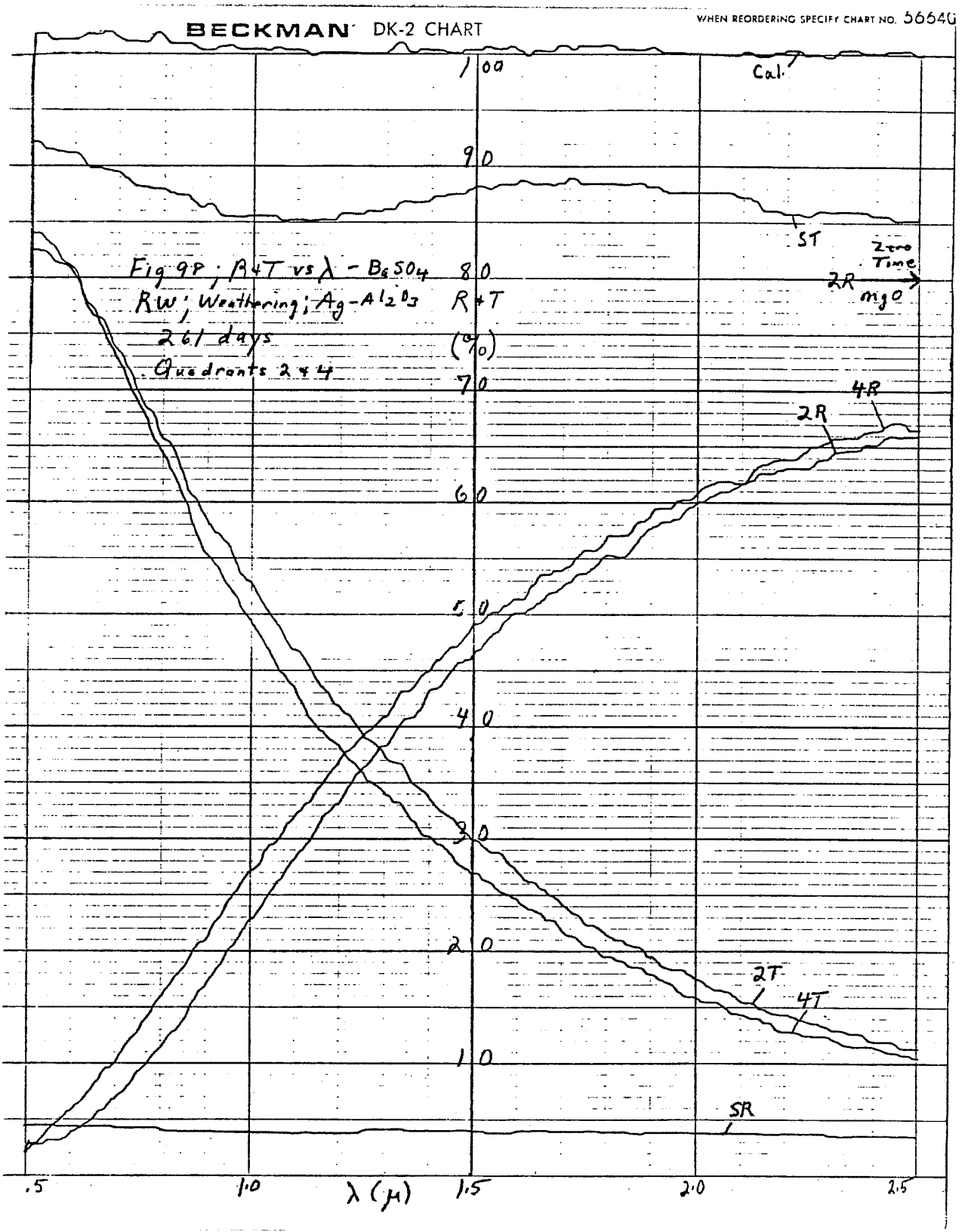
BECKMAN DK-2 CHART
WHEN REORDERING SPECIFY CHART NO. 56640
Cal.
ST
Zero Time
2R
MgO
4R
2R
2T
4T
SR
100
90
80
70
60
50
40
30
20
10
R+T (%)
.5
1.0
λ (μ)
1.5
2.0
2.5
Fig 98; R+T vs λ - BaSO4
RW; Weathering; Ag-Al2O3
261 days
Quadrants 2 4 4

water), isopropyl alcohol, acetone, trichloroethylene, lacquer thinner and 409. Since the samples might be mounted with the deposited side in, or out, full immersion tests were specified. Residential type retrofit material was used since it was more likely to be attacked than office window material. Tests were conducted on Ag-SiO_2, Ag-Al_2O_3 and Bs-Al_2O_3 systems.

The procedure was basically to immerse the sample in the solvent for 5 minutes with 3 seconds of manual agitation every 30 seconds. After removal the sample was then rinsed in a series of less active solvents which had already been shown to have no affect on performance in order to remove residual solvent films. They were than blown dry and retested optically. In general, the order of severity was that given above so that, for example, a trico test film would be rinsed in the order acetone, alcohol, ammonia water (sometimes omitted as unnecessary) and distilled water.

Tests were done on many films involving the above combinations on P and FEP substrates. Results were essentially identical for P and FEP substrates for a given metal-dielectric combination. Bs-Al_2O_3 results were also essentially identical to Ag-Al_2O_3 results. Figs. 99-110 have therefore been selected to show typical results on FEP for the Ag-SiO_2 system and on P for the Ag-Al_2O_3 system.

These solvent immersion tests were considered indicative of potential severe attack mechanisms in actual use; e.g. lacquer thinner in connection with painting, 409 in connection with cleaning etc. It was quickly discovered that 409 is a very active cleaner which readily removes oxidized paint and attacks Al and glass. The container clearly warns against its use on varnished surfaces, Al or glass. The results below show the potential problem which was only on Al_2O_3. SiO_2 was immune.

Figs. 99-104 show that none of the solvents studied had any appreciable effect on the film performance. There was also no change visibly except for wrinkling on the films due to extensive handling. This wrinkling and/or residual films are believed to be cause of some small (uniform with wavelength) decreases in R and increases in T (e.g. Fig. 100 after acetone). Other films in the same

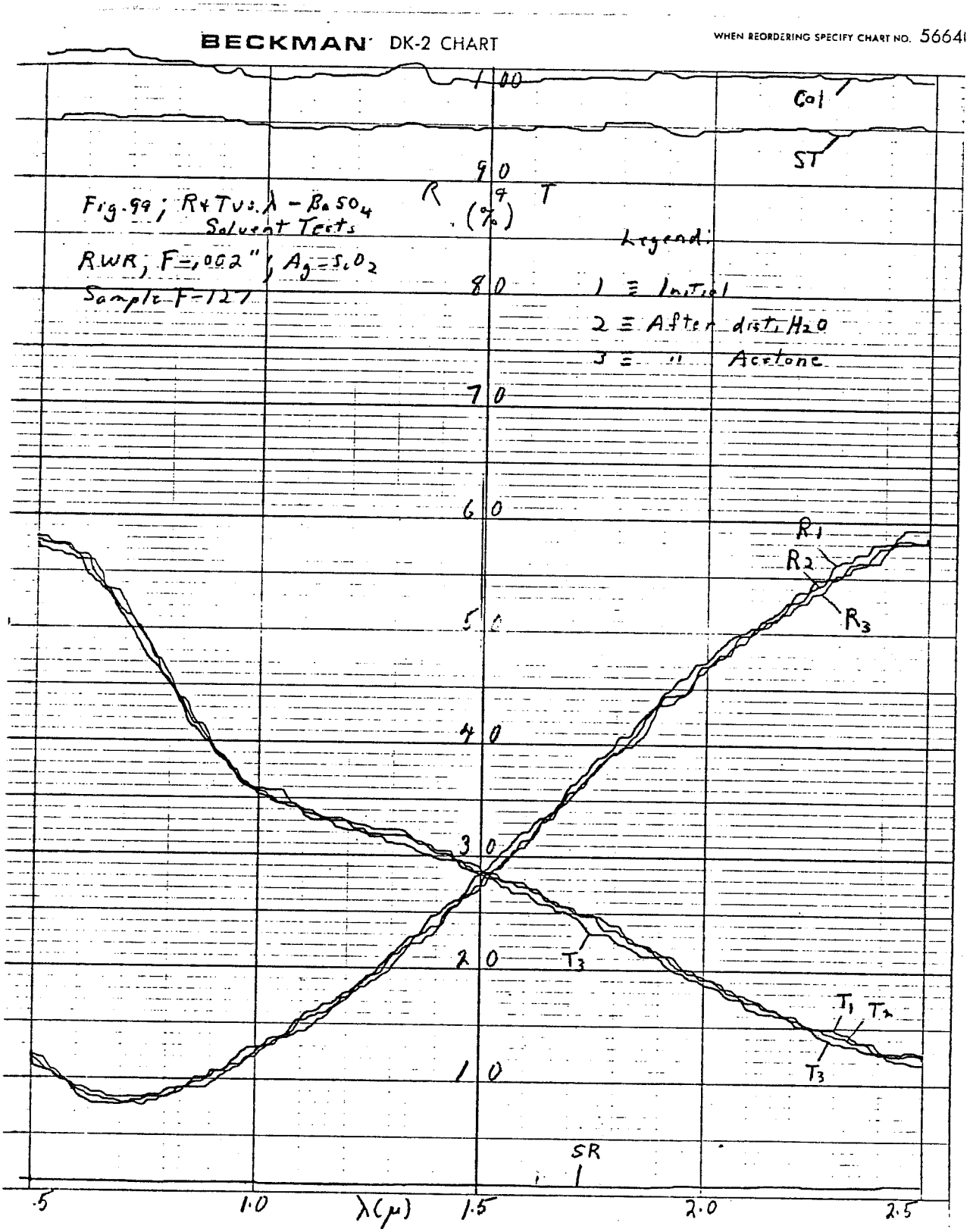
BECKMAN DK-2 CHART
WHEN REORDERING SPECIFY CHART NO. 56641
Fig. 99; R+T vs. λ - BaSO4
Solvent Tests
RWR; F=.002"; Ag=SiO2
Sample F-127
R (%) T
Legend:
1 ≡ Initial
2 ≡ After dist. H2O
3 ≡ " Acetone
Col
ST
100
90
80
70
60
50
40
30
20
10
R1
R2
R3
T3
T1 T2
T3
SR
.5
1.0
λ(μ)
1.5
2.0
2.5

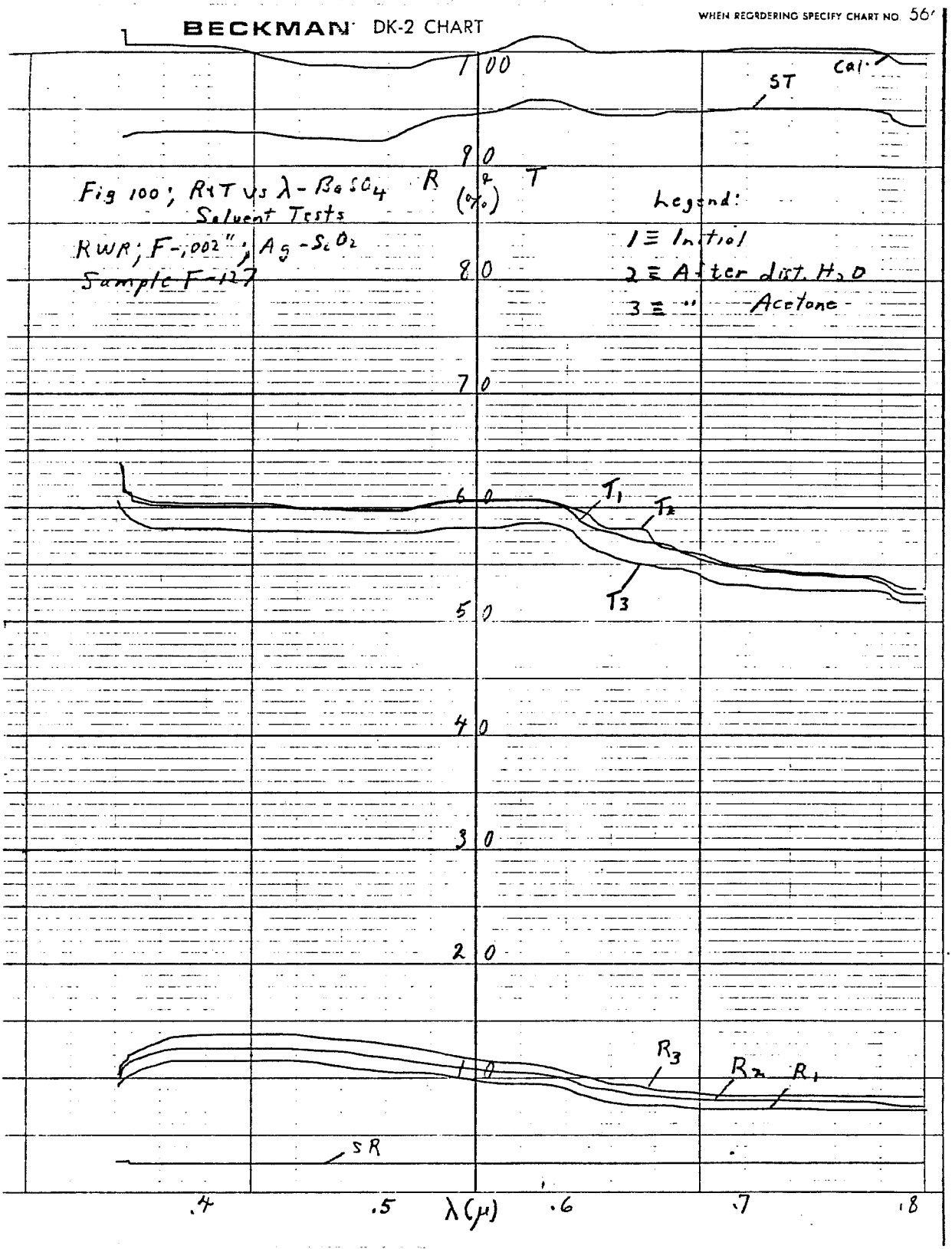
BECKMAN DK-2 CHART
WHEN REORDERING SPECIFY CHART NO. 56
100
90
80
70
60
50
40
30
20
R (%)
T
Cal.
ST
Fig 100; R+T vs λ - BaSO4
Solvent Tests
RWR; F-.002"; Ag-SiO2
Sample F-127
Legend:
1 ≡ Initial
2 ≡ After dist. H2O
3 ≡ " Acetone -
T1
T2
T3
R3
R2
R1
SR
.4
.5
λ(μ)
.6
.7
.8

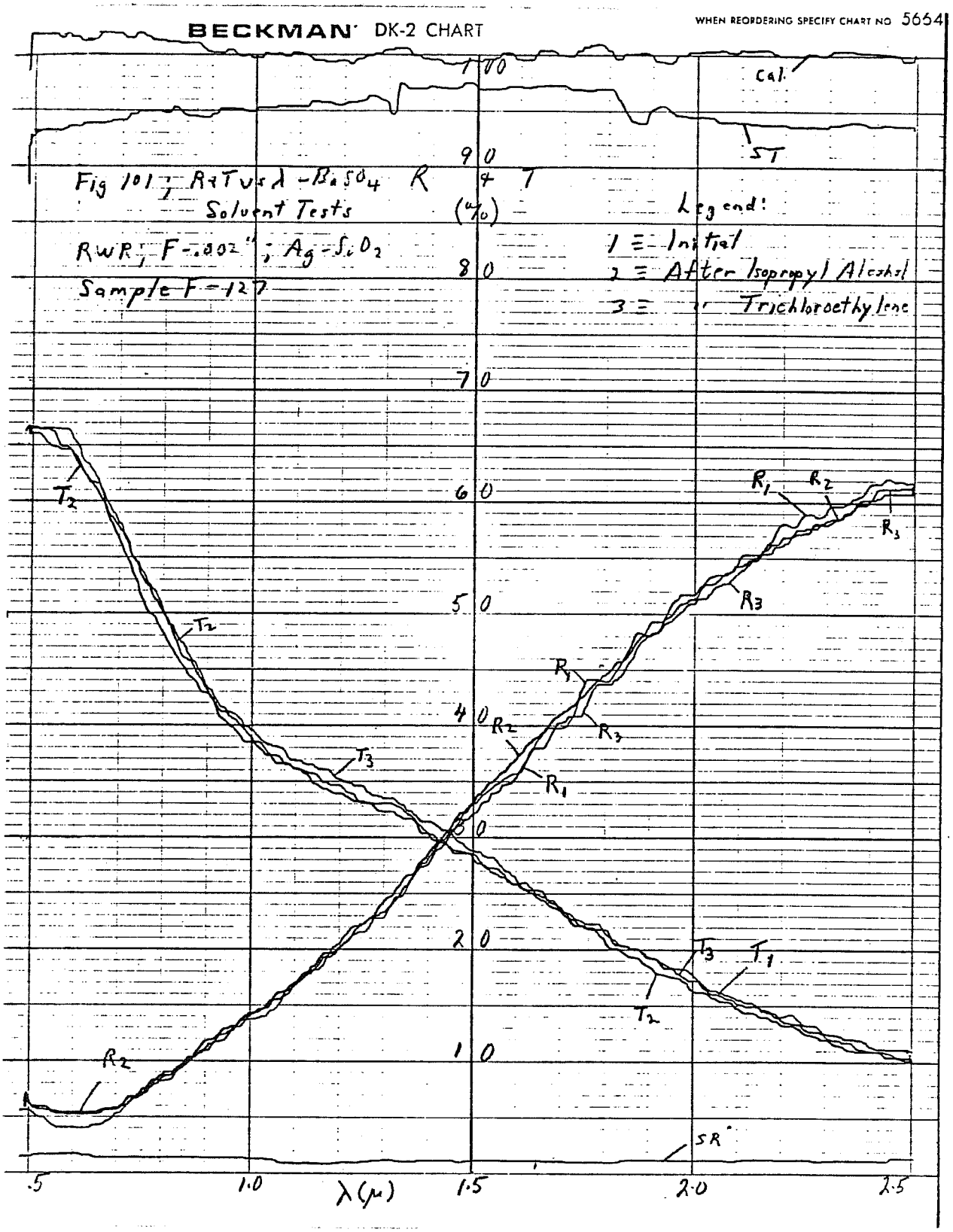
BECKMAN DK-2 CHART
WHEN REORDERING SPECIFY CHART NO 5664
100
90
80
70
60
50
40
30
20
10
Cal.
ST
Fig 101 - R+T vs λ - BaSO4 R + T
Solvent Tests (%)
RWR - F=.002" ; Ag - SiO2
Sample F-127
Legend:
1 = Initial
2 = After Isopropyl Alcohol
3 = " Trichloroethylene
T2
T2
T3
R1
R2
R3
R1
R2
R3
R3
T3
T1
T2
R2
SR
.5
1.0
λ(μ)
1.5
2.0
2.5

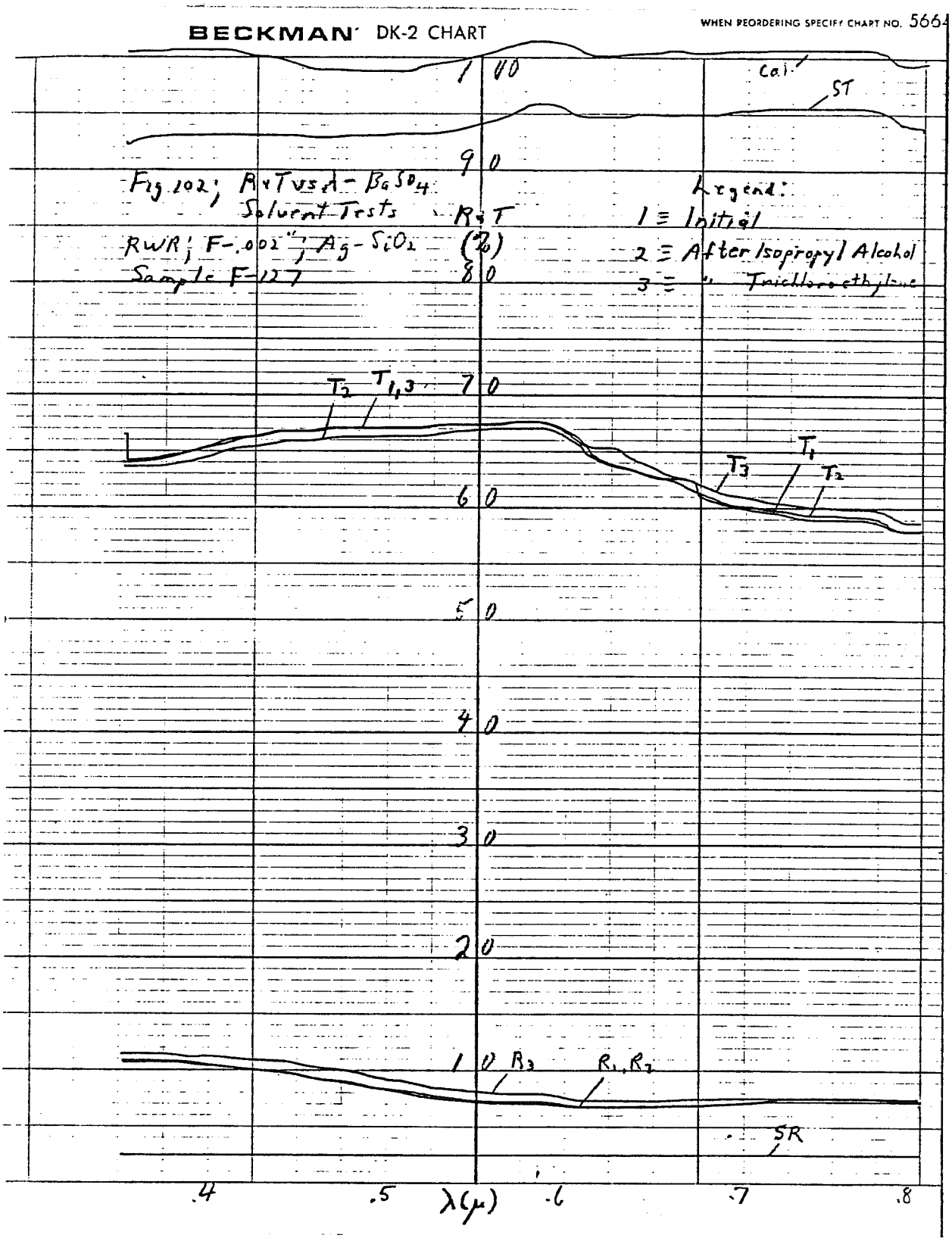
BECKMAN DK-2 CHART
WHEN REORDERING SPECIFY CHART NO. 5664
100
90
80
70
60
50
40
30
20
10
Cal.
ST
Fig 102; R+T vs λ - BaSO4 Solvent Tests
RWR; F-.002"; Ag-SiO2
Sample F-127
R+T (%)
Legend:
1 ≡ Initial
2 ≡ After Isopropyl Alcohol
3 ≡ " Trichloroethylene
T2
T1,3
T3
T1
T2
R3
R1, R2
SR
.4
.5
λ(μ)
.6
.7
.8

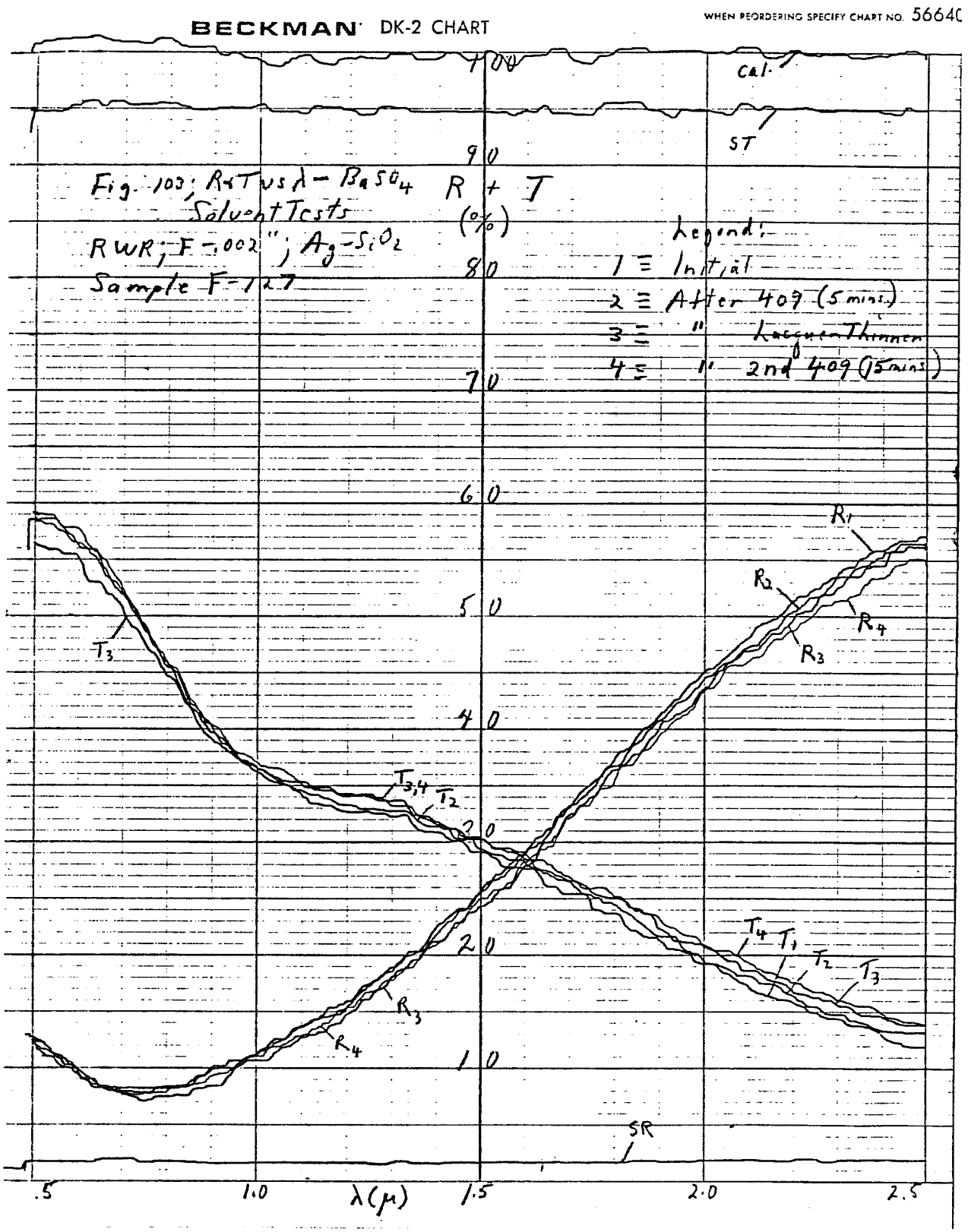
BECKMAN DK-2 CHART
WHEN REORDERING SPECIFY CHART NO. 56640
100
90
80
70
60
50
40
30
20
10
Cal.
ST
SR
R + T (%)
Fig. 103; R+T vs λ - BaSO4
Solvent Tests
RWR; F=.002"; Ag-SiO2
Sample F-127
legend:
1 ≡ Initial
2 ≡ After 40° (5 mins.)
3 ≡ " Lacquer Thinner
4 ≡ " 2nd 40° (5 mins.)
R1
R2
R4
R3
T3
T3,4
T2
T4
T1
T2
T3
R3
R4
.5
1.0
λ(μ)
1.5
2.0
2.5

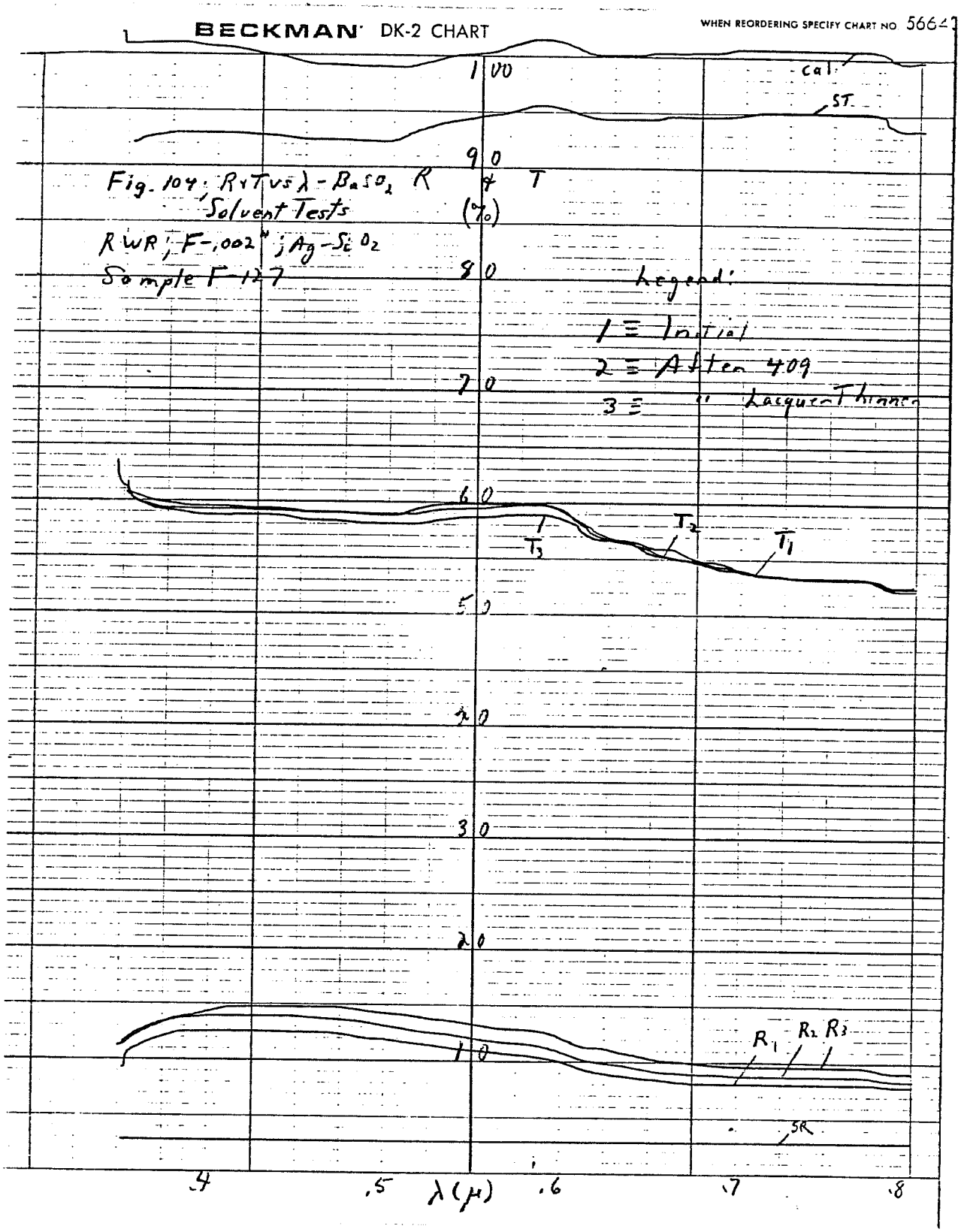
BECKMAN DK-2 CHART
WHEN REORDERING SPECIFY CHART NO 5664
100
90
80
70
60
50
40
30
20
10
R & T (%)
cal.
ST.
Fig. 104; R+T vs λ - BaSO4
Solvent Tests
RWR; F-.002"; Ag-SiO2
Sample F-127
Legend:
1 = Initial
2 = After 409
3 = " Lacquer Thinner
T3
T2
T1
R1
R2
R3
SR
.4
.5
λ(μ)
.6
.7
.8

solvents showed no change and the present figures were selected because this particular sample was studied with all solvents. Because of the effect of 409 on the Ag-Al_2O_3 films (see following), it was decided to repeat the 409 test on the same sample using a 15 minute cycle instead of the 5 minute cycle. The small changes in R and T are considered consistent with film wrinkling and/or residual film effects.

Basically, the Ag-SiO_2 system stood up extremely well under severe solvent environments. This, coupled with previous longer term weathering data, indicates that this is a very practical system.

The Ag-Al_2O_3 system (Figs. 105-110) also stood up very well to everything except 409 which produced some unusual effects. After the first 409 immersions it was observed that the coatings were getting slightly darker. To emphasize the effect, the 409 was magnetically stirred continuously in subsequent tests and the R and T curves were taken after a water rinse only. This resulted in a surprising increase in R and decrease in T as shown by curves 3 in Fig. 109. However, some spottiness was also evident visually and when the film was subsequently subjected to the normal decreasing solvent rinsing cycle, much of the film delaminated resulting in curves 4 which show a radical decrease in R and increase in T. The film removal mechanism appeared to be physical rather than chemical following the chemical attack of the 409 on the thin films.

This susceptibility to 409 would have been a severe disadvantage for the Ag-Al_2O_3 system if it were exposed but would not have affected its value for between window use. Since the Ag-Al_2O_3 system gives the best performance, KCI spent some time after the program was over developing a modified deposition technique that produced an Al_2O_3 overcoat on P that eliminated the problem.

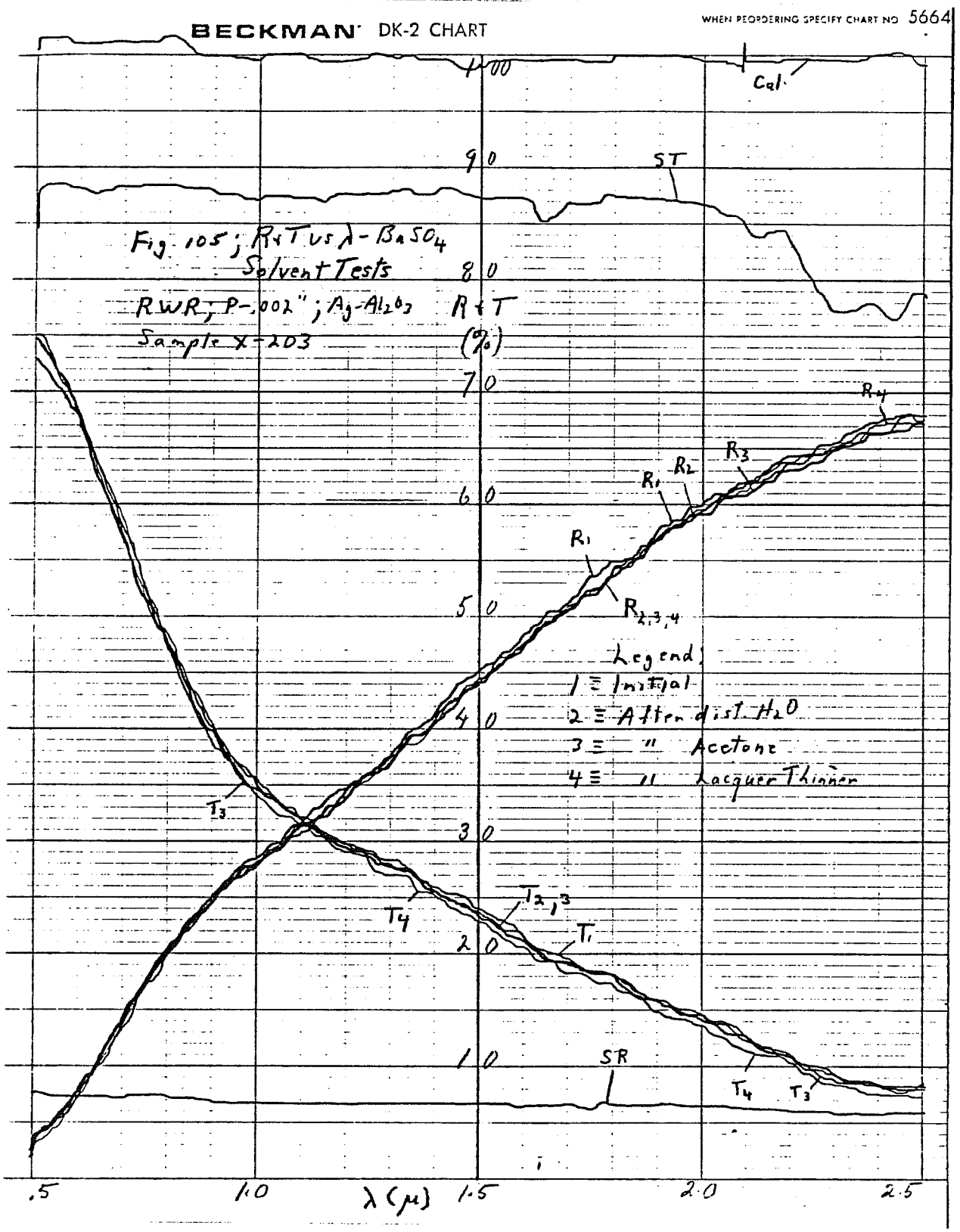
BECKMAN DK-2 CHART
WHEN REORDERING SPECIFY CHART NO 5664
Cal
ST
SR
Fig. 105; R+T vs λ - BaSO4
Solvent Tests
RWR; P-.002"; Ag-Al2O3
Sample X-203
R+T (%)
100
90
80
70
60
50
40
30
20
10
R4
R3
R2
R1
R1
R2,3,4
T3
T4
T2,3
T1
T4
T3
Legend:
1 ≡ Initial
2 ≡ After dist. H2O
3 ≡ " Acetone
4 ≡ " Lacquer Thinner
.5
1.0
λ (μ)
1.5
2.0
2.5

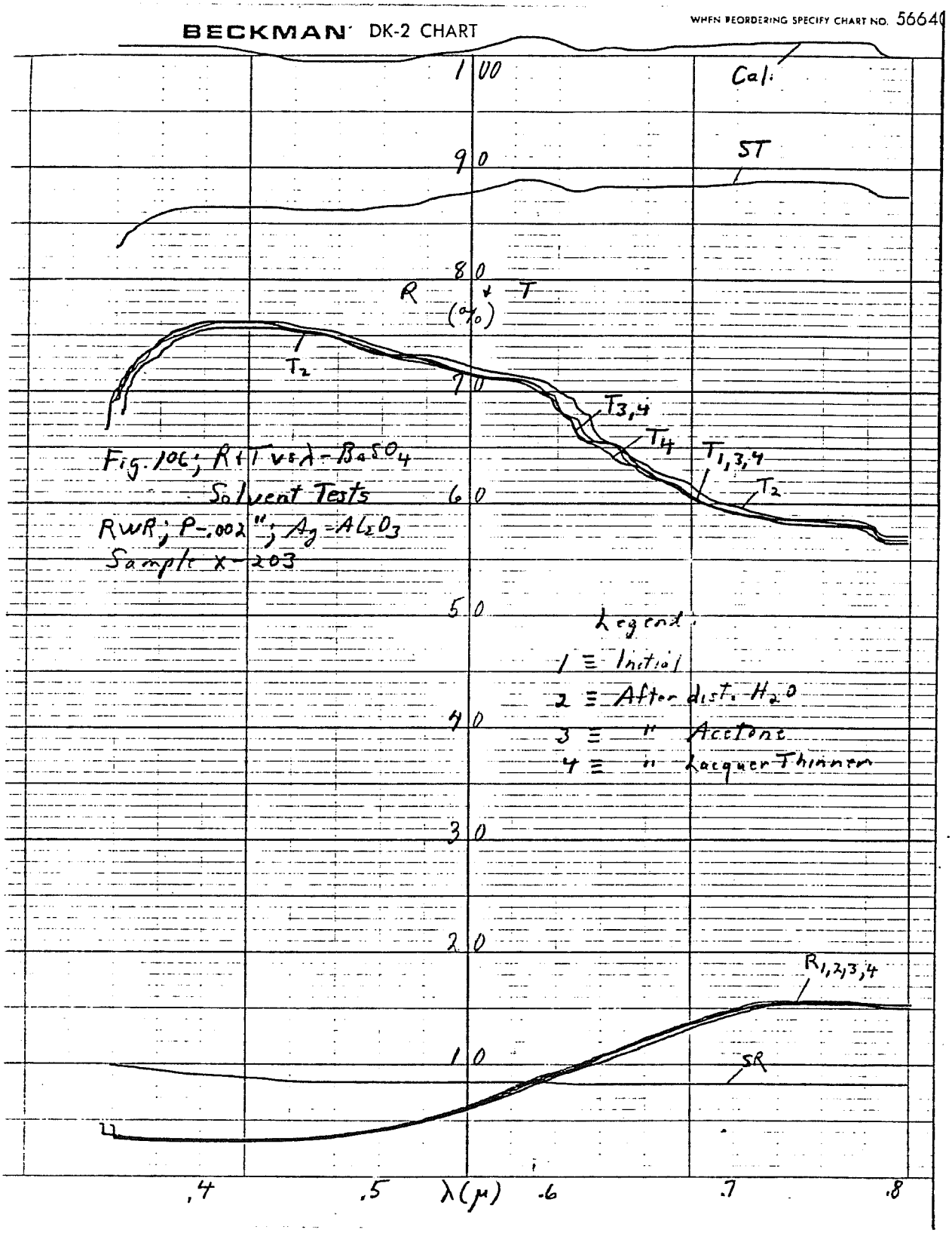
BECKMAN DK-2 CHART
WHEN REORDERING SPECIFY CHART NO. 56640
100
90
80
70
60
50
40
30
20
10
0
R + T (%)
Cal.
ST
SR
T_2
$T_{3,4}$
T_4
$T_{1,3,4}$
T_2
$R_{1,2,3,4}$
Fig. 106; R + T vs λ - $BaSO_4$
Solvent Tests
RWR; P-.002"; $Ag - Al_2O_3$
Sample X-203
Legend:
1 ≡ Initial
2 ≡ After dist. H_2O
3 ≡ " Acetone
4 ≡ " Lacquer Thinner
.4
.5
λ(μ)
.6
.7
.8

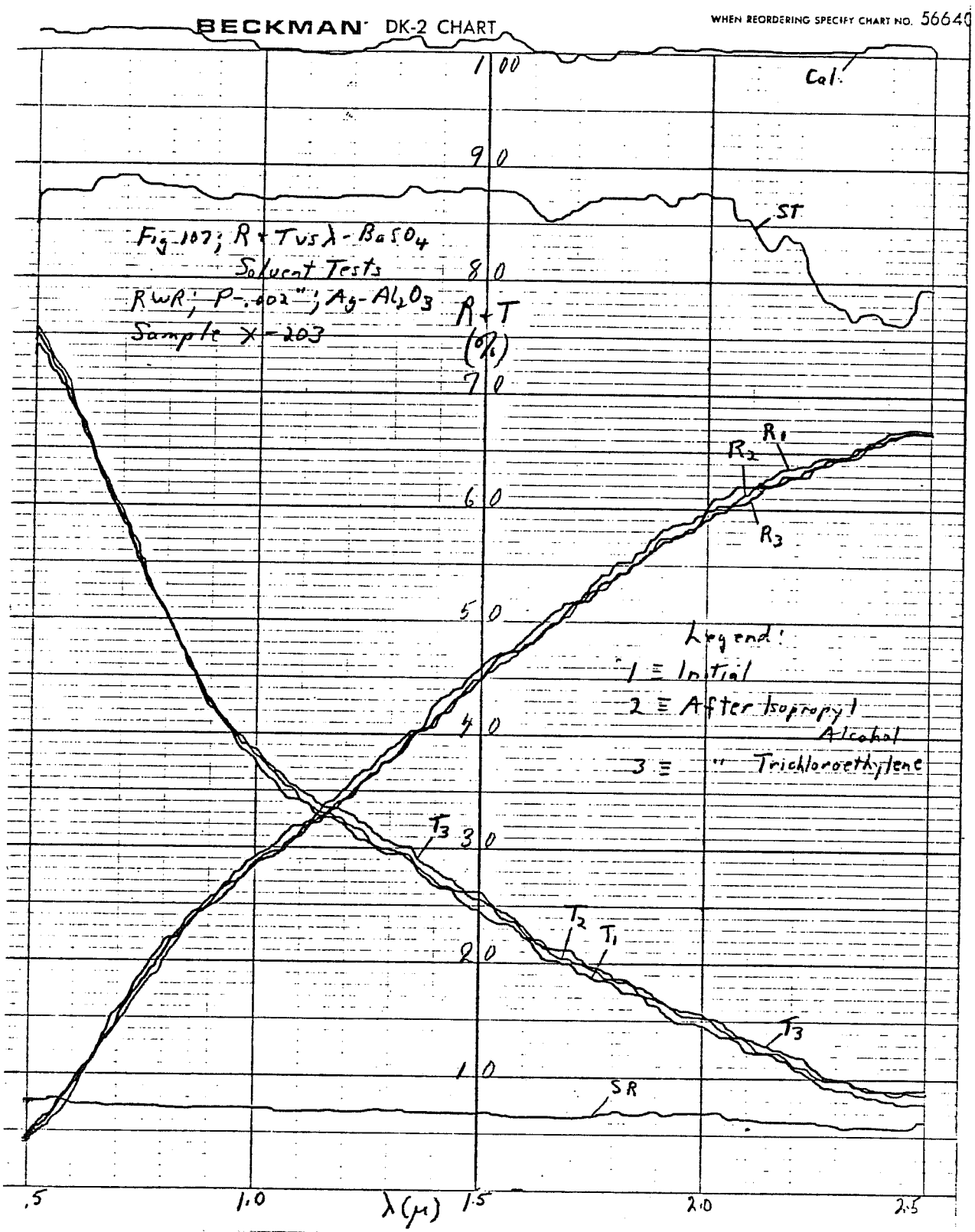
BECKMAN DK-2 CHART
WHEN REORDERING SPECIFY CHART NO. 56640
Cal.
ST
Fig-107; R+T vs λ - BaSO4
Solucat Tests
RWR; P-.402"; Ag-Al2O3
Sample X-203
R+T (%)
100
90
80
70
60
50
40
30
20
10
R1
R2
R3
T3
T2
T1
T3
SR
Legend:
1 ≡ Initial
2 ≡ After Isopropyl Alcohol
3 ≡ " Trichloroethylene
.5
1.0
λ(μ)
1.5
2.0
2.5

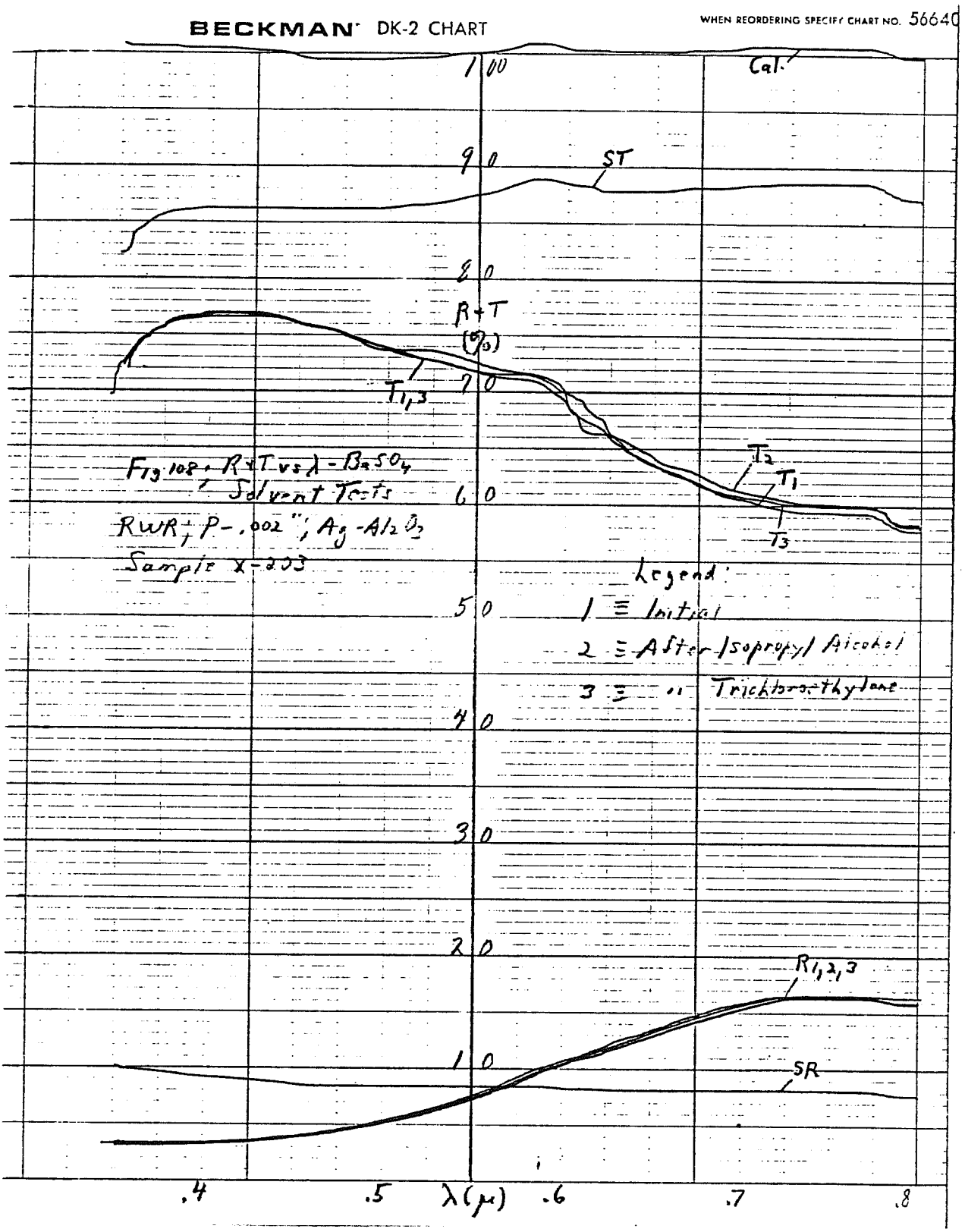
BECKMAN DK-2 CHART
WHEN REORDERING SPECIFY CHART NO. 56640
100
90
80
70
60
50
40
30
20
10
Cal.
ST
R+T
(Pb)
T1,3
T2
T1
T3
R1,2,3
SR
.4
.5
λ(μ)
.6
.7
.8
Fig 108 - R+T vs λ - BaSO4
Solvent Tests
RWR+ P-.002"; Ag-Al2O3
Sample X-203
Legend:
1 ≡ Initial
2 ≡ After Isopropyl Alcohol
3 ≡ " Trichloroethylene

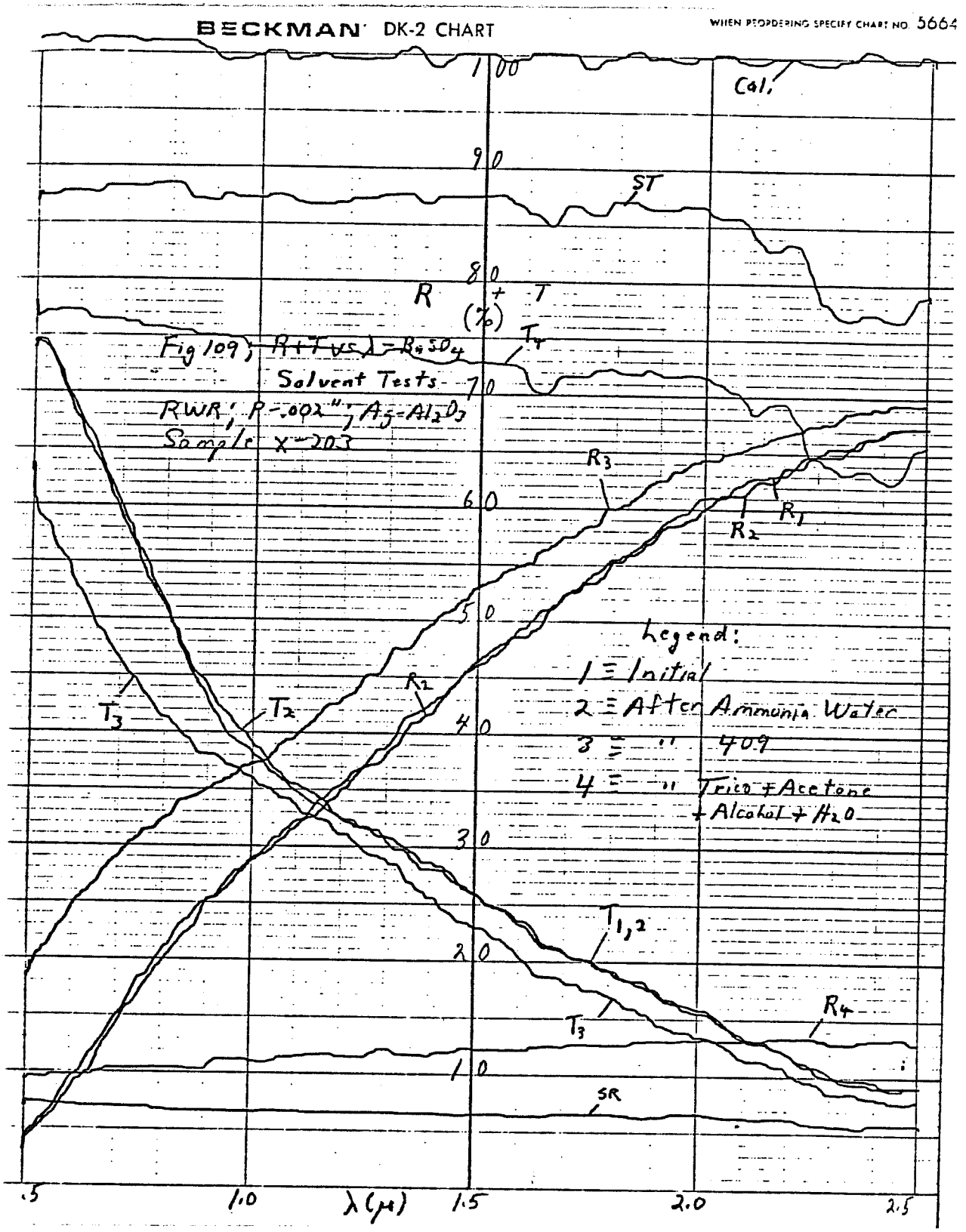
BECKMAN DK-2 CHART
WHEN REORDERING SPECIFY CHART NO. 5664
Cal.
ST
R + T (%)
Fig 109; R+T vs λ - R_6SO_4
Solvent Tests -
RWR; R-.002"; A_5-Al_2O_3
Sample X-203
T_1
T_2
T_3
R_1
R_2
R_3
R_4
$T_{1,2}$
SR
Legend:
1 ≡ Initial
2 ≡ After Ammonia Water
3 ≡ " 409
4 ≡ " Tric + Acetone + Alcohol + H_2O
λ (μ)
.5
1.0
1.5
2.0
2.5

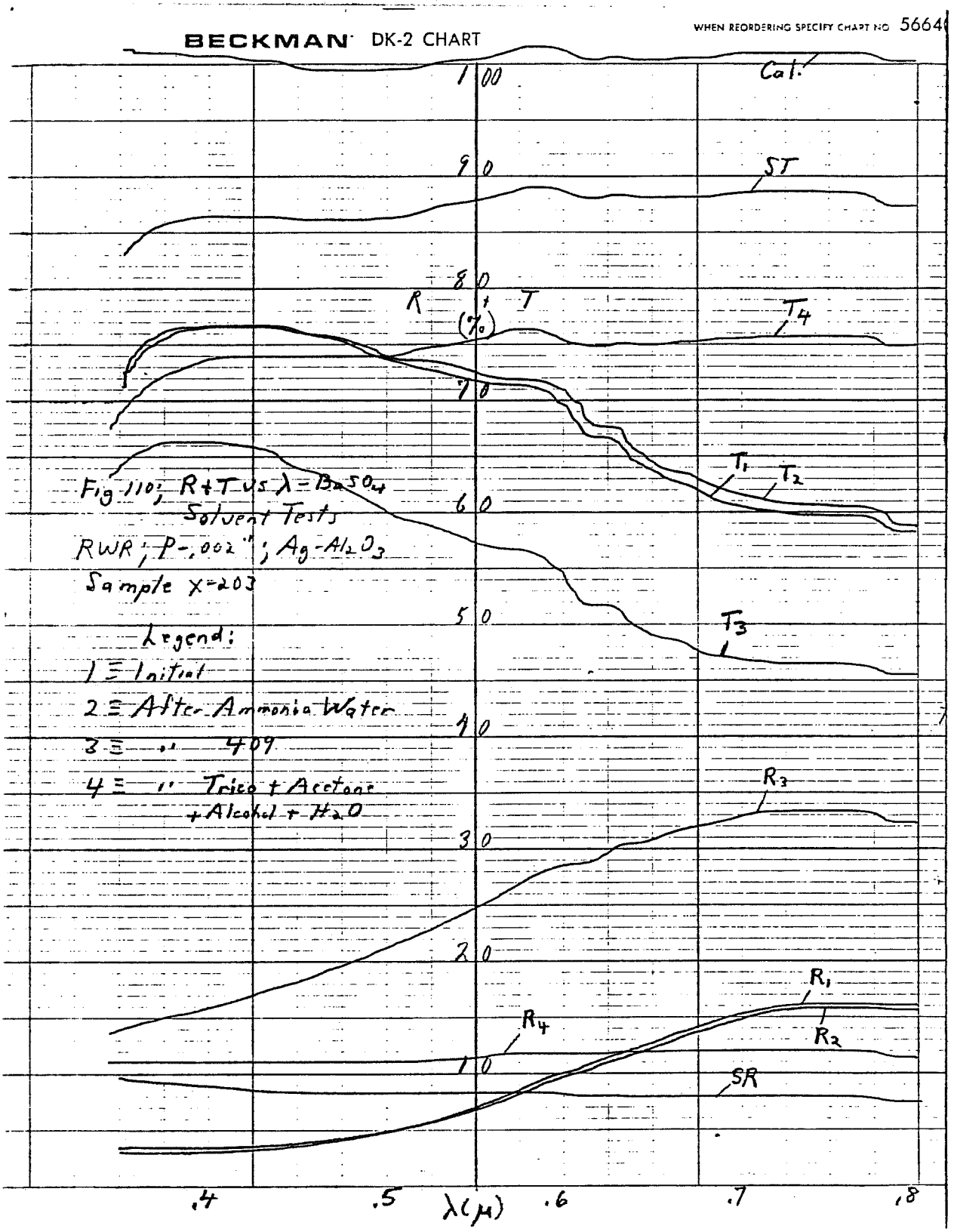
BECKMAN DK-2 CHART
WHEN REORDERING SPECIFY CHART NO 5664
Cal.
100
90
80
70
60
50
40
30
20
10
R + T (%)
ST
T4
T1
T2
T3
R3
R1
R2
R4
SR
Fig 110; R+T vs λ = BaSO4
Solvent Tests
RWR; P-.002"; Ag-Al2O3
Sample X-203
Legend:
1 ≡ Initial
2 ≡ After Ammonia Water
3 ≡ " 409
4 ≡ " Trico + Acetone
+ Alcohol + H2O
.4
.5
λ(μ)
.6
.7
.8

Absolutely no degradation was observed after one hour emmersion in 409 with this new method, and after 15 hours there was only a slight change in coloration due to etching of the oxide by the 409. Physically the Ag film was still extremely well bonded.

On PR substrates there was still some slight change with time. Fig. 111 shows the results for a modified test of the new Al_2O_3, in which the sample was repeatedly immersed in 409 for 3", towel dried and then retested. Successive immersions up to a total of 21 minutes resulted in increases in R and corresponding decreased in T. At this point there was some slight lifting of the film in small areas. The film was then left immersed for an additional 15 minutes at which point most of the film stripped (curves h). This performance is considered adequate for real world conditions but is not as good as the new Al_2O_3 on P or the SiO_2 systems. The new Ag-Al_2O_3 system is considered commercializable and was used for all demonstration samples.

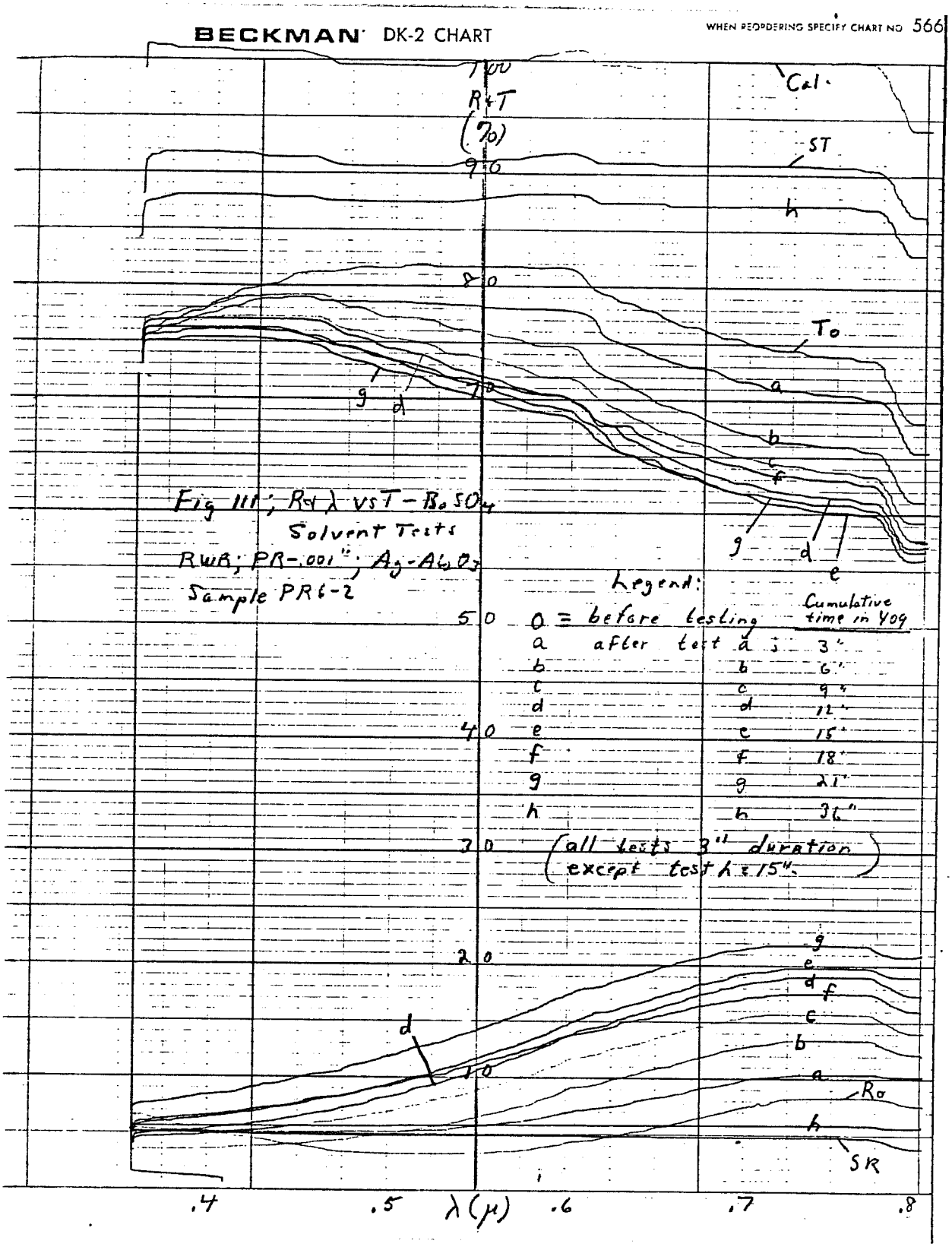
BECKMAN DK-2 CHART
WHEN REORDERING SPECIFY CHART NO 566
100
R+T
(%)
90
80
70
60
50
40
30
20
10
Cal.
ST
h
To
a
b
c
f
g
d
e
g
d
Fig III; R+λ vs T - BaSO4
Solvent Tests
RWB; PR-.001"; Ag-Al2O3
Sample PR6-2
Legend:
0 = before testing
a after test a ; 3"
b b 6"
c c 9"
d d 12"
e e 15"
f f 18"
g g 21"
h h 36"
(all tests 3" duration
except test h = 15".
g
e
d
f
c
b
a
Ro
h
SR
d
.4
.5
λ(μ)
.6
.7
.8

5 Demonstration Program

5.1 General

The original program plan called for a demonstration system in which 12" x 12" glass plates would be transferred across a 3" x 12" aperture through which the necessary films would be deposited. The intent was simply to demonstrate a continuous process, using KCI ion beam sputtering methods, to provide uniform windows with desired OW and RW characteristics. The process as demonstrated had to be expandable to commercial size.

Values for aperture size and sample size were dictated by the equipment and money available for the program. In order to demonstrate at low cost, an existing piece of KCI equipment having a vacuum chamber 4' x 3' x 2', was used. All demonstrations had to be conducted within this chamber which had to contain the ion source components, targets, and sampling handling mechanisms. Since the glass was to be translated across the aperture, the slit size was limited to 12" wide (36 - 2 x 12). In practice, with the necessary fixturing etc. this reduced to 6 1/2" which became the final aperture. The length could essentially be left open since the material itself defined the length.

A commercial system would not necessarily need the aperture, which was used primarily to limit the area of the depositing material for demonstration purposes. The deposition system, per se, was capable of depositing over a 2' x 2' area. In order to ensure uniformity, an extensive program was conducted to measure distribution using 1" x 1" stainless steel shim stock pieces positioned in rows and columns as shown in Fig. 112 (a). The shim stock pieces were mounted on a static holder positioned above the Cu (original demonstration metal) target and runs were made to deposit .3-.5 mils of material. This material could be stripped from the stainless by a combination of heating with a propane torch combined with severe flexing. After stripping, the deposited metal thickness was directly measured with a Starrett depth gauge yielding uniformity and rate.

Many runs were made, changing source and target conditions,

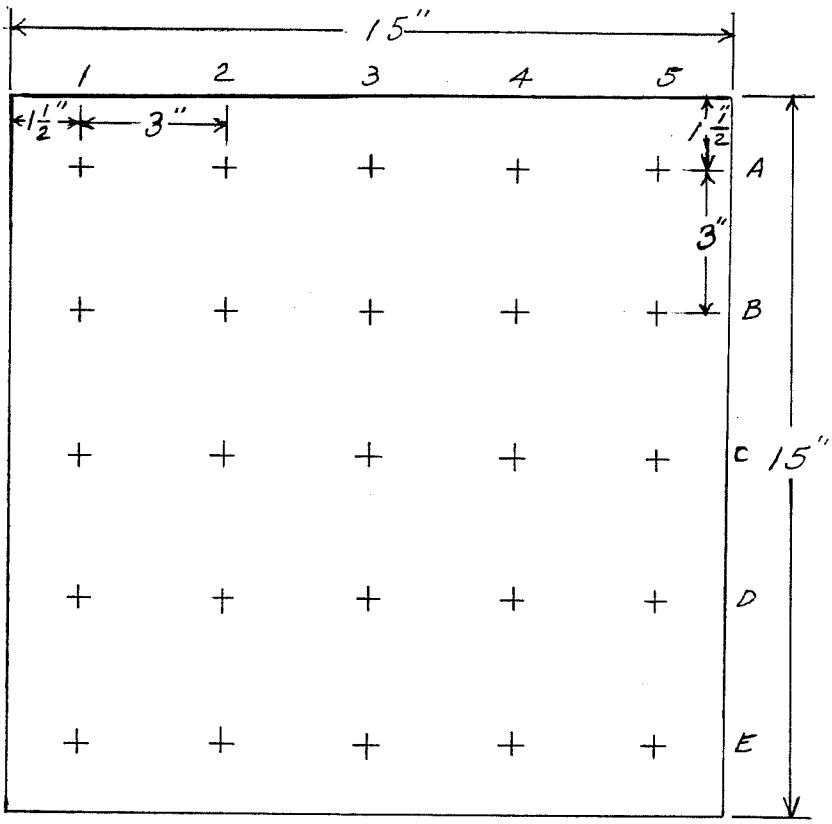

(a) UNIFORMITY TEST PATTERN

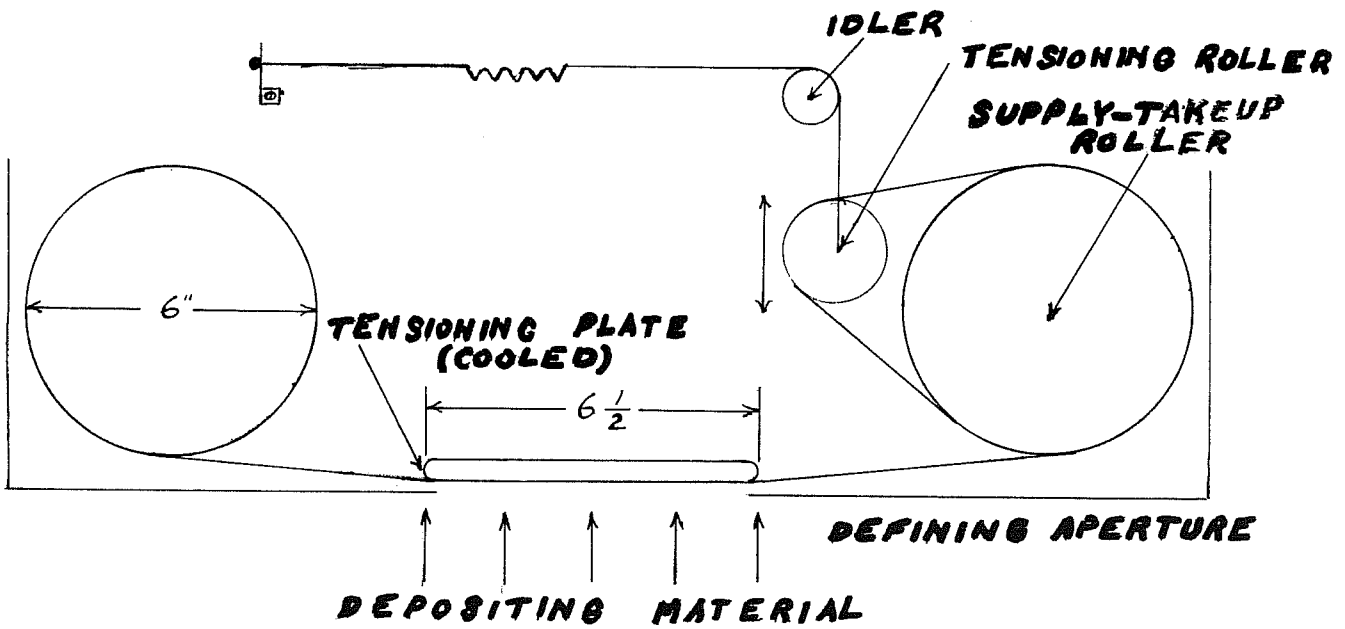

(b) ROLLER SYSTEM

Fig 112 BASIC DEMONSTRATION PROGRAM

ultimately resulting in a deposition pattern which would provide $\pm$ 4.5% uniformity for substrates traversing a 12" x 15" aperture or $\pm$ 1.4% for a 9" x 12" aperture. This distribution was therefore more than adequate for a 6" x12" aperture.

An additional problem existed, however, in that both targets (metal and dielectric) had to be mounted in the same chamber, roughly in the same position for successive passes or layers. The metal target was mounted above the dielectric target and could be swung out of the way to expose the latter. The targets were therefore not at the same distance from the substrate which had the effect of displacing their distribution centers to different positions. Compensation was made by tilting the dielectric target but a perfect fix could not be obtained.

This problem was completely an artifact of demonstrating in an existing small chamber and would not be present in production. To determine the potential effect on the finished samples, a series of runs was made in which Cu-SiO_2 (RW levels) was deposited on 15" x 15" glass plates in a static position. Visual evaluation of these plates showed a high uniformity of color and overall appearance even to the educated eye. Because of this, it was decided that building a system to transfer a piece of 12" x 12" glass past an aperture was a trivial exercise. Also, by this time the program had been heavily reoriented to heat mirror or residential applications with emphasis on retrofits. It was therefore decided to change the demonstration to a roll-to-roll system using plastic substrates.

As a final check the Cu-SiO_2 deposition system was tried on 15" x 15" FEP substrates. Fig. 113-114 shows the results for an RWR. Both R and T are slightly below design values and below the relative values achieved on the smaller IBSS, probably due to target cross-contamination. (Note: Glass backing was used to try to keep the samples flat for measurement, but actually resulted in lower R values.) The Cu absorption peak is very obvious in the visible. At this time it became evident that Cu-SiO_2 was not a preferred combination. Since stability of the Bs systems was not yet fully determined, it was decided on the basis of existing data to go with Ag-Al_2O_3 for the demonstration samples.

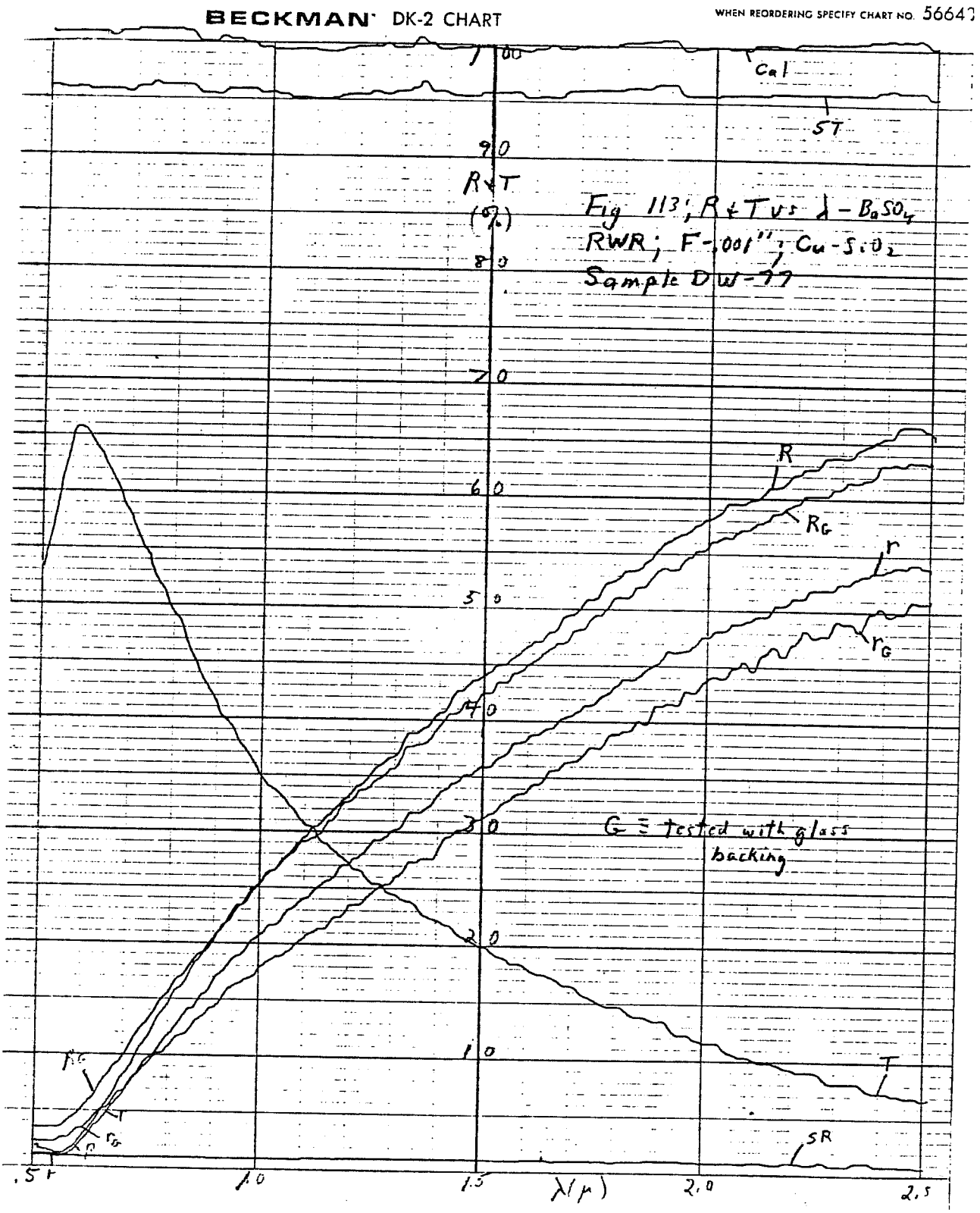
BECKMAN DK-2 CHART
WHEN REORDERING SPECIFY CHART NO. 56643
100
Cal
5T
90
R+T
(%)
80
70
60
50
40
30
20
10
R
RG
r
rG
T
5R
.5T
1.0
1.5
λ(μ)
2.0
2.5
Fig 113; R+T vs λ - BaSO4
RWR; F-.001"; Cu-SiO2
Sample DW-77
G = tested with glass backing

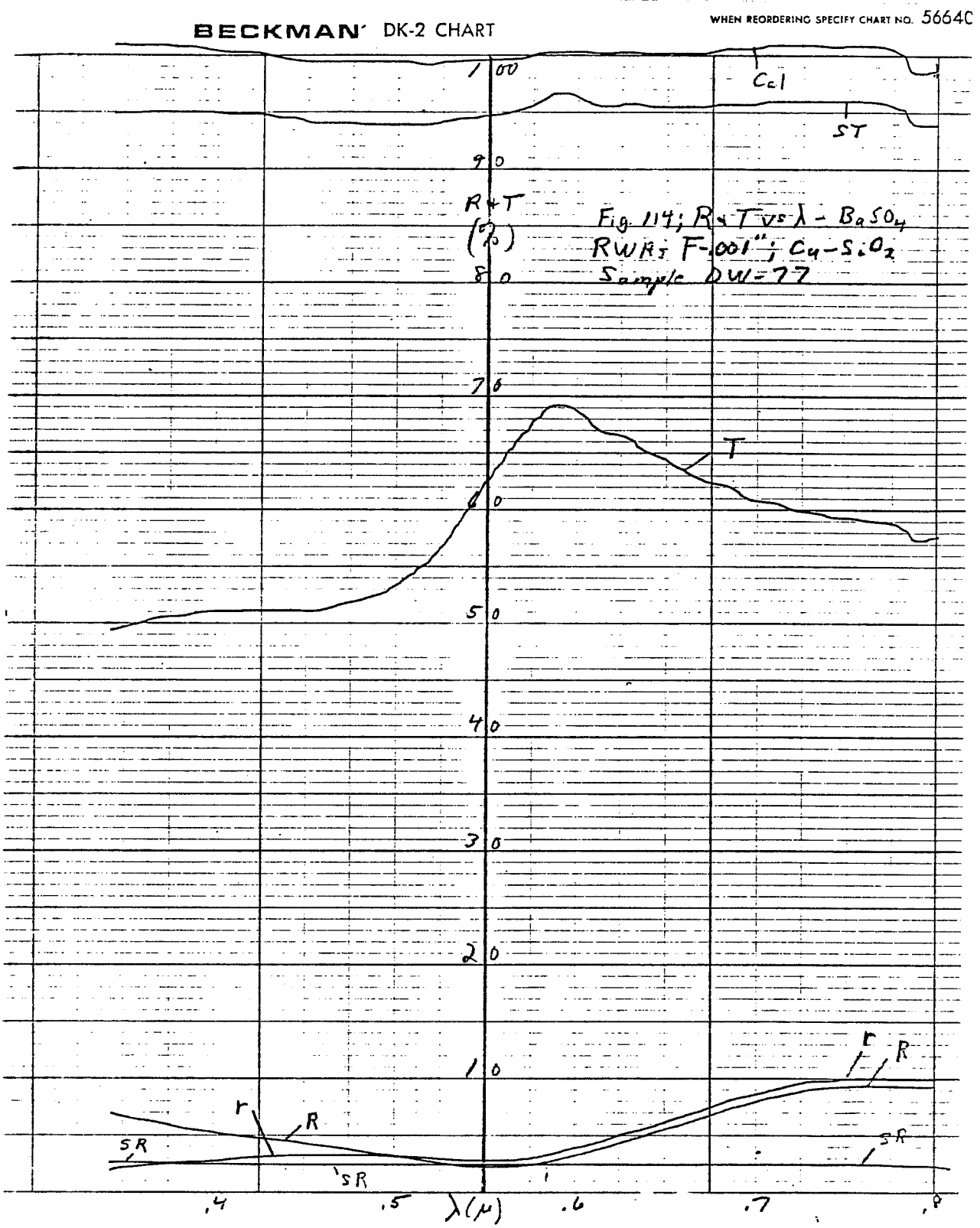
BECKMAN DK-2 CHART
WHEN REORDERING SPECIFY CHART NO. 5664C
100
90
80
70
60
50
40
30
20
10
R+T
(%)
Fig. 114; R+T vs λ - BaSO4
RWR; F-.001"; C4-SiO2
Sample DW-77
Cal
ST
T
r
R
SR
SR
.4
.5
λ(μ)
.6
.7
.8

5.2 Roller System

Fig. 112(b) shows the basic roller system that was used. Material is transferred from one supply-takeup roll (14" long) over a tensioning roller and a cooled sample plate to a second supply-takeup roller. Since the metal and dielectric are deposited in the same system, the material must be transferred from one roller to the other and then back. Both rollers therefore had to be synchronously driven (chain drive) and reversible.

The path of material was chosen so that the deposited material did not pass over the small tensioning roller with the deposit to the roller. This avoided scratching of the metal layer before the hard dielectric was applied. The cooled sample plate has rolled edges so that, under tension, the film is slightly stretched over the edges to help maintain alignment and thermal contact. In addition, one end is pivoted and the other translatable, using an eccentric lever, to align the film in the direction of motion while the system is operating.

Fig. 115 shows 4 views of the actual roller system which is mounted to the vacuum chamber door which is on rollers and can be pulled back from the system for adjustments or sample loading etc. The reversible motor (variable speed) is mounted outside of the system and connects to the chain drive through the vacuum chamber wall. Deposit thickness is controlled by a combination of source operating conditions and motor speed. In the final system a shutter system was added to allow target blow-off before the runs were initiated. A shielding system (not shown) was included to prevent any bounce material from reaching the plastic when it was not over the aperture.

Although requiring little write-up, the procedure for obtaining uniform deposits and designing and building a roller system to operate in the small available chamber consumed a large part of the engineering time on this project. These objectives were, in fact, a major goal of the program. The basic methods used, or modifications thereof, may readily be scaled to commercial sizes.

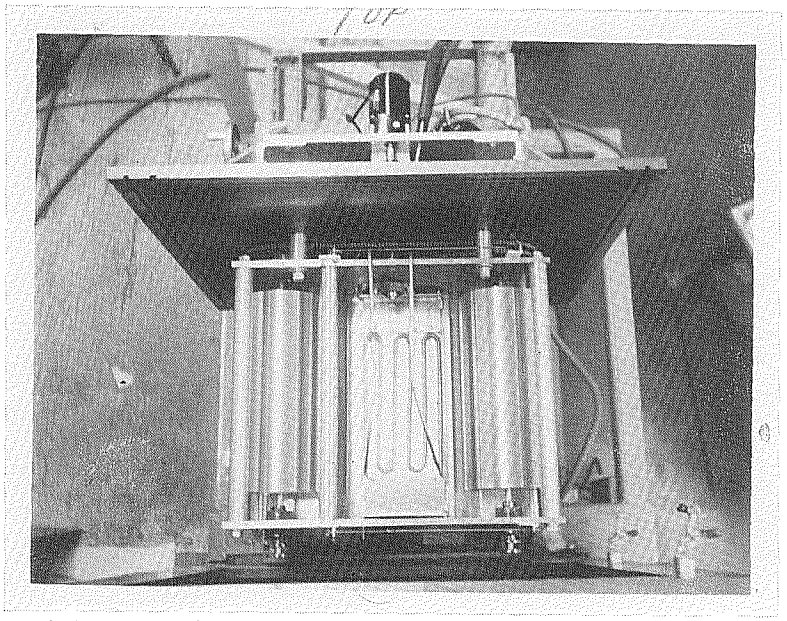

(a) Top View XBB 816-4927

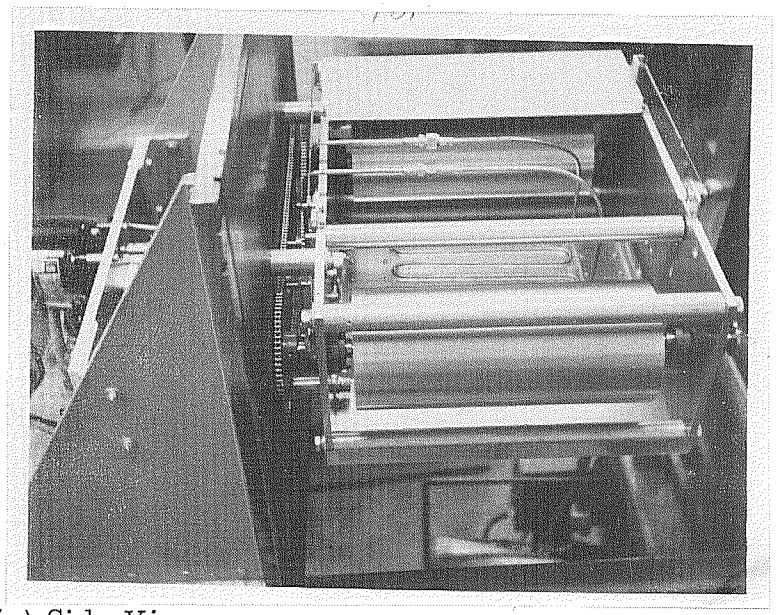

(c) Side View XBB 816-4925

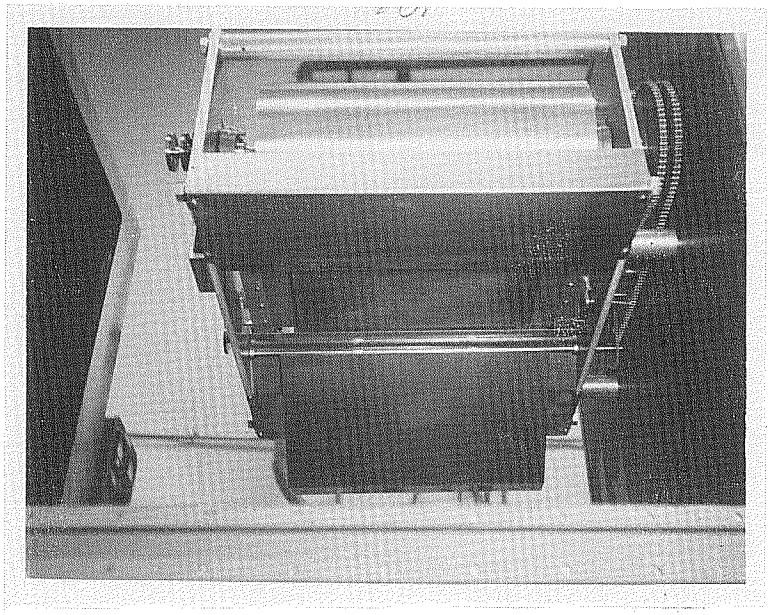

(b) Bottom View XBB 816-4928

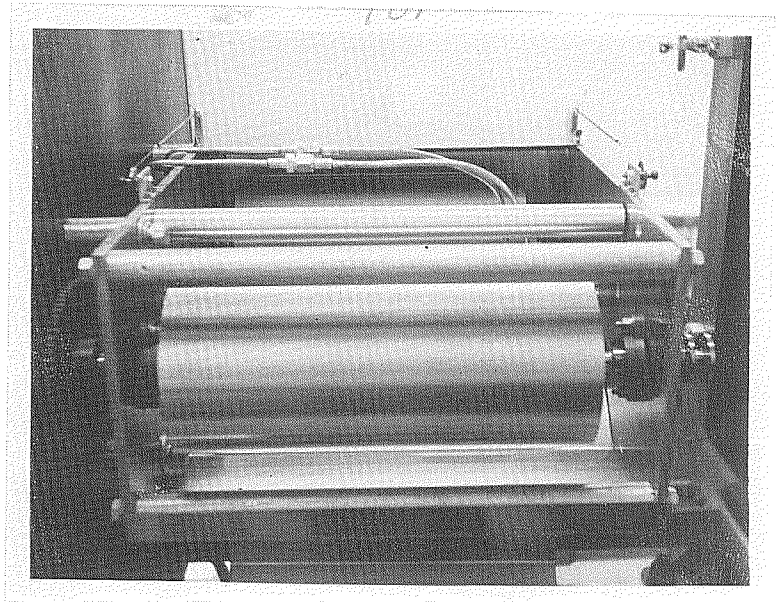

(d) Side View XBB 816-4926

Figure 115- Roller System

5.3 Demonstration Samples

Various materials have been run on the complete system. For demonstration purposes, Ag-Al_2O_3 runs were made on P substrates. Included were OWRs on 100 gauge (.001" - Melinex 42) and on 200 gauge (.002"-Melinex OW, UV stabilized), and RWRs on 100 gauge (Melinex 442), 50 gauge (.0005"-Melinex 442) and on 200 gauge (Melinex OW). Results for these combinations are given in Figs. 116-120 in which .5-2.5 μ data and .35-.8 μ data are plotted on the same graph. These samples, delivered as 10' strips, have no significant variation in R values from end to end. From side to side there is a slight drop on one edge due to the two target problem discussed previously. Coloring is quite uniform throughout the run and could be precisely duplicated from run to run. For each sample type a few runs were made at the beginning to define the desired operating parameters.

OWRs on P (.001") were run first and the run conditions were adjusted to give the characteristics shown in Fig. 116. This particular sample has a 1.0 μ R value of .74 which is at the low end of the .75-.85 objective. This was done specifically to increase visible T which averages slightly more than 40%. Better compromise conditions were achieved in the materials program on the small IBSS, but cross-contamination problems in the larger machine make it impossible to achieve quite as good performance. This difference is an artifact of having both targets at one position and would not exist for a real production machine. Reflectivity of this material at 10 μ would be 96-98%.

Fig. 117 gives data for an RWR on the same P (.001") substrate material. Measurements on samples glued on glass (see PR14, this Section) showed material of this type to have 10 μ R values of 86-88%. Since the incident solar light penetrates this material from substrate side, the reflectance from the back side, r, has also been plotted. This back reflectance averages less than 10% over the visible spectrum. Again the characteristics are slightly poorer than achieved in the small IBSS, although more than adequate.

For comparison, Fig. 118 shows the characteristics of an RWR run on thinner (.0005") P material using exactly the same conditions as for the 100 gauge material. Interestingly, the visible T values are slightly less in this

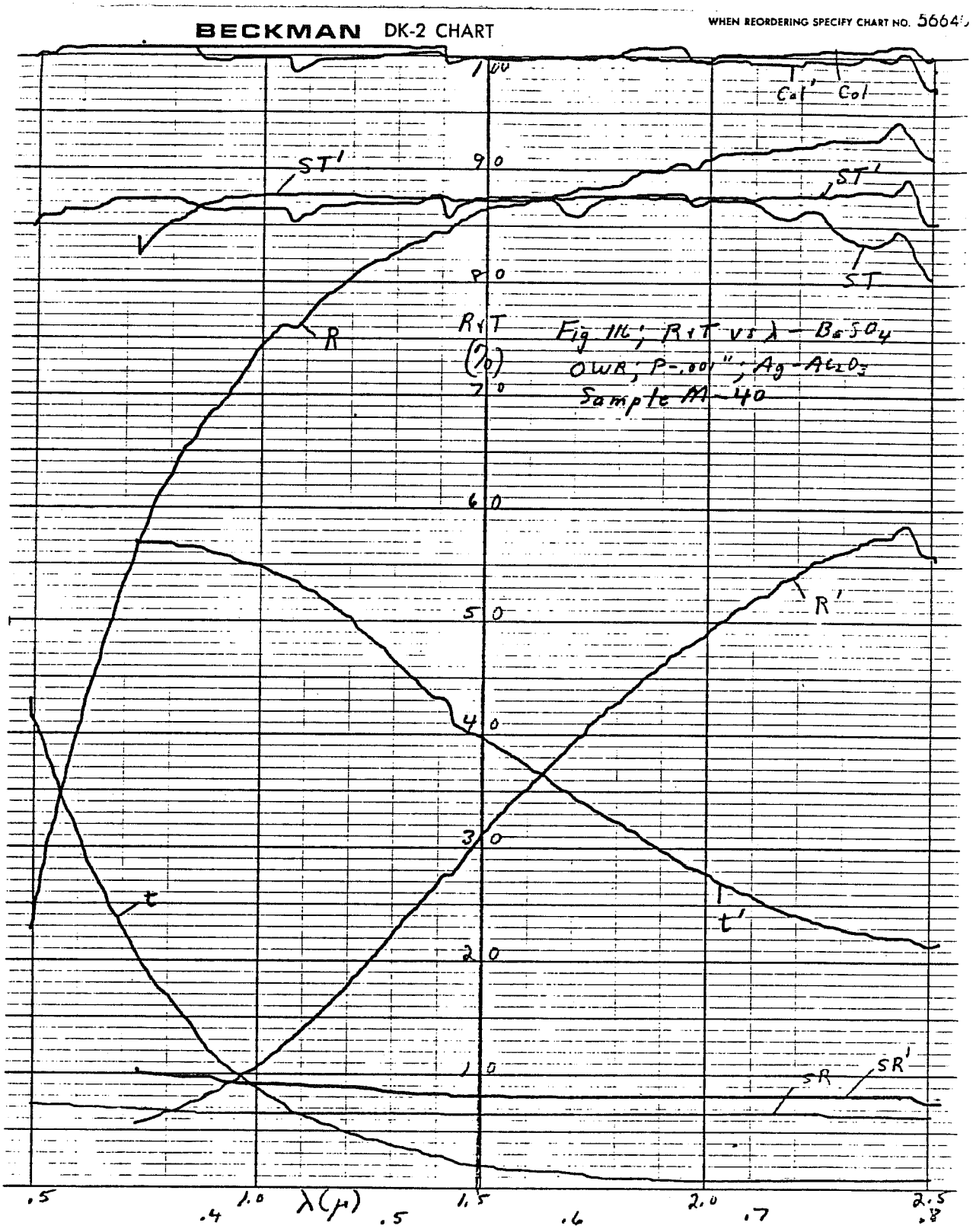
BECKMAN DK-2 CHART
WHEN REORDERING SPECIFY CHART NO. 5664
Cal'
Col
ST'
ST'
ST
R
R'
R I T (%)
Fig 11c; R I T vs λ — BaSO4
OWR; P-.001"; Ag-Al2O3
Sample A-40
t
t'
SR
SR'
λ(μ)
.5
1.0
1.5
2.0
2.5
.4
.5
.6
.7
.8
100
90
80
70
60
50
40
30
20
10

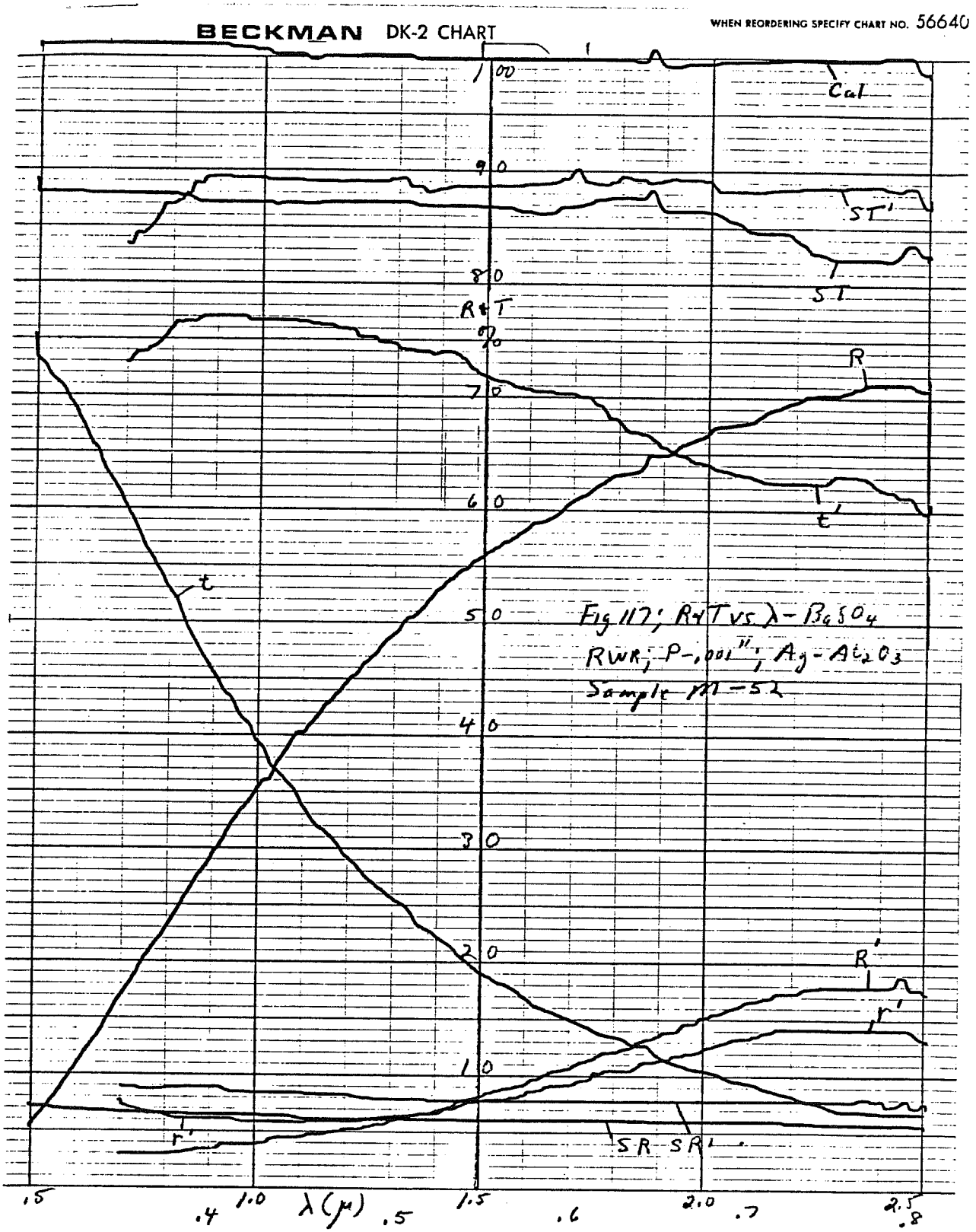
BECKMAN DK-2 CHART
WHEN REORDERING SPECIFY CHART NO. 56640
100
Cal
90
ST'
80
ST
R+T
%
70
R
60
t'
t
50
Fig 117; R+T vs λ - BaSO4
RWR; P-,001"; Ag - Al2O3
Sample M1-52
40
30
20
R'
r'
10
r'
SR SR'
.5
1.0
1.5
2.0
2.5
.4
.5
.6
.7
.8
λ(μ)

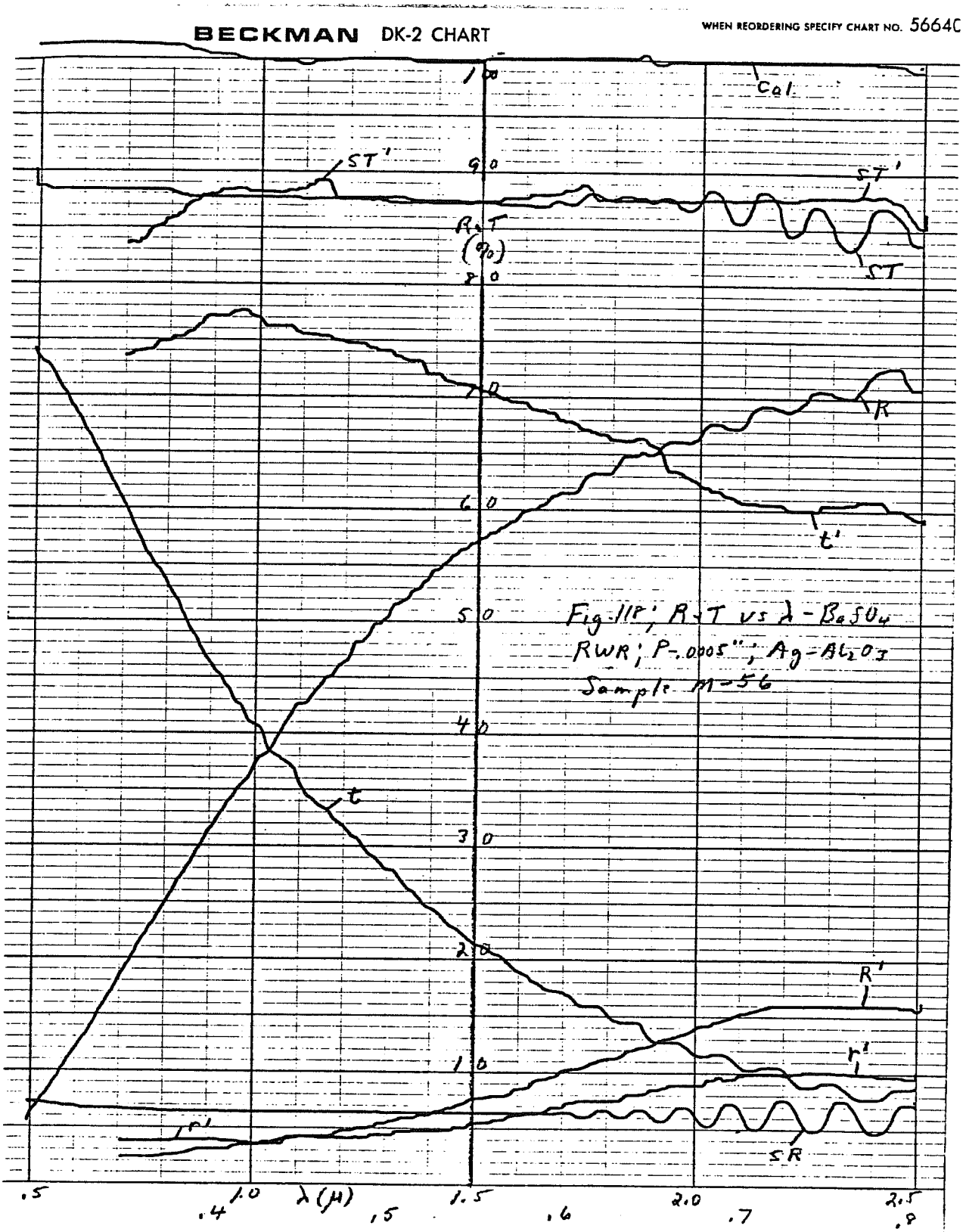
BECKMAN DK-2 CHART
WHEN REORDERING SPECIFY CHART NO. 5664C
Cal.
ST'
ST'
ST
R+T (%)
100
90
80
70
60
50
40
30
20
10
R
t'
t
R'
r'
r'
≤R
Fig-11P; R+T vs λ - BaSO4
RWR; P-.0005"; Ag-Al2O3
Sample M-56
.5
.4
1.0
λ (μ)
.5
1.5
.6
2.0
.7
2.5
.8

case and apparently corresponds to a slightly lower substrate transmission. The difference, if real, is extremely marginal and the choice in production would probably depend on economics and handling factors.

The same running conditions on UV stabilized P (.002") resulted in very similar characteristics (Fig. 119). There is a drop in T below .4 μ due to absorption in the substrate. In practice this would have only marginal significance because of the small amount of energy contained in the solar spectrum (see Fig. 1) for AM2 below this wavelength.

The final sample type was an OWR on UV stabilized P. This material was run with R at 1.0 μ pushed to the high and low extremes. Fig. 120 gives the results for a R (1.0 μ) value of .83. The average visible T value is considerably lower than for the 100 gauge P sample (Fig. 116) which had a lower R (1.0 μ) value. However, a run on the 200 gauge stabilized P with a lower R (1.0 μ) value of .73 gave a much higher average T value (approximately 52%). A mid value of R (1.0 μ) of .78 would reasonably be expected to yield an average visible T of 41-43%. Only a couple of runs were made for OWRs with this stabilized material because of limited quantity.

5.4 Glued Samples

As a final demonstration of the state-of-development of this general class of window materials, some material was used to make glued samples on glass using water soluble glue (supplied by Transilwrap). Approximately 30 of these glued samples.were assembled by spreading out the glue on the glass, scooping off the excess and then applying the retrofit plastic film and flattening it with a glass or plastic roller applied directly to the deposited film. Values of R at 10 μ were obtained for all of these samples and consistently ran in the .85-.88 range for RWRs and .95-.98 for OWRs. The extra flatness introduced by the glass backing made measurement much easier. Optically these windows were extremely good, especially the later ones. Except for a few very small bubbles, they were quite clean and flat and in many cases could not be distinguished from glass without very close observation. Coloring, or lack thereof for residential windows, was excellent.

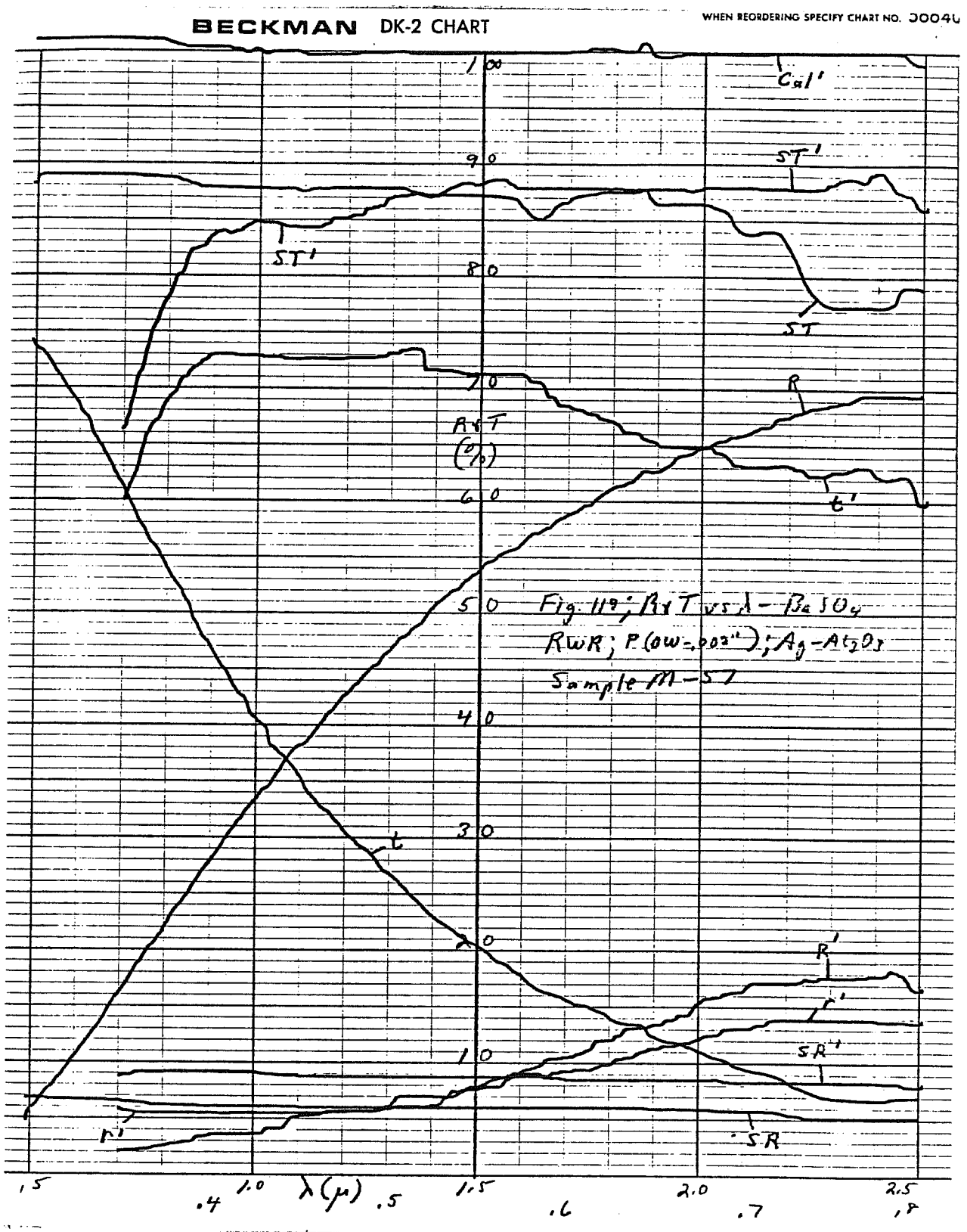
BECKMAN DK-2 CHART
WHEN REORDERING SPECIFY CHART NO. 30040
100
90
80
70
60
50
40
30
20
10
R+T (%)
Cal'
ST'
ST'
ST
R
T'
T
R'
r'
SR'
r'
SR
Fig. 119; R+T vs λ - BaSO4
RWR; P(ow=.003"); Ag-Al2O3
Sample M-57
1.5
.4
1.0
λ(μ)
.5
1.5
.6
2.0
.7
2.5
.8

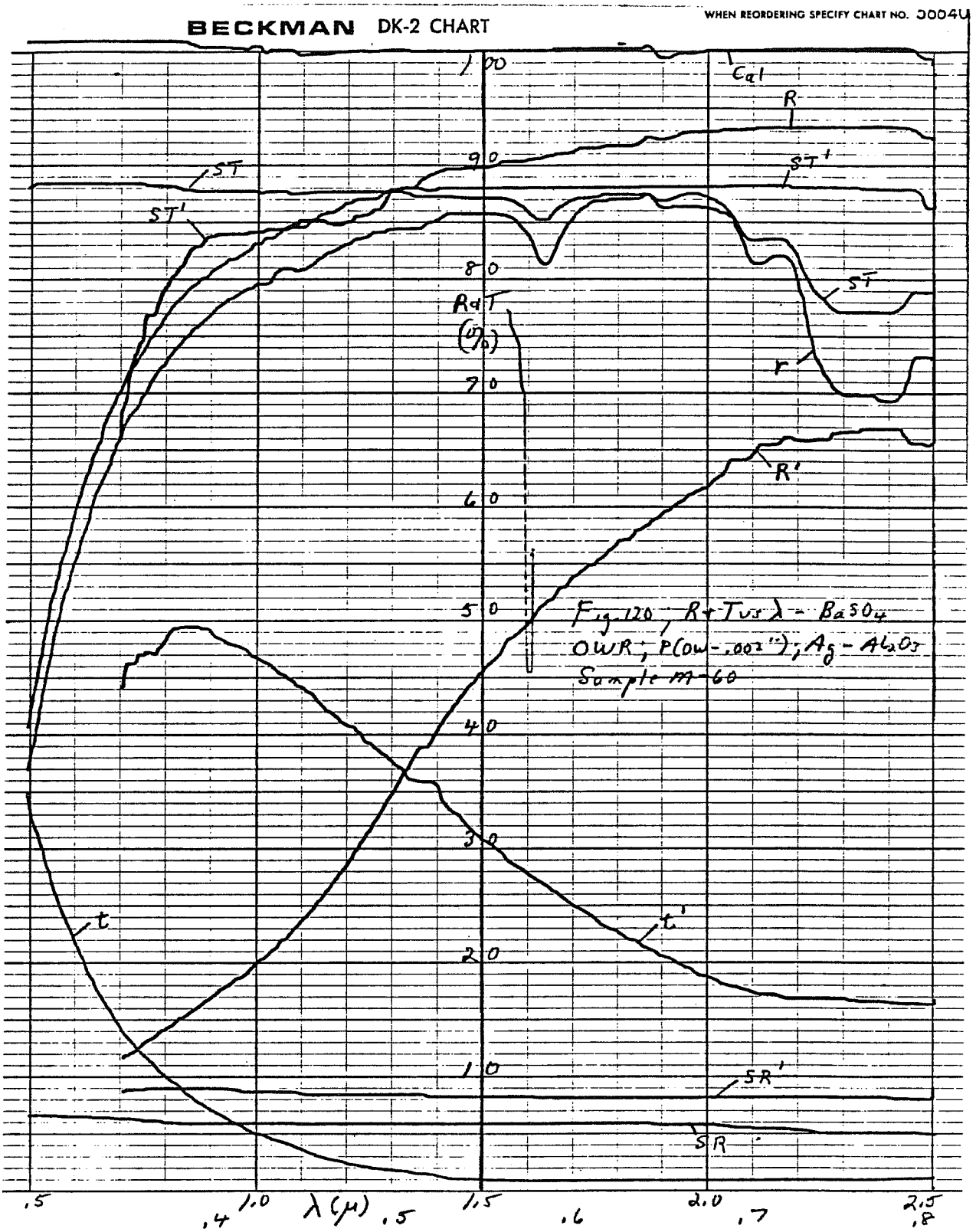
BECKMAN DK-2 CHART
WHEN REORDERING SPECIFY CHART NO. 30040
Cal
R
ST'
ST
ST'
ST
R+T (%)
r
R'
Fig 120, R+T vs λ - BaSO4 OWR; P(ow-.002"); Ag - Al2O3 Sample M-60
t
t'
SR'
SR
100
90
80
70
60
50
40
30
20
10
.5
.4
1.0
λ(μ)
.5
1.5
.6
2.0
.7
2.5
.8

Two of these samples were inserted in the weatherometer for accelerated testing but to date only limited data is available. Figs. 121-122 give data for one of these, a Ag-Al_2O_3 OWR which has been in the weatherometer for 6 weeks with the plastic facing the lamps and water. Very little change, either visual or measured, has occurred in this sample except for a small visible T change which is probably due to the glue drying. In view of the severe environment in the weatherometer, especially the large thermal swings (23°C to 64°C), the prognosis for this configuration is quite positive.

A similar RWR (Ag-Al_2O_3 on 100 gauge P) was made up and inserted in the weatherometer. Although inadvertently inserted in the wrong direction (plastic to lamps) it too had not shown any degradation at the end of 6 weeks. Both of these samples are being carefully monitored vs. time.

A final set of samples was made with the PR retrofits developed after the program was complete. Some samples were glued with the substrate side to the glass and some with the deposit side to the glass. Figs. 123-124 give the curves for a substrate to glass OWR. There was nothing of special note about this window, which is apparently stable, except that it was slightly optically inferior to the P substrate types because of material characteristics (slight striations). It was, however, quite acceptable with excellent visible transmission.

A similar RWR sample (Figs. 125-126) also had very high visible T in spite of its very high R value (.76) at 2.5 μ. Energy performance of this particular window should be as good as achievable but stability vs. time is in doubt because of its potential degradation under UV radiation.

The PR substrate system was actually developed for use with the deposit side glued to the glass for RWRs. Reasonable samples could be made this way but some difficulty was encountered in getting good gluing due to the PR physical characteristics. Optical clarity of these samples, although not as good as for the deposit side out samples, is again adequate with a slightly striated appearance on close inspection. Glue smearing etc. is much worse on these samples. Tests to date under a high intensity UV lamp (Section 3.7) indicate that this configuration may very well be stable when used in this manner.

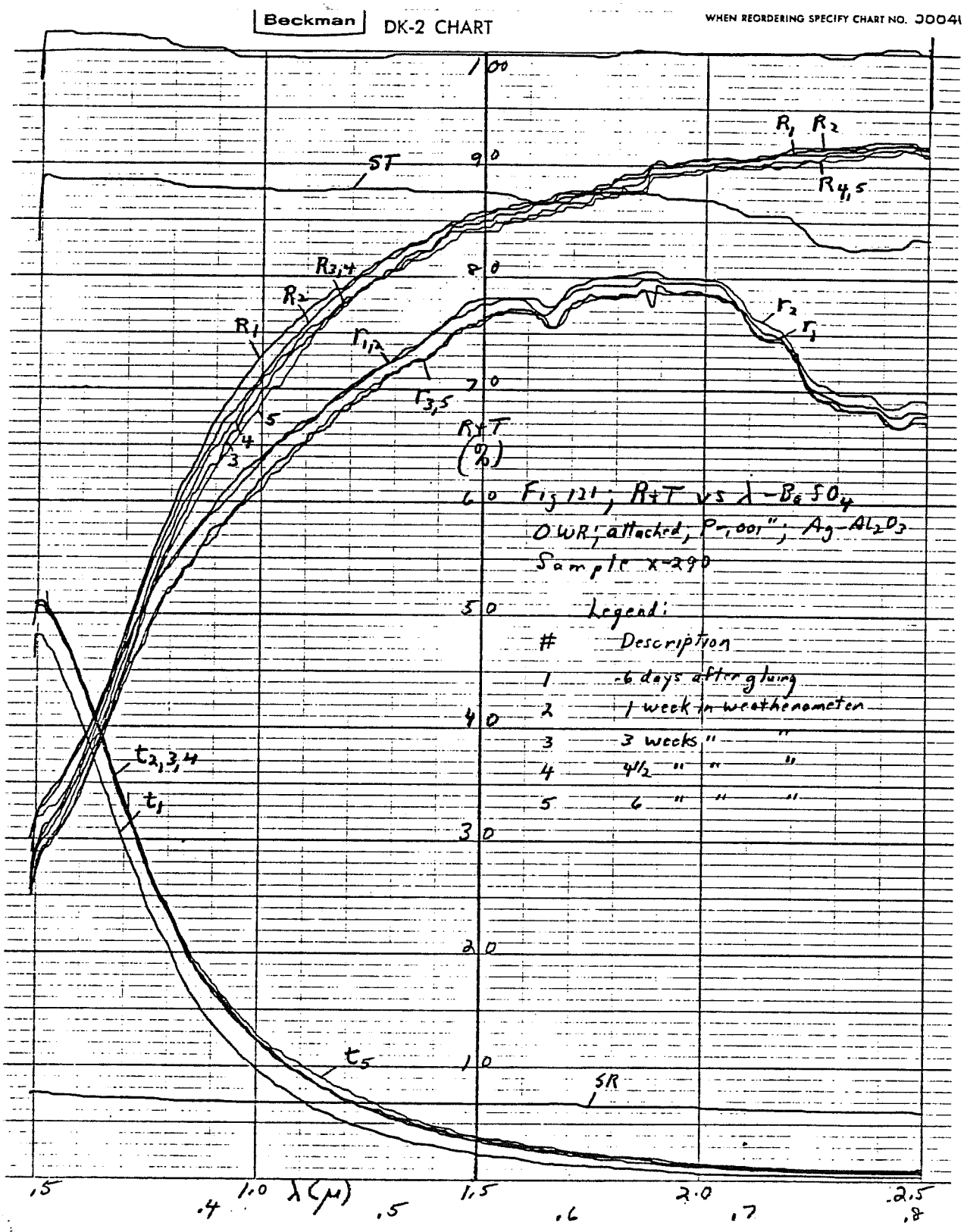
Beckman DK-2 CHART
WHEN REORDERING SPECIFY CHART NO. 30041
100
90
80
70
60
50
40
30
20
10
R, T (%)
R1 R2
R4,5
ST
R3,4
R2
R1
r1,2
r3,5
r2
r1
5
4
3
t2,3,4
t1
t5
SR
Fig 121; R+T vs λ - BaSO4
OWR; attacked; P-.001"; Ag-Al2O3
Sample x-290
Legend:
Description
1 -6 days after gluing
2 1 week in weathenometer
3 3 weeks " "
4 4½ " " "
5 6 " " "
.5
1.0
λ(μ)
1.5
2.0
2.5
.4
.5
.6
.7
.8

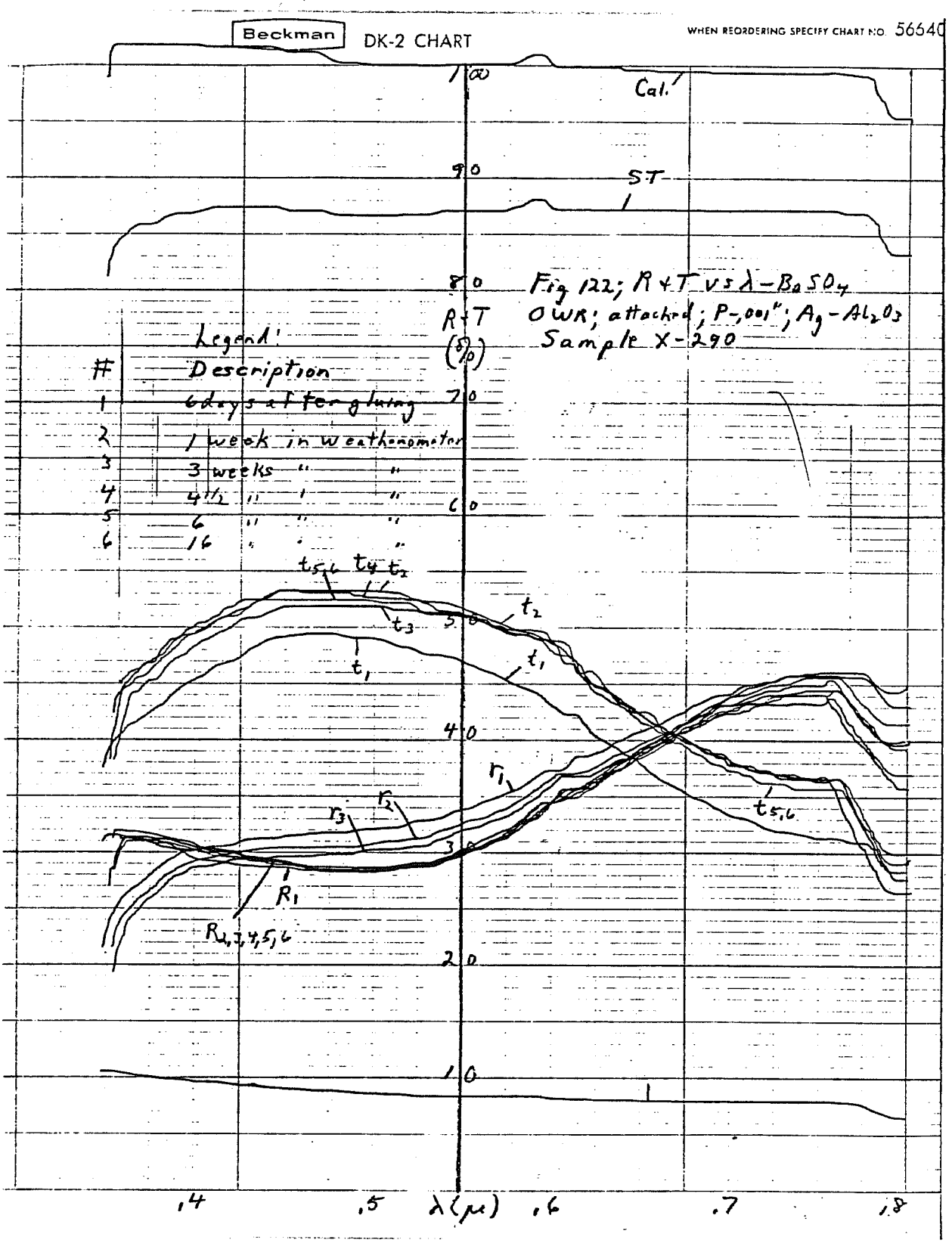
Beckman
DK-2 CHART
WHEN REORDERING SPECIFY CHART NO. 56640
Cal.
S.T.
Fig 122; R+T vs λ - BaSO4
OWR; attacked; P-,001"; Ag - Al2O3
Sample X-290
R+T (%)
Legend:
Description
1 6 days after gluing
2 1 week in weathonometer
3 3 weeks " "
4 4 1/2 " " "
5 6 " " "
6 16 " " "
100
90
80
70
60
50
40
30
20
10
.4
.5
λ(μ)
.6
.7
.8

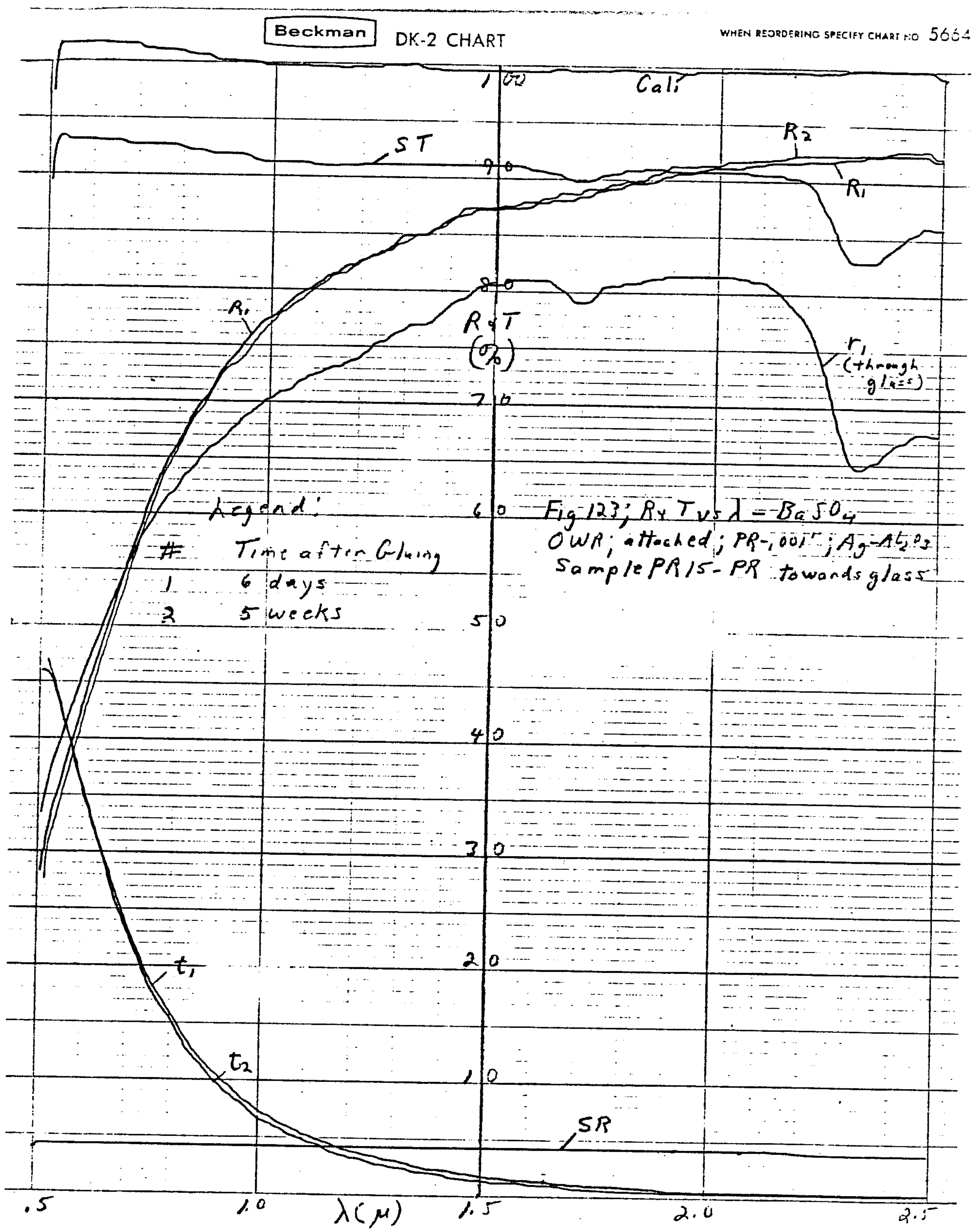
Beckman
DK-2 CHART
WHEN REORDERING SPECIFY CHART NO 5664
Cali
ST
R2
R1
r1 (through glass)
R & T (%)
Legend:
Time after Gluing
1 6 days
2 5 weeks
Fig 123; R & T vs λ - $BaSO_4$
OWR; attached; PR-.001"; Ag-Al_2O_3
Sample PR15 - PR towards glass
t1
t2
SR
λ (μ)
.5
1.0
1.5
2.0
2.5
100
90
80
70
60
50
40
30
20
10

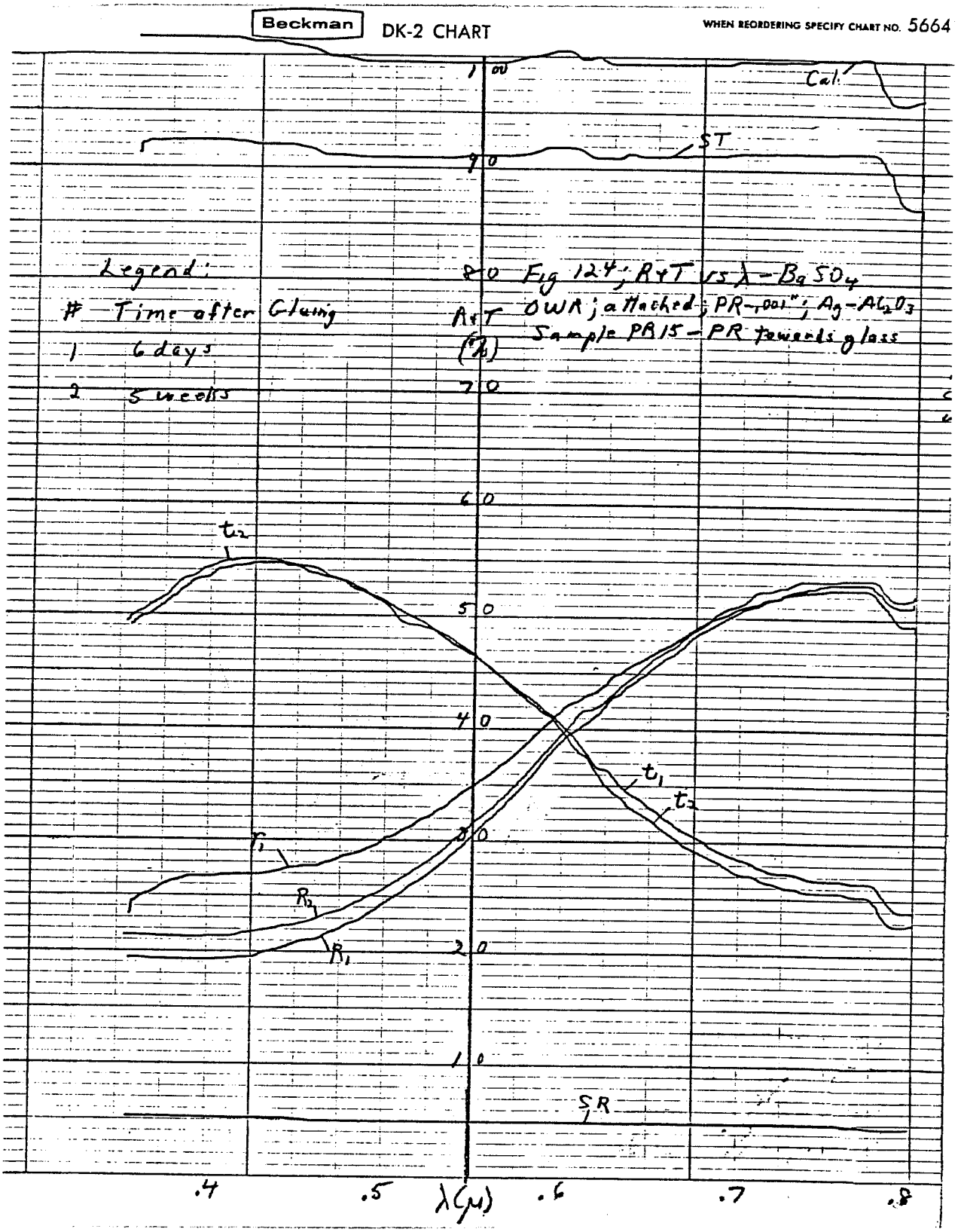
Beckman
DK-2 CHART
WHEN REORDERING SPECIFY CHART NO. 5664
100
Cal
ST
90
Legend:
Time after Glazing
1 6 days
2 5 weeks
80 Fig 124; R+T vs λ - BaSO4
R+T OWR; attached; PR-1001"; Ag-Al2O3
(%) Sample PR15 - PR towards glass
70
60
t2
50
40
t1
t2
30
R2
R1
20
10
SR
.4
.5
λ(μ)
.6
.7
.8

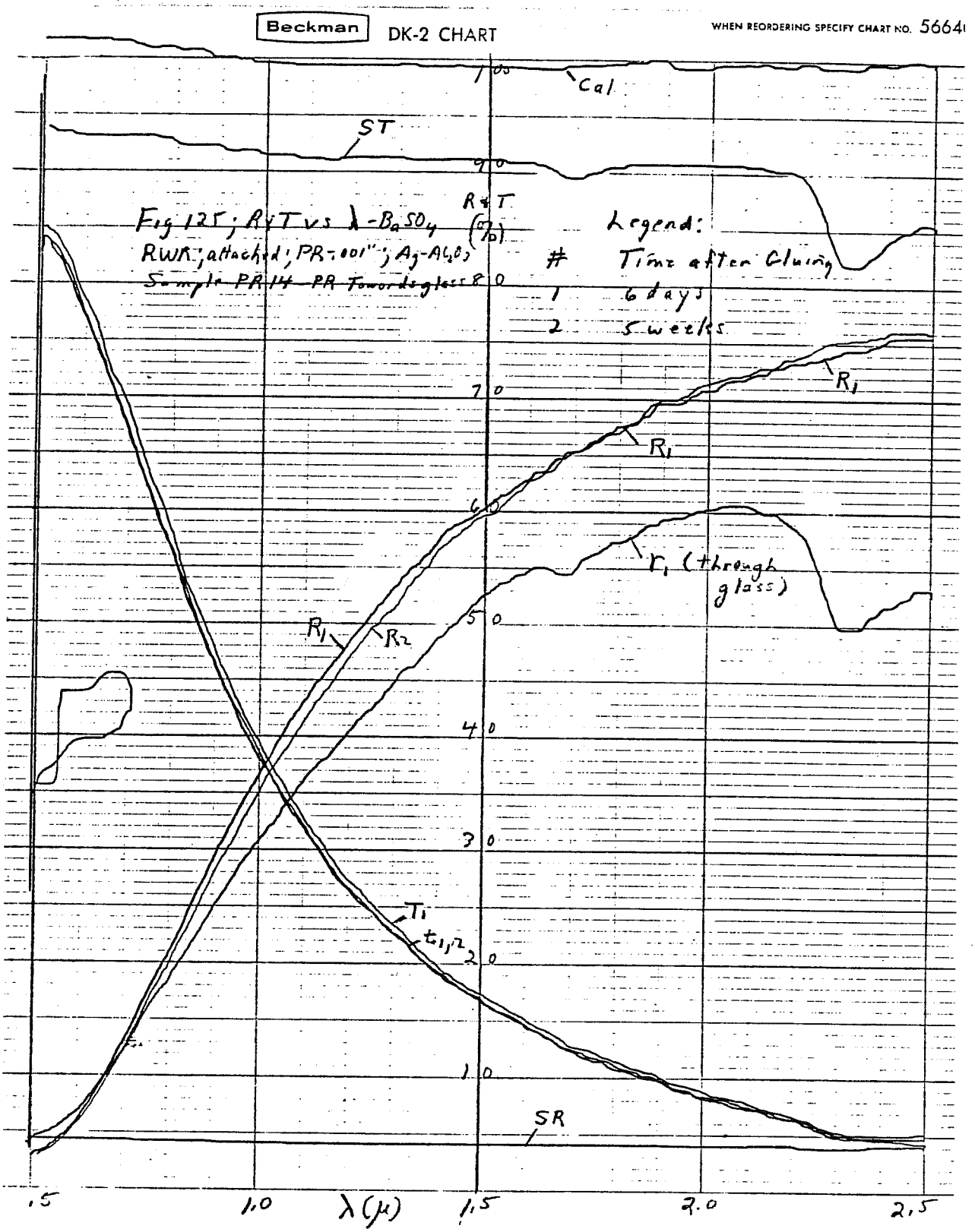
Beckman
DK-2 CHART
WHEN REORDERING SPECIFY CHART NO. 56641
Cal
ST
R+T (%)
Fig 125; R+T vs λ-BaSO4
RWR; attached; PR: .001"; Aj-Al2O3
Sample PR14 PR Towardsglass
Legend:
Time after Curing
1 6 days
2 5 weeks
R1
R1
r1 (through glass)
R1
R2
T1
t1/2
SR
100
90
80
70
60
50
40
30
20
10
.5
1.0
λ(μ)
1.5
2.0
2.5

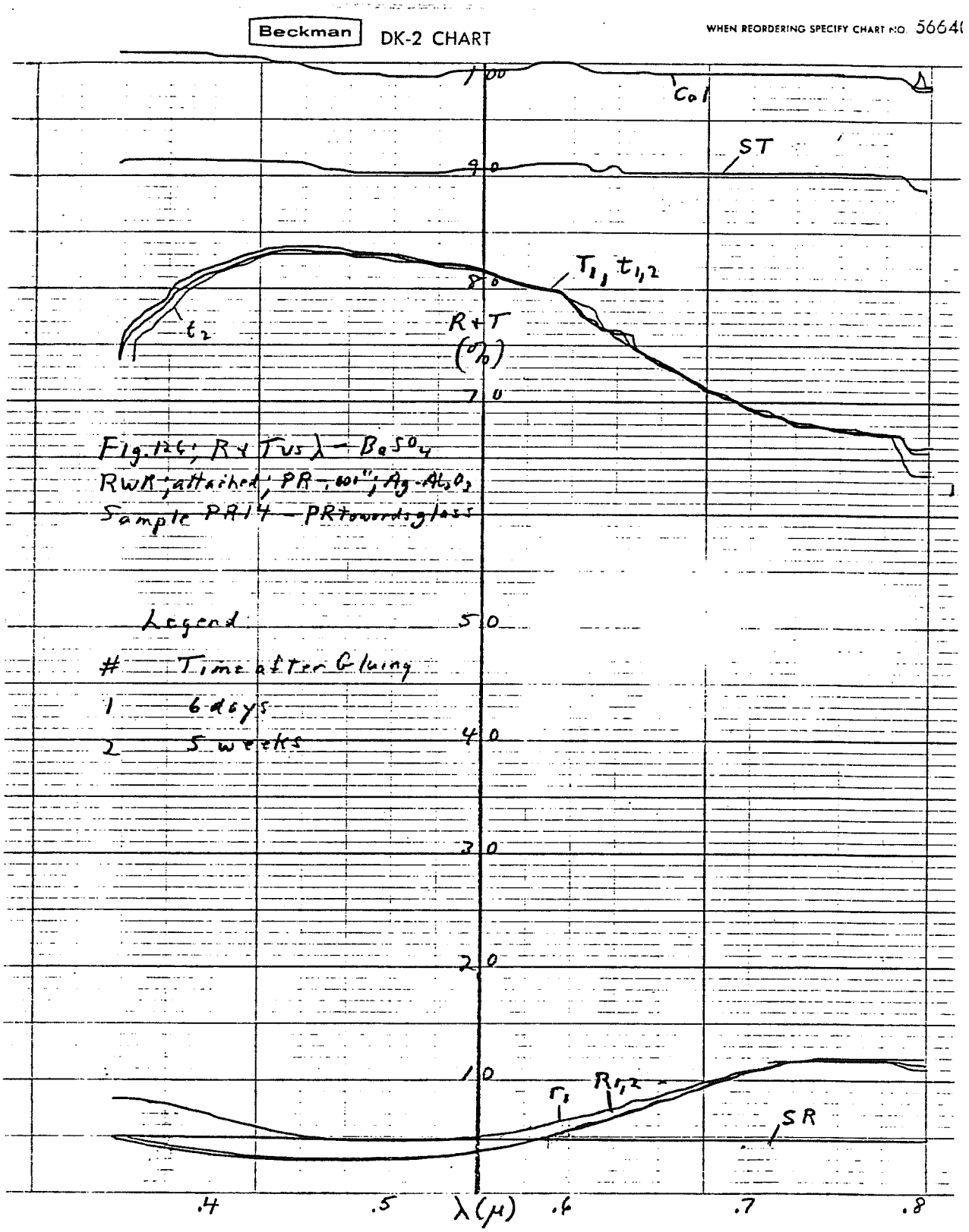
Beckman
DK-2 CHART
WHEN REORDERING SPECIFY CHART NO. 56641
100
90
80
70
50
40
30
20
10
Cal
ST
T1, t1,2
t2
R+T
(%)
Fig. 126; R+T vs λ - BaSO4
RWR; attached; PR - 001"; Ag-Al2O3
Sample PR14 - PR towards glass
Legend
Time after Gluing
1 6 days
2 5 weeks
r1
R1,2
SR
.4
.5
λ(μ)
.6
.7
.8

Figs. 127-128 give the characteristics for an OWR. The most notable difference is in visible T which is much lower than in the PR side in configuration. Stability to date looks reaonable.

The comparable RWR sample (Figs. 129-130) is interesting in that its characteristics are essentially the same when viewed from either side. The visible T values are considerably lower than the PR side in configuration (Fig. 126) but compare favorably with other RWR possibilities.

Exact values of R in the 10 μ region were obtained for these PR substrate samples. At 10 μ, PR15 had an R of . 96 and PR14 an R of . 88. The PR side out samples performance at long wavelength IR must be monitored at some other wavelength than 10 μ becuase of absorption peak there (see Fig. 68). A better monitoring wavelength is roughly 10. 95 μ where PR19 had an R of . 93 and PR21 an R of . 84.

In general, it may be stated that this program has accomplished its goal of demonstrating the ability to achieve the various window configurations discussed in Section 1. Implementation of the technology depends on marketing factors and economic considerations.

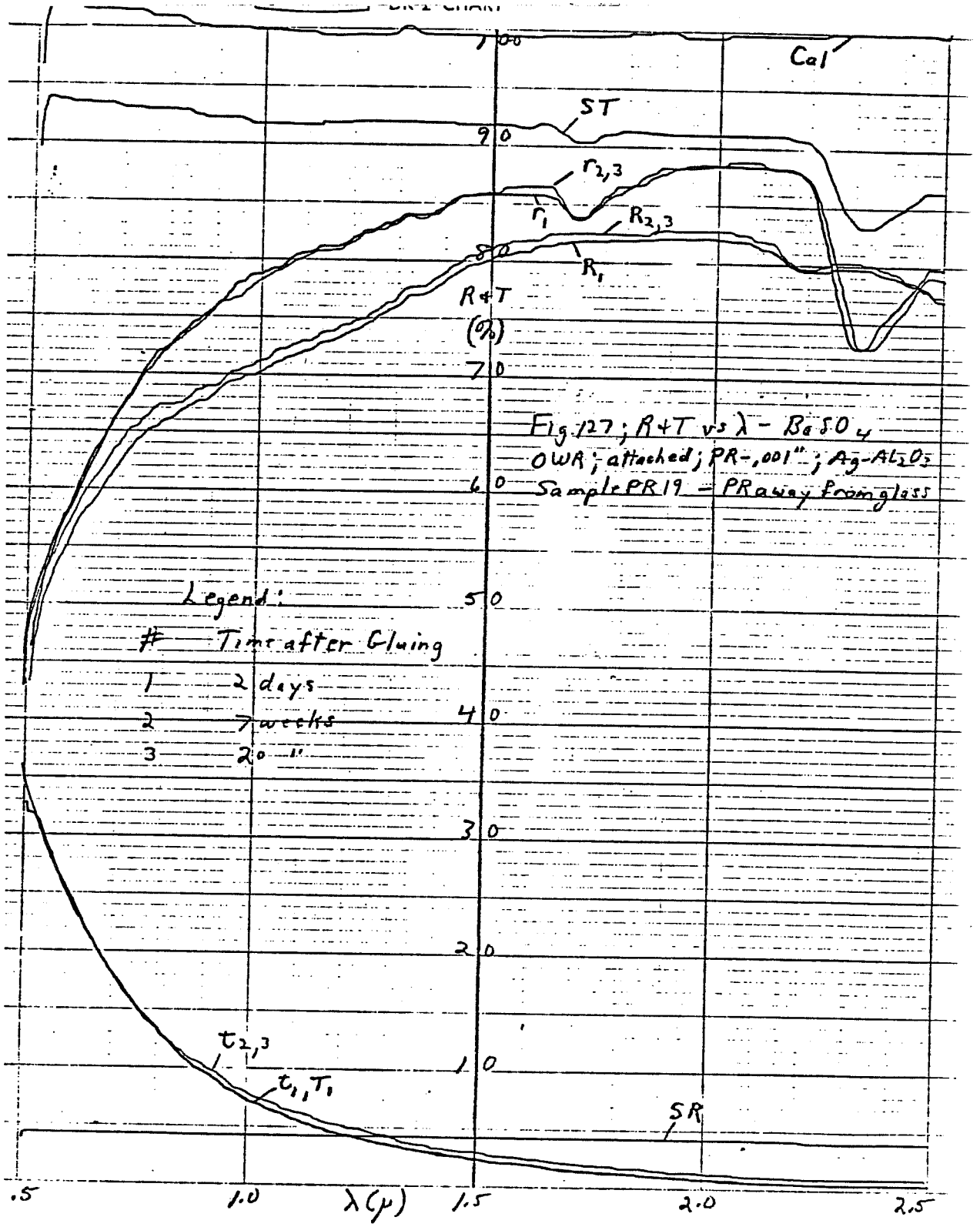

Fig. 127; R+T vs λ - $BaSO_4$ OWR; attached; PR-.001"; Ag-AL_2O_3 Sample PR19 - PR away from glass

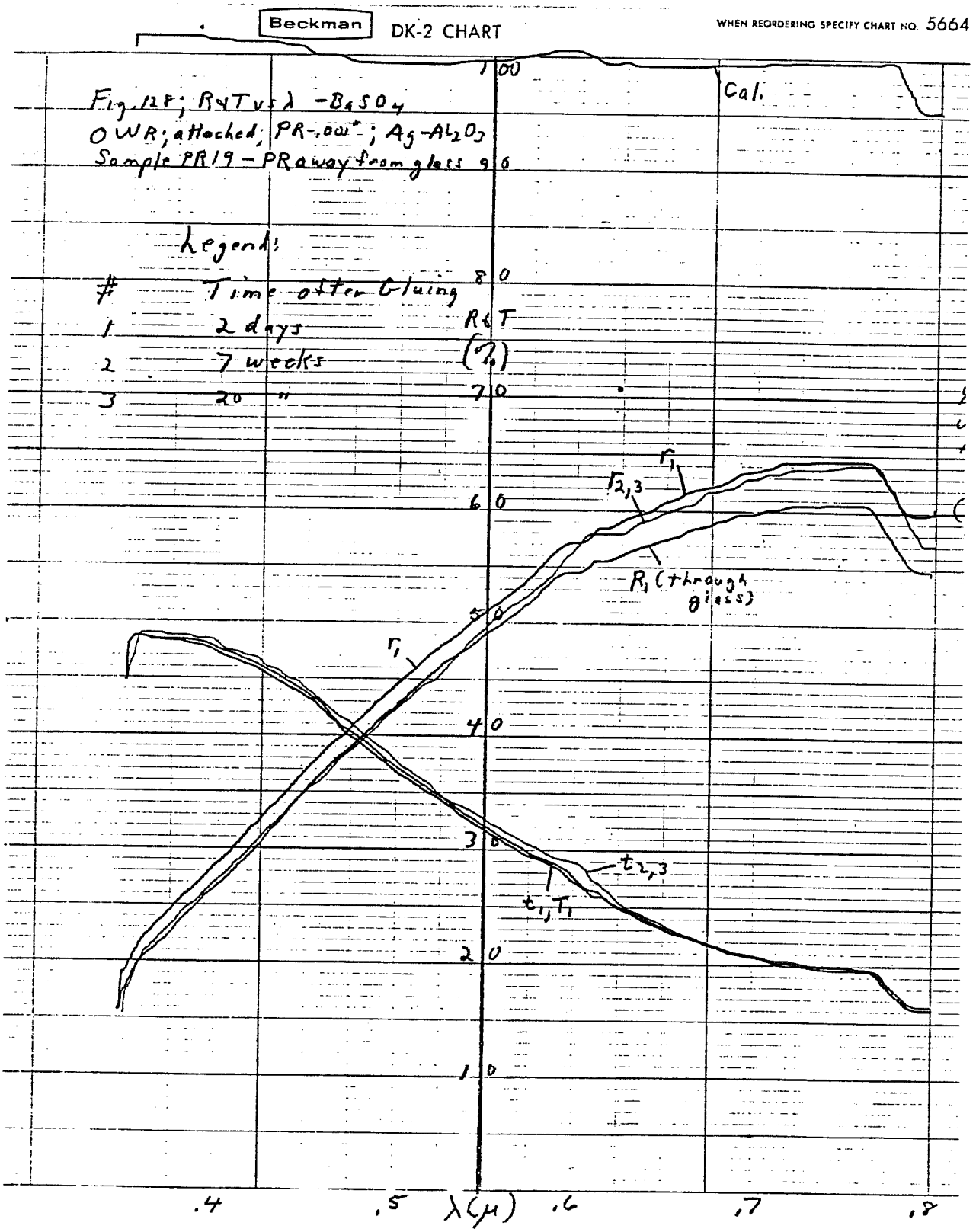
Beckman
DK-2 CHART
WHEN REORDERING SPECIFY CHART NO. 5664
Fig. 12F; R&T vs λ - B_4SO_4
OWR; attached; PR-.001"; Ag - Al_2O_3
Sample PR19 - PR away from glass
Cal.
legend:
Time after Gluing
1 2 days
2 7 weeks
3 20 "
R&T (%)
100
90
80
70
60
50
40
30
20
10
r_1
$r_{2,3}$
R_1 (through glass)
$t_{2,3}$
t_1, T_1
.4
.5
λ(μ)
.6
.7
.8

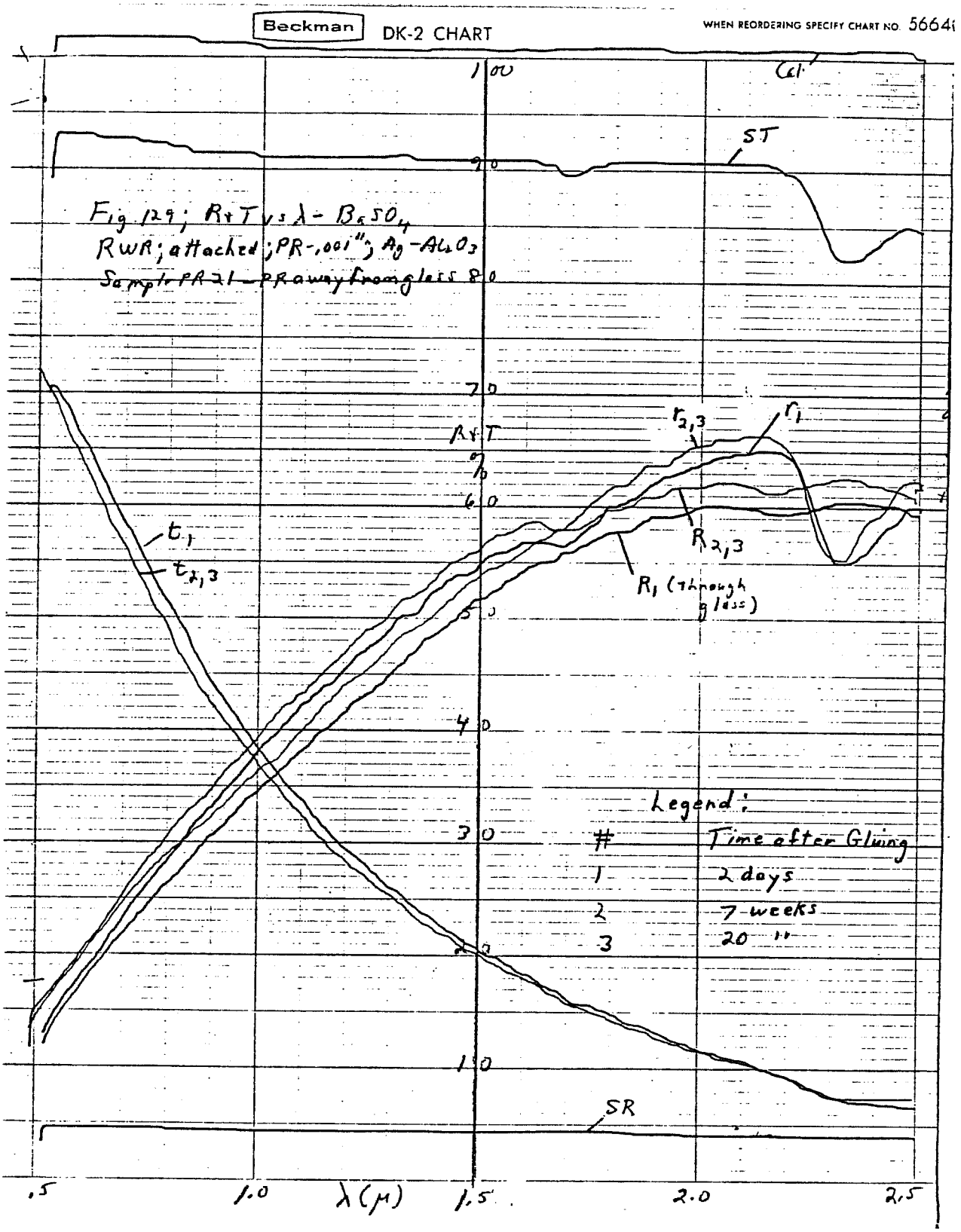
Beckman
DK-2 CHART
WHEN REORDERING SPECIFY CHART NO. 5664
100
Cal
ST
90
Fig 129; R+T vs λ - BaSO4
RWR; attached; PR-.001"; Ag-Al2O3
Sample PR21 - PR away from glass
80
70
R+T
60
50
40
30
20
10
SR
t1
t2,3
r2,3
r1
R2,3
R1 (through glass)
Legend:
Time after Gluing
1 2 days
2 7 weeks
3 20 "
.5
1.0
λ(μ)
1.5
2.0
2.5

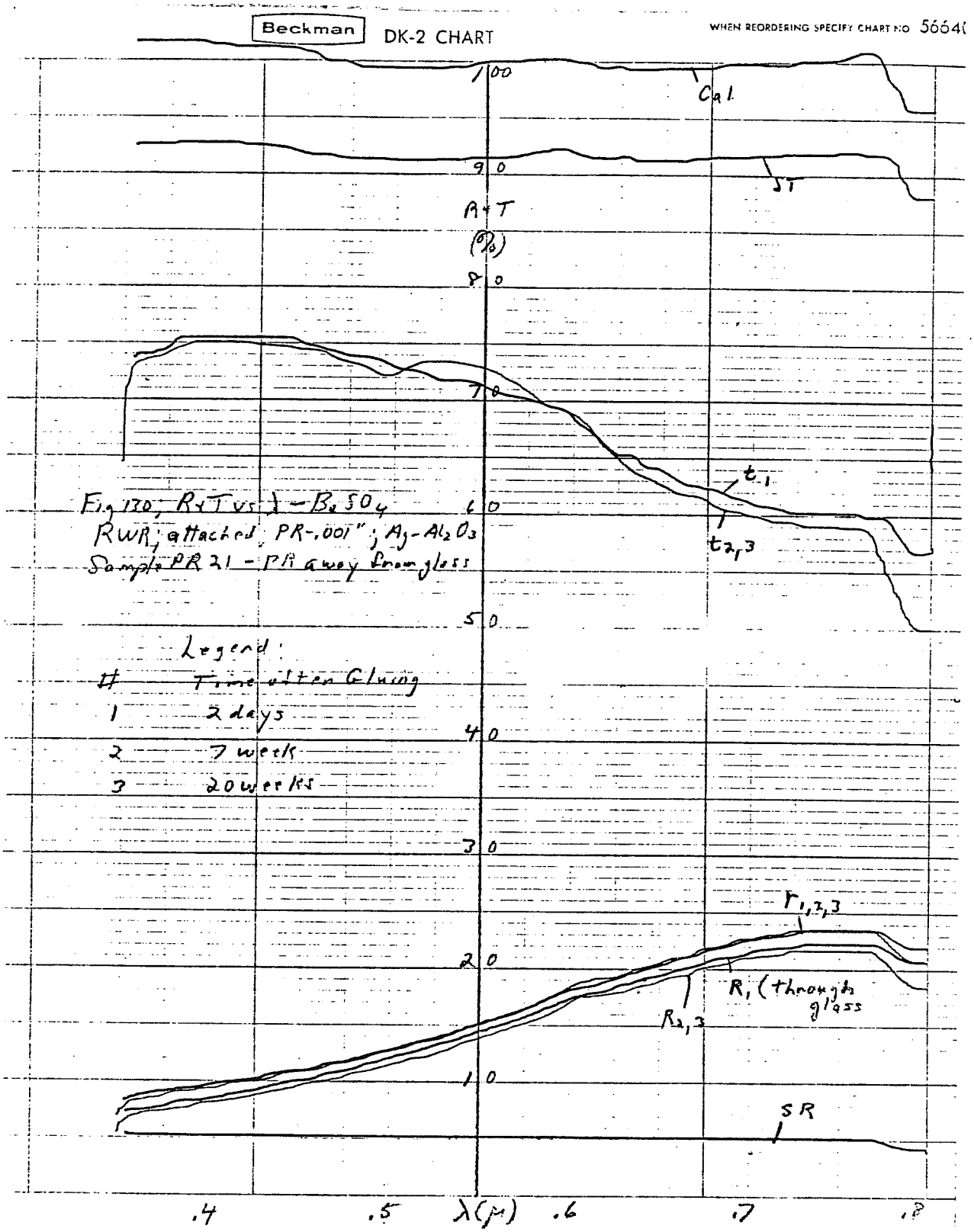
Beckman
DK-2 CHART
WHEN REORDERING SPECIFY CHART NO 5664(
100
90
80
70
60
50
40
30
20
10
R+T
(%)
Cal
ST
t1
t2,3
Fig 170; R+T vs λ - BaSO4
RWR; attached; PR-.001"; Ag-Al2O3
Sample PR 21 - PR away from glass
Legend:
Time after Curing
1 2 days
2 7 weeks
3 20 weeks
R1,2,3
R1 (through glass)
R2,3
SR
.4
.5
λ(μ)
.6
.7
.8

6. Economic Factors

A complete analysis of all of the economic factors associated with manufacturing and selling window materials of the types described is beyond the scope of this report. It is obvious that general merchandising and distribution costs will be similar to those in the established solar control industries, whether they be original equipment (glass) or retrofit (plastics). The present analysis is concerned primarily with manufacturing retrofit material. Considerations for glass substrates would be very similar except that the cost of the basic machine would be higher due to more difficult handling, and relative throughput rates would be lower. Substrate cost would, of course, also be higher but simply be carried forward to the higher selling price of the finished product.

Total production costs in the solar control retrofit film industry are estimated to run in the $\$.30$-$\$.45/ft^2$ including all normal business costs. Factors outside of the direct production costs consitute a large proportion of this cost. Such factors as handling, shipping, adhesive application (if factory applied), merchandising and normal business overhead and profit will be the same for the present material. Any fundamental differences will be connected with the actual factory manufacturing cost.

Table I gives a breakdown of the projected manufacturing cost for a factory based on one large coating machine capable of handling 20 M ft^2 of starting material per year on a 300 day, 20 hr day basis. Multiple safety factors have been taken in the calculations. A manufacturing system based on the Ag-Al_2O_3 combination was assumed. This is by far the worst case because of the cost of the materials and the slower deposition rate of Al_2O_3 compared, for example, to SiO_2. The actual calculated machine cost of \$ 3 M was arbitrarily increased to \$ 5 M to compensate for design errors and inflationary factors. Depreciation for the machine was taken over a 5 year life rather than the anticipated much longer useful life. All wages and benefits were pushed to the maximum as were space and miscellaneous overhead. For direct comparison, each item has been reduced to a cost/ft^2. The effect of varying any factor is simply an incremental addition or subtraction to the individual item and to the overall cost.

TABLE 1

PROJECTED FACTORY MANUFACTURING COST

20 M ft^2/yr - starts

18 M ft^2/yr - shipped material

Item	Total $x 1 k	Cost ¢/ft^2
Direct Labor (Eng. Foreman, 2 Sr. Tech - benefits) $20 k 2 x $15 k 20% 4 shifts	240	1.2
Factory Overhead		
Indirect Labor (Mgt. Eng., Q. C., Sec'y - benefits $30 k $25 k $12 k 20% 3 shifts 1 shift 1 shift	152	.76
Space (15,000 ft^2 at $7 - includes heat, AC, lights etc.)	105	.53
Machine Power (500 kW-300 days/yr-7¢/kWhr)	252	1.2
Misc. O. H. (maintenance, ins., machine parts etc.)	100	.5
Depr. (5 yr - straight line)	1,000	5.0
Direct Materials		
Substrates (100 gauge polyester)		1.0
Ag (at $20/oz.)		.64
Misc. (targets, gases, etc.)		.1
Total Cost ¢/ft^2		10.9
Yield factor (10% loss due to ripping etc.)		1.1
Final Cost ¢/ft^2		12.0

The breakdown can be analyzed on a line by line basis. Direct labor consists of 2 senior technicians for general operation and loading-unloading and an engineer/foreman responsible for overall operation. Four shifts are assumed, to account for 6 days a week operation and overtime. Indirect labor consists of a management engineer responsible for overall plant function on each shift, plus a quality control engineer and secretary on the day shift only. Space is based on a machine size nominally 40-50' x 8-10' in overall dimensions with surrounding space for electronics, local roll handling etc. Modified machine designs could be longer but this has been taken into account. Machine power is a straightforward assignment of costs. Miscellaneous includes machine repair parts as well as overall plant maintenance and insurance.

Depreciation is an item where relatively large shifts could be observed. If the assumed lifetime were longer, it would go down whereas if the amount of finished material went down it would go up; e.g. 10 M ft^2/yr would raise depreciation to 10¢/ft^2. On the other hand, going to SiO_2 could decrease depreciation to 2.5 - 3.5¢/ft^2. Obviously this is an important factor in direct factory costs although not nearly so important in overall manfuacturing and selling costs. Substrate costs can vary widely, with 100 gauge P (1¢/ft^2) having been assumed as the standard. Approximate costs for other materials are 2¢/ft^2 for 100 gauge PR, 4¢/ft^2 for 200 gauge (thinnest available) stabilized P (Melinex OW) and 15¢/ft^2 (estimate in large volumes) for 100 gauge FEP. An 80% use factor (not counting recovery) and a $20/oz. price have been assumed for the Ag metal layer. Other metals or alloys could be cheaper or more expensive. Miscellaneous materials consist primarily of targets.

In order to account for handling loss factors an overall yield of 90% has been assumed leading to a final direct manufacturing cost of 12¢/ft^2. This number is clearly consistent with the overall industry total factory cost factors and would result in a total factory cost of 35-50¢/ft^2 depending strongly on selling and promotional costs. Prices to the consumer would probably be $.90-$1.80 with professional installation costing $1.50-$2.50.

For residential heat conserving applications, S. Selkowitz[2] has estimated that for a five-year payback in a region with heating fuel costs of $6/MBTU, the maximum that can be spent on retrofit heat mirrors would range from $.60/ft^2 in a mild, 2000 degree day climate to $2.40/ft^2 in a cold, 8000 degree day climate. Since fuel costs are already above this and rising quickly and continuously, these are very conservative estimates. Other configurations (OWR, OW, RW) must be evaluated individually in the context of their potential use, but it is fair to say that the comparisons are similar to the one above.

A factor which is generally ignored but which is very important is that of energy pay-back; i. e. the time required to conserve as much energy as it took to make the product. Using an RWR as an example and the above numbers, it takes approximately 500 BTU of energy to coat 1 ft^2 of RWR material. At an energy savings of 10 BTU/ft^2/hr, (20°F differential) which is consistent with the expected performance of such windows in the heating season, it would take 50 hours to recover the energy used in the coating process. The energy used in making the plastic (quick calculation including oil equivalent for material and processing) is almost certainly less than an additional 500 BTU or 50 hours energy recovery time. Larger temperature differentials would actually result in faster recovery of the energy consumed in manufacturing. Total energy pay-back time is therefore of the order of 100 hours or 4 days. In these days of rapidly decreasing energy supplies, this looks like an offer that can't be refused.

---

(2) S. Selkowitz; Transparent Heat Mirrors for Passive Solar Heating Applications, LBL-7829, March 1978